



UNIVERSITÀ DEGLI STUDI DI TRENTO
Dipartimento di Ingegneria Meccanica e Strutturale
Facoltà di Ingegneria

Ph.D student: Eng. Fabio Ferrario

Analysis and modelling of the seismic behaviour of high ductility steel-concrete composite structures

Tutor: Prof. Eng. Oreste S. Bursi

Cotutor: Prof. Eng. André Plumier

Febbraio 2004

@Seismicisolation

Università degli Studi di Trento
Università degli Studi di Brescia
Università degli Studi di Padova
Università degli Studi di Trieste
Università degli Studi di Udine
Istituto Universitario di Architettura di Venezia

Ph.D. student: Eng. Fabio Ferrario

ANALYSIS AND MODELLING
OF THE SEISMIC BEHAVIOUR OF HIGH DUCTILITY
STEEL-CONCRETE COMPOSITE STRUCTURES

Tutor: Prof. Eng. Oreste S. Bursi

Co-tutor: Prof. Eng. André Plumier

February 2004

UNIVERSITÀ DEGLI STUDI DI TRENTO
Dottorato di Ricerca in Modellazione, Conservazione e Controllo delle Strutture
(XVI ciclo)

Prof. Oreste S. Bursi

Analysis and Modelling of the Seismic Behaviour of High Ductility
Steel-Concrete Composite Structures

Fabio Ferrario
Department of Mechanical and Structural Engineering
Via Mesiano 77 - 38050
University of Trento - ITALY
Phone number: +39 0461 882572
Fax number: +39 0461 882567
E-mail: fabio.ferrario@ing.unitn.it

Esame finale: 4 marzo 2004

Commissione esaminatrice:
Prof. André Plumier, Université de Liège; Belgium
Prof. Oreste S. Bursi, Università degli Studi di Trento, Italia
Prof. Alessandro De Stefano, Università degli Studi di Torino, Italia

Analysis and Modelling of the Seismic Behaviour of High Ductility Steel-Concrete Composite Structures

Fabio Ferrario
Department of Mechanical and Structural Engineering
University of Trento
Via Mesiano 77 – 38050 – ITALY
Phone number: +39 0461 882572
Fax number: +39 0461 882567
E-mail: fabio.ferrario@ing.unitn.it

ABSTRACT

In this thesis theoretical, experimental and numerical aspects and applications concerning the seismic behaviour of high ductility steel-concrete composite structure are analysed.

The interest has been focused on the capability of framed structures to dissipate seismic energy by means of inelastic deformations. The basic design parameter in this approach is the *ductility* that should be considered as a conceptual framework in the Performance-Based Seismic Engineering (PBSE). PBSE has been developed encompassing the full range of seismic engineering issues to be referred to design of structures for predictable and controlled seismic performance within established levels of risk.

The attention has been focalised on different solutions of steel and steel-concrete composite beam-to-column joints assuring the necessary ductility that can be obtained not only through careful study of building morphology, structural schemes and construction details, but also through the rational use of materials. Three specific and related topics have been analyzed and detailed analyses and experimental tests on substructures have been performed in order to ensure large inelastic deformations and the necessary energy dissipation under earthquake strong motion. The results aiming at qualifying the dissipative and rotational capacities of a particular typology of beam-to-column joints are then illustrated and discussed. The objective of this study is to provide designers with precise rules regarding constructional solutions suitable to each scheme and to the associated design methodologies necessary for evaluating their performances.

Keywords: Low-cycle fatigue, ductility, innovative beam-to-column joint design, life-safe condition.

@Seismicisolation

Ai miei genitori

@Seismicisolation

RINGRAZIAMENTI

Nello scrivere la pagina di ringraziamento penso sia comune a tutti avere la paura di escludere qualcuno che in maggior o minore misura ha contribuito a rendere questo periodo un momento della propria vita unico ed irripetibile.

Le prime persone, che meritano il mio più sincero e sentito "Grazie", sono sicuramente i miei genitori per l'affetto ed il sostegno che hanno saputo darmi in questi anni.

Ringrazio il prof. Oreste S. Bursi, relatore della tesi, che mi ha seguito con disponibilità e pazienza fornendomi preziose indicazioni in riferimento alla valutazione dei risultati sperimentali e di alcuni delicati aspetti teorici. A lui va un ringraziamento particolare per la fiducia riposta e per la possibilità concessami di lavorare in un'esperienza indimenticabile.

Un ringraziamento particolare va al prof. André Plumier, dell'Università di Liegi, correlatore della tesi, per i numerosi e preziosi consigli nelle lunghe discussioni avute nel suo ufficio. Ricordo con grande piacere le chiacchierate sulle sue esperienze di vita, sui giri in bicicletta e sui sogni di navigatore dei mari. Sicuramente il suo esempio sarà per me un punto di riferimento nel voler diventare ingegnere, ma soprattutto uomo di spessore.

Ringrazio, poi, tutti coloro che in questi tre anni mi sono stati vicini come colleghi di lavoro ma soprattutto come amici. Un sentito ringraziamento va a tutti gli studenti, dottorandi e giovani ricercatori che ho incontrato e con i quali ho avuto la fortuna di collaborare, sia all'Università di Trento, sia all'Università di Pisa, sia all'Università di Liegi. Anche se non vi nomino, voglio che sappiate che non vi ho dimenticato.

Infine, per ultimo, voglio ringraziare Colui che ha avuto il merito più grande in questo lungo cammino! Aver tracciato il mio percorso e avermi dato la possibilità di percorrerlo è stato un segno indelebile del fatto che mi vuoi bene! Ti ringrazio per avermi fatto assaporare una delle Avventure più stupende della mia vita!

Fabio Ferrario

Trento, febbraio 2004

@Seismicisolation

INDEX

1 INTRODUCTION.....	1
1.1 INTRODUCTION	1
1.2 ORGANIZATION OF THE WORK	3
1.2.1 <i>Seismic behaviour of bolted end plate beam-to-column steel joints</i>	3
1.2.2 <i>Seismic response of partial-strength composite joints</i>	4
1.2.3 <i>Seismic behaviour of RC columns embedding steel profiles</i>	5
1.3 REFERENCES	6
2 DUCTILITY AND SEISMIC RESPONSE OF STRUCTURES.....	7
2.1 INTRODUCTION	7
2.2 DUCTILITY IN SEISMIC DESIGN	8
2.2.1 <i>First developments of ductility concept</i>	8
2.2.2 <i>Modern design concepts of ductility</i>	9
2.2.3 <i>Ductility definition</i>	11
2.3 THE PERFORMANCE BASED SEISMIC DESIGN.....	14
2.3.1 <i>Performance objectives (POs)</i>	14
2.3.2 <i>Performance Levels</i>	16
2.4 REQUIRED DUCTILITY CONCEPT.....	20
2.4.1 <i>Non-linear static pushover (NSP) analysis</i>	24
2.4.2 <i>Non-linear dynamic procedure (NDP)</i>	31
2.5 AVAILABLE DUCTILITY CONCEPT.....	34
2.6 REFERENCES	37
3 SEISMIC BEHAVIOUR OF BOLTED END PLATE BEAM-TO-COLUMN STEEL JOINTS.....	40
3.1 INTRODUCTION	40
3.2 THE COMPONENT METHOD.....	42

INDEX

3.3	SEMI-RIGID PARTIAL-STRENGTH EXTENDED END PLATE CONNECTION	44
3.4	THE EXPERIMENTAL PROGRAMME CARRIED OUT AT THE DIMS	46
3.4.1	<i>Material properties</i>	50
3.4.2	<i>Fracture mechanics-based characterization</i>	51
3.4.3	<i>Testing equipment and measuring apparatus</i>	53
3.4.4	<i>Testing procedure</i>	56
3.5	MAIN RESULTS AND PRELIMINARY SEISMIC ASSESSMENT	58
3.5.1	<i>Isolated Tee stubs</i>	58
3.5.2	<i>Coupled Tee Stubs</i>	61
3.5.3	<i>Complete Joints</i>	63
3.6	VALIDATION OF THE COMPONENT METHOD.....	69
3.7	NUMERICAL ANALYSIS.....	75
3.7.1	<i>FE Models of the ITS connections</i>	75
3.7.2	<i>FE Models of the CJ specimens</i>	81
3.7.3	<i>Parametric analyses</i>	85
3.8	CONCLUSIONS	94
3.9	REFERENCES	96
4	SEISMIC RESPONSE OF PARTIAL-STRENGTH COMPOSITE JOINTS	100
4.1	INTRODUCTION.....	100
4.2	THE ECOLEADER-ECSC JOINT PROJECT.....	101
4.3	DESCRIPTION OF THE PROTOTYPE STRUCTURE	102
4.4	SEISMIC DESIGN OF THE PROTOTYPE STRUCTURE	107
4.5	SEISMIC DESIGN OF THE COMPOSITE JOINT	110
4.5.1	<i>Concrete slab resistance</i>	111
4.5.2	<i>Column web panel shear resistance</i>	115
4.5.3	<i>Joint rotational capacity evaluation</i>	120
4.6	MECHANICAL PROPERTIES OF MATERIALS.....	122
4.7	SEISMIC PERFORMANCE EVALUATION FOR THE PROTOTYPE STRUCTURE.....	122
4.8	CYCLIC TESTS OF FULL-SCALE COMPOSITE JOINT SUBASSEMBLAGES	127
4.8.1	<i>Test set-up and procedure</i>	127
4.8.2	<i>Specimen behaviour and test results</i>	130
4.8.3	<i>Validation of the analytical model</i>	136
4.8.4	<i>3D finite element (FE) model</i>	142
4.9	NUMERICAL ANALYSES OF THE PROTOTYPE STRUCTURE.....	150
4.9.1	<i>Pushover vs. incremental dynamic analysis results</i>	151
4.10	PSEUDO-DYNAMIC TESTS ON THE PROTOTYPE STRUCTURE	160
4.10.1	<i>Testing apparatus and instrumentation</i>	161
4.10.2	<i>Results of the PsD test n° 1</i>	163

INDEX

4.10.3	<i>Results of the PsD test n° 2</i>	163
4.10.4	<i>Results of the PsD test n° 3</i>	165
4.10.5	<i>Results of the PsD test n° 4</i>	167
4.10.6	<i>Results of the cyclic test</i>	167
4.11	CONCLUSIONS.....	170
4.12	REFERENCES	171
5	SEISMIC BEHAVIOUR OF RC COLUMNS EMBEDDING STEEL PROFILES	174
5.1	INTRODUCTION	174
5.2	THE INERD PROJECT.....	175
5.3	DESCRIPTION OF THE PROTOTYPE STRUCTURE	179
5.3.1	<i>Materials and mechanical properties.....</i>	179
5.3.2	<i>Load combinations.....</i>	181
5.3.3	<i>3D frame modelling.....</i>	184
5.3.4	<i>Design of the reinforced concrete columns</i>	187
5.3.5	<i>Design of the fully encased composite columns</i>	190
5.4	DESIGN OF BEAM-TO-COLUMN JOINTS	196
5.4.1	<i>Strength of the Inner Elements</i>	197
5.4.2	<i>Strength of the Outer Elements</i>	202
5.5	THE EXPERIMENTAL TEST PROGRAMME	208
5.5.1	<i>Design of the reduced section of the specimen to be tested.....</i>	208
5.5.2	<i>Test set-up and test programme</i>	211
5.5.3	<i>Global test instrumentation.....</i>	213
5.5.4	<i>Local test instrumentation.....</i>	214
5.5.5	<i>Test procedure and loading history.....</i>	216
5.6	RESULTS OF THE TESTS	222
5.6.1	<i>RCT5 Specimen</i>	222
5.6.2	<i>COT9-COT10 Specimens</i>	223
5.6.3	<i>COT11-COT12 Specimens</i>	227
5.6.4	<i>Comparison of the experimental results and comments.....</i>	227
5.7	NUMERICAL ANALYSES AND VALIDATION OF THE MECHANISMS.....	230
5.7.1	<i>FE Model of the specimens</i>	230
5.7.2	<i>Steel web panel shear mechanism verification.....</i>	232
5.7.3	<i>Concrete compression strut mechanism verification.....</i>	235
5.7.4	<i>Concrete compression field mechanism verification.....</i>	237
5.7.5	<i>Calibration of the mechanisms.....</i>	238
5.8	CONCLUSIONS.....	240
5.9	REFERENCES	242

INDEX

6 SUMMARY, CONCLUSIONS AND FUTURE PERSPECTIVES.....	244
6.1 SUMMARY.....	244
6.2 CONCLUSIONS AND FUTURE PERSPECTIVES	245
6.2.1 <i>Seismic behaviour of bolted end plate beam-to-column steel joints.....</i>	245
6.2.2 <i>Seismic response of partial-strength composite joints</i>	247
6.2.3 <i>Seismic behaviour of RC columns embedding steel profiles</i>	248

1 INTRODUCTION

1.1 Introduction

In the seismic design of framed structures the dissipation of input seismic energy plays a fundamental role. The basic parameter in this approach is *ductility*, considered as the ability of a structure to undergo serious plastic deformations without losing strength. In design practice it is generally accepted that steel is an excellent material for this purpose due to performance in terms of ductility. But the recent earthquakes of Mexico City (1985), Loma Prieta (1989), Northridge (1994) and Kobe (1995) have seriously compromised this idyllic image of steel as a perfect material for seismic areas. A series of factors contributes to the poor local ductility of steel structures. With regard to resistance these factors are the discrepancies between real and design yield stress, the value of through thickness resistance of steel, the need for requirements on toughness of the base and weld material and the effect of strain rate. With regard to the action effect, other factors contributed to a bad ductility: the past underestimates of needed plastic rotations, the existence of 3D stress states created in welded connections of high beams, the consideration of wrong stress distributions in beam ends, a bad design of connections and the influence of the composite character of beams.

Aiming at making up for this lack, the world of civil structural research is moving to give designers constructional rules that allow to design high-ductility structures in seismic areas. An important evidence of these research activities is that the verification of structure ductility must be quantified at the same level as the strength and stiffness. It must be recalled that, in that concept, specific elements of the primary lateral force resisting system are chosen and suitably designed and detailed for energy dissipation under severe imposed deformations. The critical regions of these members, often termed plastic hinges or dissipative zones, are

1. INTRODUCTION

detailed for inelastic behaviour. All other structural elements are protected against actions that could cause failure by providing them with strength greater than that corresponding to the development of the maximum feasible strength in the plastic hinge regions. The following features characterise the procedure:

- potential plastic hinge regions within the structure are clearly defined and designed to have dependable strengths and ductility;
- potential brittle regions, or those components not suited for stable energy dissipation, are protected by ensuring that their strength exceeds the demands originating from the overstrength of the plastic hinges.

To highlight the concept of capacity design, the chain shown in Figure 1.1 is often considered (Plumier, 2000). As the strength of a chain is the strength of its weakest link, one ductile link may be used to achieve ductility for the entire chain. The nominal tensile strength of the ductile link is subject to uncertainties of material strength and strain hardening effects at high strains. The other links are presumed to be brittle, but their failure can be prevented if their strength is in excess of the real strength of the ductile weak link at the level of ductility envisaged. Correct application of the capacity design principle thus requires knowledge of the material properties, both of the plastic and neighbouring zones, and the evaluation of the stresses and strains, which must be sustained by the material of the plastic zones. It is clear now that pre-Northridge or Kobe design was characterised by weaknesses in the evaluations made either on the side of resistance or on the side of action effect.

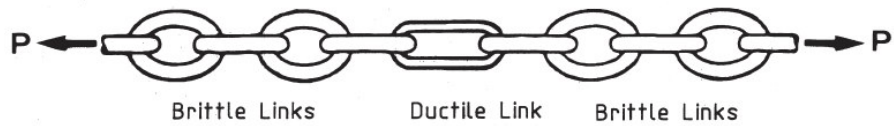


Figure 1.1. Principle of capacity design

Solutions assuring the necessary ductility can be obtained not only through careful study of building morphology, structural schemes and construction details, but also through the rational use of materials. Steel-concrete composite structures, owing to their high capacity for prefabrication and rational use of the materials, seem able to provide high levels of performance in terms of ductility and dissipation energy, while at the same time containing construction costs. However, the adoption of such structural solutions in design practice has been precluded to date by the lack of suitable constructional solutions. In fact, Eurocode 8 (prEN 1998-1, 2002) sets forth general principles for designing composite structures for seismic areas and

1. INTRODUCTION

imposes precise constructional and performance guidelines; however it does not furnish adequate information on the use of the various structural schemes, or on the associated constructional solutions and design methodologies, for which it often refers designers to codes and regulations regarding non-earthquake-resistant structures. Thus, it is necessary to conduct systematic studies of structural schemes by analysing their constructional requirements as well as their performance in terms of ductility and dissipative capacity. Such analysis must provide designers with precise rules regarding the constructional solutions suitable to each scheme and to the associated design methodologies necessary for evaluating their performances.

1.2 Organization of the work

On the basis of the aforementioned developments in earthquake design, in this thesis the attention will be focused on new solutions assuring the necessary ductility, which can be obtained not only through careful study of building morphology, structural schemes, and construction details, but also through a rational use of materials. The attention will be focused on detailed analyses, design and tests of beam-to-column joints that can ensure the necessary ductility by their plastic deformations, and then the necessary energy dissipation under earthquake strong motion. Three main topics are analyzed and briefly introduced below.

1.2.1 Seismic behaviour of bolted end plate beam-to-column steel joints

The study conducted in the first year of the research activity is part of a research programme which has a two-fold purpose: (i) to analyse the seismic performance of partial strength bolted extended end plate joints with fillet welds, which represent an alternative to fully welded connections for use in seismic force resisting moment frames; (ii) to verify the feasibility of the mechanical approach adopted for joints undergoing monotonic loading in a low-cycle fatigue regime, whereby the properties of a complete joint are understood and obtained by assembling the properties of its component parts. The experimental investigation clearly showed that failure of connections and components always happened due to initiation and stable growth of microcracks at the weld toe. These issues represent fundamental aspects of research and code developments on the seismic design of beam-to-column extended end plate joints, and they are the issues explored by this the

1. INTRODUCTION

research: (i) mechanical and metallurgic characterization of the connection material in order to estimate fracture toughness parameters like the inelastic crack tip opening displacement (CTOD); (ii) development of adequate numerical models taking into account the initiation and subsequent crack growth as well as the cyclically stable stress-strain curve; (iii) parametric study on some design parameters which influence the fracture resistance of steel bolted extended plate connections. More specifically, the effects of the weld-to-base metal yield strength ratio, the residual stress influence, and the end plate yield-to-ultimate strength ratio have been determined through detailed two- and three-dimensional non-linear finite element analyses of isolated Tee stub connections and complete joints.

1.2.2 Seismic response of partial-strength composite joints

This research activity is part of a ECOLEADER Project (3D Full-Scale Seismic Testing of a Steel-Concrete Composite Building at Elsa, 2004), in which the University of Trento plays the role of technical coordination. The project was partially conducted jointly with an ECCS Project (Applicability of Composite Structures to Sway Frames - 7210-PR-250 Project). In order to evaluate the feasibility and effectiveness of the composite constructions with partial-strength beam-to-column joints and partially encased columns in earthquake-prone regions, the study aims at calibrating design rules affecting the aforementioned components and the participation of the concrete slab in the relevant transfer mechanisms. The results of this project led to improved design procedures for composite constructions (Section 7, Part 1 of Eurocode 8, 2002). On the basis of constructional considerations and of the favourable seismic behaviour of both the column web panel and the end plate connection of the previous activity, the composite solution adopted in the tested structure relies on plain steel columns. Cyclic and Pseudo-Dynamic (PsD) tests have been conducted on a virtually full-scale steel-concrete composite 3D structure with two-storey two-bay layout. Pseudo-dynamic tests were performed in order to evaluate the performance of the structure in terms of complex hysteretic behaviour under earthquake-like loading. Moreover, new performance-based seismic design guidelines require that steel-concrete composite buildings be analysed by using non-linear static pushover analyses or non-linear dynamic analyses in order to control local and global performances. For this reason, experimental data of beam-to-column joints performed with the ECCS Project were then used to validate 3D model assembled with the ABAQUS code and 1D composite frame set up with the IDARC-2D code. The 3D model is used to analyse the local behaviour of composite members and

1. INTRODUCTION

joints whilst 2D model allows the behaviour of moment resisting composite frames to be understood.

1.2.3 Seismic behaviour of RC columns embedding steel profiles

This last research activity, conducted in the third year of the Ph.D. course, is part of another European Project titled Two Innovations For Earthquake Resistant Design - INERD Project, that deals with the improvement of the resistance and ductility of reinforced concrete (RC) structures using the performance of structural steel profiles.

The general objective is to establish a new standard constructional rule able to improve the seismic safety of reinforced concrete structures, without great changes to traditional constructional practice. This rule consists in promoting one specific construction measure for lower storeys of reinforced concrete structures, by which steel profiles would be encased in RC columns in order to provide them with a basic reliable shear and compression resistance. The introduction of this new concept is justified by the fact that the main safety problem for RC structure is the *soft storey* failure, that is a localization of buildings seismic deformations and rupture in one or two lower storeys as a consequence of the major discrepancy existing between design assumptions and real requirements. The proposed idea is to use encased steel sections as ductile fuses able to dissipate the energy of the earthquake in the lower storeys of buildings in a cyclic way.

1. INTRODUCTION

1.3 References

- Bursi O.S., Caramelli S., Fabbrocino G., Molina J., Salvatore W., Taucer F. (2004): *3D Full-scale seismic testing of a steel-concrete composite building at ELSA*. Contr. No. HPR-CT-1999-00059. Eur Report, European Community.
- Plumier A. (2000): *General report on local ductility*. Journal of Constructional Steel Research, 55, 91–107.
- prEN 1998-1:2002: *Design of structures for earthquake resistance. Part 1: general rules, seismic actions and rules for buildings* - Draft n°5.

2 DUCTILITY AND SEISMIC RESPONSE OF STRUCTURES

2.1 Introduction

Engineers have recognized the need to take into account the plastic design in the design of framed structures subjected to seismic actions. Regarding the seismic design, the interest is focused on dissipation of input seismic energy. The basic design parameter in this approach is *ductility*, considered as the ability of the structure to undergo serious plastic deformations without losing strength. In design practice it is generally accepted that steel is an excellent material for this purpose objectives due to performance in terms of ductility. But in the last decades specialists have recognized that the so-called good ductility of steel structures may be, in some particular conditions, only a dogma, which disagrees with reality. In fact, the recent earthquakes of Mexico City (1985), Loma Prieta (1989), Northridge (1994), and Kobe (1995) have seriously compromised this idyllic image of steel as a perfect material for seismic areas. In some cases the performance of steel joints and members was very bad and large damage was produced, showing that the present design concepts are not sufficient in special conditions.

Aiming at making up for this lack, modern codes for building in seismic areas allow to design high-ductility structures and to provide designers with some constructional rules considering whose fulfilment is suppose to assure a good ductility. But the above mentioned bad behaviour of steel structures has shown that this conception is not proper and the verification of structure ductility must be quantified at the same level as the strength and stiffness.

In fact, in the conventional practice for non-seismic loads, structures are designed only according to demands of strength and rigidity, which correspond to a good structural performance. The strength checking, including stability, is related to the ultimate limit state, assuring that the force level developed in the structure remain

2. DUCTILITY AND SEISMIC RESPONSE OF STRUCTURES

in the elastic range, or some limited plastic deformations can occur in agreement with the design assumptions. The rigidity check is generally related to the serviceability limit state, for which the structure displacements must remain within certain limits, which assure that no damage occurs in non-structural elements. Although it is recognized that damage is also due to deformations, strength checking plays the leading role in designs for conventional loads. Conversely, in case of earthquake design, a new demand must be added to the two previous ones, that is the ductility demand. The performance of a structure under strong seismic actions relies on its capacity to deform beyond the elastic range, and to dissipate seismic energy through plastic deformations. So, the ductility check controls whether the structure is able to dissipate the given quantity of seismic energy considered in structural analysis or not (Gioncu and Mazzolani, 2002).

2.2 Ductility in seismic design

2.2.1 *First developments of ductility concept*

The preliminary design concepts were conceived after the severe earthquakes at the beginning of the 20th century. The great builder Gustave Eiffel had the intuition to model the earthquake forces by means of an equivalent wind load. The city of San Francisco was rebuilt after the 1906 great earthquake using a 1.4 kPa equivalent wind load. It was not until after the Santa Barbara earthquake in 1925 and the Long Beach earthquake in 1933, that the concept of lateral forces proportional to the mass was introduced into practice. The buildings have been designed to withstand lateral forces of about 7.5 percent for rigid soil and 10 percent for soft soil of their dead load. This rule was a consequence of the observation that the great majority of well designed and constructed buildings survived strong ground motions, even if they were designed only for a fraction of the forces that would develop if the structure behaved entirely linearly elastic (Fajfar, 1995). In 1943, the Los Angeles city code recognized the influence of flexibility of structures, and considered the number of structure levels in design forces. The San Francisco recommendations were the first ones where the influence of the fundamental period of the structure was introduced with a relation stating that the seismic forces are inversely proportional to this period (Bertero, 1992, Popov 1994).

2. DUCTILITY AND SEISMIC RESPONSE OF STRUCTURES

These preliminary concepts are based on grossly simplified physical models, engineering judgment and a number of empirical coefficients. Influenced by conventional design concepts, earthquake actions are considered as static loads and the structures as elastic systems. This simple concept has been the standard design methodology for several decades, well understood by structural engineers because relatively easy to implement. These are the reasons for the success of this design approach, even if, in some cases, it may lead to inadequate protection (Krawinkler, 1995). Because of this limits new concepts have been developed.

2.2.2 Modern design concepts of ductility

The beginning of the modern design concepts can be fixed in the 1930s, when the concepts of response spectrum and plastic deformation were introduced into earthquake engineering. The first concept considering the elastic response spectrum was used by Benioff in 1934 and Biot in 1941. Linear elastic response spectra provide a reliable tool to estimate the level of forces and deformations developed in the structures. In 1935 Tanabashi proposed an advanced theory, which suggested that the earthquake resistance capacity of a structure should be measured by the amount of energy that the structure can absorb before collapse. In term used nowadays, this energy can be interpreted as the dissipated energy through the ductility of the structure.

The first attempts to combine these two aspects, the response spectrum and the dissipation of seismic energy through plastic deformations, was made by Housner (1997), who made a quantitative evaluation of the total amount of energy input that contributes to the building response, using the velocity response spectra in the elastic system. Moreover, assuming that the energy input, responsible for the damage in the elastic-plastic system, is identical to that in the elastic system (Akiyama, 1985). Housner verified his hypothesis by examining several examples of damage. So, his method proposed a limit design type analysis to ensure that there is sufficient energy-absorbing capacity to give an adequate factor of safety against collapse in the event of extremely strong ground motion. Velestos and Newmark conducted the first study on the inelastic spectrum in 1960. They obtained the maximum response deformation for the elastic-perfectly plastic structures. Since its first application in seismic design, the response spectrum has become a standard measure of the demand of ground motion. Although it is based on a simple Single-Degree-of-Freedom (SDoF) linear system, the concept of the response spectrum has been extended to Multiple-Degree-of-Freedom (MDoF) systems, non-linear elastic systems and inelastic hysteretic systems. The utility of the response spectrum lies in the fact that it gives a simple and direct indication of

2. DUCTILITY AND SEISMIC RESPONSE OF STRUCTURES

the overall displacement and acceleration demands of earthquake ground motion for structures having different period and damping characteristics, without the need to perform detailed numerical analyses. A new concept was proposed in 1960 by Newmark and Hall, by constructing spectra based on accelerations, velocities and displacements, in short, medium and long period ranges, respectively. This concept remained a proposal until after the Northridge and Kobe earthquakes, when the importance of the velocity and displacement spectra was recognized.

More recently, another methodology based on the drift spectrum of a continuous medium in opposition to the concepts of discrete medium has been elaborated for structures situated in near-field region of an earthquake (Iwan, 1997). This concept is based on the observation that the ground motions in near-field regions are quantitatively different from that commonly used for far-field earthquake regions. For near-field earthquakes, the use of the equivalence of MDof systems with only SDof gives inaccurate results, because the effects of the higher vibration modes are ignored. Therefore, a new direction of research works for ductility of structures in near-field regions began to be explored.

Moreover, the recent technological computer advances permit static and dynamic analyses in elastic and elasto-plastic ranges and allow to obtain more refined results, using the design spectra in current design, with a more correct calibration of the design values. At the same time, a time-history methodology can be applied for important structures using a recorded accelerograms and the behaviour of the structures under seismic actions can be evaluated in a more precise way, according to the spectrum methodology.

Recently, this concept has been criticized because large deformations, such as those necessary for the building components to provide the required ductility, are associated to strong earthquakes with local buckling, cracking and other damage in structural and non-structural elements, with a very high cost of repair after each event. In order to minimize this damage, a new approach in seismic design has been developed, mainly based on the idea of controlling the response of the structure, by reducing the dynamic interaction between the ground motion and the structure itself. This concept is very different from the conventional one, according to which the structure is unable to behave successfully when subjected to load conditions different from the ones it has been designed for. The control of the structural response produced by earthquakes can be obtained by various means, such as modifying rigidities, masses, damping and providing passive or counteractive forces (Housner et al, 1997). This control is based on two different approaches, either the modification of the dynamic characteristic or the modification of the energy absorption capacity of the structure. In the first case, the structural period is shifted away from the predominant periods of the seismic input,

2. DUCTILITY AND SEISMIC RESPONSE OF STRUCTURES

thus avoiding the risk of resonance occurrence. In the second case, the capacity of the structure to absorb energy is enhanced through appropriate devices which reduce damage to structural elements (Mele and De Luca, 1995).

These response control systems are used to reduce floor response and interstorey drift. The reduction of floor response and of inter-storey drift may ensure seismic safety and decrease the amount of construction materials, reduce damage to non-structural elements and increase design freedom; but there are some limitations in the use of these systems:

- there are situations where more than one source are depicted in the same region and, generally, these sources have different characteristics. It is very difficult to design a control system, which has a variable response as a function of the ground motion type;
- it is not technically possible to design a control system, which assures that the structure remains elastic during a strong earthquake. An open question is the behaviour of a structure when it falls in the inelastic range. The development of plastic hinges could in fact reduce the difference in period between fixed base and isolated schemes, reducing the effectiveness of the isolators and leading to fast deterioration of the dynamic response. In some cases, a sudden increase of damage is observed at some level of acceleration;
- in case of near-field ground motion, as the energy content and velocity are very high, the required isolator displacements are very large and very often exceed available displacements of isolators. These cases result in a high impact load to the isolated portion of building (Iwan, 1995).
- when the vertical displacements are very high (as for near-field zones), the efficiency of devices for response control is disputable.

Thus, even in cases of response control, the ductility control remains a very important method for preventing any unexpected behaviour of a structure during severe earthquakes.

2.2.3 Ductility definition

Before the 1960s the ductility notion was used only for characterizing the material behaviour, after Baker's studies in plastic design and Housner's research works in earthquake problems (1997), this concept was extended to the level of structure and associated with the notions of strength and stiffness of the whole structure. But after years of use this concept continues to be an ambiguous parameter. In the practice of plastic design of structures, ductility defines the ability of a structure to undergo deformations after its initial yield without any significant reduction in

2. DUCTILITY AND SEISMIC RESPONSE OF STRUCTURES

ultimate strength. The ductility of a structure allows prediction of the ultimate capacity of a structure, which is the most important criterion for designing structures under conventional loads. In the practice of earthquake resistant design the term ductility is used for evaluating the seismic performance of structures, by indicating the quantity of seismic energy, which may be dissipated through plastic deformations. The use of this concept of ductility gives the possibility to reduce seismic design forces and allows the production of some controlled damage in the structure, also in case of strong earthquakes. The following ductility types are widely used in literature (see Figure 2.1):

- material ductility, or axial ductility, which characterizes the material plastic deformations;
- cross-section ductility, or curvature ductility, which refers to the plastic deformations of cross-section, considering the interaction between the parts composing the cross-section itself;
- member ductility, or rotation ductility, when the properties of member are considered;
- structure ductility, or displacement ductility, which considers the behaviour of the whole structure.

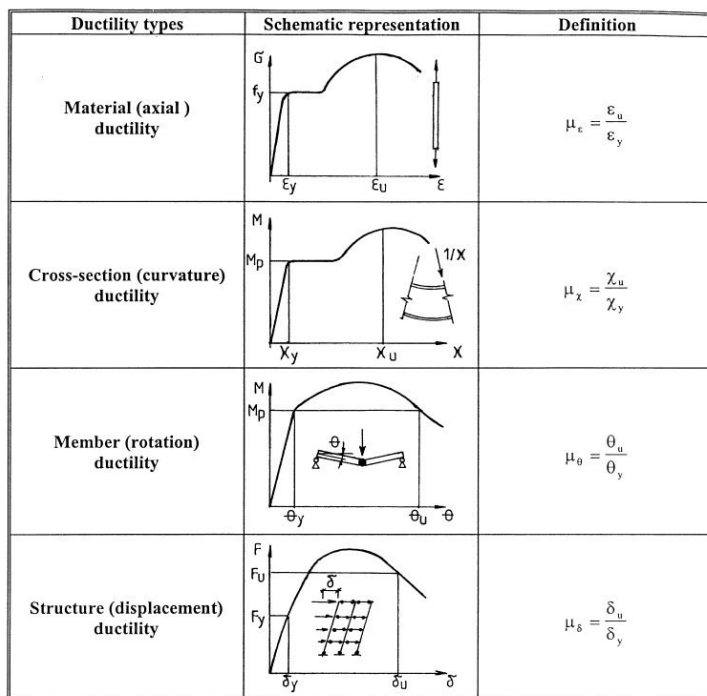


Figure 2.1. Ductility types

2. DUCTILITY AND SEISMIC RESPONSE OF STRUCTURES

A very important value in seismic design is the ductility limit. This limit is not necessarily the largest possible energy dissipation, but a significant changing of structural behaviour must be expected at ductilities larger than this limit. Two ductility limit types can be defined:

- available ductility, resulting from the behaviour of structures and taking into account its information, material properties, cross-section type, gravitational loads, degradation in stiffness and strength due to plastic excursions, etc;
- required ductility, resulting from earthquake actions, in which all factors influencing these actions are considered: magnitude, ground motion type, soil influence, natural period of the structure versus ground motion period, number of important cycles, etc.

Ductility of a structure is provided by satisfying the limit state criterion:

$$\frac{D_a}{\gamma_m} \geq \gamma_F D_r \quad (2.1)$$

where D_a is the available ductility determined from the local plastic deformation and D_r is the required ductility obtained from the global plastic behaviour of a structure. The partial safety factors γ_m for available ductility and γ_F for required ductility must be determined considering the scatter of data with a mean plus one standard variation and the uncertainties in available and required capacities. Values of $\gamma_m=1.3$ and $\gamma_F=1.2$ are proposed (Gioncu, 2000) for this check, if the ductility is obtained by deformation ductility (see Figure 2.2). If the available ductility results from fracture, a greater value for γ_F must be used (i.e. $\gamma_F=1.5$). This check must be included in a *performance based seismic design*.

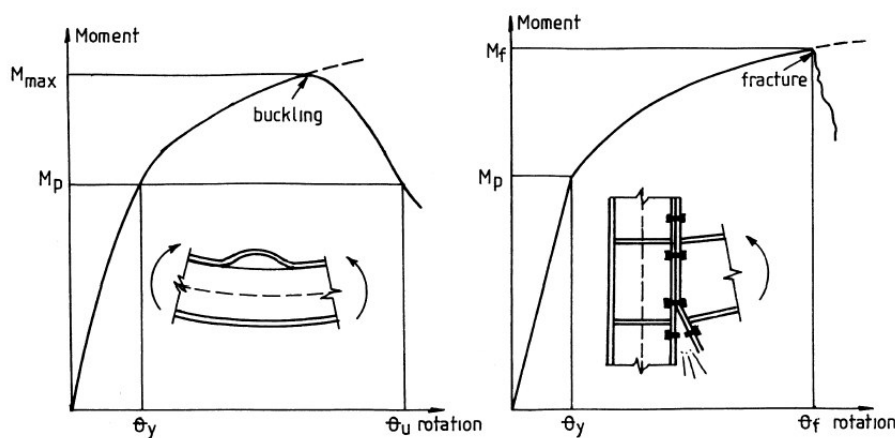


Figure 2.2. Deformation and fracture ductilities

2. DUCTILITY AND SEISMIC RESPONSE OF STRUCTURES

2.3 The performance based seismic design

During recent earthquakes, including those of California and Japan, structures in conformity with modern seismic codes performed as expected; and, as expected, the loss of lives was minimal. However, the economic loss due to sustained damage was substantial. Earthquakes in urban areas have demonstrated that the economic impact of physical damage, loss of function and business interruption was huge and damage control must become a more explicit design consideration. A promising approach to such needed development is the performance-based engineering (PBE); its application to significant seismic hazards is commonly known as performance-based seismic engineering (PBSE). An important phase of performance-based seismic engineering is the performance-based seismic design (PBSD), that is defined as "identification of seismic hazards, selection of the performance levels and performance design objectives, determination of site suitability, conceptual design, numerical preliminary design, final design, acceptability checks during design, design review, specification of quality assurance during the construction and of monitoring of the maintenance and occupancy (function) during the life of the building." (Bertero and Bertero, 2002). Therefore, a comprehensive performance based design involves several steps:

- selection of the performance objectives;
- definition of multi-level design criteria;
- specification of ground motion levels, corresponding to the different design criteria;
- consideration of a conceptual overall seismic design;
- options for a suitable structural analysis method;
- carrying out comprehensive numerical checking.

2.3.1 *Performance objectives (POs)*

A conceptual framework for the performance base seismic design has been developed encompassing the full range of seismic engineering issues to be referred to design of structures for predictable and controlled seismic performance within established levels of risk. The first step is the selection of the performance design objectives (POs). These objectives are selected and expressed in terms of expected levels of damage resulting from expected levels of earthquake ground motions (SEAOC, 1995). POs will range from code minimum requirements (usually based on fully operational under minor earthquake ground motions and on life

2. DUCTILITY AND SEISMIC RESPONSE OF STRUCTURES

safety under a rare earthquake ground motion) to fully operational in a maximum credible (capable or considered) earthquake ground motion.

A PO is a coupling of expected performance levels with levels of seismic ground motions. A performance level represents a distinct band in the spectrum of damage to the structural and non-structural components and contents, and also considers the consequences of the damage to the occupants and functions of the facility. Four discrete performance levels are identified in Figure 2.3, which gives a table that define them in terms of the various components of the building. The seismic hazard at a given site is represented as a set of earthquake ground motions and associated hazards with specified probabilities of occurrence. For instance, the term 'rare earthquake' refers to a set of potential earthquake ground motions that can produce a defined level of damage with a specific mean annual frequency (e.g. 475 years return period for standard buildings). The set of earthquake ground motions will vary not only for different seismic regions but also from site to site within a region because of variations in site conditions (topography and soil profile). Note that the return period, T_R , and the exceeding probability in N years, p_N , are two different ways of expressing the same concept and they are related by:

$$p_1 = \frac{1}{T_R}, \quad p_N = 1 - (1 - p_1)^N \quad (2.2)$$

where p_1 is the annual probability of exceedance. The validity of these equations assumes that earthquake occurrences are independent events. This is not strictly correct, but the above relations are widely used to simplify the discussion of probability.

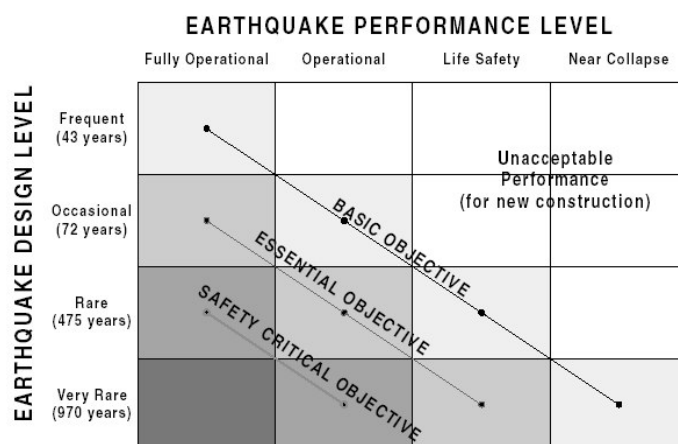


Figure 2.3. Recommended minimum seismic performance design objectives for buildings after Bertero and Bertero (2002)

2. DUCTILITY AND SEISMIC RESPONSE OF STRUCTURES

Performance objectives (POs) typically include multiple goals for the performance of the constructed building: for example that it will be fully operational in the 43-year-event, that it offers life safety in the 475-year-event, and it will not collapse in the 970-year-event. The selection of POs sets the acceptability criteria for the design. Design criteria are rules and guidelines, which must be met to ensure that the usual three major objectives of design, i.e. performance of function, safety, economy, are satisfied. The performance levels are keyed to limiting values of measurable structural response parameters, such as drift and ductility (monotonic and cumulative), structural damage indexes, storey drift indexes, and rate of deformations such as floor velocity, acceleration and even the jerk (in case of frequent minor earthquake ground motions). When the performance levels are selected, the associated limiting values become the acceptability criteria to be verified in later stages of the design. Note that once the limit value of the parameter has been selected for a particular earthquake hazard level, in order to completely define the design criteria it is still necessary to define the acceptable conditional probability of going beyond that limit state (failure probability).

2.3.2 Performance Levels

A building can be subjected to low, moderate, or severe earthquakes. It may cross these events undamaged, it can undergo slight, moderate or heavy damage, it may be partially destroyed or it can collapse. These levels of damage depend on the earthquake intensities. Low intensity earthquakes occur frequently, moderate earthquakes more rarely, while strong earthquakes may occur once or maximum twice during the life of the structure. It is also possible that no devastating earthquake will affect the structure during its life. In these conditions, the checks, required to guarantee a good behaviour of a structure during a seismic attack, must be examined in the light of a multi-level design approach. The structure design procedure on the basis of multi-level criteria is not a new concept. Under gravity, live, snow, wind loads, the limit state design considers the service and ultimate levels. In the case of seismic loading, the declared intent of building codes is to produce buildings capable of achieving the following performance objectives (Fajfar, 1998):

- to resist minor earthquakes without significant damage;
- to resist moderate earthquakes with repairable damage;
- to resist major earthquakes without collapse.

However, as a rule, the majority of codes consider explicitly only one performance objective, defined as protection, in cases of rare major earthquakes, of occupants

2. DUCTILITY AND SEISMIC RESPONSE OF STRUCTURES

against injury or death. Criteria for structure checking to minor or moderate earthquakes that may occur relatively frequently in the life of the building are not specified explicitly. A review of 41 codes elaborated all over the world shows that 38 are based on just one level, the principal design being concentrated on strength requirements (Bertero, 1997). So, the first step in the performance basic design philosophy is to define an acceptable level of damage due to an earthquake, and this is the purpose of the design code.

Performance-based seismic engineering, elaborated by the Vision 2000 Committee of SEAOC (1995) and ATC (1995), consists of a selection of appropriate systems, layout and detailing of a structure, and of non-structural components and contents so that, at specified levels of ground motion and defined levels of reliability, the structure will not be damaged, beyond certain limit states. The performance levels have been defined for four levels as a combination of damage to structure and to non-structural elements, building facilities and required repairs.

1. *Near collapse level*: collapse prevention is directly related to the prevention of casualties and of damage to the contents of buildings. The structure can undergo serious damage during the major earthquakes, but it must be standing after the ground motion.
2. *Life safe level*: the casualties in a building are usually caused by the collapse of the building components during an earthquake. The evaluation of the number of casualties as an economic damage in an optimisation process, as suggested in some studies, poses very difficult ethical problems.
3. *Operational level*: a distinction is made between structural damage which cannot be repaired and damage which can be repaired. Irreparable damage is a specific subject for individual engineering judgement of experts. The damage refers both to structure and to non-structural elements.
4. *Fully operational level*: in some cases the value of the business is more important than the value of the buildings themselves and the interruption of this activity is intolerable. If the owner of a building wishes to avoid the cost of interruptions, it is necessary to fulfil more than the minimum requirement of design codes. By using stronger and stiffer designs, it is possible to reduce or even eliminate, the interruption of the building function after a strong earthquake, but this results in a more expensive structure.

These limit states are presented in Figure 2.4, as a function both of the structure and of non-structural elements. In the seismic load-top sway displacement curve,

2. DUCTILITY AND SEISMIC RESPONSE OF STRUCTURES

there are three very significant points: the limit of elastic behaviour without any damage, the limit of damage with major damage and, finally, the limit of collapse, for which the structure is at the threshold of breakdown. By taking different limit states for the structure and for non-structural elements, some multi-level approaches are possible.

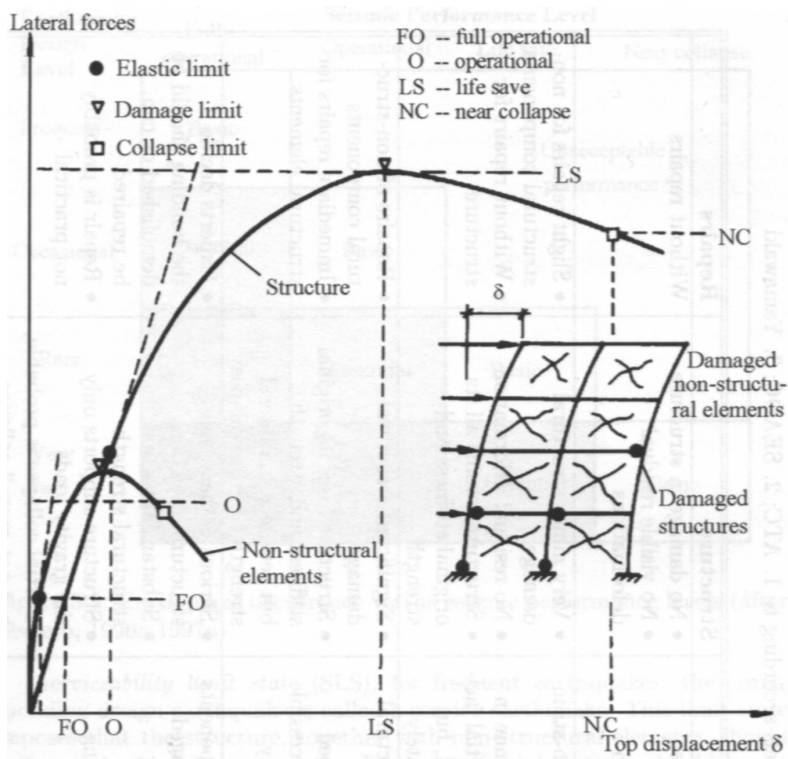


Figure 2.4. Performance levels

A verification at three performance levels has been proposed by different researchers (Gioncu and Mazzolani, 2002):

1. *Serviceability limit state (SLS)* for frequent earthquakes; the corresponding design earthquake is called a service earthquake. This limit state imposes that the structure, together with non-structural elements, should suffer minimum damage and the discomfort for inhabitants should be reduced to a minimum. Therefore, the structure must remain within the elastic range or it can suffer unimportant plastic deformations;
2. *Damageability limit state (DLS)* for occasional earthquakes: this limit state considers an earthquake intensity which produces damage in non-structural elements and moderate damage in a structure, which can be repaired without great technical difficulties;

2. DUCTILITY AND SEISMIC RESPONSE OF STRUCTURES

3. *Survivability-ultimate limit state (ULS)* for earthquakes which may rarely occur represents the strongest possible ground shaking. For these earthquakes, both structural and non-structural damage are expected, but the safety of inhabitants has to be guaranteed. In many cases damage is so substantial that structures are not repaired and demolition is the recommended solution.

Although it is recognized that the ideal methodology would use four or three levels for design, today current European Code methodologies and seismic design philosophy can be based on just two levels (Eurocode 8, 2002):

1. *Serviceability limit state*, for which structures are designed to remain elastic, or with minor plastic deformations and the non-structural elements remain undamaged or have minor damage;
2. *Ultimate limit state*, for which structures exploit their capability to deform beyond the elastic range, the non-structural elements being partially or totally damaged.

In the Eurocode 8, the accelerations corresponding to the serviceability limit state are given as a fraction of the corresponding ones for the ultimate limit state. Generally, this methodology cannot assure controlled damage, also because the determination of this relationship is not clearly assigned in the code.

When the number of performance levels is discussed, one must recognize that the use of four levels is the most rational proposal and that two levels represent the minimum acceptable option. Since it is questionable to ask design engineers to perform too much verification, it seems more rational to introduce no more than three levels of verifications: serviceability, damageability and ultimate (survivability) levels. To achieve these levels of verifications, the seismic design problem is laid out through required-available formulation. Currently, the required-available pairs of three mechanical characteristics considered in seismic design are:

$$\text{Required rigidity} < \text{Available rigidity} \quad (2.3)$$

$$\text{Required strength} < \text{Available strength} \quad (2.4)$$

$$\text{Required ductility} < \text{Available ductility} \quad (2.5)$$

The rigidity verification is a problem of the serviceability level, the strength verification is related to the damageability level and ductility verification is a

2. DUCTILITY AND SEISMIC RESPONSE OF STRUCTURES

problem of survivability. Other verifications at each level are only optional or not necessary, as a function of building importance or earthquake intensities. The relationship between performance levels and the other parameters of structure-seismic design are:

- for serviceability level, under frequent low earthquakes, the strategy calls for the elastic response of a structure. The lateral deformations are limited for the interstorey drift limits, given for the non-structural elements. Due to their integrity, interaction structure-non-structural elements must be considered. The basic verification refers to the structure rigidity and the strength verification (condition to elastic behaviour) is only optional;
- for damageability level, under occasional moderate earthquakes, an elasto-plastic analysis must be performed. The basic verification refers to the structure member strengths, verifications for rigidity or ductility being optional. The non-structural elements are partially damaged, so the analysis must consider only the structure behaviour, without any interaction with non-structural elements;
- for ultimate (survivability) level, under rare severe earthquakes, a kinematic analysis, which considers the behaviour of possible formed plastic mechanisms, must be performed. The basic verification refers to the ductility, the strength verification being only optional. The design strategy refers to the control of the formation of a pre-selected plastic mechanism and the rotation capacities of plastic hinges. Non-structural elements are completely damaged.

2.4 Required ductility concept

The *required ductility* is directly influenced by ground motions (source, distance from source, site conditions) and structural systems (foundations, structure types, non-structural elements). The control of ductility demand requires, firstly, attention to be given to some important aspects:

- i. Seismic macro-zonation, which is an official zoning map to country scale, based on a hazard analysis elaborated by geologists and seismologists. This map divides the national territory into different categories and provides each area with values of earthquake intensities, on the basis of design spectra. At the same time, this macro-zonation must characterize the possible ground motion types, as a surface or deep source an

2. DUCTILITY AND SEISMIC RESPONSE OF STRUCTURES

- interplate or intraplate fault, etc. Ductility demands vary depending on each ground motion type.
- ii. Seismic micro-zonation, which considers the possible earthquake sources at the level of region or town, on the basis of common local investigation. The result of these studies is a local map indicating the position and the characteristic of the sources, general information about the soil conditions and design spectra. It is very useful to accompany the time-history accelerograms with very precise indications about the place where they have been recorded (directions, distance from epicentre, soil conditions, etc.). Recordings such as magnitude, distance from source, attenuation and duration are directly involved in ductility demand.
 - iii. Site condition, established through the examination of the stratification under the proposed structure site. This is a very important step, because dramatic changes of earthquake characteristic within a few hundred meter distance are not unusual during an earthquake. These differences are mainly caused by the difference in soil conditions. For soft soil the ductility demand is more important than for rigid soil.

Differently from the past, when the developed design methods was based on simple hypotheses because the reduced number of records during severe earthquakes, today several measurements of ground motions for different distance from the sources and on different site conditions are available thanks to a large network of instrumentation all over the world,. This situation allows to underline a new very important aspect, which was previously neglected in the current concept: the difference in ground motion between *near-field* and *far-field* earthquakes. The near-field region of an earthquake is the area, which extends for several kilometres from the projection on the ground surface of the fault rupture zone. Since in the past the majority of ground motions were recorded in the far-field region, the current concept refers to this earthquake type only. The great amount of damage during the Northridge and Kobe earthquakes is due to the fact that these towns are situated in a near-field region. Thus, ground motion recorded in far-field regions cannot be used to describe in proper manner the earthquake action in near-field regions. The differences, as presented in Figure 2.5, consist in:

- the direction of the propagation of the fault rupture has the main influence for near-field regions, the local site stratification having a minor consequence. On the contrary, for far-field regions, soil stratification for travelling waves and site conditions are of first importance;
- in near-field regions, the ground motion has a distinct low-frequency pulse in acceleration time history and a pronounced coherent pulse in velocity

2. DUCTILITY AND SEISMIC RESPONSE OF STRUCTURES

and displacement history. The duration of ground motion is very short. For far-field regions, the records in acceleration, velocity and displacement have the characteristic of a cyclic movement with a long duration;

- the velocities in near-field regions are very high. During the Northridge and Kobe earthquakes, velocities with values of 150-200 cm/sec were recorded at the soil level, while for far-field regions these velocities did not exceed 30-40 cm/sec. Therefore, in case of near-field regions the velocity is the most important parameter in design concept, replacing accelerations, which are a dominant parameter for far-field regions;
- the vertical components in near-field regions may be greater than the horizontal components, due to the direct propagation of P waves, which reach the structure without important modifications due to soil conditions, their frequencies being far from the soil frequencies.

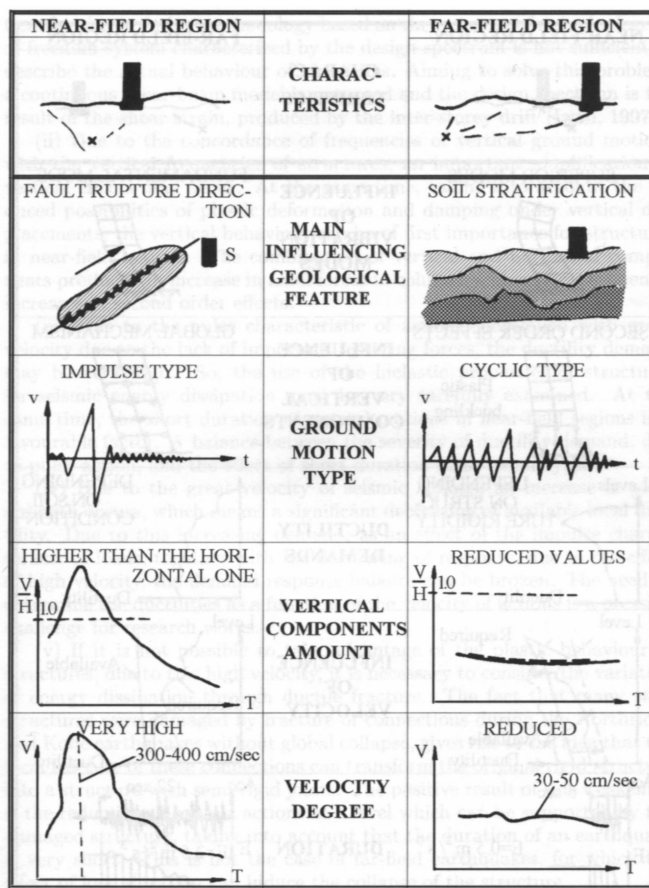


Figure 2.5. Near-field vs. far-field ground motion features after Gioncu and Mazzolani (2002)

2. DUCTILITY AND SEISMIC RESPONSE OF STRUCTURES

As a consequence of the above-mentioned differences in ground motions, there are some very important modifications in the design concepts:

- in near-field regions, due to the very short periods of ground motions and to pulse characteristic of loads, the importance of higher vibration mode increases, in comparison with the case of far-field regions, where the first fundamental mode is dominant. For structures subjected to pulse actions, the impact propagates through the structure like a wave, causing large localized deformation and/or important interstorey drifts. In this situation the classic design methodology based on the response of a single-degree of freedom system characterized by the design spectrum is not sufficient to describe the actual behaviour of structures. Aiming at solving this problem, a continuous shear-beam model is proposed and the design spectrum is the result of the shear strain, produced by the inter-storey drift. (Iwan, 1997).
- due to the concordance of the frequencies of vertical ground motions with the vertical frequencies of structures, an important amplification of vertical effects may occur. At the same time, taking into account the reduced possibilities of plastic deformation and damping under vertical displacements, the vertical behaviour can be of first importance for structures in near-field regions. The combination of vertical and horizontal components produces an increase in axial forces in columns and, as a consequence, increases in second order effects.
- due to the pulse characteristic of the actions, developed with great velocity due to the lack of important restoring forces, the ductility demand may be very high. So, the use of inelastic properties of structures for seismic energy dissipation must be very carefully examined. At the same time, the short duration of the ground motions in near-field regions is a favourable factor. A balance between the severity of ductility demand, due to pulse action, and the effect of short duration must be analyzed.
- due to the great velocity of the seismic actions, an increase in yield strength occurs, which means a significant decrease of the available ductility. The demand-response balance can be broken due to this increasing demand, as an effect of the impulse characteristic of loads, together with the decreasing of the response, owing to the effect of high velocity. The need to determine ductility as a function of the velocity of actions is a pressing challenge for research works.
- if it is impossible to take advantage of the plastic behaviour of structures, at this high velocity, it is necessary to consider the variation of energy dissipation through ductile fracture. The fact that many steel structures

2. DUCTILITY AND SEISMIC RESPONSE OF STRUCTURES

were damaged by fracture of connections during the Northridge and Kobe earthquakes without global collapse, gives rise to the idea that the local fracture of these connections can transform the original rigid structure into a structure with semi-rigid joints. The positive result of the weakening is the reduction of the seismic actions at a level, which can be supported by the damaged structure, taking into account that the duration of an earthquake is very short. This is not the case of far-field earthquakes, for which the effect of long duration can induce the collapse of the structure.

Required ductility on the other hand is associated with the global behaviour of the structure, which is a function of members of plastic hinges as well as of the amount of plastic rotation they undergo. For the plastic analysis of a moment resisting frame, the methods available to the designer are either monotonic static non-linear analyses, i.e. *pushover type*, or dynamic *time-history* analyses. Of course the last ones are more effective, but they require special computer programs, which are not available to all design offices. At the same time, time-history methods are large computation time consumer and they are very expensive. The pushover methods, if the conditions of load and local behaviour are properly designed, may provide sufficient information on the expected behaviour for design purposes.

2.4.1 Non-linear static pushover (NSP) analysis

The purpose of the pushover analysis is to evaluate the expected performance of a structural system by estimating its strength and deformation demands in design earthquakes by means of a static inelastic analysis, and comparing these demands to available capacities at the performance levels of interest (Krawinkler and Seneviratna, 1998). The evaluation is based on an assessment of important performance parameters, including global drift, interstorey drift, inelastic element deformations (either absolute or normalized with respect to the yield value), deformations between elements, and element and connection forces (for elements and connections that cannot sustain inelastic deformations). The inelastic pushover analysis can be viewed as a method for predicting seismic force and deformation demands, which takes into account in an approximate manner the redistribution of internal forces occurring when the structure is subjected to inertia forces that can no longer be resisted within the elastic range of the structural behaviour.

The pushover analysis is expected to provide information on many response characteristics that cannot be obtained from an elastic static or dynamic analysis. The following are examples of such response characteristics:

- the realistic force demands on potentially brittle elements, such as axial force demands on column, force demands on brace connections, moment

2. DUCTILITY AND SEISMIC RESPONSE OF STRUCTURES

demands on beam-to-column connections, shear force demands in deep reinforced concrete beams, shear force demands in unreinforced masonry wall piers, etc;

- estimates of the deformation demands for elements that have to deform inelastically in order to dissipate the energy imparted to the structure by ground motion;
- consequences of strength deterioration of individual elements on the behaviour of a structural system;
- identification of the critical regions in which the deformation demands are expected to be high and that have to become the focus of detailing;
- identification of strength discontinuities in plan and elevation that will lead to changes in the dynamic characteristic in the inelastic range;
- estimates of the interstorey drifts that account for strength or stiffness discontinuities and that may be used to control damage and to evaluate P-delta effects.

Clearly, this benefits come at the cost of additional analysis effort, associated with incorporation of all important elements, the modelling of their inelastic load-deformation characteristic, and the execution of incremental inelastic analysis, preferably with a three-dimensional (3D) analytical model. At this time adequate analytical tools for this purpose are either cumbersome or not available, but several good tools are under development, primarily through the recent publication of the FEMA 273 document (1997), that includes extensive recommendations for load-deformation modelling of individual elements and for acceptable values of force and deformation parameters for performance evaluation. Based on the capacity spectrum method originally developed by Freeman et al. (1975) and Freeman (1978), the NSP procedure could be summarized in the following steps (Chopra and Goel, 1999):

1. Develop the relationship between base shear V_b and roof (N^{th} floor) displacement u_N , depicted in Figure 2.6, commonly known as pushover curve.

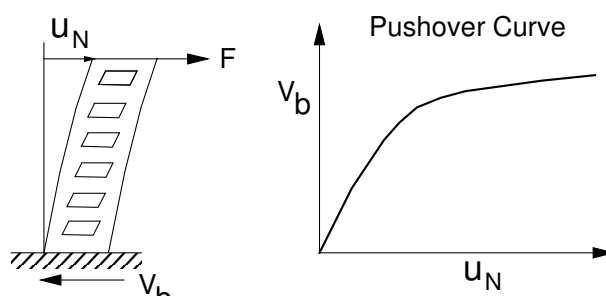


Figure 2.6. Development of a pushover curve

2. DUCTILITY AND SEISMIC RESPONSE OF STRUCTURES

2. Convert the pushover curve to a capacity diagram, see Figure 2.7, where

$$\Gamma_1 = \frac{\sum_{j=1}^N m_j \phi_{j1}}{\sum_{j=1}^N m_j \phi_{j1}^2} \quad M_1^* = \frac{\left(\sum_{j=1}^N m_j \phi_{j1} \right)^2}{\sum_{j=1}^N m_j \phi_{j1}^2} \quad (2.6)$$

and m_j = lumped mass at the j^{th} floor level, ϕ_{j1} is the j^{th} -floor element of the fundamental mode ϕ_j , N is the number of floors, and M_1^* is the effective modal mass for the fundamental vibration mode.

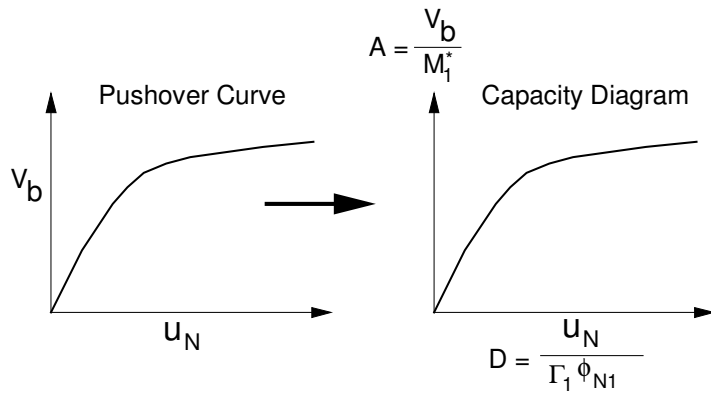


Figure 2.7. Conversion of a pushover curve to a capacity diagram

3. Convert the elastic response (or design) spectrum from the standard pseudo-acceleration A versus natural period T_N format to the $A-D$ format, where D is the deformation spectrum ordinate, defined as

$$D = \frac{T_N^2}{4\pi^2} \cdot A \quad (2.7)$$

4. Plot the demand diagram and capacity diagram together and determine the displacement demand as illustrated in Figure 2.8. Involved in this step are dynamic analyses of a sequence of equivalent linear systems with successively updated values of the natural vibration period T_{eq} and equivalent viscous damping ξ_{eq} . To define the above-mentioned quantities we have to consider an inelastic SDoF system with bi-linear force-deformation relationship on initial loading. The stiffness of the elastic branch is k and that of the yielding branch is αk .

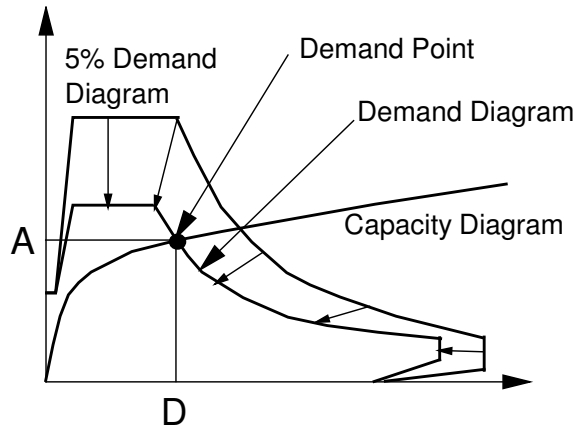


Figure 2.8. Determination of a displacement demand

The yield strength and yield displacement are denoted by f_y and u_y , respectively. If the peak (maximum absolute) deformation of the inelastic system is u_{max} , the ductility factor is defined as

$$\mu = \frac{u_{max}}{u_y} \quad (2.8)$$

For the same bi-linear system, the natural vibration period of the equivalent linear system with stiffness equal to the secant stiffness k_{sec} is

$$T_{eq} = T_N \sqrt{\frac{\mu}{1 + \alpha\mu - \alpha}} \quad (2.9)$$

where T_N is the natural vibration period of the system vibrating within its linear elastic range ($u \leq u_y$). Moreover, the most common method for defining an equivalent viscous damping is to equate the energy dissipated in a vibration cycle of the inelastic system and of an equivalent linear system. Based on this concept, it can be shown that the equivalent viscous damping ratio is (Chopra, 1995)

$$\xi_{eq} = \frac{1}{4\pi} \frac{E_D}{E_S} \quad (2.10)$$

where the energy dissipated in the inelastic system is given by the area E_D enclosed by the hysteresis loop and $E_s = k_{sec}u_m^2/2$ is the strain energy of

2. DUCTILITY AND SEISMIC RESPONSE OF STRUCTURES

the system with stiffness k_{sec} . Substituting the expressions of E_d and E_s in Eq. (2.10) on gets:

$$\xi_{eq} = \frac{2(\mu-1)(1-\alpha)}{\pi\mu(1+\alpha\mu-\alpha)} \quad (2.11)$$

The total viscous damping of the equivalent linear system is

$$\bar{\xi}_{eq} = \xi + \xi_{eq} \quad (2.12)$$

where ξ is the viscous damping ratio of the bilinear system vibrating within its linearly elastic range ($u \leq u_y$).

For elasto-perfect plastic systems, $\alpha = 0$ and both Eqs. (2.9) and (2.11) reduce to

$$T_{eq} = T_N \sqrt{\mu} \quad \bar{\xi}_{eq} = \frac{2}{\pi} \frac{\mu-1}{\mu} \quad (2.13)$$

Eqs. (2.9) and (2.11) are plotted in Figure 2.9 where the variation of T_{eq}/T_N and ξ_{eq} vs. μ is shown for four values of α . For yielding systems, viz. $\alpha > 1$, T_{eq} is longer than T_N and $\xi_{eq} > 0$. The period of the equivalent linear system increases monotonically with μ for all α . For a fixed μ , T_{eq} is longest for elasto-plastic systems and is shorter for systems with $\alpha > 0$. For $\alpha = 0$, ξ_{eq} increases monotonically with μ but not for $\alpha > 0$. For the latter case, ξ_{eq} reaches its maximum value at a μ value, which depends on α , and then decreases gradually.

5. Convert the displacement demand determined in Step 4 to global (roof) displacement and individual component deformation and compare them to the limiting values for the specified performance goals.

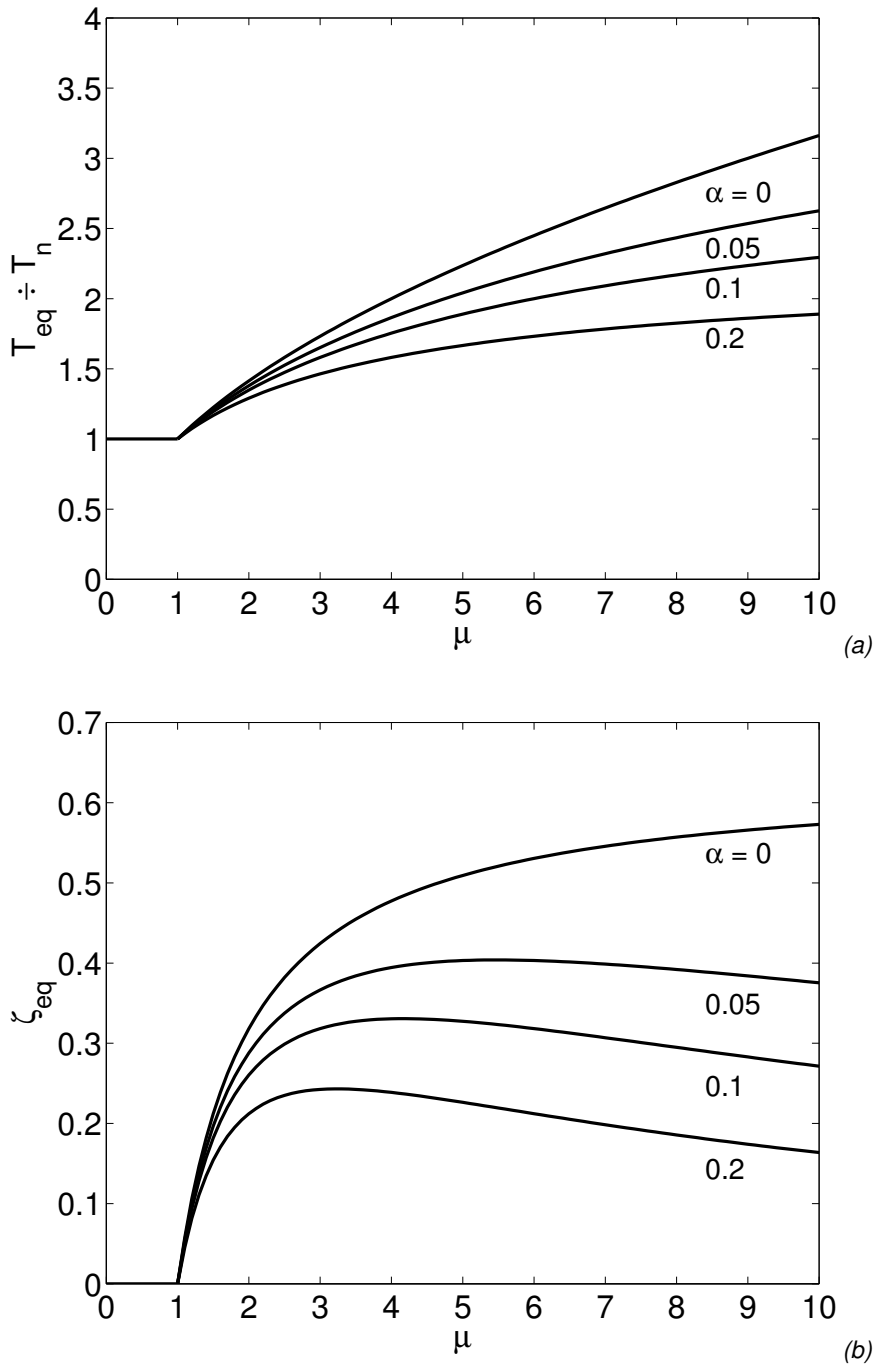


Figure 2.9. Variation of period and viscous damping of an equivalent linear system vs. ductility

2. DUCTILITY AND SEISMIC RESPONSE OF STRUCTURES

Approximations are implicit in the various steps of this simplified analysis of an inelastic MDof system. Implicit in Steps 1 and 2 is a lateral force distribution assumed to be fixed, and based only on the fundamental vibration mode of the elastic system; however, extensions to take into account higher mode effects have been proposed. Implicit in Step 4 is the belief that the earthquake-induced deformation of an inelastic SDof system can be estimated satisfactorily by an iterative method requiring analysis of a sequence of equivalent linear SDof systems, thus avoiding the dynamic analysis of the inelastic SDof system.

Both force distribution and target displacement are based on the assumption that the response is controlled by a single shape vector (the fundamental mode) and that the mode shape remains unchanged after the structure yields. Parameter studies have shown that for frame and wall structures with a first mode period of less than 2 seconds this assumption is rather accurate for elastic systems and conservative (overestimates the MDof displacement) for inelastic systems.

In all cases, the determined target displacement becomes the base line for predicting the inelastic displacement demand, which needs to be accomplished with due consideration to the hysteretic characteristic of the equivalent SDof system. The effects of yield strength, strength and stiffness degradation, pinching during hysteretic loops, P-delta incremented forces caused by gravity loads acting on the deformed configuration of the structure can be taken into account through cumulative modification factors applied to the elastic displacement demand. The loop illustrated in Figure 2.10 assumes that stable relationships can be found between the spectral displacement demand at the first mode period of the structure and the system and element deformation demands (Gupta and Krawinkler, 2000), using the following definitions:

- *MDof modification factor*, α_{MDOF} , a factor that relates the elastic spectral displacement demand at the first mode period of the structure to the elastic roof drift demand of the MDof structure, neglecting P- Δ effects.
- *Inelasticity modification factor*, α_{INEL} , a factor that relates the elastic roof drift demand to the inelastic roof drift demand, neglecting P- Δ effects.
- *P- Δ modification factor*, $\alpha_{P\Delta}$, a factor that takes into account the effect of P- Δ on the inelastic roof drift demand.
- *Storey drift modification factor*, α_{ST} , a factor that relates individual storey drift demands to the roof drift demand.
- *Element deformations modification function*, a function that relates storey drift demand to element plastic deformation demands.

2. DUCTILITY AND SEISMIC RESPONSE OF STRUCTURES

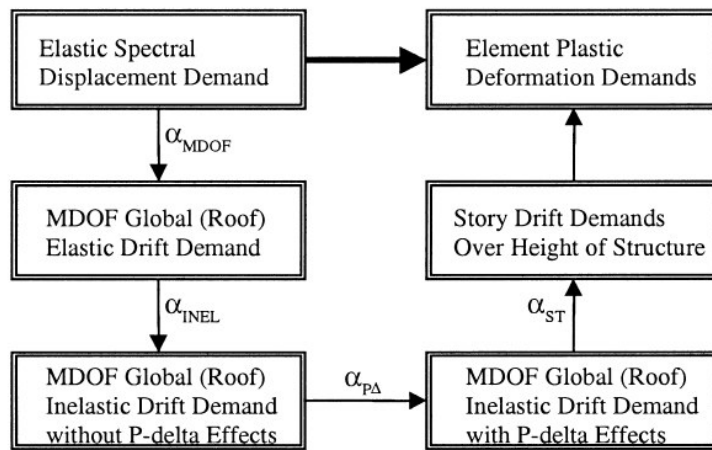


Figure 2.10. Process for simplified demand estimation Gupta and Krawinkler (2000)

However, such satisfactory predictions of seismic demands are mostly restricted to low- and medium-rise structures in which the inelastic action is distributed throughout the height of the structure (Krawinkler and Seneviratna, 1998; Gupta and Krawinkler, 2000). None of the invariant force distributions can take into account the contributions of higher modes to response, or for a redistribution of inertia forces because of structural yielding and the associated changes in the vibration properties of the structure. To overcome these limitations, several researchers have proposed adaptive force distributions that attempt to follow more closely the time-variant distributions of inertia forces [Fajfar and Fischinger, 1988; Gupta and Kunnath, 2000]. While these adaptive force distributions may provide better estimates of seismic demands, they are conceptually complicated and computationally demanding for routine application in structural engineering practice. Attempts have also been made to consider more than the fundamental vibration mode in pushover analysis.

2.4.2 Non-linear dynamic procedure (NDP)

Under the non-linear dynamic procedure (NDP), design seismic forces, their distribution over the height of the building, and the corresponding internal forces and system displacements are determined by using an inelastic dynamic analysis (IDA). The concept was mentioned as early as 1977 by Bertero, and has since been cast in several forms in the work of many researchers. Recently, it has also

2. DUCTILITY AND SEISMIC RESPONSE OF STRUCTURES

been adopted by U.S. guidelines (FEMA Reports) and European Code (EC8, 2002) as the state-of-the art method to determine the global collapse capacity. The IDA study is now a multi-purpose and widely applicable method and its objectives, only some of which are evident in Figure 2.11, include (Vamvatsikos and Cornell, 2001):

1. thorough understanding of the range of response or demands versus a range of potential levels of a ground motion record;
2. better understanding of the structural implications of rarer/more severe ground motion levels;
3. better understanding of changes in the nature of the structural response as the intensity of ground motion increases, e.g. changes in peak deformation patterns with height, onset of stiffness and strength degradation and their patterns and magnitudes;
4. producing estimates of the dynamic capacity of the global structural system;
5. finally, given a multi-record IDA study, understanding how stable or variable all these items are from one ground motion record to another.

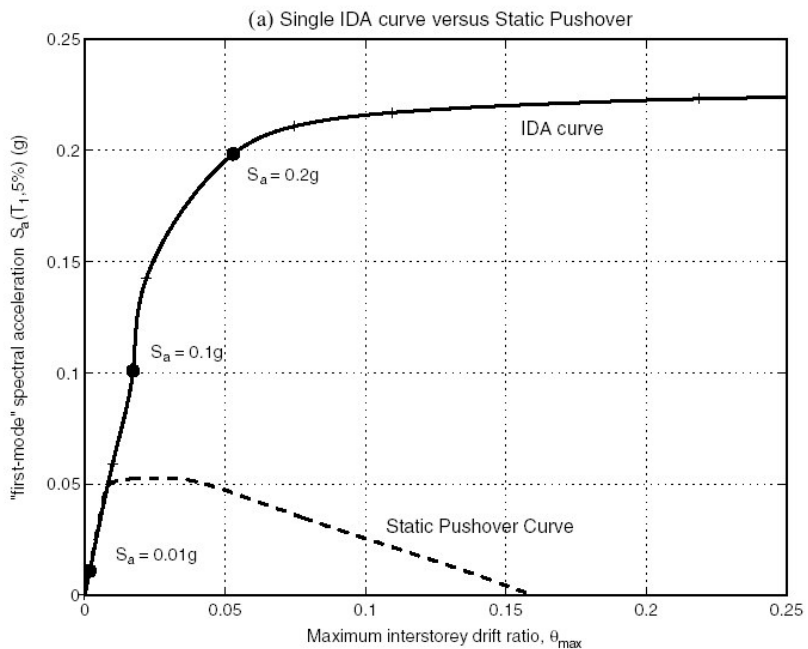


Figure 2.11. An example of information extracted from a single-record IDA study of a $T_1=4$ s, 20-storey steel moment-resisting frame with ductile members and connections, including global geometric nonlinearities ($P-\Delta$) subjected to the El Centro (1940) record after Vamvatsikos and Cornell (2001)

2. DUCTILITY AND SEISMIC RESPONSE OF STRUCTURES

The basis, modelling approaches, and acceptance criteria of the NDP are similar to those of the NSP. The main exception is that the response calculations are carried out using a *time-history* analysis. With the NDP, design displacements are not established using a target displacement, but are determined directly through dynamic analysis using ground motion histories instead. Calculated responses can be highly sensitive characteristics of individual ground motions; in fact, when subjected to different ground motions, a model will often produce quite dissimilar responses that are difficult to predict *a priori*. Therefore, it is recommended to carry out analyses with more than one ground motion record. This variability also leads to the need for statistical treatment of multi-record IDA output in order to summarize the results and in order to use them effectively in a predictive mode, as for example in a PBE context. In accordance with Eurocode 8 (2002), depending on the nature of the application and on the information actually available, the description of the seismic motion may be made by using artificial accelerograms and recorded or simulated accelerograms. Artificial accelerograms shall be generated so as to match the elastic response spectra for 5% viscous damping ($\xi = 5\%$). The duration of the accelerograms shall be consistent with the magnitude and the other relevant features of the seismic event underlying the establishment of a_g . When site-specific data are not available, the minimum duration T_s of the stationary part of the accelerograms should be equal to 10 s. Recorded accelerograms or accelerograms generated through a physical simulation of source and travel path mechanisms may be used, provided that the samples used are adequately qualified with regard to the seismogenetic features of the sources and to the soil conditions appropriate to the site, and their values are scaled to the value of a_gS for the zone under consideration. The suite of artificial and recorded or simulated accelerograms should observe the following rules:

- a. a minimum of 3 accelerograms should be used;
- b. the mean of the zero period spectral response acceleration values (calculated from the individual time histories) should not be smaller than the value of a_gS for the site in question;
- c. in the range of periods between $0,2T_1$ and $2T_1$ where T_1 is the fundamental period of the structure in the direction where the accelerogram will be applied no value of the mean 5% damping elastic spectrum, calculated from all time histories, should be less than 90% of the corresponding value of the 5% damping elastic response spectrum.

The seismic motion, represented in terms of ground acceleration time-histories and related quantities (velocity and displacement) shall consist of three simultaneously acting accelerograms. The same accelerogram may not be used simultaneously

2. DUCTILITY AND SEISMIC RESPONSE OF STRUCTURES

along both horizontal directions. Since the numerical model takes into account directly effects of the material inelastic response, the calculated internal forces will be reasonable approximations of those expected during a design earthquake.

2.5 Available ductility concept

In an effort to develop methods based on ductility it is clear that the evaluation of the inelastic response is required. For moment resisting frames (MRFs), inelastic deformations correspond to the formation of plastic hinges at localized positions (Gioncu, 200). *Available ductility* is therefore associated with the rotation capacity of plastic hinges. The design philosophy must consider that inelastic deformations occur in one or more of the three components of a node i.e. beam or column ends, connections and panel zones (Figure 2.12).

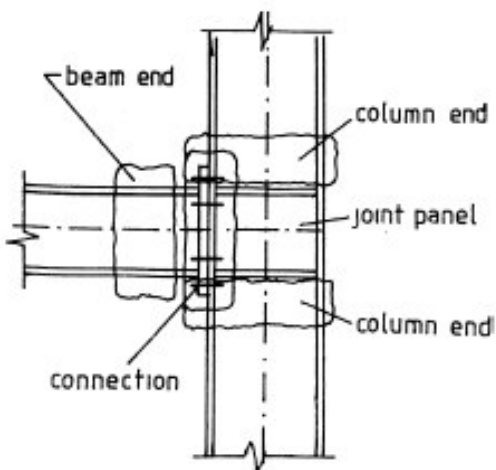


Figure 2.12. Components of a frame node

Modern codes impose that plastic deformation must occur only at beam ends and column bases, without considering *joint panels*, even if it is well-known that these show a stable behaviour under plastic shear deformations (Eurocode 8, 2002). But in reality the required conditions (the joint capacity must be 30% stronger than the adjacent members) do not assure the elastic behaviour of joints and as a consequence, the panel zone can be in some cases the weakest component of a joint. Results of the so called weak panel zone-strong column system (WP-SC),

2. DUCTILITY AND SEISMIC RESPONSE OF STRUCTURES

are that panel zones are designed to be the weakest element of the node and inelastic deformations are expected to occur in panel zones.

The ductility of *members* is another reason for dispute between the code provisions and researchers, concerning the use of ductility determined at the level of cross-section (as in Eurocode 3, 2000) or the necessity to use the ductility of members as proposed by Gioncu and Mazzolani (2002). Code provisions are particularly qualitative and therefore this procedure is inadequate for a methodology in which the available ductility is compared with the required one. The basic requirement for plastic analysis is that large rotations (theoretical infinite) be possible without significant changes in the resistant moment. But these theoretical large plastic rotations may not be achieved because some secondary effects occur. Flexural-torsional instability, local buckling or brittle fracture of members usually imposes the limitation to plastic rotation. A proper available ductility must be determined taking into account that the members and joints belong to a structure with a complex behaviour. But this is a very difficult task owing to the great number of factors influencing the behaviour of actual members and joints. The problem of evaluating the rotation capacity has recently been of primary interest, as witnessed by the numerous published papers, presenting different methods which can be classified as theoretical methods, based on the use of FEM, or integrating the moment-curvature relationship; approximate methods, based on the use of the collapse plastic mechanism; and empirical methods, based on statistical analysis of experimental tests.

Joint ductility depends on the importance of all component behaviours. For welded joints ductility is given by the plastic shear deformation, by crushing of web of joint panel or weld fracture, while for bolted joints ductility results from plastic deformations up to fracture of the column flanges, connection elements, i.e. end plates, or by fracture of bolts or welds as summarized in Figure 2.13.

Recent great seismic events have shown that the concentration of inelastic phenomena into joints leads to a brittle fracture of welds. Therefore, in the last period great efforts were devoted to the definition of adequate different detailing of joints able to provide a more satisfactory behaviour. New types of joint have been proposed, based on the idea of moving the plastic hinge away from the column-beam interface, in the field where the welding or bolts do not govern the node behaviour. This solution can be obtained by weakening the specific beam near to the connection by trimming the beam flanges, i.e. the *dog-bone solution* proposed by Plumier (1994) or by strengthening the specific beam near to the connection by adding vertical ribs or cover plates. The weakening of the beam offers the possibility of reducing the dimensions of columns, while strengthening requires an increase of these dimensions, showing the superiority of the dog-bone solution.

2. DUCTILITY AND SEISMIC RESPONSE OF STRUCTURES

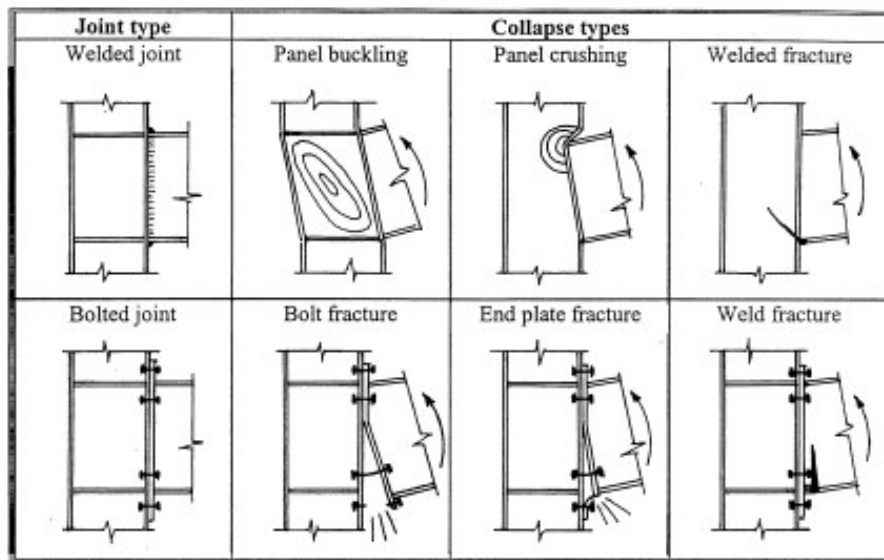


Figure 2.13. Joint collapse type after Gioncu and Mazzolani (2002)

Due to the relevant number of influencing parameters, a macroscopic view of the joint obtained by subdividing it into individual basic components has proved to be most appropriate. This approach, which allows to determine the local strength and rotation capacity, is known as the *component method* (Eurocode 3, 2001). The assumption considered in this method allows us to determine the overall rotation as the sum of the all components and the node ductility by the ductility of the weaker component (see Figure 2.14).

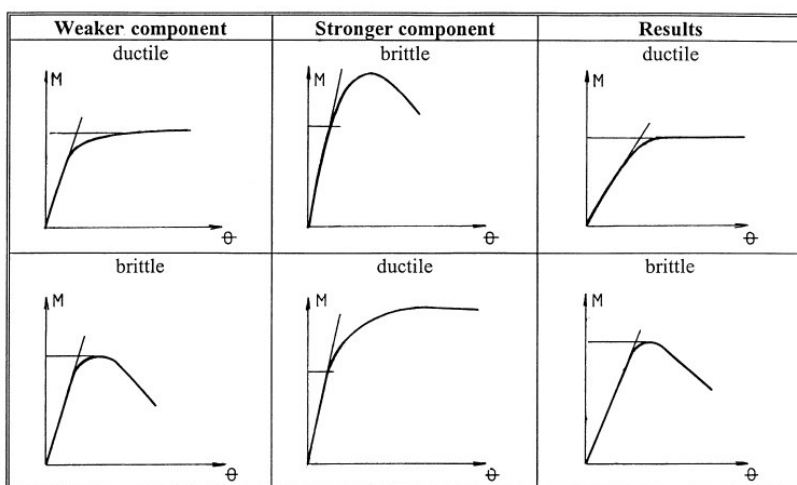


Figure 2.14. The component methodology

2. DUCTILITY AND SEISMIC RESPONSE OF STRUCTURES

2.6 References

- Akiyama H. (1985): *Earthquake-resistant limit-state design for buildings*. University of Tokio Press.
- ATC – Applied Technology Council (1995): *Guidelines and commentary for seismic rehabilitation of buildings*. ATC Report 33.03, Redwood City, California.
- Bertero R.D. and Bertero V.V. (2002): *Performance-based seismic engineering: the need for a reliable conceptual comprehensive approach*. Earthquake Engineering And Structural Dynamics, Vol. 31, 627–652.
- Bertero V.V. (1992): *Major issues and future directions in earthquake resistant design*. In 10th World Conference on Earthquake Engineering, Madrid, 19-24 July 1992, Balkema, Rotterdam, 6407-6444.
- Bertero V.V. (1997): *Performance-based seismic engineering: a critical review of proposed guidelines*. In Seismic Design Methodologies for the Next Generation of Codes, (Eds. P. Fajfar, H. Krawinkler), Bled, 24-27 June 1997, Balkema, Rotterdam, 1-31.
- Chopra A. K. (1995): *Dynamics of structures: theory and applications to earthquake engineering*. Chapters 3, Prentice Hall, New Jersey.
- Chopra A.K. and Goel R.K. (1999): *Capacity-demand-diagram methods for estimating seismic deformation of inelastic structures: SDof systems*. Report No. PEER-1999/02 Pacific Earthquake Engineering Research Center, College of Engineering, University of California, Berkeley.
- Fajfar P. (1995): *Design spectra for new generation codes: Eurocode 8 achieves the half-way mark*. In 10th European Conference on Earthquake Engineering (Ed. G. Duma), Vienna, 28 August – 2 September 1994, Balkema, Rotterdam, Vol. 4, 2969-2974.
- Fajfar P. (1998): *Trends in seismic design and performance evaluation approaches*. In 11th European Conference on Earthquake Engineering, Paris, 6 – 11 September 1998, Balkema, Rotterdam, Invited Lectures, 237-249.
- Fajfar P. and Fischinger M. (1988): *N2- A method for non-linear seismic analysis of regular structures*. In 9th World Conference on Earthquake Engineering, Tokio-Kyoto, Japan, Vol. 5, 111-116.
- FEMA 273 (1997): *HEHRS Guidelines for the seismic rehabilitation of buildings*. Federal Emergency Management Agency.
- Freeman S. A., Nicoletti J. P., and Tyrell J. V. (1975): *Evaluations of existing buildings for seismic risk - A case study of Puget Sound Naval Shipyard*. Bremerton, Washington. Proceedings of 1st U.S. National Conference on Earthquake Engineering, EERI, Berkeley, 113-122.

2. DUCTILITY AND SEISMIC RESPONSE OF STRUCTURES

- Freeman S. A. (1978): *Prediction of response of concrete buildings to severe earthquake motion.* Publication SP-55, American Concrete Institute, Detroit, MI, 1978, 589-605.
- Gioncu V. (2000): *Framed structures. Ductility and seismic response.* General Report. Journal of Constructional Steel Research, Vol. 55, 125–154.
- Gioncu V. and Mazzolani F.M. (2002): *Ductility of seismic resistant steel Structures.* Spon Press, London, 1-40.
- Gupta A., Krawinkler H. (2000): *Estimation of seismic drift demands for frame structures.* Earthquake Engineering and Structural Dynamics, Vol. 29, 1287-1305.
- Housner G.M. et al (1997): *Structural control: past, present and future.* Journal of Engineering Mechanics, Vol. 123, No. 9, 897-971.
- Iwan W.D. (1995): *Near-field considerations in specification of seismic design motion of structures.* In 10th European Conference on Earthquake Engineering (Ed. G. Duma), Vienna, 28 August – 2 September 1994, Balkema, Rotterdam, Vol. 1, 257-267.
- Iwan W.D. (1997): *Drift spectrum: measures of demand for earthquake ground motions.* Journal of Structural Engineering, Vol. 123, No. 4, 397-404.
- Krawinkler H. (1995): *New trends in seismic design methodology.* In 10th European Conference on Earthquake Engineering (Ed. G. Duma), Vienna, 28 August – 2 September 1994, Balkema, Rotterdam, Vol. 1, 821-830.
- Krawinkler H. and Seneviratna G.D.P.K. (1998): *Pros and cons of a pushover analysis of seismic performance evaluation.* Journal of Engineering Structures, Vol. 20, No. 4-6, 452-464.
- Newmark N.M. and Hall W.J. (1969): *Seismic design criteria for nuclear reactor facilities.* Proc. 4th World Conference on Earthquake Engineering, Santiago, Chile, 2 (B-4), 37-50.
- Mele E. and De Luca A. (1995): *State of the art report on base isolation and energy dissipation.* In Behaviour of Steel Structures in Seismic Areas, Stessa 94, (Eds. F.M. Mazzolani and V. Gioncu), Timisoara, 26 June – 1 July 1994, E&FN Spon , London, 631-658.
- prEN 1993-1 (2001): *Eurocode 3: Design of steel structures. Part 1: General rules for buildings.* CEN, European Committee for Standardization.
- PrEN 1998-1 (2002): *EC8 Final Draft. Design of Structures for earthquake resistance.* CEN, European Committee for Standardization, Draft No. 5.
- Plumier A. (1994): *Behaviour of connections.* Journal of Constructional Steel Research, Vol. 38, 95–123.
- Popov E.P. (1992): *Development of U.S. codes.* Journal of Constructional Research, Vol. 29, 191-207.

2. DUCTILITY AND SEISMIC RESPONSE OF STRUCTURES

- SEAOC Vision 2000 Committee (1995: *Performance-based seismic engineering*). Report prepared by Structural Engineers Association of California, Sacramento, CA.
- Vamvatsikos D. and Cornell C.A. (2001): *Incremental dynamic analysis*. Earthquake Engineering And Structural Dynamics, Vol. 31, 491–514.
- Velestos A. and Newmark N.M. (1960): *Effect of inelastic behaviour on response of simple system to earthquake motions*. Proc. 2th World Conference on Earthquake Engineering, Tokio, Japan, 855-912.

3 SEISMIC BEHAVIOUR OF BOLTED END PLATE BEAM-TO-COLUMN STEEL JOINTS

3.1 Introduction

In high seismic risk areas such as California and Japan, steel-framed buildings have frequently been employed because of their excellent performances in terms of strength and ductility. Nevertheless, a large number of entirely unexpected severe brittle cracks of welded beam-to-column connections were found in the recent Northridge (1994) and Kobe (1995) earthquakes (Bertero et al., 1994, Kuwamura, 1998). The failures raised many questions regarding the validity of design and construction procedures used for these connections at the time. Since the earthquake, several extensive analytical and experimental studies have been conducted to investigate the various aspects believed to be associated with the failure observed in the pre-Northridge connection and to improve connection performance. The majority of the thorough investigations established that premature cracking in welded steel connections resulted from a combination of factors, such as high strain demands coupled with large inherent flaws and stress risers, overreliance on low-toughness materials, deficient field welding and insufficient quality control.

As a result of poor performance of flange-welded moment connections, end plate moment connections may represent, especially in Europe, an alternative to welding in seismic regions. But because of limited cyclic testing of moment end plate connections, extensive research has been initiated. In the framework of a research programme conducted by the Department of Mechanical and Structural Engineering of the University of Trento and sponsored by a MIUR-PRIN project devoted to the analysis of semi-rigid beam-to-column connections, the presented study has a two-fold purpose:

3. SEISMIC BEHAVIOUR OF BOLTED END PLATE BEAM-TO-COLUMN STEEL JOINTS

- analysing the seismic performance of partial strength bolted extended end plate joints with fillet welds, which represent an alternative to fully welded connections for use in seismic force resisting moment frames;
- verifying in a low-cycle fatigue regime the feasibility of the mechanical approach adopted for joints undergoing monotonic loading, whereby the properties of a complete joint are understood and obtained by assembling the properties of its component parts.

The study was limited to one basic connection geometry representative of a typical European design, viz. bolted extended end plate connections with overmatching fillet welds, as depicted in Figure 3.1. However, different design parameters, among which the end plate thickness and the bolt diameter, were addressed. A series of tests on connection substructures and subassemblages subjected both to monotonic and cyclic displacement regime was carried out. These results allow *the component method* to be appraised. Also mechanical and metallurgic characterization test data of the connection material are collected.

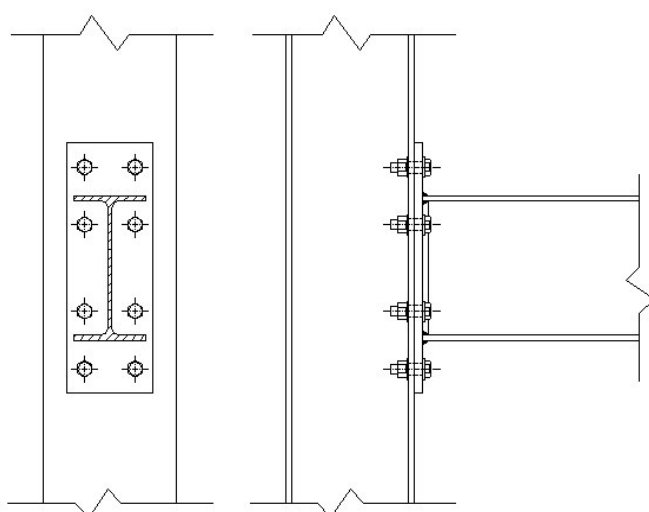


Figure 3.1. Bolted extended end plate beam-to-column joint

On the basis of the experimental results and the data collection, inelastic finite element (FE) analyses carried out by means of the ABAQUS code (Hibbit, Karlsson & Sorensen Inc., 2001), both on isolated Tee Stub (ITS) connections and on Complete Joints (CJ) have been performed. Therefore, both FE models were calibrated and the stress and strain state of the aforementioned connections was simulated both in the monotonic and in the cyclic displacement regime. Finally, some design parameters which influence the fracture resistance of steel bolted

3. SEISMIC BEHAVIOUR OF BOLTED END PLATE BEAM-TO-COLUMN STEEL JOINTS

extended plate connections have been analysed. In detail, the effects of the weld-to-base metal yield strength ratio, the end plate yield-to-ultimate strength ratio and the residual stress influence have been determined through detailed two- and three-dimensional non-linear finite element analyses. Such analyses conducted in the monotonic regime permitted fracture toughness demands in terms of performance indices to be evaluated. In addition, the analyses provided insights to develop a better intuitive understanding of fracture in the aforementioned connections.

3.2 The component method

Design of MR frame with semi-rigid partial strength joints is one of the major developments in the structural design of steel and composite steel-concrete buildings.

The importance of joint action has been perceived since the beginning of the last century. However, only in the 80's the tools available to the practitioners, and in particular the structural analysis programs, made the new methodology ready for practical use. Since then a number of research studies were carried on worldwide, aimed at building up the necessary knowledge to develop design tools ranging from general criteria to specific methods and rules for joints and frames (Bjorhovde et al, 1988; Narayanan, 1988; Bjorhovde et al, 1992; Colson, 1992; Lorenz et al, 1993; Wald, 1994; Bjorhovde et al, 1996; Maquoi, 1999; Easterling and Leon, 2002).

All the key facets of the problem were investigated via experimental, numerical and theoretical analysis, including the behaviour of a wide range of joint types, the design models to approximate joint response and the influence of joint action on frames performance. Design criteria as well as specific recommendations were set up and included in Codes (Eurocode 3, 2001) and design aids were developed in order to make the new philosophy accepted in practice.

Following the recommendation included in Eurocode 3 (2001), it is possible to classify the joint by stiffness or by strength. Depending on the stiffness, a joint can be classified as rigid, nominally pinned or semi-rigid on the basis of particular or general experimental evidence or significant experience of previous satisfactory performance in similar cases or by calculations based on test evidence. A rigid joint shall be so designed that its deformations have no significant influence on the distribution of the internal forces and moments in the structure or on its overall

3. SEISMIC BEHAVIOUR OF BOLTED END PLATE BEAM-TO-COLUMN STEEL JOINTS

deformation. A nominally pinned joint shall be designed so that it cannot develop significant moments, which might adversely affect members of the structure, and should be able to transmit the forces calculated in the design and accept the resulting rotations. A joint that does not meet the criteria for a rigid joint or a nominally pinned joint shall be classified as a semi-rigid joint.

Depending on the strength, a joint can be classified as full-strength, nominally pinned or partial strength by comparing its moment resistance with the moment resistances of the connected members. The design resistance of a full-strength joint shall not be inferior to the members connected. A full-strength joint should be so rigid that, under the design loads, the rotations at the necessary plastic hinges do not exceed their rotation capacities. A nominally pinned joint shall be capable of transmitting the calculated design forces, without developing significant moments, which might adversely affect members of the structure. The rotation capacity of a nominally pinned joint should be sufficient to enable all the necessary plastic hinges to develop under design loads. The design resistance of a partial-strength joint shall be not be less than that necessary to transmit the calculated design forces and moments, but may be less than that of connected members. The rotation capacity of a partial-strength joint, which occurs at a plastic hinge location, shall not be inferior to the capacity needed to enable all the necessary plastic hinges to develop under the design loads.

A vital requisite of any design approach incorporating joint response as a key parameter, is the capability of enabling adequate approximation of the whole beam-to-column joint response in terms of stiffness, strength and rotation capacity. As regard to this aspect, many of the traditional methods were developed with the sole purpose of determining the connection resistance capacity. Furthermore, the complexity of the stress state in the nodal zone makes the range of application of most methods rather limited (Nethercot & Zandonini, 1988). An attempt to overcome these difficulties, and to provide a general and comprehensive tool is given by the so-called *component model*, which identifies the various elemental joint components, and builds up the overall response of the joint on the individual response of these components (Eurocode 3, 2001). The advantages of this approach, schematically shown in Figure 3.2, are multi-faceted: (i) the attention of research and design is focussed on the elemental components, whose behaviour is easier to be determined (either experimentally or numerically) and modelled; (ii) the range of applicability is potentially unlimited, and actually bounded only by the range of geometrical and/or mechanical data, on which the component model is based; (iii) the response of the joint can be controlled in design through the control of the critical component(s), i.e., of the component(s) governing the key aspect of the behaviour for the limit state considered.

3. SEISMIC BEHAVIOUR OF BOLTED END PLATE BEAM-TO-COLUMN STEEL JOINTS

A number of validation and calibration studies were carried out in the last decade, and design criteria and recommendations were developed and included in the Eurocodes 3 (2001) and Eurocode 4 (2002).

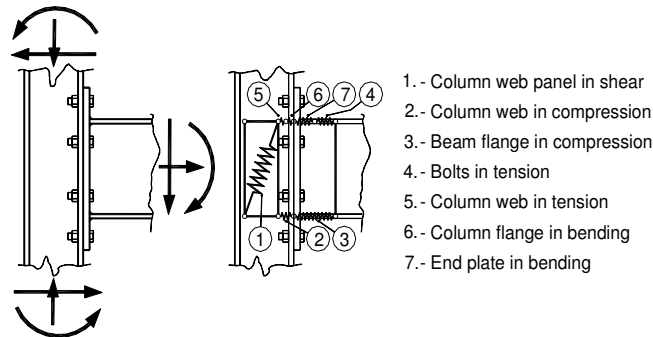


Figure 3.2. Mechanical model of the EC3 - Design of joints

A similar development, as to the novel importance of joints in design, took place in earthquake engineering. The possible role of joints in the energy dissipation mechanism was in fact recognised and the potential of semi-continuous frames in seismic areas investigated. Design approaches based on conceptual design were also proposed for steel as well as for composite frames. The limits of the traditional approaches in appraising the joint response become even more evident when cyclic loads are considered. A clear need for catching stiffness and strength deterioration, and possible pinching effects associated with buckling and fracturing of components and with the increase of lack-of-fit due to plastic deformations (in particular in bolted connections), makes the requirements to be met by prediction models more strict than in the case of static loading. The peculiar features listed above for the component method make it a fairly appealing solution for modelling joints also in seismic analysis. In particular, it should be stressed that it would allow to concentrate on the cyclic response of individual components, which can be investigated in a far more simple and economic way than the response of the whole joint.

3.3 Semi-rigid partial-strength extended end plate connection

Extended end plate as well as flush end plate connections allow to realize joints covering a rather wide range of strength and stiffness. In many instances they also possess an adequate rotation capacity for plastic design. The complexity of the

3. SEISMIC BEHAVIOUR OF BOLTED END PLATE BEAM-TO-COLUMN STEEL JOINTS

response - influenced by the geometrical and mechanical parameters defining the key structural components, i.e. the end plate, the bolts, the column flange and web, the column panel zone - makes the experimental analysis vital research tool. Numerous studies were also devoted to the simulation of joint behaviour through numerical methods, in particular FE analysis with interesting results, which complemented the test outcomes permitting their extension to a larger range of cases of practical interest (Nethercot & Zandonini, 1988; Bose et al, 1996; Bursi and Jaspart, 1997; Bursi and Jaspart, 1998; Bahaari and Sherbourne, 2000). Despite important continuous advances in FE analysis, which enable more and more refined approximations, the reliability of the results is still remarkably affected by the importance of localised effects, e.g., the evolution of plate-contact area, bolt-plate interaction, low ductility of the Heat Affected Zones (HAZ) near welds, etc. Besides, the associated burden makes this approach unfeasible in design practice, and its cost efficiency remains rather low even for research purposes. However, the knowledge of the behaviour of end plate connections under static loading was more than adequate to develop and validate design models, which meet the recent demand of semi-continuous frame design.

An extended end plate connection consists of a plate with bolt holes drilled or punched, and shop welded to a beam section. The connection is completed in the field when the beam end is bolted to a column. The extended end plate connection is termed "extended" because the plate extends above or below the flange that will be in tension under monotonic loading. In the case of extended end plate devoted to seismic design, the end plate is extended above and below beam flanges.

The behaviour of this type of connection under cyclic loading has been investigated, though at a lower extent than for the static case, and the main features clearly identified, including the stiffness and strength deterioration, the dependence on the loading history, and the typical modes of failure (Ghobarah et al, 1990; Ghobarah et al, 1992; Bernuzzi et al, 1996; Kukreti and Biswas, 1997; Adey et al, 1998). On the one hand, the increasing degree of complexity of the phenomena involved with respect to the monotonic case is apparent, like also the higher difficulty in setting up a model capable of approximating the hysteretic behaviour under any type of loading history, with the accuracy level required in seismic design (Deng et al, 2000). On the other hand, recent studies pointed out that moment resisting semi-continuous steel frames can possess a satisfactory seismic performance at competitive cost (Nader & Astaneh, 1991), which underlines once more the lack of simplified, yet reliable, design criteria and joint models. Such a limited knowledge hampers the practical use of semi-rigid frames in seismic areas, despite they are accepted by recent Codes (AISC, 1997 and Eurocode 8, 2002).

3. SEISMIC BEHAVIOUR OF BOLTED END PLATE BEAM-TO-COLUMN STEEL JOINTS

3.4 The experimental programme carried out at the DIMS

The study intends to discuss the main outcomes of research work related to the experimental analysis of the cyclic behaviour of end plate joints and their Tee-stub components, conducted by the Department of Mechanical and Structural Engineering (DIMS) of the University of Trento. This study aims at developing joint models enabling their seismic response to be captured in all its aspects, including the damage initiation and evolution up to and at failure. The results of the extensive experimental analysis were evaluated in terms of the main behavioural parameters of interest in seismic design. They were then used to appraise the component method, because of the particular interest in the extension of the model to the cyclic range. Within a plane frame, an exterior joint connecting an IPE beam with an HE exterior column is considered. In accordance with the Eurocode 3, the key component, on which the attention is focussed, is assumed to be the Tee stub. Along this line, isolated Tee stubs (ITS), Complete Tee stubs (CTS) and Complete Joints (CJ) have been tested. The overall programme consists of 36 tests on three sets of specimens of different complexity in terms of number of components involved: the first set of specimens is illustrated in Figure 3.3a and comprises 10 Isolated Tee Stub connections assumed to be the elemental components of end plate connections.

The basic geometrical characteristics of ITS connections are collected in Columns 2 of Table 3.1 while the corresponding bolt diameters are gathered in Column 3. The second 8 specimens coupling a Tee stub with a column section as depicted schematically in Figure 3.3b. These specimens reflect both the behaviour of ITS and of column components. Relevant properties of CTS specimens are collected in Table 3.2. Moreover, ITS and column stubs are coupled to generate different typical thickness over bolt diameter ratios. The third set includes 18 complete beam-to-column joints. Specimens are illustrated schematically in Figure 3.3c while the corresponding geometrical properties are reported in Table 3.3. Specimens were designed to achieve a partial strength and ductile behaviour through plasticity both at the beam-to-column connection and at the column web panel.

The parameters investigated were:

- the joint geometry in terms of: end plate thickness 12 and 18mm, bolt diameter, 16, 20 and 24 mm, column section, i.e. HEA180 and 280, HEB180 and 280;
- the loading history: 7 histories depicted in Figure 3.4 were considered in addition to the monotonic loading.

3. SEISMIC BEHAVIOUR OF BOLTED END PLATE BEAM-TO-COLUMN STEEL JOINTS

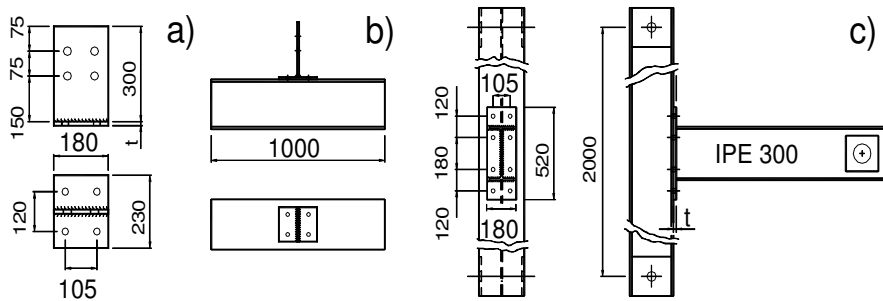


Figure 3.3. (a) Isolated Tee stub; (b) Coupled Tee stub; (c) Complete Joint

Specimen	t_p (mm)	Bolt diameter (mm)	Displacement test procedure
TM-1	12	16	Monotonic
TC-1	12	16	SDTP - 2
TM-2	12	20	Monotonic
TC-2	12	20	SDTP - 2
TM-3	18	20	Monotonic
TC-3	18	20	SDTP - 2
TM-4	18	24	Monotonic
TC-4	18	24	SDTP - 2
TC-5	25	20	SDTP - 2
TC-6	25	24	SDTP - 2

Table 3.1. Properties of Isolated Tee Stubs

Specimen	t_p (mm)	Bolt diameter (mm)	Column	t_{ef} (mm)	Displacement test procedure
CIB1-1	12	16	HEB180	14	SDTP - 2
CIB2-1	12	16	HEB280	18	SDTP - 2
CIA1-2	12	20	HEA180	9.5	SDTP - 2
CIA2-2	12	20	HEA280	13	SDTP - 2
CIB1-3	18	20	HEB180	14	SDTP - 2
CIB2-3	18	20	HEB280	18	SDTP - 2
CIB1-4	18	24	HEB180	14	SDTP - 2
CIA2-4	18	24	HEA280	13	SDTP - 2

Table 3.2. Properties of Coupled Tee Stubs

3. SEISMIC BEHAVIOUR OF BOLTED END PLATE BEAM-TO-COLUMN STEEL JOINTS

Specimen	t_p (mm)	Bolt diameter (mm)	Column	t_{cf} (mm)	Displacement test procedure
<i>JA1-2A</i>	12	20	HEA180	9.5	<i>SDTP - 1</i>
<i>JA1-2B</i>	12	20	HEA180	9.5	<i>SDTP - 1</i>
<i>JA1-2C</i>	12	20	HEA180	9.5	<i>SDTP - 3</i>
<i>JA1-2D</i>	12	20	HEA180	9.5	<i>SDTP - 4</i>
<i>JA1-2E</i>	12	20	HEA180	9.5	<i>SDTP - 5</i>
<i>JA1-2E</i>	12	20	HEA180	9.5	<i>SDTP - 6</i>
<i>JA1-2M</i>	12	20	HEA180	9.5	<i>Monotonic</i>
<i>JA1-2R</i>	12	20	HEA180	9.5	<i>SDTP - 7</i>
<i>JB1-3A</i>	18	20	HEB180	14	<i>SDTP - 1</i>
<i>JB1-3B</i>	18	20	HEB180	14	<i>SDTP - 1</i>
<i>JB1-3C</i>	18	20	HEB180	14	<i>SDTP - 3</i>
<i>JB1-3D</i>	18	20	HEB180	14	<i>SDTP - 4</i>
<i>JB1-3E</i>	18	20	HEB180	14	<i>SDTP - 5</i>
<i>JB1-3F</i>	18	20	HEB180	14	<i>SDTP - 6</i>
<i>JB1-3M</i>	18	20	HEB180	14	<i>Monotonic</i>
<i>JB1-3R</i>	18	20	HEB180	14	<i>SDTP - 7</i>
<i>JB1-4</i>	18	24	HEB180	14	<i>SDTP - 1</i>
<i>JA2-4</i>	18	24	HEA280	13	<i>SDTP - 1</i>

Table 3.3. Properties of Complete Joints

All bolts are 8.8 grade bolts preloaded to the 40% of the actual yield strength in order to roughly simulate the condition corresponding to the pretension induced by hand tightening up to the snug tight condition. The geometries of the components (Tee stubs, bolts and column section) are coupled in such a way to cover a range of relative component stiffness (Tee stub thickness to bolt diameter for the isolated Tee stubs and Tee stub thickness to column flange thickness for the coupled Tee stubs and full joint specimens) of significance for practical interest.

3. SEISMIC BEHAVIOUR OF BOLTED END PLATE BEAM-TO-COLUMN STEEL JOINTS

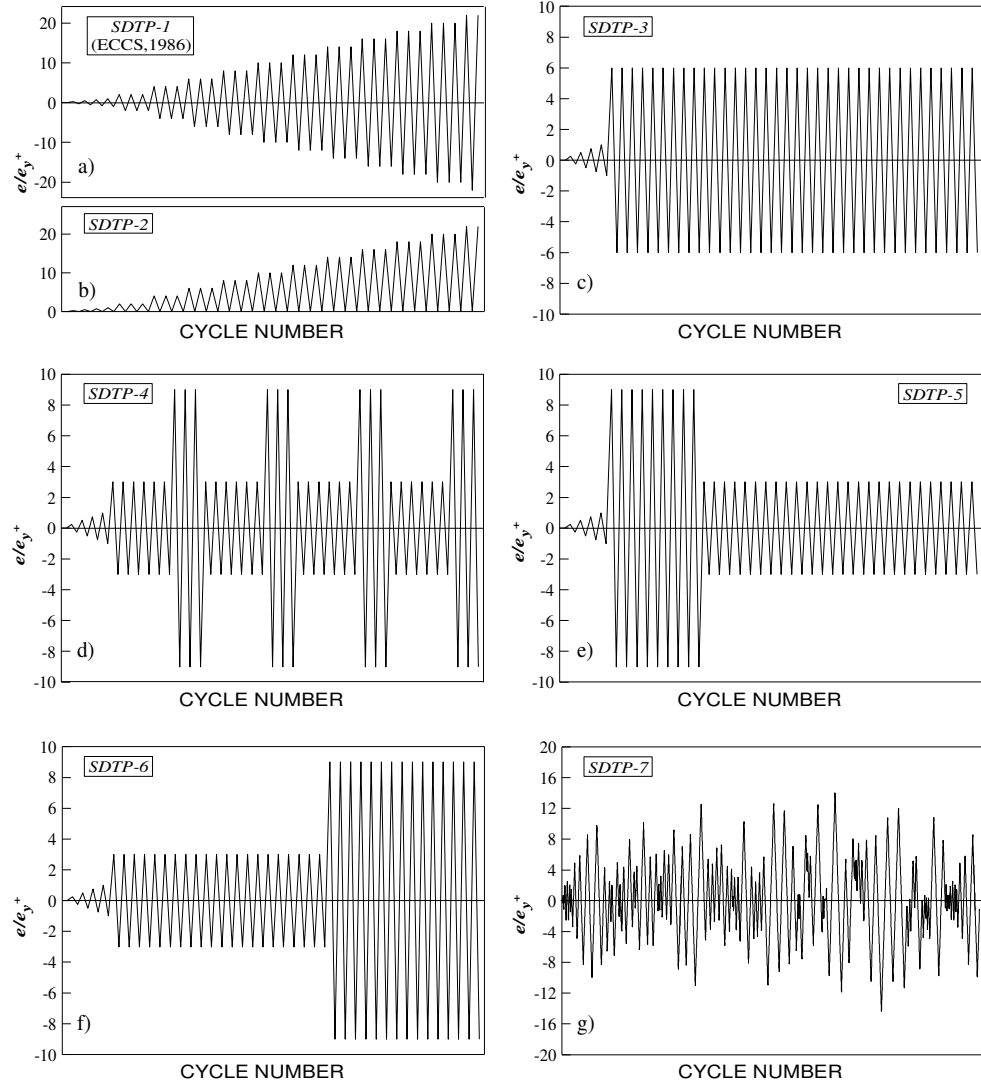


Figure 3.4. Controlled displacement test protocols: a) and b) Variable amplitude cycles in accordance with the ECCS Procedure (1986); c) Constant amplitude cycles; d), e) and f) Large amplitudes cycles superimposed upon constant amplitude cycles; g) Random amplitude cycles.

3. SEISMIC BEHAVIOUR OF BOLTED END PLATE BEAM-TO-COLUMN STEEL JOINTS

3.4.1 Material properties

Particular attention was paid to the mechanical and fracture-related properties of the structural components and of the fasteners (welds and bolts). The relevant results of tension coupon tests conducted on samples from end plates, bolts, profiles and fillets of weld are collected in Table 3.4.

Component		t (mm)	ϵ_y (%)	ϵ_u (%)	ϵ_u/ϵ_y	f_y (MPa)	f_{max} (MPa)	f_{max}/f_y
<i>IPE 300</i>	<i>Flange</i>	10.2	0.16	43.58	272.4	307	471	1.53
	<i>Web</i>	7.1	0.17	40.88	240.5	328	477	1.46
<i>HEA 180</i>	<i>Flange</i>	9.4	0.18	38.99	216.6	317	471	1.49
	<i>Web</i>	6.0	0.18	37.14	206.3	373	494	1.32
<i>HEB 180</i>	<i>Flange</i>	13.8	0.12	43.61	363.4	292	478	1.64
	<i>Web</i>	8.3	0.17	43.01	253.0	316	493	1.56
<i>HEA 280</i>	<i>Flange</i>	12.4	0.17	34.61	203.6	413	528	1.28
	<i>Web</i>	8.6	0.23	31.64	137.6	428	545	1.27
<i>HEB 280</i>	<i>Flange</i>	16.7	0.16	34.61	216.3	266	440	1.65
	<i>Web</i>	10.6	0.10	45.39	453.9	270	462	1.71
<i>End Plate</i>		12.5	0.13	43.65	335.8	260	442	1.70
<i>End Plate</i>		18.0	0.16	22.14	138.4	318	441	1.39
<i>End Plate</i>		25.8	0.11	31.44	285.8	262	434	1.66
<i>Weld Met.</i>		5.4	0.19	26.76	140.8	355	489	1.38
<i>Weld Met.*</i>		5.4	0.18	3.9	21.7	441	528	1.20
<i>Bolt</i>		16	0.52	2.59	5.0	813	890	1.10
<i>Bolt</i>		20	0.43	4.50	10.5	888	948	1.07
<i>Bolt</i>		24	0.42	6.25	14.9	816	882	1.08

*Specimen with flaws

Table 3.4. Mechanical Properties of Specimens

The strength properties of structural elements are in satisfactory accordance with the nominal values for S275 steel, whose yield strength f_y and ultimate tensile strength f_u are equal to 275 and 430 MPa respectively (Eurocode 3, 2001). The material performance generally meets the Codes requirements both for strength and deformation capacity: the ultimate elongation ϵ_u is greater than 20% and the ultimate material ductility (ϵ_u/ϵ_y) achieves fairly high values. However, as far as strength limitation are concerned, in a few cases $f_y/f_{y,nom}$ was beyond the limit of 35 per cent allowed by Eurocode 8 (2002) recommendation on the material overstrength. Moreover, the strength f_{max}/f_y ratio very often exceeds the value of

3. SEISMIC BEHAVIOUR OF BOLTED END PLATE BEAM-TO-COLUMN STEEL JOINTS

1.25 specified by the seismic provisions of AISC (1992) and therefore, hardening of cyclic stress-strain curve is expected.

The performance of structural joints under recent strong earthquakes pointed out the significant importance of weld design and execution. Therefore, beam stubs were connected to end plates by means of fillet welds, executed with special care by licensed welders. The welding technology was Flux Cored Arc Welding (FCAW) with Metal Active Gas (MAG) shielding and no preheating. A filler metal was selected, characterized by a nominal yield stress f_y equal to 420 MPa and a nominal ultimate strength f_u of about 520 MPa, respectively. This deliberate strength overmatch by the filler metal aimed at shifting the expected failure planes to the base metal adjacent to the weld. The test values of the yield and ultimate tensile strength for the weld metal samples extracted from virgin specimens comply well with the nominal ones as reported in Table 3.4.

3.4.2 Fracture mechanics-based characterization

A series of laboratory tests was carried out to characterize the end plate material in its different microstructural states. As a matter of fact owing to the filler metal and the uneven temperature distribution, a welded joint is a compound of three different metallurgical regions: the fusion zone, the heat affected zone (HAZ), and the unaffected base metal. The HAZ is the area adjacent to the fusion zone, where the material has undergone a thermal cycle that alters the microstructure of the base material, though the temperature is too low to determine fusion.

The microstructural characterization was performed by means of the optical microscope in order to determine the microstructural state in the different zones. Then, Vickers hardness measurements were carried out on different regions of the specimens highlighted by etching. Such results are reported in Table 3.5

A further important characteristic in seismic design is the material toughness, in particular in the HAZ. In order to meet this requirement filler material was selected with nominal toughness, as obtained through a Charpy V-Notch impact energy test (ASTM, 1988) greater than 70 J at -20 °C and 50 J at -40 °C.

A series of Charpy impact tests was then carried out to characterize the notch toughness values both of base metal and of weld metal in two different directions. Columns 3 and 4 of Table 5 collect sample values extracted along (L) and orthogonally (T) the rolling-mill direction as shown schematically in Figure 3.5.

More specifically, one may observe that large differences exist between the relevant impact energy values. This trend may be explained recalling that along the rolling-mill direction, the material microstructure is an aligned multi-layered structure with ductile behaviour made up of ferrite and perlite.

3. SEISMIC BEHAVIOUR OF BOLTED END PLATE BEAM-TO-COLUMN STEEL JOINTS

Specimen	Material	CVN J @ 20° C		HV (daN)
		L	T	L
JA1-2**	Weld (W)	75	-	259
	End Plate (EP)	294	-	180
JB1-3**	W	91	-	234
	EP	232	-	188
JA1-2B**	W	24	152	151
	EP	75	244	151
JB1-3B**	W	27	103	143
	EP	83	>300	139
TC-2*	W	67	-	288
	EP	107	196	133
TC-2**	W	79	-	297
	EP	105	198	159
TC-3*	W	78	-	241
	EP	124	223	180
TC-3**	W	82	-	297
	EP	246	205	130

* Virgin

** Failed

Table 3.5. Fracture Properties of Specimens

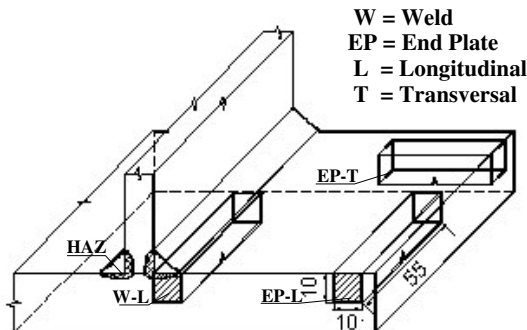


Figure 3.5. Locations and sample for Charpy V-Notch Impact Energy Test

Therefore, more energy dissipation capacity can be provided. Moreover, the impact energy tests show that both the base metal and the weld metal are endowed with satisfactory CVN levels at room temperature, viz. with values higher than the minimum ones established by design codes. As the above impact tests were instrumented, we could track the evolution of the applied load in addition to the total absorbed energy. This allows identification of the various deformation and fracture process stages. More specifically, the crack initiates after considerable plastic deformation of the specimen. After an initial unstable propagation, it

3. SEISMIC BEHAVIOUR OF BOLTED END PLATE BEAM-TO-COLUMN STEEL JOINTS

propagates in a stable way converting a large part of the absorbed energy into plastic work.

Both the material characterization and the specimen failure mechanisms pointed out the need of fracture mechanics tests in order to define the fracture toughness of the base material in the elastic-plastic regime. These tests, performed according to the ASTM E 813-89 code (1989), permitted the determination of the critical value J_{1c} , viz. the change of the elastic-plastic work per unit crack extension at the onset of stable crack extension. Moreover, the critical value of the crack tip opening displacement (CTOD), in agreement with ASTM E 1290-93 code (1993) was measured. It provides a unique estimate of localized plastic strain. The samples used to determine J_{1c} embodied a mechanical notch that was sharpened with a fatigue pre-crack induced by a constant amplitude sinusoidal loading. The multiple-specimen technique was adopted being the specimens drawn from the end plate normal to the weld bead. After fatigue pre-cracking, the specimens were subjected to a displacement controlled three-point bending test up to the crack extension. A value of J_{1c} equal to 115 kJ/m^2 was obtained in accordance with literature data (SAC Background Reports, 1997). In addition, the critical value of the crack tip opening displacement (CTOD) was measured. In detail, the crack mouth opening displacement was detected through a displacement gauge, by means of quasi-static bending tests on a pre-cracked specimen. A value of 0.31 mm was obtained, showing a good correlation with the corresponding J_{1c} value. As a matter of fact, the J_{1c} value can be converted into the CTOD index through the following relationship:

$$J_{1c} = m\sigma_y CTOD \quad (3.1)$$

where m is the so-called constraint factor. It is worthwhile to emphasize that CTOD values computed through the correlation in Equation (3.1) are approximate owing to the inherent variation of toughness properties of materials in building construction.

3.4.3 Testing equipment and measuring apparatus

All specimens were tested in a rigid reaction frame, illustrated in Figure 3.6. In detail, ITS specimens were connected directly to the rigid counter-beam of the frame while a column stub was attached to the counter-beam in order to test CTS specimens as illustrated in Figure 3.6a. The loading arrangement relevant to CJ specimens is depicted in Figure 3.6b. The column is kept horizontal and hinged at both ends at the distance of 2000 mm while the horizontal loading is applied at the

3. SEISMIC BEHAVIOUR OF BOLTED END PLATE BEAM-TO-COLUMN STEEL JOINTS

beam top. Displacements were applied to the free end of the specimen by means of a servo-controlled hydraulic actuator while a jack imposed an axial load of 300 kN to one column end.

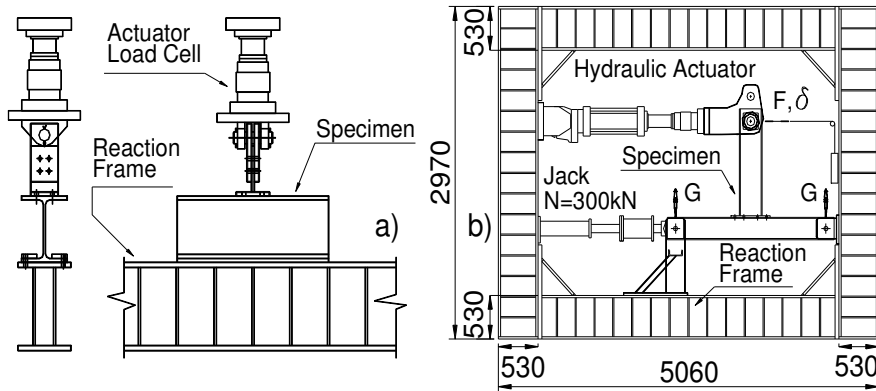


Figure 3.6. Test set-up and boundary condition for: a) Isolated Tee stubs and coupled Tee stubs specimens; b) Complete Joint specimens.

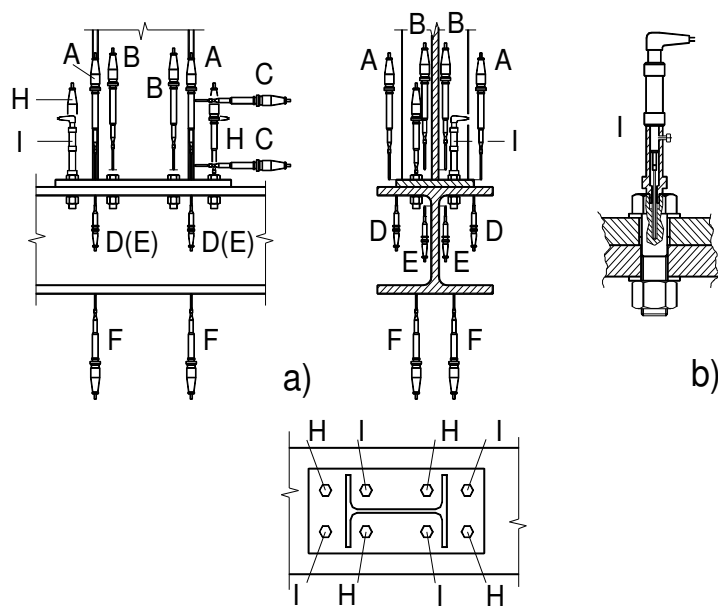


Figure 3.7. Details of the measuring apparatus for a Complete Joint

For brevity, only the instrumentation used in the CJ specimens is illustrated in Figure 3.7. It allows to detect the overall joint displacements as well as the contributions of the various components. In detail, displacement transducers (LVDTs) enabled detection of the following average quantities:

1. Connection uplift (LVDTs A);

3. SEISMIC BEHAVIOUR OF BOLTED END PLATE BEAM-TO-COLUMN STEEL JOINTS

2. Connection uplift measured on the beam web at 20 mm above the end plate (LVDTs B);
3. Lateral displacements measured on the beam flange in the web plane (LVDTs C);
4. Column flange movement along the end plate edge (LVDTs D);
5. Column web movement along the beam flange (LVDTs E);
6. Bottom column flange displacements located at 20 mm from the column web plane (LVDTs F);
7. Displacements of the column ends (see LVDTs G in Figure 3.6).

We note that all the above measurements are taken with respect to a reference frame. Moreover, four LVDTs H were adopted to measure the vertical movement of bolts, while the bolt shank elongation was detected by means of LVDTs I as illustrated in Figure 3.7b. The calibration of LVDTs I by means of companion bolts tested under a universal machine allowed also bolt forces to be detected. As a result, the prying forces that were developed at the end plate-column flange interface were estimated indirectly in a rather accurate fashion.

Joint components can be characterized directly by means of LVDT measurements while the joint behaviour of CJ specimens can be summarized in moment-rotation relationships. In detail, the joint rotation reads

$$\varphi = \varphi_b - \varphi_f - \varphi_r \quad (3.2)$$

in which φ_b represents the rotation of the beam at the end plate level as illustrated in Figure 3.8, φ_f denotes the elastic deformation of the column while φ_r denotes any rigid rotation of the column owing to the flexibility of the equipment supporting the column. Such a rigid rotation was detected by means of LVDTs G illustrated in Figure 3.6b. Besides the joint rotation φ defined in Eq. (3.2), the measuring apparatus allows the following rotations to be estimated:

$$\varphi_{conn} = \varphi_b - \varphi_c \quad (3.3)$$

$$\gamma = \varphi_c - \varphi_f - \varphi_r \quad (3.4)$$

viz. the connection rotation φ_{con} and the shear deformation γ of the column web panel, respectively.

3. SEISMIC BEHAVIOUR OF BOLTED END PLATE BEAM-TO-COLUMN STEEL JOINTS

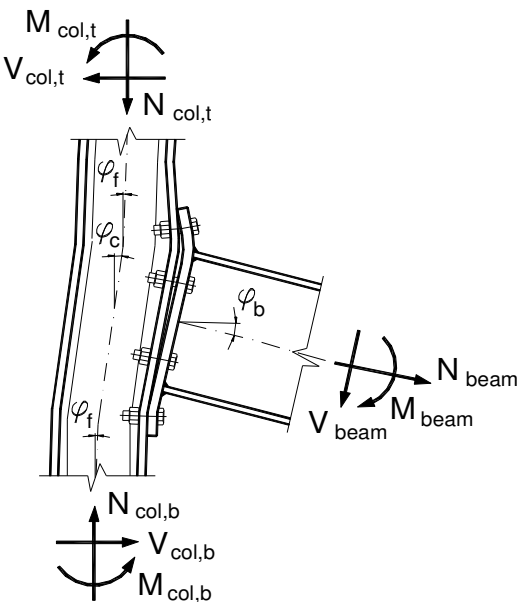


Figure 3.8. Definition of rotations for a Complete Joint

3.4.4 Testing procedure

Predefined representative displacement histories are usually applied in order to characterize the behaviour of specimens under hysteretic loading. The problem of the displacement pattern arises especially under seismic loading, as unique fatigue relationships are strictly valid only for constant-amplitude displacement reversals. Real structures, however, seldom conform to this ideal as they can be subjected to multitude of displacement patterns of varying degrees of complexity. In these instances, probability-density curves able to characterize random-amplitude displacements should be employed. In order to reduce the problem complexity, a heuristic approach is adopted in this study, applying to the specimens several displacement histories lying between the extremes of constant-amplitude and random-amplitude displacement reversals.

In order to define conveniently displacement patterns, a conventional elastic limit state characterized by the displacement e_y^+ and the corresponding force F_y^+ can be defined on the first part of each non-linear response envelope obtained from monotonic tests as depicted in Figure 3.9, schematically. The tri-linear approximation of each curve, is determined on the basis of best-fitting and of the equivalence of the dissipated energy between the actual non-linear response and the idealized tri-linear approximation up to (e_{\max}^+, F_{\max}^+) . Then, the linear elastic response with slope K_e^+ and the linear strain-hardening response with slope K_h^+

3. SEISMIC BEHAVIOUR OF BOLTED END PLATE BEAM-TO-COLUMN STEEL JOINTS

define the coordinates (e_y^+, F_y^+) , of concern for the serviceability limit state. Imposing the condition $F^+ = F_y^+ = F_u^+$ the ultimate displacement capacity e_u^+ can be evaluated. Being $F_u^+ < F_{max}^+$, this definition implies a certain level of strength degradation. Such procedure can also be applied to the non-linear force-displacement envelope of the cyclic response of a specimen and therefore, the ultimate displacement ductility factor e_u^+/e_y^+ can be evaluated also in a cyclic regime.

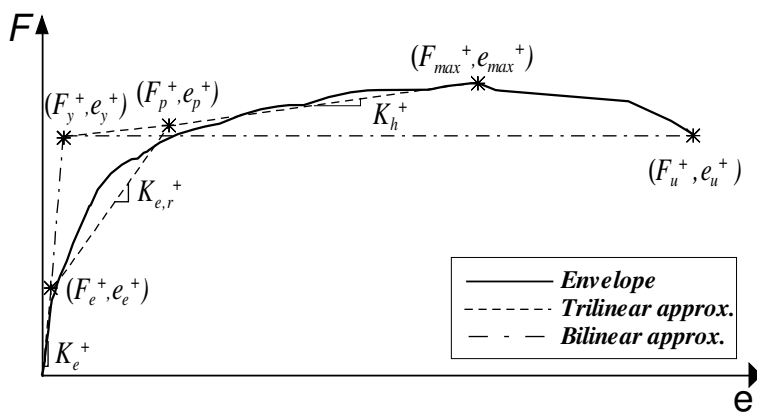


Figure 3.9. Bi- and tri-linear fits of a force-displacement envelope

To acquire comprehensive sets of information from the specimens, the so-called Complete Testing Procedure proposed by the European Convention for Constructional Steelwork (ECCS Procedure, 1986) was used. This sequential displacement test protocol SDTP-1, which is illustrated in Figure 3.4a, is adopted to acquire data on the specimen capacity such as the maximum strength, ultimate displacement ductility e_u^+/e_y^+ , maximum absorbed energy, etc. A variant of this procedure, labelled SDTP-2, and suitable to ITS and CTS is depicted in Figure 3.4b. The procedure SDTP-3 illustrated in Figure 3.4c, is characterized by a set of equi-amplitude constant displacements at $6e_y^+$, in agreement with the Cumulative Damage Testing Program (1992). This procedure provides the basis for developing fatigue-life relationships. Moreover, additional test protocols were conceived to investigate the displacement sequence effects on cumulative damage. In particular, the SDTP-4-SDTP-6 test protocols illustrated in Figure 3.4d-f, are characterized with large displacement reversals reproducing seismic pulses superimposed upon constant amplitude displacement fluctuations. Finally, the SDTP-7 test protocol is plotted in Figure 3.4g and was derived from simulations on steel frames exposed to an artificial accelerogram matching the Type 1 elastic response spectrum suggested in Eurocode 8 (2002) for subsoil class A. This type of displacement sequence provides a convenient benchmark for compare random

3. SEISMIC BEHAVIOUR OF BOLTED END PLATE BEAM-TO-COLUMN STEEL JOINTS

amplitude testing. The different loading histories considered are built up to appraise the influence on the cyclic joint response, and in particular on the damage evolution, of different sequences of cycle amplitudes, simulating some features of the seismic input. Tests were carried out quasi-statically. Therefore, an increase in the ductility capacity compared to equivalent specimens loaded dynamically would be expected, considering that fracture toughness of steel decreases with the strain rate growth. However, tests on welded beam-to-column connections performed by Saita et al. (1998) pointed out the equivalence between quasi-static and dynamic tests with regard to ductility. Moreover, the strength as well as the absorbed energy is larger for dynamic loading than for quasi-static loading confirming that quasi-static test procedures lead to a conservative appraisal of these key parameters.

3.5 Main results and preliminary seismic assessment

The results of the study are briefly presented in this section, focused on the experimental outcomes and their first assessment in the perspective of seismic design. The three sets of tests are here considered separately. The significance of these results in view of the validation of the component method is dealt with in Section 3.6.

3.5.1 *Isolated Tee stubs*

The applied load versus the upward displacement curves of the Tee stub web represent an important overall indicator of the specimen's behaviour to be associated with the failure mode in order to understand the influence of the parameters investigated, i.e., the plate thickness, the bolt diameter and their ratio. Figure 3.10 illustrates a typical Tee stub response with reference to the case of 12 mm end plate thickness t and 20 mm diameter bolts. Both the monotonic and cyclic responses are plotted, showing that the envelope of the latter one lies very close to the monotonic curve for a first significant portion of the loading process. Progressive strength deterioration, associated to the increase of end plate plastic deformations and damage at the weld toe, is then occurring. As illustrated in Figure 3.11, at the ultimate limit state the TM-2 specimen was characterized by a collapse mechanism with four yield lines located at the bolt-holes and at the weld toes in accordance with Mode 1 failure (Eurocode 3, 2001). The corresponding specimen

3. SEISMIC BEHAVIOUR OF BOLTED END PLATE BEAM-TO-COLUMN STEEL JOINTS

subject to cyclic loading, TC-2, experienced premature plate fractures at a hot spot of plastic strain concentration located at weld toes.

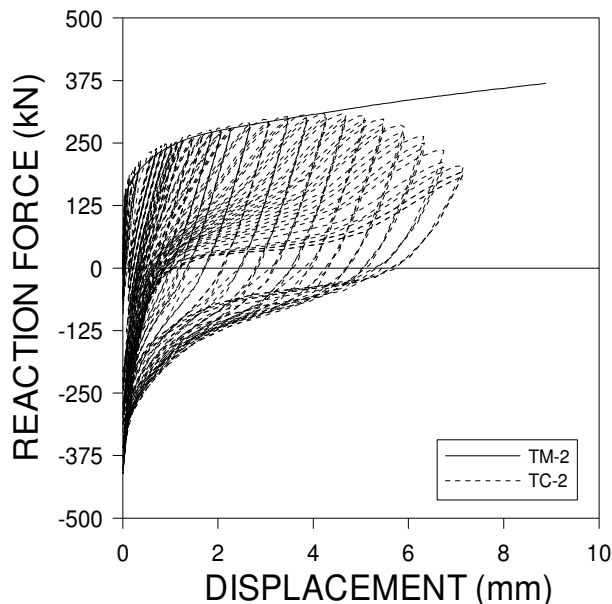


Figure 3.10. Experimental response of TM-2 and TC-2 Isolated Tee stubs

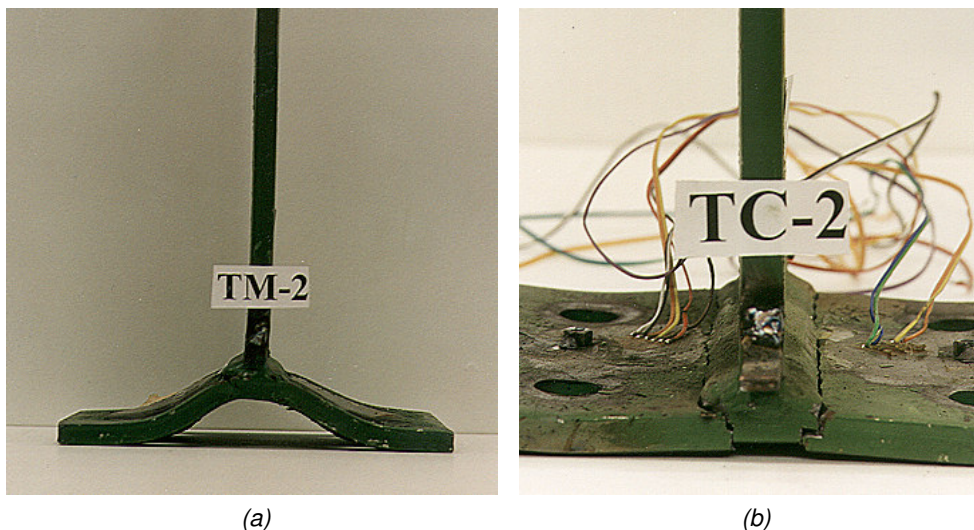


Figure 3.11. Collapse mechanism for (a) the TM-2 specimen; (b) TC-2 specimen

As a result, cyclic loading reduces significantly both the ultimate strength and the displacement ductility factors. Close observation of the plate failure reveals that brittle fracture evolved in three sequential phases: i) the initiation of a ductile crack at the steel surface owing to plastic strains; ii) a stable growth of a ductile crack in

3. SEISMIC BEHAVIOUR OF BOLTED END PLATE BEAM-TO-COLUMN STEEL JOINTS

the plate thickness; iii) a sudden propagation of the crack in a brittle fracture mode. However, the test indicates that the fillet welds performed well and were able to develop the required cyclic strength.

Similar considerations apply to the specimens with plate thickness equal to 18 mm. As expected, the specimen TM-3 was characterized by a Mode 2 failure according to Eurocode 3, with two yield lines located at the weld toes, whilst specimen TC-3 failed by plate fracture close to the weld toes following the same sequence described above for the TC-2 specimen.

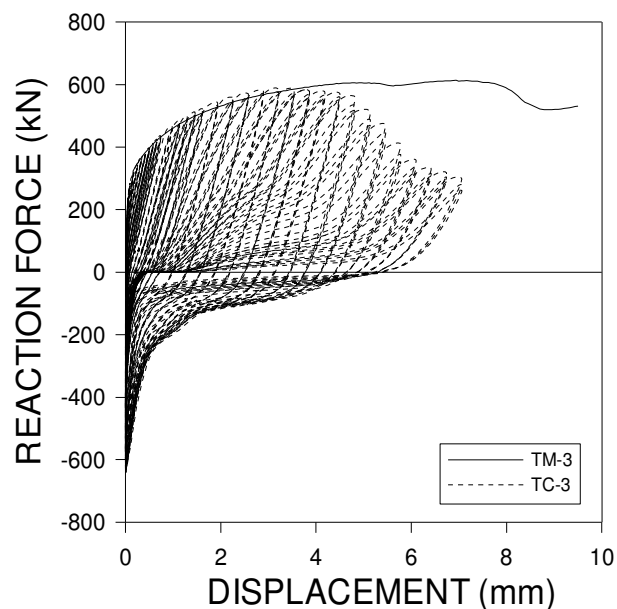


Figure 3.12. Experimental response of TM-3 and TC-3
Isolated Tee stubs

A comparative assessment of the hysteretic performances of TC-2 and TC-3 specimens can be based on the relation between the mean energy ratio (i.e., the ratio between the absorbed energy, averaged on three cycles, and the energy dissipated per complete cycle by an equivalent elastic-plastic oscillator) and the maximum ductility e/e_y (ECCS, 1986). Such a comparison pointed out that: (i) owing to the Mode 1 failure pattern which involves four yield lines, the TC-2 specimen is able to absorb greater amounts of energy also at smaller ductility ratios; (ii) the ultimate displacement ductility factor e^+/e_y^+ (see Figure 3.9) are 73 and 53 for the TC-2 and TC-3 specimen, respectively. Thereby, the TC-2 specimen performs better both in terms of absorbed energy and of ductility, as illustrated in Figure 3.13.

3. SEISMIC BEHAVIOUR OF BOLTED END PLATE BEAM-TO-COLUMN STEEL JOINTS

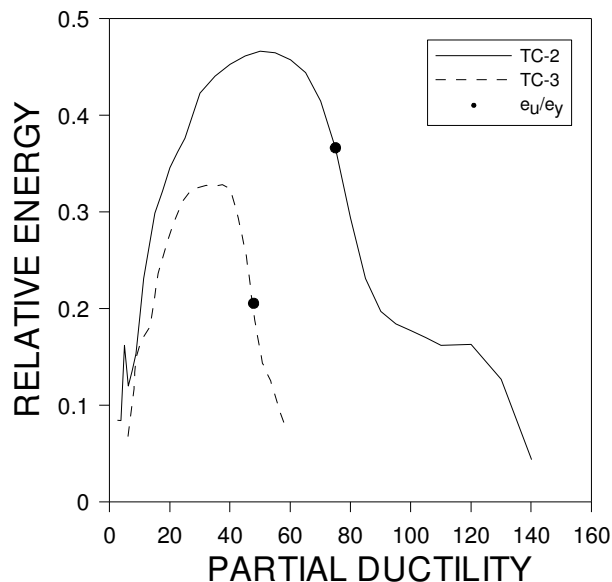


Figure 3.13. Relative dissipated energy vs. partial ductility for the TC-2 and TC-3 Isolated Tee stubs

3.5.2 Coupled Tee Stubs

Different inelastic mechanisms were observed in coupled Tee stub tests, associated with different relative stiffness and strength of the relevant components: the Tee stub, the column flange and the bolts. The total thickness of the connected parts; i.e. column flange and Tee stub plate, also seems to affect the response.

Figure 3.14a compares the responses of specimens C1A1-2 and C1A2-2, different for the column section, which is a HEA180 in the former and a HEA280 in the latter test. It is apparent that specimen C1A1-2 is characterized by large energy absorption and displacement ductility, due to the extensive plastic deformation occurring in both the Tee stub with $t = 12\text{mm}$ and the column flange with $t_f = 9.5\text{ mm}$. Failure was attained by brittle fracture of the Tee stub weld toes after crack propagation. The C1A2-2 specimen has a thicker column flange, i.e. $t_f = 13\text{mm}$, which caused inelastic phenomena to concentrate in the Tee stub only. This results in lower displacement ductility and energy absorption, while pinching phenomena appear in last cycles. As to the corresponding two 18 mm plate thickness specimens (see Figure 3.14b), specimen C1B1-3 with a HEB180 column section with $t_f = 14\text{mm}$ experienced inelastic phenomena in the sole column flange, which resulted in a limited energy absorption and maximum displacements capability, while in the specimen C1B2-3 with a HEB280 profile and $t_f = 18\text{mm}$ plastic phenomena occurred both in the Tee stub and in the column flange, enabling

3. SEISMIC BEHAVIOUR OF BOLTED END PLATE BEAM-TO-COLUMN STEEL JOINTS

larger displacement ductilities to be achieved; pinching phenomena appeared in the last cycles, when brittle failure developed at the weld toes of the tee stub.

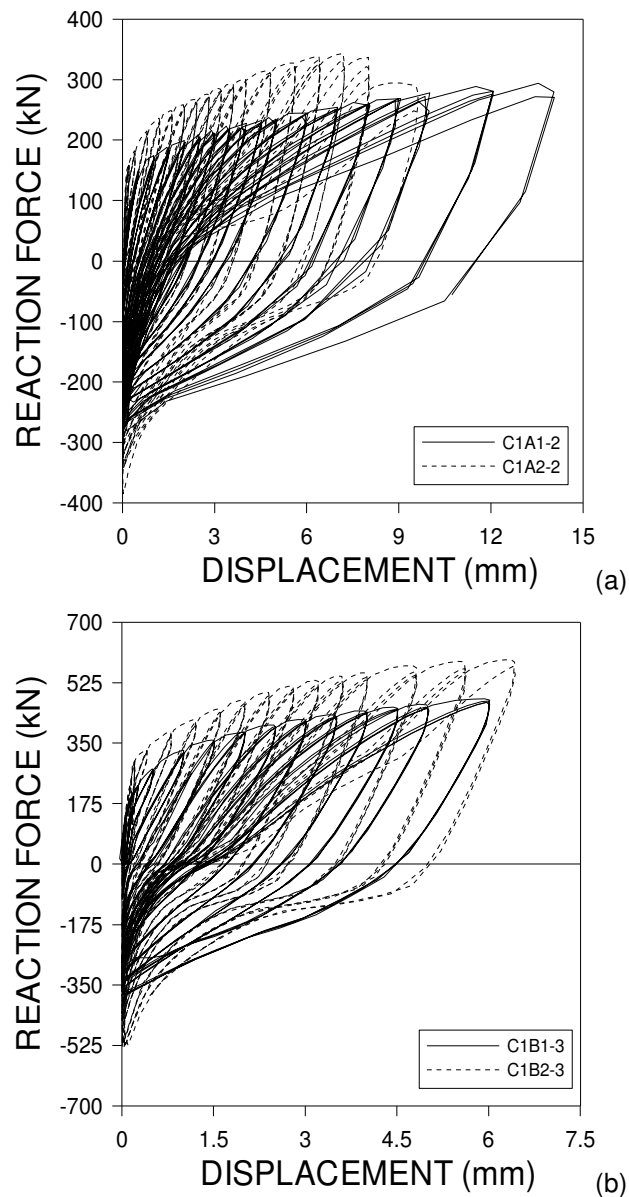


Figure 3.14. Experimental response of (a) C1A1-2 and C1A2-2; (b) C1B1-3 and C1B2-3 Coupled Tee stubs

Pinching somehow depends on the relative thickness of the connection plate to the column flange, and increased with the increase of this ratio. However, all the coupled Tee stub specimens showed less important pinching than the isolated corresponding isolated Tee stubs. On the one hand, the C1A1-2 specimen, which

3. SEISMIC BEHAVIOUR OF BOLTED END PLATE BEAM-TO-COLUMN STEEL JOINTS

is associated with the coupling of two ‘thin’ elements with relatively heavy bolts, showed the best performance in terms of mean energy ratio. On the other hand, the coupling of a thick Tee stub with a column flange of similar thickness like the C1B2-3 specimen ensues the lowest energy ratio.

3.5.3 Complete Joints

On the basis of the results of the coupled Tee stub tests, attention is focused on joints JA1-2 and JB1-3, which appear to be more adequate in terms of seismic design requirements. In this subsection the monotonic tests will be discussed as well as the cyclic tests adopting the ECCS displacement procedure (1986). The subsequent set of tests adopting the different procedures shown in Figure 3.4 aimed at providing data for the calibration of damage models considered but will not be discussed in this study. Both the monotonic and the cyclic moment rotation response relative to the Complete Joint endowed with a 12 mm end plate thickness coupled with the column of HEA180 profile, i.e. JB1-2M and JB1-2A specimen, respectively are illustrated in Figure 3.15.

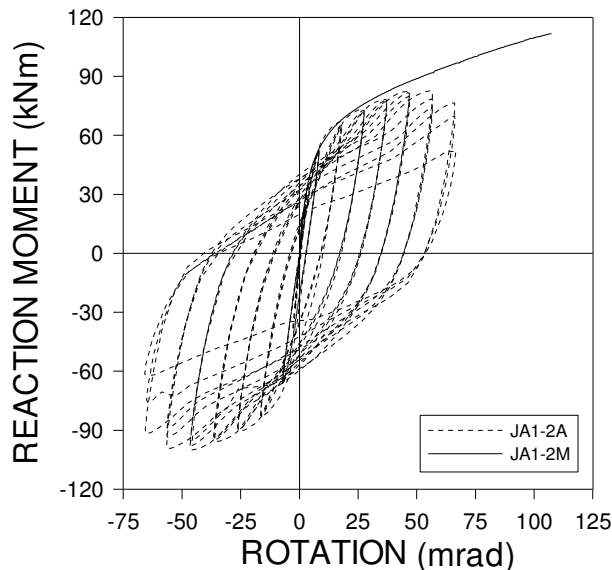


Figure 3.15. Experimental response of JA1-2M and JA1-2A Complete Joints

Similar behavioural features were observed for the joint JB1-3A, and for the twin specimens JA1-2B and JB1-3B (see Figure 3.16). These joints exhibited failure at weld toes in the end plate part outside the beam section owing to fragile crack propagation, as illustrated in Figure 3.17. This indicates a satisfactory behaviour of the fillet welds. The monotonic response is characterized by inelastic phenomena

3. SEISMIC BEHAVIOUR OF BOLTED END PLATE BEAM-TO-COLUMN STEEL JOINTS

activated in the end plate, the column flange and the column web panel in shear. With regard to the cyclic response, one can observe that total rotations of CJ reach values higher than 45 mrad, implying a suitable ductile behaviour for high ductile (class H) structures in seismic applications (Astaneh-Asl, 1995; Eurocode 8, 2002).

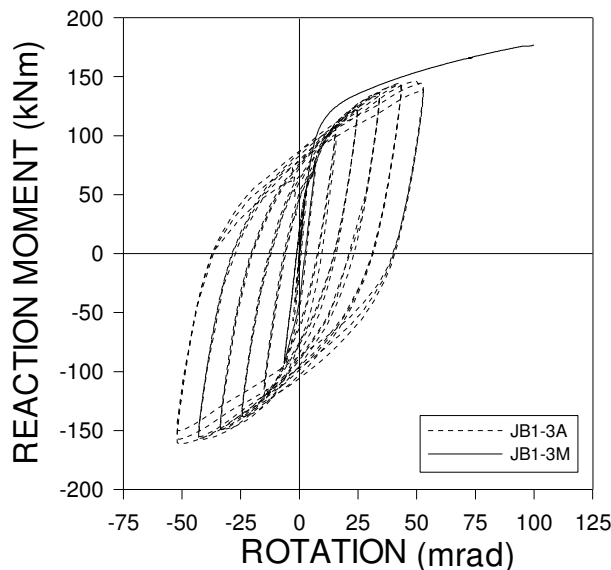


Figure 3.16. Experimental response of JB1-3M and JB1-3A Complete Joints



Figure 3.17. Fracture of an end plate in a Complete Joint

The percentage of the energy dissipated by the different component of the joint is reported in Figure 3.18. The most ductile components are:

- the column web panel in shear (component 1 of Figure 3.2);
- the column flange in bending (component 6);

3. SEISMIC BEHAVIOUR OF BOLTED END PLATE BEAM-TO-COLUMN STEEL JOINTS

- the end plate in bending (component 7).

It is evident that the contribution of the column web panel is significant in all cases.

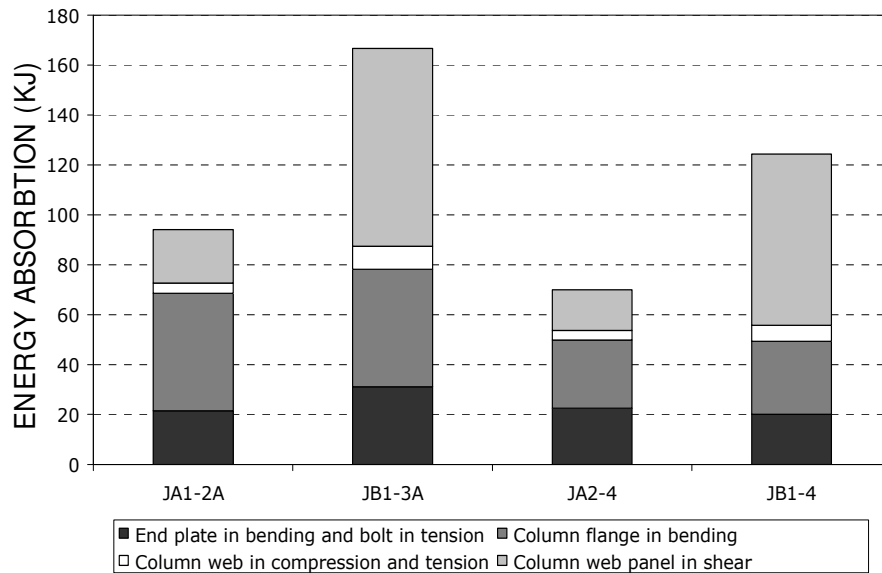


Figure 3.18. Percentage of energy dissipated by the components

The mean energy ratios as well as the ultimate ductility ratios indicate a satisfactory cyclic performance. All joint components can reach mean energy ratios higher than 0.5, while ultimate rotational ductilities $\phi_{j,u}/\phi_{j,y}$ range from 8 to 21. The results for the component 6 (column flange in bending) and for the component 7 (end plate in bending) of the specimens JA1-2 and JB1-3 are illustrated in Figure 3.19. Joint JA2-4, which also reached plastic rotations greater than 30 mrad, was characterized by a mean energy ratio below 0.5.

As far as the joint classification is concerned, it is important to underline that the Eurocode 3 (2001) permits a classification valid only for monotonic loads. In this study this approach is taken into account for an extension under seismic loading history. The response envelopes lie within the semi-rigid range of Eurocode 3 for unbraced frames, when typical beam lengths ranging from 4 to 8 m are taken into account.

3. SEISMIC BEHAVIOUR OF BOLTED END PLATE BEAM-TO-COLUMN STEEL JOINTS

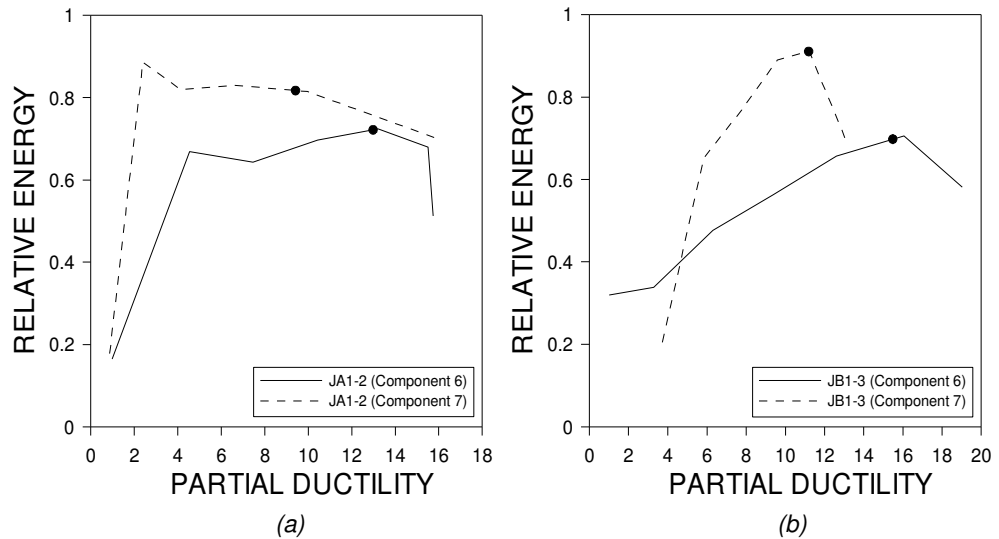


Figure 3.19. Relative dissipated energy vs. partial ductility for the components 6 and 7 of:
(a) JA1-2 and (b) JB1-3 Complete joints

According to stiffness, a joint can be classified as:

- *rigid*: its deformations has no significant influence on the distribution of the internal forces and moments in the structure or on its overall deformation.
Numerically we obtain:
i) for moment resisting unbraced frames:

$$\text{if } \bar{m} \leq \frac{2}{3} \quad \Rightarrow \quad \bar{m} \geq 25 \cdot \bar{\phi} \quad (3.5)$$

$$\text{if } \frac{2}{3} < \bar{m} \leq 1,0 \quad \Rightarrow \quad \bar{m} \geq \frac{25 \cdot \bar{\phi} + 4}{7} \quad (3.6)$$

- ii) for braced frames:

$$\text{if } \bar{m} \leq \frac{2}{3} \quad \Rightarrow \quad \bar{m} \geq 8 \cdot \bar{\phi} \quad (3.7)$$

$$\text{if } \frac{2}{3} < \bar{m} \leq 1,0 \quad \Rightarrow \quad \bar{m} \geq \frac{20 \cdot \bar{\phi} + 3}{7} \quad (3.8)$$

whit:

$$\bar{m} \leq \frac{M}{M_{pl,Rd}} \quad (3.9)$$

3. SEISMIC BEHAVIOUR OF BOLTED END PLATE BEAM-TO-COLUMN STEEL JOINTS

$$\bar{\phi} \leq \frac{E_s I_b}{L_b M_{pl,Rd}} \cdot \phi \quad (3.10)$$

where:

- $M_{pl,Rd}$ beam plastic moment;
- I_b moment of inertia of the beam;
- L_b beam length;
- E_s steel Young modulus.

- *nominally pinned*: it cannot develop significant moments, which might adversely affect members of the structure

Numerically we obtain:

$$\text{if } \bar{\phi} \leq 0,5 \Rightarrow \bar{m} \leq \frac{\bar{\phi}}{2} \quad (3.11)$$

$$\text{if } \bar{\phi} \geq 0,5 \Rightarrow \bar{m} \leq 0,25 \quad (3.12)$$

- *semi-rigid*: a joint, which does not meet the criteria for a rigid joint or a nominally pinned joint, shall be classified as a semi-rigid joint.

The aforementioned formulas are represented in the following Figure 3.20.

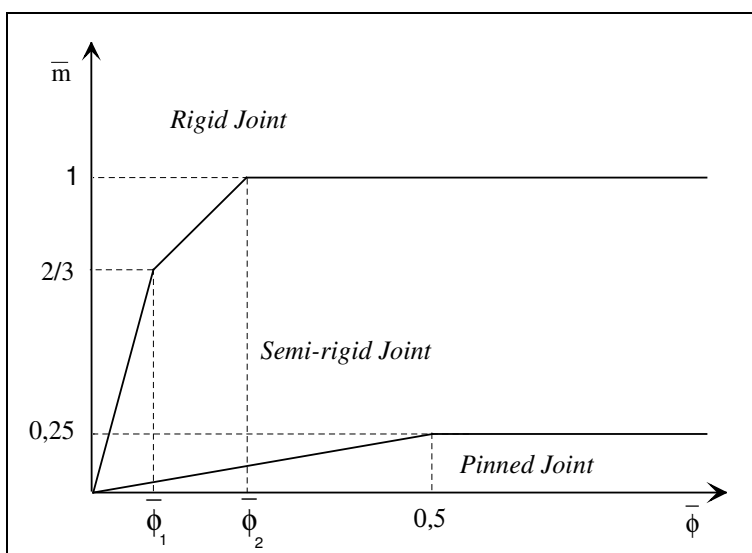


Figure 3.20. Classification of the Joint in accordance with Eurocode 3

According to strength, a joint can be classified as full-strength, partial strength or nominally pinned by comparing its moment resistance with the moment resistances of the connected members. In detail:

3. SEISMIC BEHAVIOUR OF BOLTED END PLATE BEAM-TO-COLUMN STEEL JOINTS

$$\text{Full strength joint: } \bar{m} \geq 1 \quad (3.13)$$

$$\text{Partial strength joint: } 0,25 \leq \bar{m} \leq 1 \quad (3.14)$$

$$\text{Nominally pinned joint: } \bar{m} \leq 0,25 \quad (3.15)$$

Furthermore, all the considered joints can be classified as partial strength joints, as illustrated in Figure 3.21 for the JA1-2 specimen endowed with an end plate thickness of 12 mm and in Figure 3.22 for the JB1-3 specimens endowed with an end plate thickness of 18 mm.

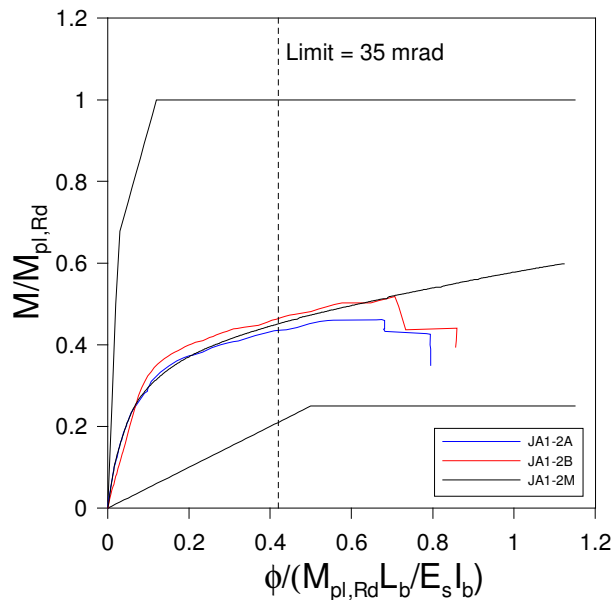


Figure 3.21. Classification of the JA1-2 Complete Joint for $L_b = 8m$

3. SEISMIC BEHAVIOUR OF BOLTED END PLATE BEAM-TO-COLUMN STEEL JOINTS

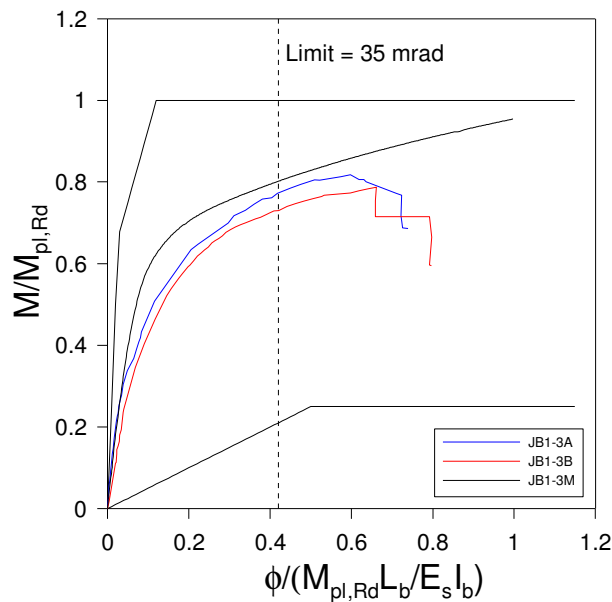


Figure 3.22. Classification of the JB1-3 Complete Joint for $L_b = 8m$

3.6 Validation of the component method

The complete set of measured parameters provides detailed information on the responses of the various components to the applied displacement history. These data enable a quantitative appraisal of the role played by each component, pointing out the effect of relative stiffness and strength of the components associated with geometry and material of the specimen. The attention is hence focused on the use of these data in order to check the general validity of the joint model by component with reference to the approximation of the cyclic response.

A first appraisal can be achieved by comparing the response of the same individual component as part of different specimens (isolated Tee stub, coupled Tee stub and complete joint). Such a comparison is somehow difficult because of the type of displacement history adopted, which determines the amplitude of the inelastic cycles as a multiple of the elastic limit displacement. As this parameter depends on the specimen, a direct comparison of cyclic responses related to different specimens is not feasible. However, reference can be made to the maximum and minimum values of parameters such as forces and displacements, ductility indices and absorbed energy.

3. SEISMIC BEHAVIOUR OF BOLTED END PLATE BEAM-TO-COLUMN STEEL JOINTS

The end plate represents an important component for the joints considered. The end plate responses of the isolated Tee stub TC-2 and Complete Joint JA1-2A are plotted in Figure 3.23. As mentioned above, the testing procedure imposes different cycle amplitudes and affects the number of cycles at failure. However, the collapse mode is the same, i.e., by plate fracturing, and the evolution of the hysteretic behaviour has similar features. A comparison between the maximum force and displacement shows an overestimate of the first parameter of 7% and an underestimate of the second of 13% with reference to the Tee stub response. The influence of the interaction between the different components in the joint appears to be limited. The same comparison between the joint JB1-3 and the corresponding Tee stubs TC-3 shows similar results, as evidenced in Figure 3.24.

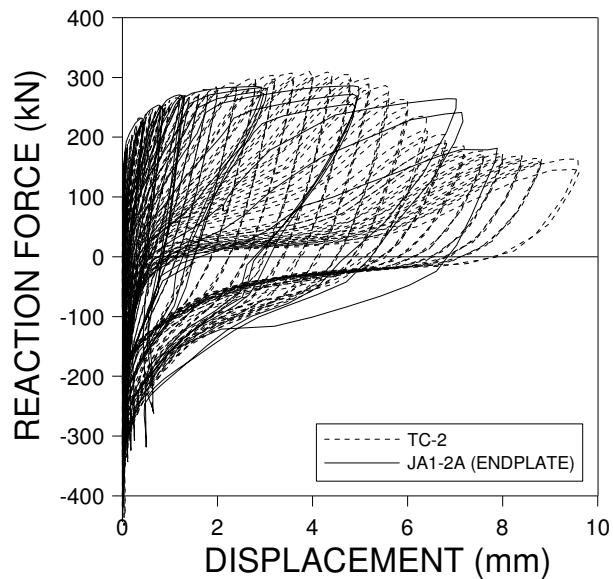


Figure 3.23. Comparison of the experimental response of the Tee stub TC-2 and the End plate of the Complete Joint JA1-2A

A more accurate appraisal of the responses of the elemental components can be obtained if reference is made to key parameters, such as the initial elastic stiffness and the plastic failure strength, which characterize the envelope of the cyclic response. A conventional elastic stiffness K_e , a plastic failure strength F_p and an ultimate displacement ductility factor ϵ_u/ϵ_y were determined by the bi- and tri-linear approximations of the envelope curve, traced on the basis of best-fitting and dissipated energy-equivalence criteria. Values of the elastic stiffness K_e relevant to the components of joints JA1-2 and JB1-3 and to the corresponding isolated and coupled Tee stubs are presented in Table 3.6.

3. SEISMIC BEHAVIOUR OF BOLTED END PLATE BEAM-TO-COLUMN STEEL JOINTS

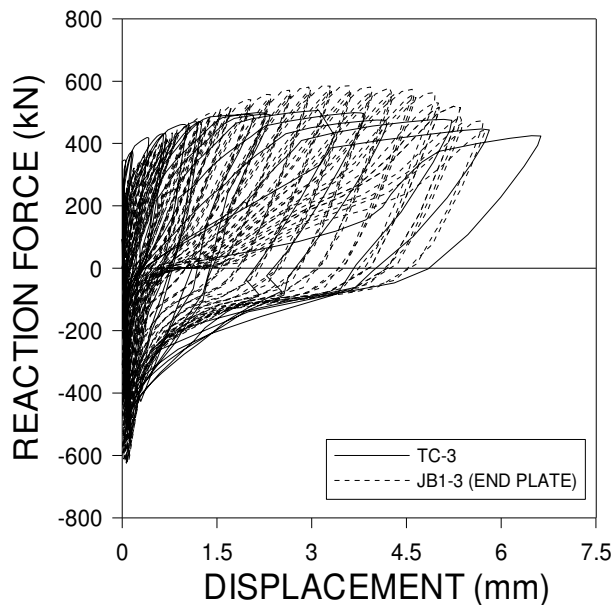


Figure 3.24. Comparison of the experimental response of TC-3 and End plate of JB1-3A Complete Joint

	EXPERIMENTAL Ke (kN/mm)					EUROCODE 3 Ke,code (kN/mm)			$\frac{Ke}{Ke,code}$		
	TC-2	C1A1-2	JA1-2A	JA1-2B	JA1-2M	TC-2	C1A1-2	JA1-2	TC-2	C1A1-2	JA1-2
Component 1	---	---	248	205	206	---	---	685	---	---	0,3
6	---	744	334	236	633	---	776	776	---	1,0	0,5
7	1393	795	1979	428	2539	378	378	378	3,7	2,1	4,4
Component	TC-3	C1B1-3	JB1-3A	JB1-3B	JB1-3M	TC-3	C1B1-3	JB1-3	TC-3	C1B1-3	JB1-3
1	---	---	266	286	256	---	---	796	---	---	0,3
6	---	1417	869	568	1093	---	3790	3790	---	0,4	0,2
7	3003	2363	2507	345	1931	1020	1020	1020	2,9	2,3	1,6

	EXPERIMENTAL Fp (kN)					EUROCODE 3 Fp,code (kN)			$\frac{Fp}{Fp,code}$		
	TC-2	C1A1-2	JA1-2A	JA1-2B	JA1-2M	TC-2	C1A1-2	JA1-2	TC-2	C1A1-2	JA1-2
Component 1	---	---	193	235	279	---	---	288	---	---	0,8
6	---	184	226	229	228	---	326	326	---	0,6	0,7
7	234	201	264	258	257	146	146	146	1,6	1,4	1,8
Component	TC-3	C1B1-3	JB1-3A	JB1-3B	JB1-3M	TC-3	C1B1-3	JB1-3	TC-3	C1B1-3	JB1-3
1	---	---	344	352	469	---	---	346	---	---	1,1
6	---	322	388	422	379	---	564	564	---	0,6	0,7
7	417	359	417	423	402	396	396	396	1,1	0,9	1,0

Components: 1. Column web panel in shear; 6. Column flange in bending; 7. end plate in bending

Table 3.6. Elastic stiffness k_e and plastic failure strength f_p of joint components

The elemental components, which give the most significant contribution, have been considered. Joints JA1-2 and JB1-3 have been selected for their satisfactory performance and as representative of joints with thin and thick extended end plates respectively. Differences among the stiffness of the same elemental components

3. SEISMIC BEHAVIOUR OF BOLTED END PLATE BEAM-TO-COLUMN STEEL JOINTS

as part of different specimen are noticeable. However, it has to be noted that the initial stiffness is very sensitive to boundary conditions and lack of fit. Table 3.6 also gathers the elastic stiffness $K_{e,code}$ computed in accordance with Eurocode 3 (2001). The stiffness ratios $K_e/K_{e,code}$ lie in a wide range, with the level of accuracy of the EC3 models being generally unsatisfactory.

With regard to the experimental plastic failure strength F_p , defined in accordance with the tri-linear approximation of the response envelope, the differences for the same component in different specimens are more limited than the ones for the elastic stiffness. However, they are still remarkable. Such differences are a consequence of the interaction, which affects the location and evolution of plastic zones. With regard to the Eurocode 3 prediction model, the plastic strength ($F_{p,code}$) was computed using measured material properties and no resistance factors. These strength values are also collected in Table 3.6. The Eurocode underestimates significantly the strength of thin end plates, while it tends to overestimate, even remarkably, most of the other components. This seems to depend mainly on the coupling effects among different components, which is not considered in the code. Moreover, non-seismic codes do not consider the development of low cycle fatigue phenomena, which lead to initiation and propagation of cracks, and affect the yield lines sequence.

A further comparison relevant to the absorbed energy was limited to the 6th elemental component *column flange in bending* and to the 7th elemental component end plate *in bending*, which dissipate most of the energy within the connection. The comparison is performed with reference to the relation between the mean energy ratio and the displacement ductility in the i-th cycle (ECCS, 1986).

The elemental component *column flange in bending* for component parts and joints embodying a thin (12mm) extended end plate showed similar mean energy ratios approaching values of about 0.7 in the coupled Tee stubs and in the complete joints, but ultimate positive partial ductilities e^+_{u}/e^+_y vary between 13 and 23, with the higher value related to the coupled Tee stubs. With reference to the 7th component, the ultimate partial ductility ranges from 9 (Complete Joint) to 13 (Isolated Tee Stub), while the mean energy ratios vary between 0.6 (Isolated Tee Stub) to 0.8 (Coupled Tee stub). A similar comparison for the 6th and 7th elemental components in joints embodying thick extended end plate of $t = 18$ mm shows even greater differences of ultimate displacement ductility factors e^+_{u}/e^+_y and maximum values of the mean energy ratios. An evaluation of these results leads to consider the component method not sufficiently accurate for approximating the cyclic response, at least for the joint configuration considered in the study. The extension of this model in seismic analysis does not seem straightforward, when

3. SEISMIC BEHAVIOUR OF BOLTED END PLATE BEAM-TO-COLUMN STEEL JOINTS

based on elemental components as defined in the Eurocodes. An alternative within the same philosophy was then explored employing *macro-components*, as the coupled Tee stubs, which take into account the influence of the key components in the compression and tension zone of the joint as well as of their interactions. The schematic model of the joint is represented in Figure 3.25.

The responses of joints JA1-2A and JB1-3A were simulated by means of this model and compared with the connection experimental responses, modified to achieve consistency. Figure 3.26 shows such a comparison for the joint JA1-2A. The overall agreement all over the response is quite good, and is confirmed by the curves of the cumulated energy illustrated in Figure 3.27. According to these first results, the macro-component model appears a viable tool for approximating the cyclic response of end plate joints.

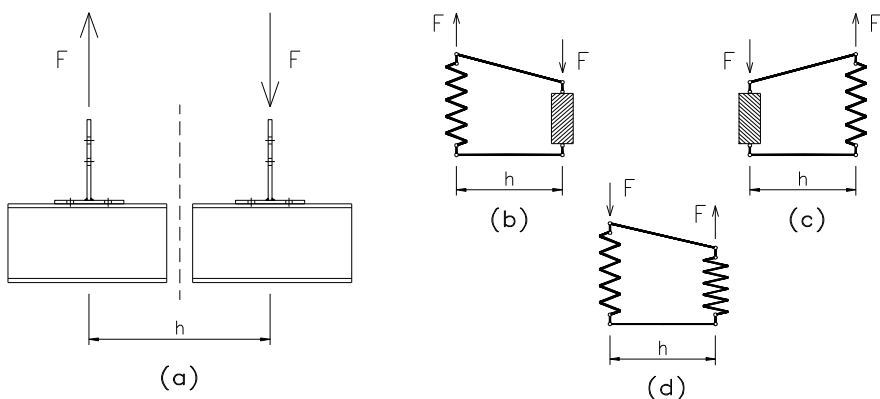


Figure 3.25. Macro-component method

3. SEISMIC BEHAVIOUR OF BOLTED END PLATE BEAM-TO-COLUMN STEEL JOINTS

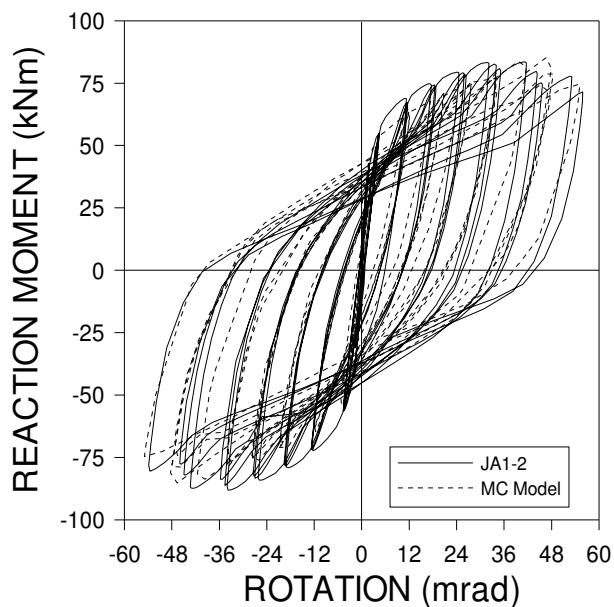


Figure 3.26. Comparison between the macro-component model and the joint response (JA1-2 specimen)

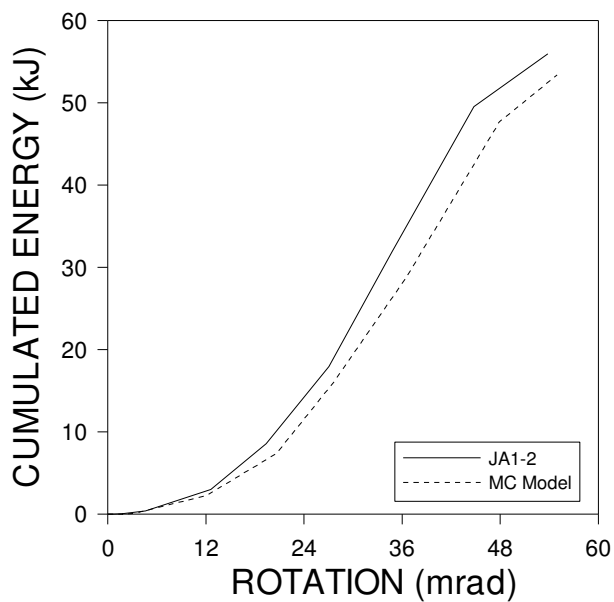


Figure 3.27. Energy absorption of the macro-component model and of the modified joint

3. SEISMIC BEHAVIOUR OF BOLTED END PLATE BEAM-TO-COLUMN STEEL JOINTS

3.7 Numerical analysis

In this section, the inelastic finite element (FE) analyses carried out by means of the ABAQUS 5.8 code (Hibbit, Karlsson & Sorensen Inc., 2001) both on isolated Tee Stub (ITS) connections and on Complete Joints (CJ) are discussed. Therefore, both FE models were calibrated and the stress and strain state of the aforementioned connections was simulated both in the monotonic and in the cyclic displacement regime. Finally, some design parameters which influence the fracture resistance of steel bolted extended plate connections are commented upon. In detail, the effects of the weld-to-base metal yield strength ratio, the end plate yield-to-ultimate strength ratio, and the residual stress influence have been determined.

3.7.1 FE Models of the ITS connections

Non-linear FE analyses of the tested Isolated Tee-Stubs were carried out both in a monotonic and in a cyclic loading regime. As a matter of fact, 3D finite element analyses of bolted connections are very demanding from a computational standpoint because contact problems as well as low-cycle fatigue phenomena need to be simulated. Hence, 2D models endowed with eight-node CPS8 plane stress elements were adopted to reduce the computational expense. Specimen symmetry permitted the modelling of only one half of the specimen.

2D models exploited FE layers to reproduce the end plate and additional FE layers to simulate the bolt shank. The pre-stressing condition was introduced in the model imposing a stretching of the bolt shank, in order to entail a final average shank stretch equal to 0.065 mm, similar to the one detected during testing.

Welding-induced residual stresses develop unavoidably in the welds and in the base metal owing to thermo elasto-plastic deformation. Therefore, an idealised stress magnitude/distribution as the one highlighted in Figure 3.28 has been introduced. Such distribution of residual stresses, which takes into account the presence of the crack, was proposed by Monahan on the basis of experimental tests performed by Porter Goff and Payne (1985). More specifically, such distribution assumes that part of the residual stresses is released as the low-cycle fatigue crack penetrates the end plate, and that the remaining residual stress is somehow redistributed throughout the uncracked ligaments. Clearly, tensile stresses at the top and bottom end plate thickness are balanced by compression stresses. Such distribution has been imposed to the mesh through several trials in order to achieve equilibrium, compatibility and the proper stress magnitude required.

3. SEISMIC BEHAVIOUR OF BOLTED END PLATE BEAM-TO-COLUMN STEEL JOINTS

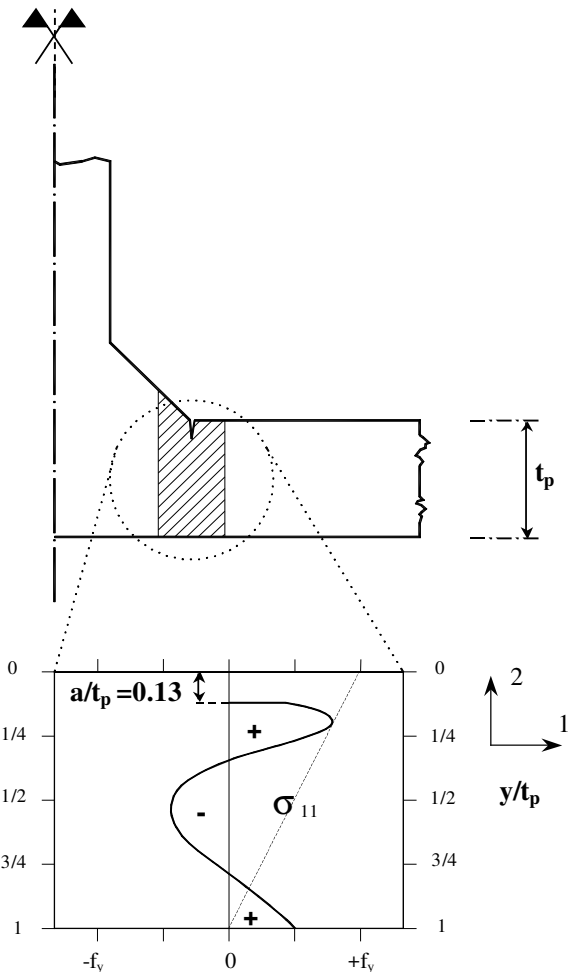


Figure 3.28. Transverse residual stress distribution in a cracked plate

Moreover, different mechanical properties are assigned to the base metal, the weld metal and the HAZ. Two-node gap contact elements are located below the end plate surface to cater for the unilateral contact condition imposed by the rigid counterbeam. In the finite element model, the gap between the bolt shank and the hole, about 1 mm, was modelled too. Hence, the contact between the shank and the end plate is modelled by using contact surfaces whilst the contact between the end plate and the nut is reproduced through gap elements. Moreover, the friction between the end plate and the column flange is neglected because its effects on the force-displacement response of this connection type are not significant (Bursi and Jaspart, 1998).

At the weld toe where stress concentrations are expected, a refined FE mesh is adopted. A crack endowed with a length of 0.26 mm (small-to-moderate root

3. SEISMIC BEHAVIOUR OF BOLTED END PLATE BEAM-TO-COLUMN STEEL JOINTS

defect) was modelled at the weld toe in order to investigate the behaviour of cracked connections. More specifically, cracking is studied through contour integral evaluation in order to infer J values. Therefore, focused meshes are set to induce the singularity at the crack tip and the crack propagation is not traced. Sharp cracks have to embody singular strain fields at the crack tip for fracture mechanics evaluations. Therefore, three nodes of the same side of eight-node isoparametric elements (CPS8) have the same geometric location at the crack tip to produce a $1/r$ strain singularity field. The FE mesh used for the ITS connections is illustrated in a. A detail of the mesh with a *spider web* configuration is reported in b where the innermost ring of elements degenerate to triangles, as described above. As the large-strain zone is very localised, sharp cracks adopted in the onset of cracking method are modelled using small-strain assumptions, and therefore large deformations are ignored. The FE analyses account for material nonlinearities using the von Mises yield criterion. Isotropic hardening is assumed for the analyses. In the analysis the measured stress-strain properties of the materials obtained by tensile test were used. The elastic modulus and the Poisson's ratio were assumed as $E=210000$ and $\nu=0.3$, respectively.

Convergence studies on elastic and inelastic models have been conducted to evaluate and arrive at the final mesh for the finite element models. The finite element model was verified by comparing the measured experimental responses with the predicted response.

The ITS connections endowed with end plate thickness of 12 mm and 18 mm, subjected to monotonic and cyclic loading respectively, have been simulated. A typical deformed configuration at failure is reported in Figure 3.30. It is possible to observe two different meshes relevant to the bolt shank and to the plate around the hole, respectively. Moreover, an attentive reader may observe how the crack with a fixed length of 2.34 mm exhibits a width increase at the tip. As a matter of fact, the nodes at the crack tip are untied in order to generate the singularity by means of inelastic elements.

The reaction force vs. the controlled displacement relevant to the TM-2 specimen is illustrated in Figure 3.31a, where the numerical simulations are compared to the experimental response. One may observe that experimental data and numerical prediction are in a good agreement. The numerical simulation relevant to the cyclic regime of the ITS TC-2 connection and the experimental response are reported in Figure 3.31b. Only a few significant displacement cycles are simulated in order to reduce the computational effort. The specimen yield strength is well captured as expected owing to the use of the isotropic strain-hardening model.

3. SEISMIC BEHAVIOUR OF BOLTED END PLATE BEAM-TO-COLUMN STEEL JOINTS

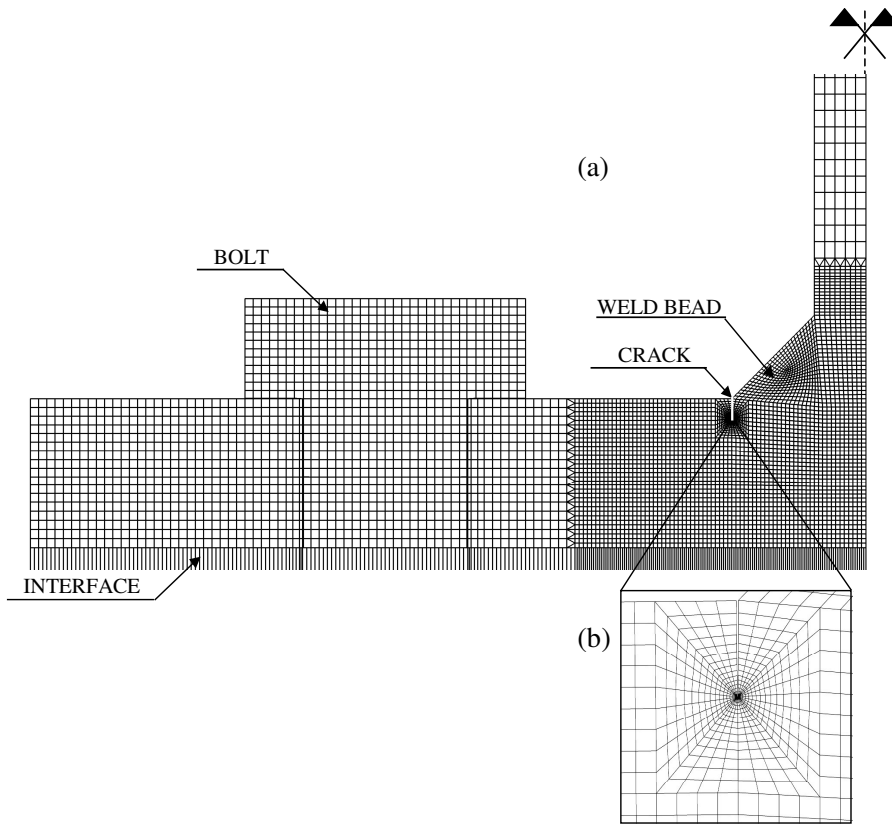


Figure 3.29. (a) 2D FE model of isolated Tee stub; (b) details of the "spider web" mesh

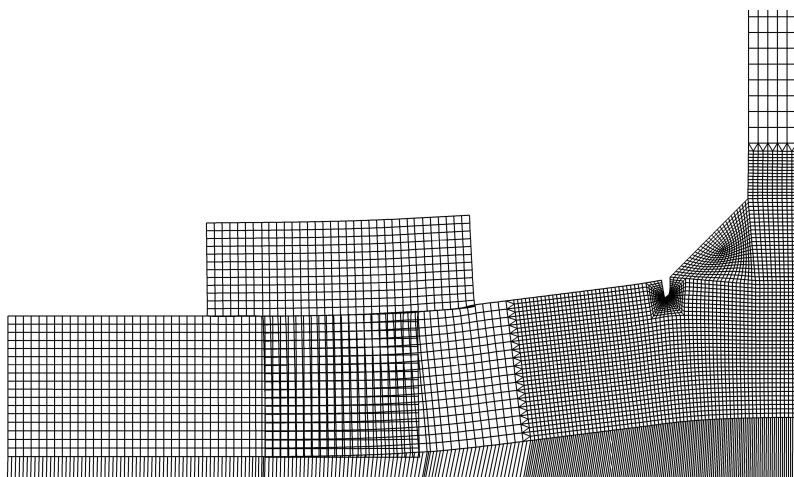


Figure 3.30. Deformed configuration of TM-3 specimen with the onset of cracking method (magnification factor 1)

3. SEISMIC BEHAVIOUR OF BOLTED END PLATE BEAM-TO-COLUMN STEEL JOINTS

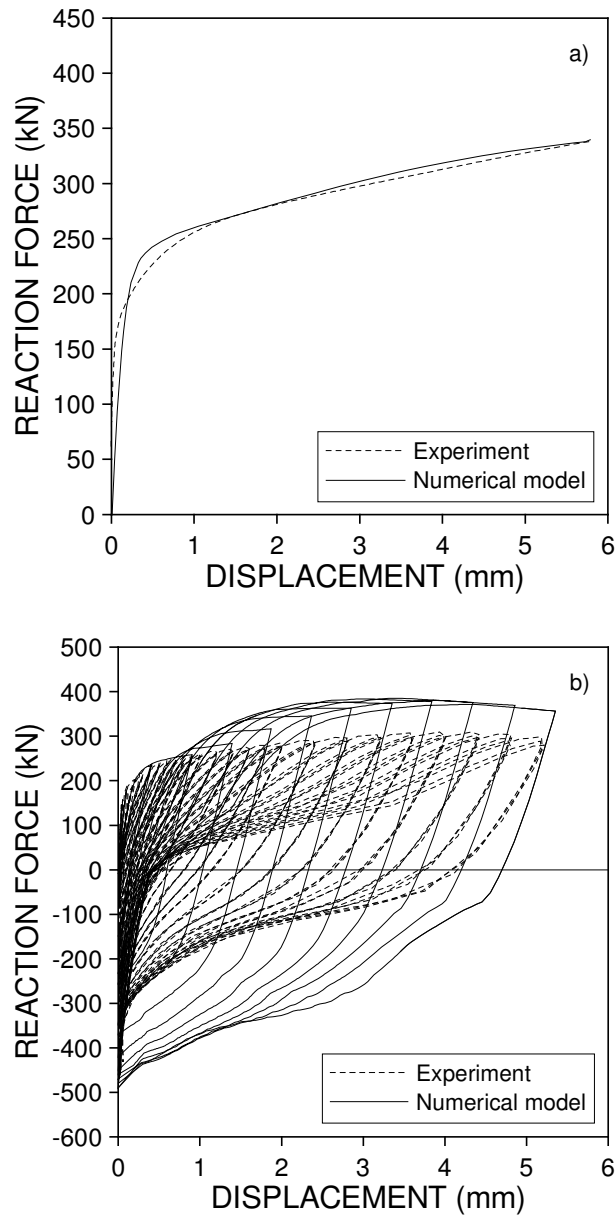


Figure 3.31. Experimental and predicted force vs. displacement of: (a) TM-2 specimen; (b) TC-2 specimen

Nonetheless, the simulation overestimates the response at large displacements owing to the lack of strength degradation.

It is possible to make similar consideration for the ITS TM-3 and TC3 specimens. The experimental reaction force vs. the controlled displacement relevant to the ITS TM-3 specimen is illustrated in Figure 3.32a, whereas the numerical simulation of

3. SEISMIC BEHAVIOUR OF BOLTED END PLATE BEAM-TO-COLUMN STEEL JOINTS

the TC-3 joint relevant to the cyclic regime with the isotropic strain-hardening model and the experimental response are reported in Figure 3.32b. Experimental data and numerical prediction are in a good agreement; this indicates a satisfactory behaviour of the numerical models employed.

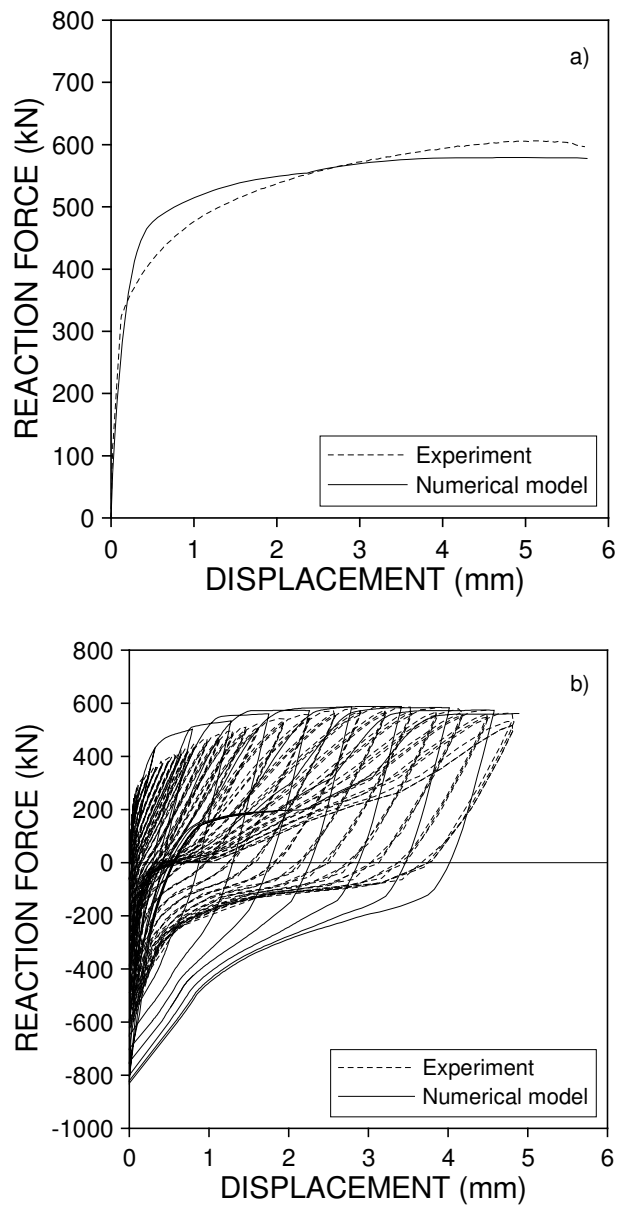


Figure 3.32. Experimental and predicted force vs. displacement of: (a) TM-3 specimen; (b) TC-3 specimen

3. SEISMIC BEHAVIOUR OF BOLTED END PLATE BEAM-TO-COLUMN STEEL JOINTS

3.7.2 FE Models of the CJ specimens

Non-linear FE analyses of the tested Complete Joints were carried out both by 2D and 3D models in a monotonic loading regime. As a matter of fact, 3D finite element analyses of bolted connections are very demanding from a computational standpoint. Hence, 2D models endowed with eight-node CPS8 plane stress elements were adopted to reduce the computational expense. For completeness some analyses have been repeated with 3D FE models, as 2D models tend to average stresses along the joint width.

In a way similar to the models used for the Isolated Tee Stubs, 2D models of the CJ specimens exploited FE layers to reproduce the end plate and additional FE layers to simulate the bolt shank. Both the specimens endowed an end plate with flange thickness of 12 mm and 18 mm are modelled. The models include details such as boltholes and bolts; surface-to-surface contact elements are used to model the surface interaction, neglecting friction, which has a negligible effect on the joint response (Bursi and Jaspart, 1998). Moreover, constraint equations are introduced to make the bolt heads continuous with the end plate. Bolt pre-tensioning is applied by prescribed displacements at the end of the bolt shank, in order to entail a final average shank stretch equal to 0.065 mm, similar to that detected during testing. These displacements are held constant throughout the loading. Welding-induced residual stresses develop unavoidably in the welds and in the base metal owing to thermo elasto-plastic deformation. Therefore, an idealised stress distribution as the one highlighted in Figure 3.28 has been introduced. One more time, at the weld toe where stress concentrations are expected, a refined FE mesh is adopted. A crack endowed with a length of 0.26 mm (small-to-moderate root defect) was modelled at the weld toe in order to investigate the behaviour of cracked connections. More specifically, cracking is studied through contour integral evaluation in order to infer J values. The model is shown in Figure 3.33 and represents the JA1-2 CJ specimen, endowed with a 12 mm end plate thickness coupled with the column of HEA180 profile.

Keeping the above-mentioned characteristics of the 2D model, a very complex 3D model of the specimen was performed in order to investigate the real stress and strain distribution along the width of the joint. With a view to confirming the hypotheses of 2D analyses, one of the main objectives that it was be obtained with the 3D model was increased accuracy in the computed local stress-strain state of the beam flange region due to weld residual stress and high gradients of stresses, where the connection has the highest fracture potential. The realised model is reported in Figure 3.34 and it represents the JB1-3 CJ specimen, endowed with an 18 mm end plate thickness coupled with the column of HEB180 profile. It is

3. SEISMIC BEHAVIOUR OF BOLTED END PLATE BEAM-TO-COLUMN STEEL JOINTS

characterized by reduced integration twenty-node solid elements (C3D20R in the ABAQUS library).

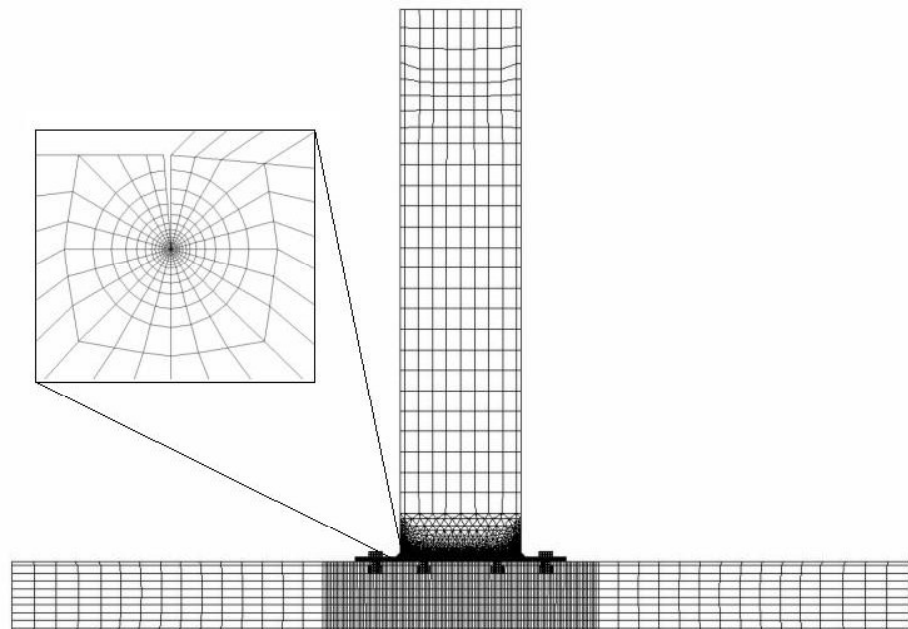


Figure 3.33. 2D FE model of a complete joint JA1-2

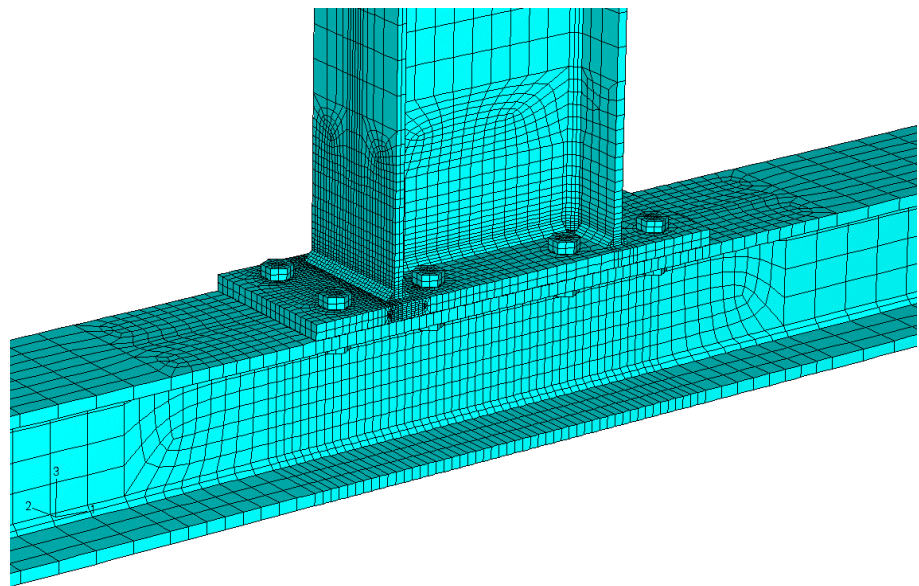


Figure 3.34. 3D FE model of a complete joint JB1-3

3. SEISMIC BEHAVIOUR OF BOLTED END PLATE BEAM-TO-COLUMN STEEL JOINTS

Both the 2D and 3D FE analyses account for material non-linearities through classical plasticity based on the Von Mises yield criterion. Isotropic hardening is assumed for the analyses. The measured stress-strain properties of the different materials (column flange, column web, end plate, beam flange, beam web and bolts) obtained by tensile test were used. Elastic and inelastic convergence studies have been conducted to evaluate and arrive at the final mesh for the finite element models. The finite element model was verified by comparing the measured monotonic and cyclic response of specimens with the predicted monotonic response (see Figure 3.35). As far as it concerns the cyclic test, the envelope curve of the experimental tests was found and compared to the curve found using the finite element model. Experimental data and numerical prediction are in a very good agreement. The specimen yield strength is well captured as expected; moreover the numerical simulation captures very well the hardening branch of the experimental response, both in term of strength and stiffness; this indicates a satisfactory behaviour of the numerical models. It is important to underline that the 3D numerical model seems to be more efficient by comparison with the experimental data. This means that the model is able to capture the 3D effects in terms of stress and strain distribution that have a significant effect on the global response of the joint.

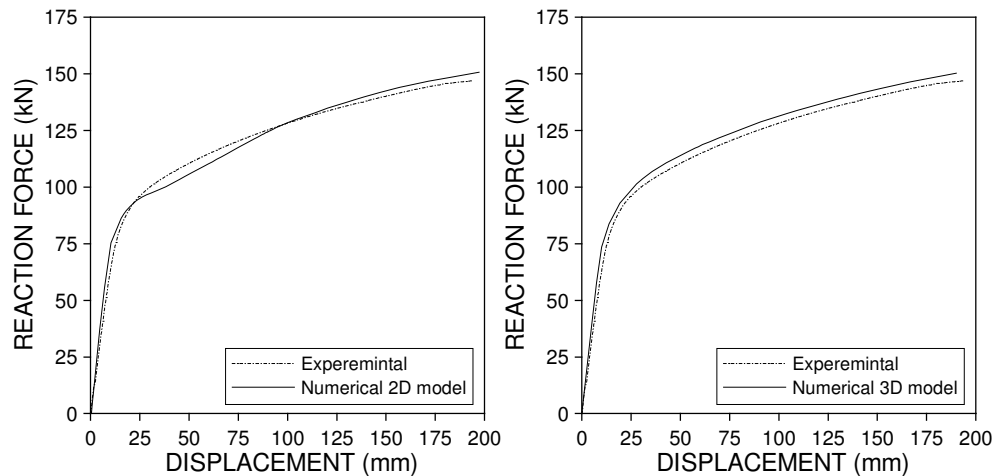


Figure 3.35. Experimental and predicted force vs. displacement of JB1-3 specimen

Moreover, the deformed configuration and the shear stress distribution in the steel joint can be estimated, for instance, through the plot of Figure 3.36. The 3D model allows the distribution of shear stresses in the panel zone to be appraised. As a result, high von Mises stresses approach values in a large zone of the web panel.

3. SEISMIC BEHAVIOUR OF BOLTED END PLATE BEAM-TO-COLUMN STEEL JOINTS

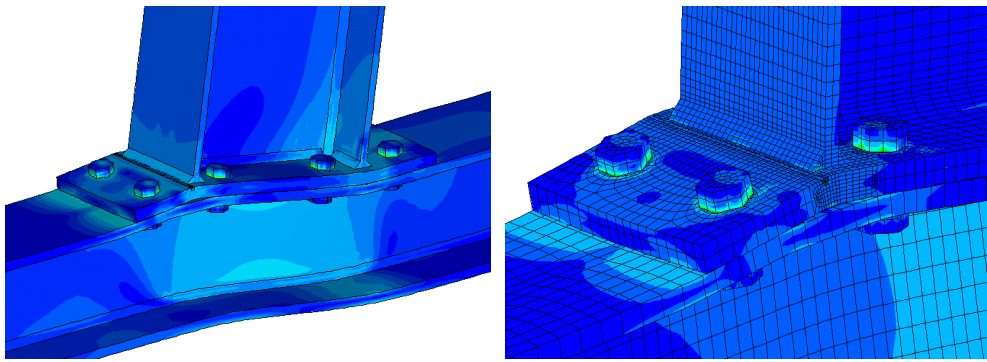


Figure 3.36. Von Mises stress distribution on the deformed joint configuration

High tensile residual stresses are known to promote brittle fracture and fatigue; and for fatigue problems, the residual stresses appear as mean stresses imposed on the exterior damage-inducing stress cycles. Thereby, both the magnitude and the distribution of residual stresses need to be included to accurately estimate weld fatigue life (Zhang and Dong, 2000). In a view to confirming the hypotheses of 2D analyses, a sub-model shown in Figure 3.37 was developed to obtain increased accuracy in the computed local stress-strain state of the beam flange region of the connection due to weld residual stress, where the connection has the highest fracture potential. Figure 3.37 depicts a substructure composed of 9314 DC3D20 elements of the JB1-3 joint, which was subjected to a total effective thermal input of 10.08 kW according to the parameters of Table 3.7, with a total arc efficiency η equal to 0.9. The displacement results of the global model are used for the boundary conditions around the perimeter boundary of the sub-model.

Solid wire (1,2 mm diameter)	Arc voltage (V)	Welding current (A)	Arc travel speed (mm/s)
AWSA5.18-R70S-6	32	350	5

Table 3.7. Welding parameters adopted for partial fillet welds

The distribution of residual stresses provided by the substructure along the flange thickness is reported in Figure 3.38, for three different flange sections. One may observe the variability of longitudinal stresses along the flange width; moreover, the distribution of residual stresses exploited in the 2D model, is inaccurate only at the top surface of the end plate.

3. SEISMIC BEHAVIOUR OF BOLTED END PLATE BEAM-TO-COLUMN STEEL JOINTS

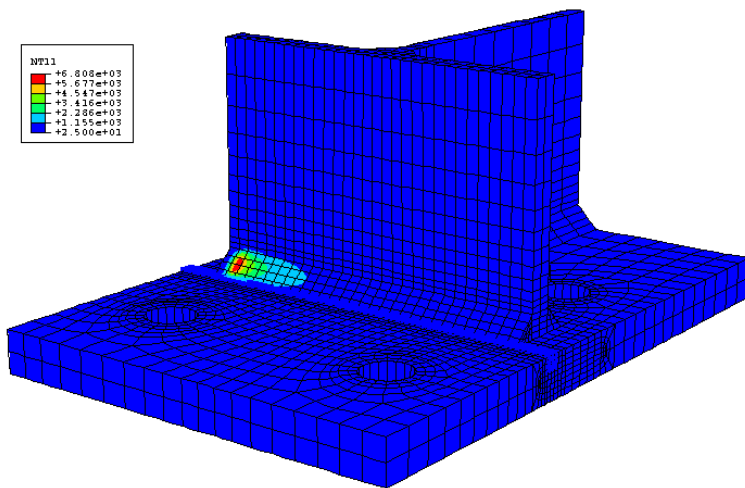


Figure 3.37. 3D substructure of the JB1-3 joint used for the single-pass weld

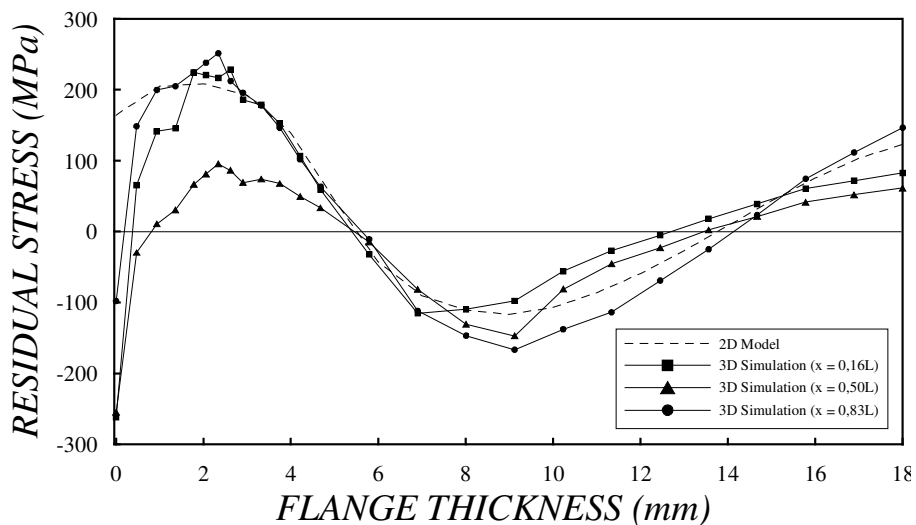


Figure 3.38. Transverse residual stress distribution

3.7.3 Parametric analyses

The parametric analyses presented in the foregoing investigate the influence of some design parameters on the fracture resistance of bolted steel component parts. In detail, the effects of the weld-to-base metal yield strength ratio, of the residual stress influence and of the end plate yield-to-ultimate strength ratio are determined through 2D and 3D non-linear finite element analyses of ITS and CJ connections, respectively. Furthermore, as noted above, the parametric study is

3. SEISMIC BEHAVIOUR OF BOLTED END PLATE BEAM-TO-COLUMN STEEL JOINTS

conducted for monotonic loading conditions only. As in prior analytical studies on welded moment connections performed by El-Tawil et al. (1998), it is assumed that the conclusions drawn from this study are qualitatively applicable to cyclic conditions.

In order to reduce the computational effort, the onset of cracking method is considered in the models. Hence, the J-integral is adopted to characterize the energy release associated with the crack growth. As sharp cracks are considered, see Figure 3.29b, an accurate evaluation of the contour integral is obtained.

Toughness demands are quantified in the analyses by means of the CTOD index, that represents the tearing at the crack tip. In detail, the CTOD is determined in the analyses evaluating the J-integral and converting it into the CTOD value by means of Eq. (3.1).

To evaluate and compare the different analyzed connection configurations for ductile fracture potential, a rupture index is computed at different locations of the connection. Others [6] have used the same approach in analytical connection studies. The rupture index (RI) is defined as:

$$RI = \frac{\frac{\varepsilon_p}{\varepsilon_y}}{\exp\left(-1.5 \frac{\sigma_m}{\sigma_{eff}}\right)} \quad (3.16)$$

where ε_p , ε_y , σ_m and σ_{eff} are, respectively, the equivalent plastic strain, yield strain, hydrostatic stress, and equivalent stress (also known as von Mises stress). The rupture index was motivated by the research of Hancock and MacKenzie (1976) on the equivalent plastic rupture strain of steel for different conditions of stress triaxiality. The process of ductile fracture initiation is caused by high tensile triaxial stresses (i.e., high tensile hydrostatic stress) that result in damage accumulation through microvoid nucleation and coalescence. The ratio of hydrostatic stress-to-von Mises stress (σ_m/σ_{eff}) that appears in the denominator of (16) is called the triaxiality ratio (TR). High triaxiality can cause a large reduction in the rupture strain of a material, thereby limiting its ductility (Lemaitre, 1996). For instance, a value of triaxiality ratio in the range $0.75 < \sigma_m/\sigma_{eff} < 1.5$ may cause a large reduction of the ultimate strength in metals, whereas a triaxiality ratio $\sigma_m/\sigma_{eff} > 1.5$ entails fragile behaviour. Thus, locations in a connection with higher values for RI have a greater potential for fracture. The ratio of equivalent plastic strain-to-yield strain that appears in the numerator of (1) is called the plastic equivalent strain (PEEQ) index. This index is a measure of the local inelastic strain demand, and is also useful in comparing the different analyzed configurations. The PEEQ index is computed by:

3. SEISMIC BEHAVIOUR OF BOLTED END PLATE BEAM-TO-COLUMN STEEL JOINTS

$$\text{PEEQ Index} = \frac{\sqrt{\frac{2}{3}\epsilon_{ij}^p\epsilon_{ij}^p}}{\epsilon_y} \quad (3.17)$$

where ij are the plastic strain components.

The triaxiality ratio and PEEQ index are also computed at different locations of the connection to provide additional means of comparing the analyzed connection configurations. The locations determined to have the highest fracture potential in the different analyzed configurations are in the weld toe region, near the interface of the weld metal and base metal.

Weld matching effects

Analyses with different weld matching conditions were carried out to investigate the joint response in terms of toughness demand. In detail, two models have been analysed: the first with overmatching welds characterized by mechanical properties very close to those of the experimental specimens; the second with matching welds in which the mechanical properties of welds are equal to those of the end plate material. Analyses with this different weld-matching conditions were carried out for:

- the TM-2 specimens. The Tee stub models are designated ITS2-1 and ITS2-2, respectively, and the corresponding mechanical properties are collected in Table 3.8. A crack length equal to 1.30 mm has been considered in order to maximize the effect of residual stresses when included.
- the TM-3 specimens. The Tee stub models are designated ITS3-1 and ITS3-2, respectively, and the corresponding mechanical properties are collected in Table 3.8. A crack length equal to 2.34 mm has been considered in order to maximize the effect of residual stresses when included.
- the JB1-3 specimen. The CJ models are designated CJ3-1 and CJ3-2, respectively, and the corresponding mechanical properties are collected in Table 3.8. The same crack length of the TM3 specimen, equal to 2.34 mm, has been considered.

For brevity, only the results of one specimen will be illustrated. The reaction force vs. the applied displacement for the TM-3 specimen is reported in Figure 3.39a. However differently from the overall behaviour, the corresponding CTOD demands are similar until a total displacement of 0.35 mm (see Figure 3.39b), from which the CTOD demand increases rapidly for the ITS3-1.

3. SEISMIC BEHAVIOUR OF BOLTED END PLATE BEAM-TO-COLUMN STEEL JOINTS

For the joint configuration under exam, the matching weld condition, viz. the ITS3-2 case, appears to be the most beneficial in terms of fracture toughness demand.

Specimen	Material	E (MPa)	f_y (MPa)	f_u (MPa)
ITS2-1	Base metal	210000	265	600
	Weld Metal	220000	520	640
ITS2-2	Base metal	210000	265	600
	Weld Metal	210000	265	600
ITS3-1	Base metal	210000	307	517
	Weld Metal	220000	520	640
ITS3-2	Base metal	210000	307	517
	Weld Metal	210000	307	517
CJ3-1	Base metal	210000	307	517
	Weld Metal	220000	520	640
CJ3-2	Base metal	210000	307	517
	Weld Metal	210000	307	517

Table 3.8. Parameters of the constitutive laws for TM-2, TM-3 and JB1-3 models

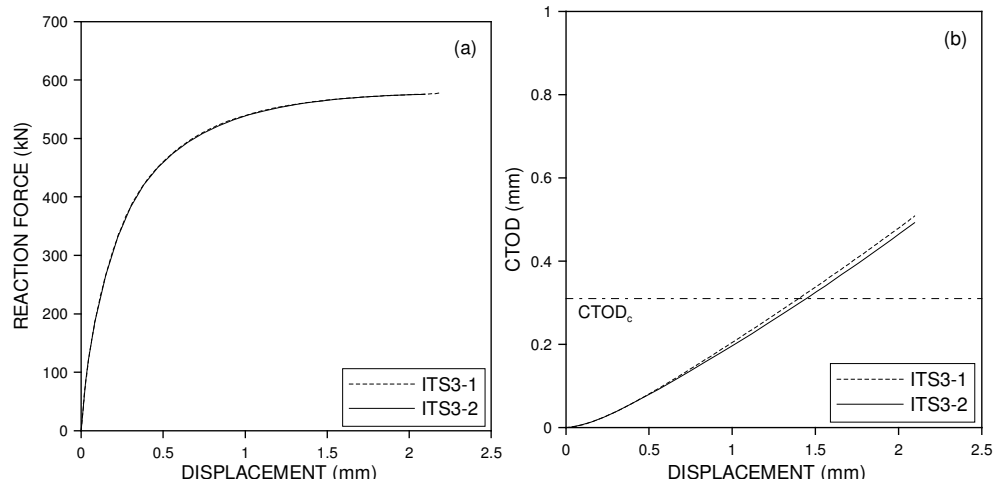


Figure 3.39. Predicted force and CTOD vs. displacement of TM-3 specimens with overmatching (ITS3-1) and matching (ITS3-2) welds

This behaviour can be explained through the equivalent plastic strain (PEEQ) distributions highlighted in Figure 3.40. During the loading process, identified by the two displacement levels (L1) and (L2), the yielded material in the weld metal corresponding to the ITS3-2 condition shields the crack tip from a stress increase.

3. SEISMIC BEHAVIOUR OF BOLTED END PLATE BEAM-TO-COLUMN STEEL JOINTS

Therefore, the CTOD demand at the crack tip is low. The aforementioned effect is less marked in the overmatching weld condition ITS3-1.

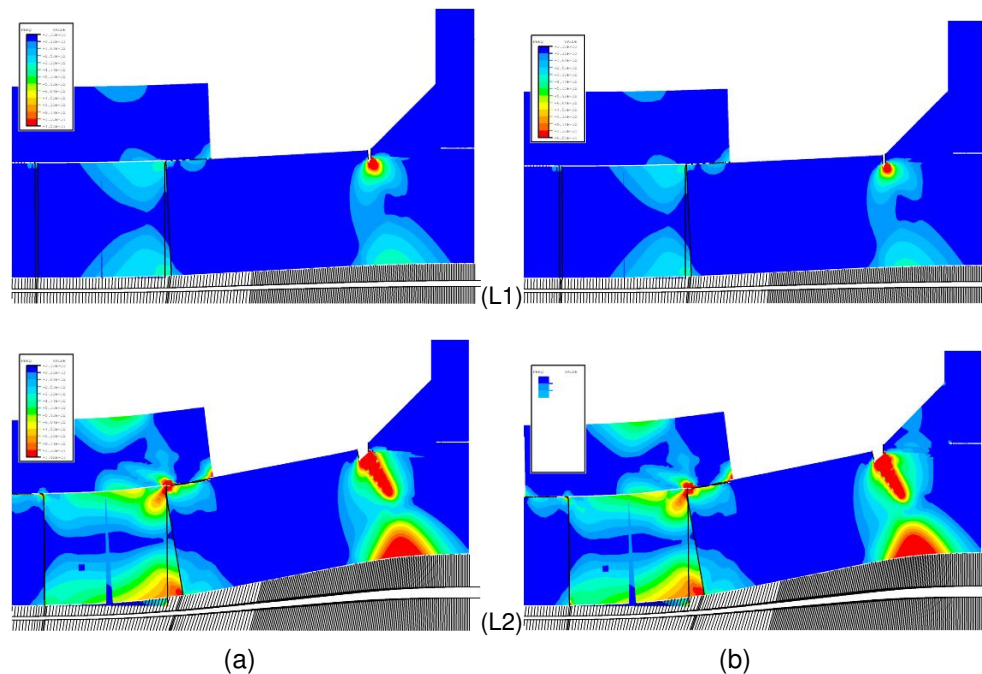


Figure 3.40. Equivalent plastic strain (PEEQ) distribution of TM-3 specimens at two levels of applied displacements: (a) overmatching weld (ITS3-1); (b) matching weld (ITS3-2)

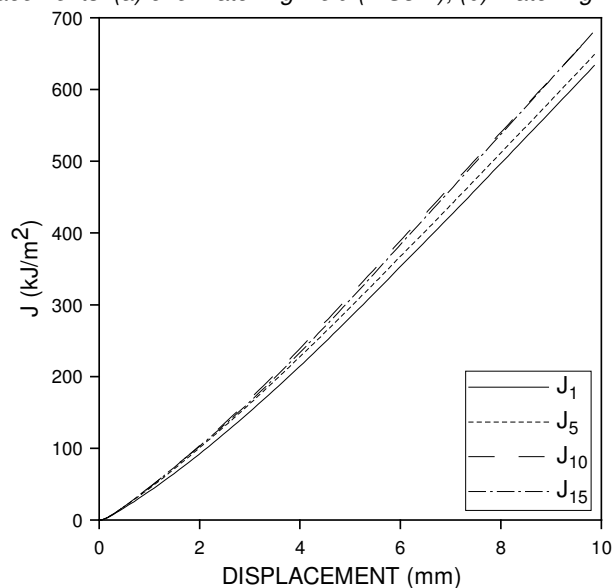


Figure 3.41. Values of J-integral for different contours as functions of the applied displacement

3. SEISMIC BEHAVIOUR OF BOLTED END PLATE BEAM-TO-COLUMN STEEL JOINTS

Similar results are obtained for the TM-2 and JB1-3 specimens. In order to verify the quality of these analyses, the values of J-integral for different paths 1, 5, 10 and 15 are plotted in Figure 3.41 as a function of the applied displacement with reference to the specimens ITS2. More specifically, 1 represents the J-integral computation from the first ring of elements abutting the crack tip whilst 15 corresponds to the path surrounding all the elements of the “spider web” mesh illustrated in Figure 3.29b. The values of J1, J5, J10, and J15 agree with each other entailing path independence at the given applied displacement. It is worthwhile to recall that the estimate provided through the first ring of elements surrounding the crack tip does not provide high accurate results (Bursi et al, 2002).

Residual stress effects

Rapid uneven heat removal in welded connections entails large welding-induced residual stresses that can influence the joint behaviour in several ways. A detailed investigation of these effects for welded beam-to-column moment connections can be found in (Zhang et Dong, 2000). For the ITS connections of 12 mm thickness, an idealised residual stress pattern like the one highlighted in Figure 3.28 has been used, assuming a crack length equal to 1.30 mm and considering an overmatching weld. Relevant results are reported in Figure 3.42a and Figure 3.42b: results show clearly that the presence of residual stresses increases the toughness demand.

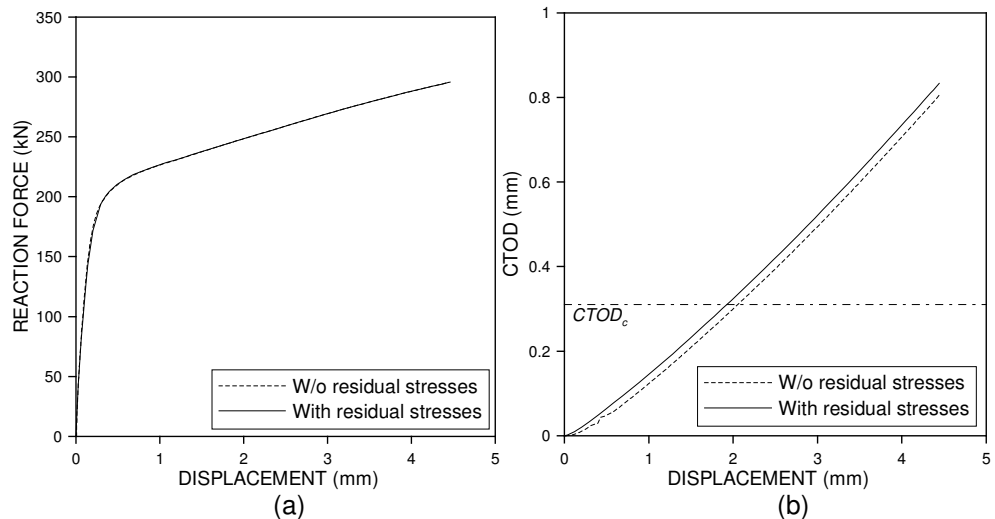


Figure 3.42. (a) Predicted force vs. displacement and (b) CTOD vs. displacement of TM-2 specimens with and without residual stresses

The same idealised residual stress pattern has been used also for the ITS connections with 18 mm thickness with a crack length equal to 2.34 mm and for the

3. SEISMIC BEHAVIOUR OF BOLTED END PLATE BEAM-TO-COLUMN STEEL JOINTS

CJ connection with 18 mm thickness with the same crack length. The results are then compared. The maximum CTOD required along the end plate width close to the weld toe predicted both by 2D and 3D analyses is depicted in Figure 3.43. The 3D analysis reveals a significant gradient across the width of the flange with a peak value in correspondence with the web. The CTOD ratio between 3D and 2D FE models is around 16 per cent.

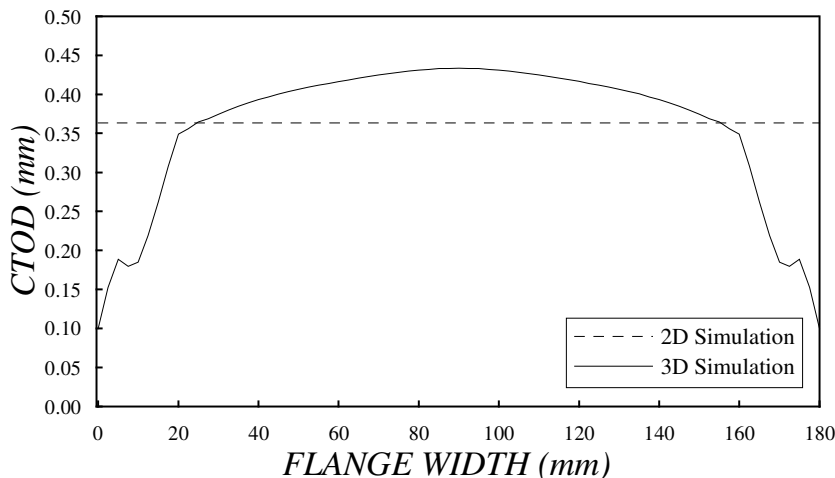


Figure 3.43. 2D versus 3D CTOD distribution at the weld toe for a crack depth of 2.34 mm

Yield-to-ultimate stress ratio effects

The plastic hinge region in a steel structure decreases as the yield-to-ultimate strength ratio σ_y/σ_u increases. In fact, a smaller yielded region imposes greater inelastic strain demands to achieve a specified plastic deformation. Since the production of American structural steel has resulted in steel with much higher ratios (Frank, 1997), recently published specifications from AISC (1997) recognized this effect and limited the yield-to-ultimate strength ratio to 0.85. A similar limitation is required by Eurocode 3 (2001), when plastic analysis has to be performed.

In order to study the yield-to-ultimate strength ratio effect on the joint configuration with 12 mm and 18 mm thickness, two strength ratios for the end plate material have been considered. More specifically, for the TM-2 specimen, σ_y/σ_u has been chosen to be 0.45 and 0.90 whilst the corresponding specimens are designated ITS2-45 and ITS2-90, respectively. However, two crack lengths equal to 1.30 mm and 2.86 mm have been considered for the specimen ITS2-45 and ITS2-90, respectively, to take account of the increase of crack-initiation threshold with the reduction of a strain hardening amount (Barsom and Rolfe, 1987). The reaction force vs. the controlled displacement of the TM-2 model is shown in Figure 3.44a,

3. SEISMIC BEHAVIOUR OF BOLTED END PLATE BEAM-TO-COLUMN STEEL JOINTS

whilst the corresponding CTOD demand is illustrated in Figure 3.44b. From the above-mentioned plots, one may observe that at large displacements, the condition in which σ_y/σ_u tends to 0.90, viz. ITS2-90, is the most favourable from a fracture mechanics standpoint.

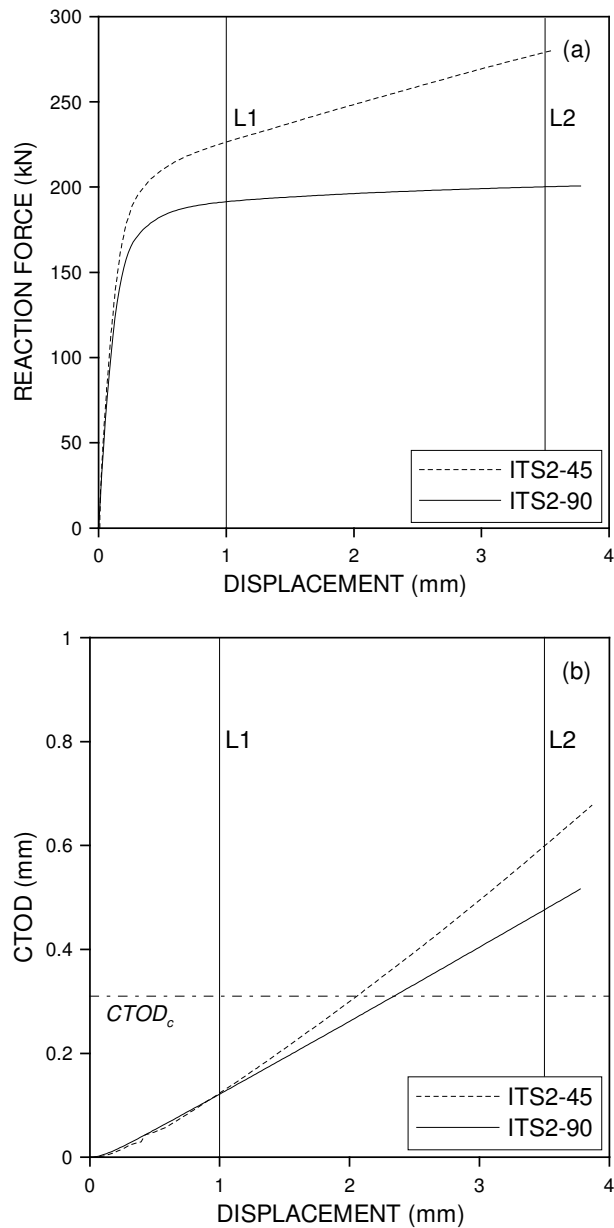


Figure 3.44. Predicted force and CTOD vs. displacement of TM-2 specimens at $\sigma_y/\sigma_u=0.45$ and $\sigma_y/\sigma_u=0.90$

3. SEISMIC BEHAVIOUR OF BOLTED END PLATE BEAM-TO-COLUMN STEEL JOINTS

On the other hand, the corresponding strain distributions highlighted in Figure 3.45 indicate that the end plate yield zone is smaller for the specimen labelled ITS2-90. Therefore, a balance between the two opposite requirements has to be found.

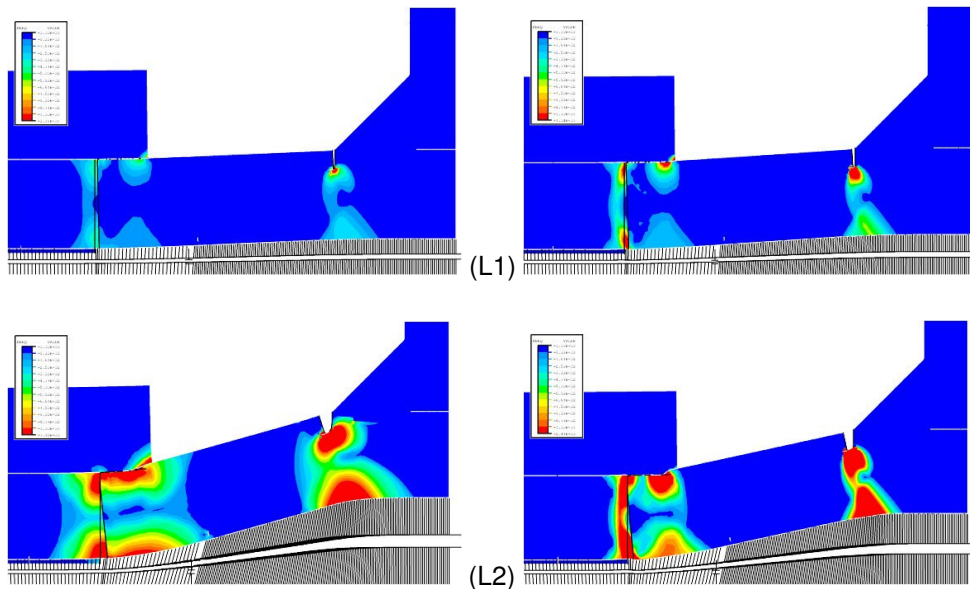


Figure 3.45. Equivalent plastic strain (PEEQ) distributions of TM-2 specimens at two levels of applied displacements: (a) $\sigma_y/\sigma_u=0.45$ (ITS2-45); (b) $\sigma_y/\sigma_u=0.90$ (ITS2-90)

As far as the ITS connections with 18 mm thickness is concerned, two strength ratios σ_y/σ_u for the end plate material equal to 0.60 and 0.90 have been considered and the corresponding specimens are called ITS3-60 and ITS3-90, respectively. Again, to take into account that the crack-initiation threshold increases with a strain-hardening reduction, two crack lengths equal to 2.34 mm and 4.95 mm have been chosen for the specimen ITS3-60 and ITS3-90, respectively. Similar results are obtained, as shown in Figure 3.46.

So far we have estimated critical states both in 2D and 3D models through the use of a critical value of the CTOD, which amounts to 0.31 mm for the joints under examination. It is possible to define critical stress states through the use of response indices, which do not require a crack modelling. One of these indices is the Rupture Index related to the stress triaxiality ratio σ_m/σ_{eff} , where σ_m defines the hydrostatic stress and σ_{eff} is the von Mises stress. Several FE analyses were conducted to estimate this index at the weld toe. 2D simulations confirm that end plates with $\sigma_y/\sigma_u = 0.6$ exhibit a favourable value of the triaxiality ratio of about 0.49, implying a ductile behaviour. The corresponding 3D analyses yield a maximum triaxiality ratio sampled at the weld toe in the middle of the end plate of

3. SEISMIC BEHAVIOUR OF BOLTED END PLATE BEAM-TO-COLUMN STEEL JOINTS

about 0.62; such value does not entail a limited ductility of the joints or a high potential for crack initiation.

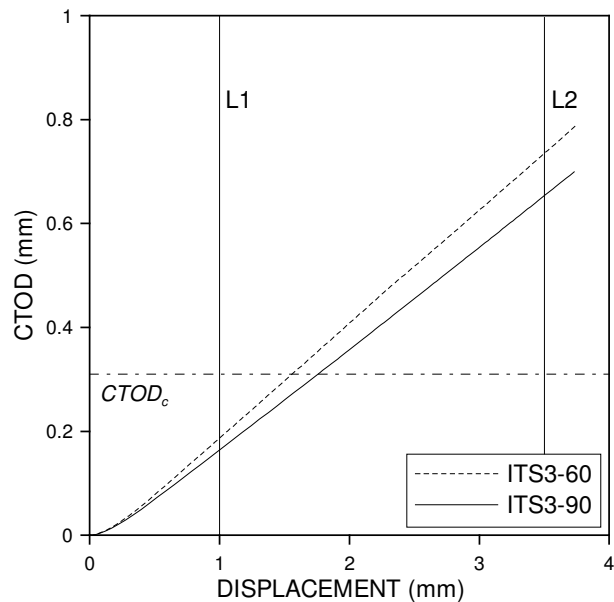


Figure 3.46. Predicted CTOD vs. displacement of TM-3 specimens at $\sigma_y/\sigma_u=0.60$ and $\sigma_y/\sigma_u=0.90$

3.8 Conclusions

A general test programme was presented, comprising partial strength bolted extended end plate joints with fillet welds and component parts, which represent an alternative to fully welded connections for use in seismic force resisting moment frames. The main results indicate that partial strength bolted extended end plate connections are suitable for use in seismic moment resisting frames. They represent an alternative to fully welded connections, as together with the column web panel yielding, they can exhibit favourable ductility and energy dissipation properties.

As far as the understanding of the low-cycle fracture behaviour of ITS, CTS, and CJ connections is concerned, experiments and numerical analyses under monotonic and cyclic loading have provided insights in order to develop rules able to reduce fracture in the aforementioned connection components. The main conclusions of this study follow.

3. SEISMIC BEHAVIOUR OF BOLTED END PLATE BEAM-TO-COLUMN STEEL JOINTS

- i. When proper consideration is given to material selection and detailing, extended end plates show a cyclic performance adequate for seismic design. The considered joints exhibit a plastic rotation greater than 35 mrad; therefore, they can be classified as *ductile* in accordance to Eurocode 8 (2002). In detail, test results on isolated bolted Tee stubs as well complete extended end plate bolted joints have shown that the overall behaviour of the specimens under investigation is governed by the material endowed with the lowest strength, viz. the base metal, in which yielding occurs, effectively. In fact, the weld metal persists in the elastic regime while the contiguous zones are weakened owing to the sharp thermal treatments and to structural as well as shape discontinuities.
- ii. Component cyclic tests enable identification of the failure mode. Moreover, they allow the Code requirements on the rotational capacity of the joint to be checked. Moreover, the mechanical models provided by the Eurocodes to determine the stiffness and strength characteristics of the individual components showed little agreement with the experimental data.
- iii. A *component model*, which approximates the cyclic response of the joints on the basis of the responses of the elemental components, does not seem to possess sufficient accuracy. Conversely, the use of *macro-components*, incorporating some of the interaction effects among elemental components, appears to be more adequate.
- iv. The simulations relevant to isolated Tee stub and Complete Joint connections indicate that the numerical model with isotropic hardening rule is able to capture both the monotonic and the cyclic responses but is not able to reproduce properly stiffness and strength degradation.
- v. A number of parametric analyses have been performed by considering fractures initiating from weld-root defects by means of the onset cracking method. Conclusions drawn from the models indicate that:
 - a. fracture driving force demands are reduced by using fillet welds matching the end plate material;
 - b. welding-induced residual stresses increase the fracture demand;
 - c. connections with $\sigma_y/\sigma_u = 0.9$ exhibit reduced fracture driving force demands but also limited plastic regions. The yield-to-ultimate strength reduction must comply with the requirements of plastic analysis.

Besides, the study is currently concentrating on the damage evolution aspect both for the components and the joint. The availability of adequate damage assessment methods is a pre-requisite to the development of reliable hysteretic models for research as well for design purposes.

3. SEISMIC BEHAVIOUR OF BOLTED END PLATE BEAM-TO-COLUMN STEEL JOINTS

3.9 References

- Adey B.T., Grondin G.Y. and Cheng J.J.R. (1998): *Extended End Plate Moment Connections under Cyclic Loading*. J. of Construct. Steel Res., Elsevier Applied Science, UK, 46:1-3, 435-436.
- AISC (1992): *Seismic provisions for structural steel buildings*, Chicago, USA.
- AISC (1997): *Shape Material – ASTM A572 Gr. 50 with Special Requirements*. Tech. Bull. N. 3, Chicago.
- Astaneh-Asl A. (1995): *Seismic design of bolted steel moment-resisting frames*. In Steel Tips, Structural Steel Education Council, Moraga, Calif., p. 82.
- ASTM E 813-89 (1989). *Standard Test Method for J1c, a Measure of Fracture Toughness*. Annual Book of ASTM Standards, Philadelphia; 646-660.
- ASTM E 1290-93 (1993): *Standard Test Method for Crack-Tip Opening Displacement (CTOD) Fracture Toughness Measurement*. Philadelphia: Annual Book of ASTM Standards; 866-875.
- ATC (1992): *Guidelines for cyclic seismic testing of components of steel structures for buildings*. Rep. No. ATC-24, Applied Technology Council, Redwood City, CA.
- Bahaari M. R. and Sherbourne A.N. (2000): *Behavior of eight-bolt large capacity end plate connections*. Computers & Structures, Pergamon Press, UK, 77, 315-325.
- Barsom JM. and Rolfe ST. (1987): *Fracture and Fatigue Control in Structures – Applications of Fracture Mechanics*. Prentice-Hall.
- Bernuzzi C., Zandonini R. and Zanon P. (1996): *Experimental analysis and modelling of semi-rigid steel joints under cyclic reversal loading*. J. of Construct. Steel Res., Elsevier Applied Science, UK, 38:2, 95-123.
- Bertero V.V., Anderson J.C. and Krawinkler H. (1994): *Performance of Steel Building Structures During the Northridge Earthquake*. Rep. No. UCB/EERC-94/04. California: University of California, Berkeley.
- Bjorhovde R., Brozzetti J. and Colson A. (1988): *Connections in Steel Structures: Behaviour, Strength & Design*. Elsevier Applied Science, London, UK, 395.
- Bjorhovde R. et al. (1992): *Connections in Steel Structures II: Behaviour, Strength & Design*. AISC, Chicago, USA, 464.

3. SEISMIC BEHAVIOUR OF BOLTED END PLATE BEAM-TO-COLUMN STEEL JOINTS

- Bjorhovde R., Colson A. and Zandonini R. (1996): *Connections in Steel Structures III: Behaviour, Strength & Design*. Pergamon Press, London, UK, 594.
- Bose B., Sarkar S., and Bahrami M. (1996): *Extended end plate connections: comparison between three-dimensional non-linear finite element analysis and full scale tests*. Structural Engineering Review, Pergamon Press, UK, 8:4, 315-328.
- Bursi O.S. and Jaspart J.P. (1997): *Calibration of a finite element model for isolated bolted end plate steel connections*. J. of Construct. Steel Res., Elsevier Applied Science, UK, 44:3, 225-262.
- Bursi O.S. and Jaspart J.P. (1998): *Basic issues in the finite element simulation of extended end plate connections*. Computers & Structures, Pergamon Press, UK, 69, 361-382.
- Bursi O.S., Ferrario F. and Fontanari V. (2002): *Non-linear Analysis of the Low-cycle Fracture Behaviour of Isolated Tee Stub Connections*. Computers and Structures, 80, 2333-2360.
- Colson A. (1992): *First State of the Art Workshop, EU Project COST C1: Semi-rigid Behaviour of Civil Engineering Structural Connections*. European Commission, Belgium, 582.
- Deng C.G., Bursi O.S. and Zandonini R. (1998): *Analysis of Moment Resisting Steel Connections under Reversed Cyclic Loading*. Proc. of the Fourth Int. Conf. on Computational Structures Technology, Edinburgh, UK.
- ECCS (1986): Recommended Testing Procedure for Assessing the Behaviour of Structural Steel Elements under Cyclic Loads. ECCS Publication n°45.
- El-Tawil S., Mikesell T., Vidarsson E. and Kunnath, S.K. (1998): *Strength and ductility of FR welded-bolted connections*. Report No. SAC/BD-98/01, SAC Joint Venture, Sacramento, CA.
- Easterling, S.W. and Leon R.T. (2002): *Connections in Steel Structures IV: Behaviour, Strength & Design*. AISC, Chicago, USA, 473.
- European Committee for Standardization (2001): *Eurocode 3: Design of Steel Structures. Part 1.1: General Rules and Rules for Buildings*. European Prestandard – ENV 1993-1-1, Belgium.
- European Committee for Standardization (2002): *Eurocode 4: Design of composite steel and concrete structures, Part 1.1 General rules and rules for buildings*. European Prestandard – prEN 1994-1-1, CEN/TC250/SC4 N259, Belgium.

3. SEISMIC BEHAVIOUR OF BOLTED END PLATE BEAM-TO-COLUMN STEEL JOINTS

- European Committee for Standardization (2002): *Eurocode 8: Design of Structures for Earthquake Resistance. Part 1: General Rules, Seismic Actions and Rules for Buildings.* European Prestandard – ENV 1998-1;
- Frank K.H. (1997): *The Physical and Metallurgical Properties of Structural Steels.* Report No SAC 95-09. California: Applied Technology Council, Redwood city, 1997.
- Ghobarah A., Osman A. and Korol R.M. (1990): *Behavior of extended end plate connections under cyclic loading.* Engineering Structures, 12:1, 15-27.
- Ghobarah A., Korol R.M. and Osman A. (1992): *Cyclic behavior of extended end plate joints.* J. Struct. Engr., ASCE, USA, 118:5, 1333-1353.
- Hancock J.W. and MacKenzie A.C. (1976): *On the mechanisms of ductile failure in high-strength steels subjected to multi-axial stress states.* Journal Mech. Phys. of Solids; 24, 147–69.
- Hibbit, Karlsson & Sorensen Inc. (2001): *ABAQUS - User's Manual.* Version 6.2. Vol. 1-3.
- Kukreti A.R. and Biswas P. (1997): *Finite element analysis to predict the cyclic hysteretic behavior and failure of end plate connections.* Computers & Structures, Elsevier Science Ltd., UK, 65, 127-147.
- Kuwamura H. (1998): *Fracture of Steel During an Earthquake: State of the Art in Japan.* Engineering Structures, Vol. 20, No 4-6, 310-322.
- Lemaitre J. (1996): *A course on damage mechanics.* Berlin: Springer Verlag.
- Lorenz R.F., Kato B. and Chen W.F. (1993): *Semi-rigid Connections in Steel Frames.* Council on Tall Buildings and Urban Habitat, Mc Graw Hill, USA, 318.
- Maquoi R. (1999): *Control of the semi-rigid behaviour of civil engineering structural connections.* Proc. of the International Conference, EU Project COST C1, Publication EUR 18854 EN, Belgium, 579.
- Monahan C.C. (1985): *Early fatigue crack growth at welds.* Computational Mechanics Publications, Southampton, UK.
- Nader M.N. and Astaneh-Asl A. (1991): *Dynamic behavior of flexible, semi-rigid and rigid steel frames.* J. of Construct. Steel Res., Elsevier Science Ltd., UK, 18, 179-192.
- Nethercot D. and Zandonini R. (1988): *Methods of prediction of joint behaviour – Beam-to-column connections, Structural Connections – Stability and Strength.* Ed. R. Naranayan, Elsevier Applied Science, London, UK, 23-62.

3. SEISMIC BEHAVIOUR OF BOLTED END PLATE BEAM-TO-COLUMN STEEL JOINTS

- SAC Joint Venture. Interim Guidelines (1995): *Evaluation, Repair, Modification and Design of Welded Steel Moment Frame Structures.* Report No. SAC-95-02, FEMA 267, August.
- SAC Joint Venture. Background Reports (1997): *Metallurgy, Fracture Mechanics, Welding, Moment Connections and Frame System Behaviour.* Report No. SAC-95-09, FEMA 288, March.
- Wald F. (1994): Second State of the Art Workshop, EU Project COST C1: *Semi-rigid Behaviour of Civil Engineering Structural Connections.* European Commission, Belgium, 561.
- Zhang J. and Dong P. (2000): *Residual Stresses in Welded Moment Frames and Implications for Structural Performance.* Journal of Structural Engineering, 126:306-315, 2000.

4 SEISMIC RESPONSE OF PARTIAL-STRENGTH COMPOSITE JOINTS

4.1 Introduction

In seismic design practice, the possibility of relying appreciably on dissipation effects translates into seismic design actions lower than those called for in brittle structures, which can count on elastic resources alone. In turn, lower design actions, which standards provide through higher values of the behaviour factor, allow for lower design values of plastic resistance, and therefore smaller structural sections and lower weights as well. The savings in terms of structural weight, when coupled with sufficient ease of execution, may render ductile structures very competitive in seismic areas. Solutions assuring the necessary ductility can be obtained not only through careful study of building morphology, structural schemes and construction details, but also through the rational use of materials.

Composite construction design, which represents a good compromise in term of strength and ductility solution, has been increasingly used over recent decades (USA, Japan and some European countries) mostly in office buildings, commercial buildings, parking areas and bridges. However, despite the advantages it presents, composite construction is still scarcely used in seismic design.

The main reasons could possibly be the lack of experience, skilled workers and appropriate equipment on the one hand and the non-existence of codes for the design of these structures on the other hand. In fact, Eurocode 8 (prEN 1998-1, 2002) sets forth general principles for designing composite structures for seismic areas and imposes precise constructional and performance guidelines; however it does not provide adequate information on the use of the various structural schemes, or on the associated constructional solutions and design methodologies, for which it often refers designers to codes and regulations regarding non-earthquake-resistant structures.

4. SEISMIC RESPONSE OF PARTIAL-STRENGTH COMPOSITE JOINTS

When analysing the possible structural solutions, it becomes immediately evident that the use of composite columns and beams, by stiffening the structural elements and therefore significantly limiting second-order effects, can allow the erection of buildings of considerable height without the need to use bracings. This advantage, combined with the introduction of partial strength joints, guarantees the formation of global dissipative frame mechanisms for seismic loadings, and it avoids unwanted storey or local mechanisms. If associated to suitable constructional solutions, such structural types can undoubtedly provide significant advantages in terms of both economy and performances (Braconi et al., 2003).

Clearly, the choice of such structural systems in current design practice cannot leave out the preliminary evaluation and mechanical definition of the different possible connection types and the associated structural details.

The present study illustrates the results of a European research (Ecoleader-ECSC joint Project) aimed at evaluating the rotational and dissipative capacities of a particular type of connection between a concrete partially encased column and a steel-concrete composite beam. The design of the connection, successively verified on the basis of experimental substructure tests, has been conducted by extending to the inelastic range the method described in Section 8 of Eurocode 4 (Bursi et al, 2003). From the obtained knowledge on connection and member response, a numerical model of the prototype structure has been developed to examine its seismic behaviour through non-linear static (push-over) and dynamic analyses. Simulated ground motion time histories that match the design response spectrum were used in the dynamic analyses. This analytical work permitted to predict the performance of the frame and to propose an appropriate magnitude level of ground motion for the pseudo-dynamic tests on a full-scale model of a frame building expressly designed using the connections and structural details suggested by the results of the analyses.

4.2 The Ecoleader-ECSC joint project

The objective of the Ecoleader-ECSC joint project is to develop an experimental database on the behaviour of low-rise steel-concrete composite structures with partial strength semi-rigid connections subjected to gravity and lateral loads. In particular, information was needed on the behaviour of the beam-to-column joints and the structural overstrength exhibited by composite frames. Moreover, in order to evaluate the feasibility and effectiveness of the composite construction with

4. SEISMIC RESPONSE OF PARTIAL-STRENGTH COMPOSITE JOINTS

semi-rigid partial-strength beam-to-column joints and partially encased columns in earthquake-prone regions, the project aims at calibrating design rules affecting the aforementioned components and the participation of the concrete slab in the relevant transfer mechanisms. Another objective of the project was also the development of non-linear mechanical models combined with smooth hysteretic and damage models of composite members, joints and frames capable of reproducing the experimental response. As a matter of fact, it is intended to calibrate damage models for members and connections and correlate the damage obtained at the inter-storey levels with the damage obtained at the members and connections.

A basic construction typology was selected for the study that includes regular composite beams connected to partially encased composite columns with partially restrained end plate connections. Within the project, a prototype 2-storey, 4-bay structure was designed to obtain representative dimensions, member sizes and connection details to examine the seismic behaviour of the structural system. Pseudo-dynamic testing of a full-scale specimen including 3 of the 5 frames of the prototype structure will be conducted in 2003 at the JRC ELSA Unit in Ispra (Italy) to examine its seismic response.

4.3 Description of the prototype structure

The prototype structure considered for this study is shown in Figure 4.1. It is a 2-storey, 12.0 m x 12.0 m x 7.0 m structure, which includes five two-bay moment resisting frames with unequal spans (5 m + 7 m). All five moment resisting frames are identical and one frame is illustrated in Figure 4.2. In the direction perpendicular to the moment resisting frames, simply supported secondary beams are used at column lines to link the frames together and lateral resistance is provided by two concentrically braced steel frames located along the exterior walls. Only the behaviour of the structure in the direction parallel to the moment resisting frames (X direction in Figure 4.1) is considered herein. The frame to be tested at Ispra only includes the three interior moment resisting frames, along with the secondary beams and the transverse cross bracing.

The columns are partially encased composite columns, which guarantee significant structural efficiency with respect to static, seismic loads and fire resistance. They are fixed at their base and continuous over the full height of the structure. The steel profiles are HEB260 and HEB280 for the exterior and interior columns,

4. SEISMIC RESPONSE OF PARTIAL-STRENGTH COMPOSITE JOINTS

respectively. As shown in Figure 4.3, longitudinal ($\phi 12$) and transversal ($\phi 8$) reinforcing steel was provided in the concrete portions of the columns and shear studs are used to ensure composite action between the concrete and the steel shapes. The spacing of the stirrups and shear studs varies along the column height. At the base and near the beam-column joints, the stirrups are spaced at 50 mm for both column types. Elsewhere, the spacing is increased to 150 mm. No concrete is used at both floor levels over the depth of the beams.

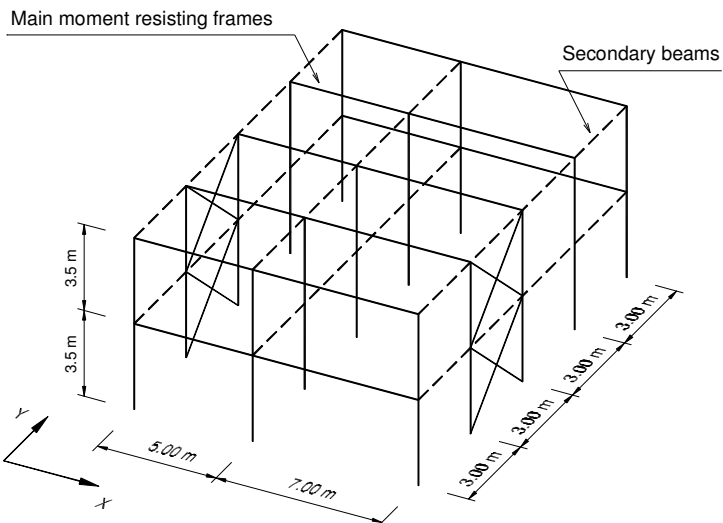


Figure 4.1. Three-dimensional view of the prototype structure

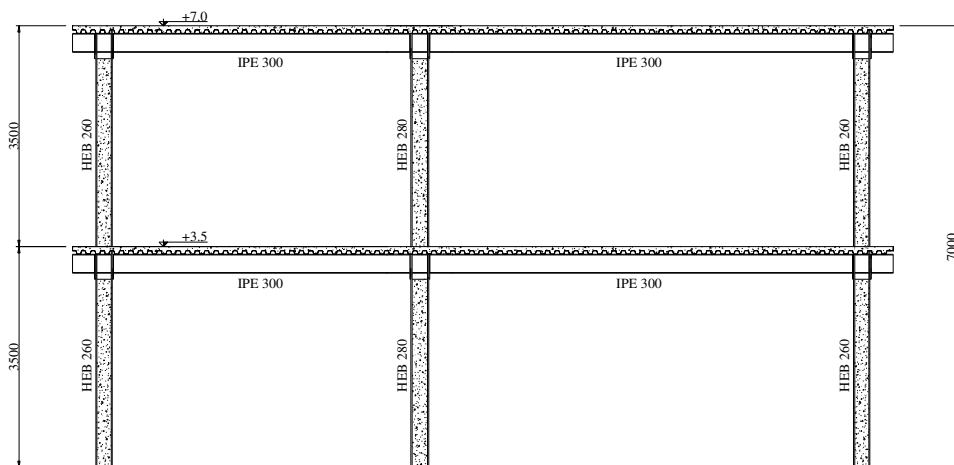


Figure 4.2. Elevation of a typical 2D Moment Resisting Frame

Photos on Figure 4.4 and Figure 4.5 show details of the column bases. The base plate is 40 mm thick and measures 400 mm x 600 mm. It is connected to the

4. SEISMIC RESPONSE OF PARTIAL-STRENGTH COMPOSITE JOINTS

foundations by means of 6 anchor bolts made with $\phi 32$ hooked reinforcing steel bars with their upper ends being threaded. A 150 mm long stub made of a HEB140 profile is welded under the base plate to transfer the horizontal shear to the foundation in the direction parallel to the loading. Base plate stiffeners are installed on each side of the columns to improve fixity about the column strong axis. They are made of 12 mm thick plates that extend over a height of 250 mm. The distance between the underside of the base plate and the top of the first floor slab is 3500

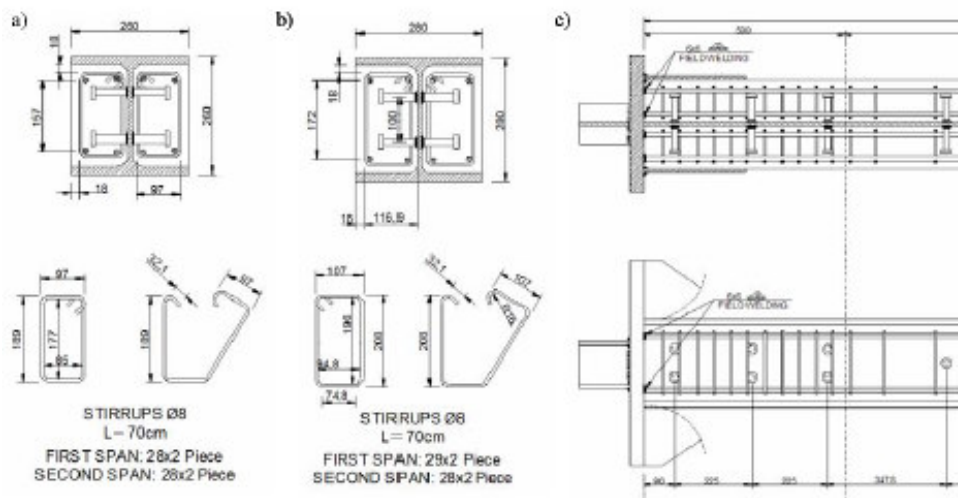


Figure 4.3. 2.3 Details of the column bases: a) cross-section of the exterior columns; b) cross-section of the interior columns; c) longitudinal cross-section and side view



Figure 4.4. Details of the column bases during fabrication of the Ispra test frame

4. SEISMIC RESPONSE OF PARTIAL-STRENGTH COMPOSITE JOINTS



Figure 4.5. Column base plate during fabrication of the Ispra test frame

The beams of the moment frames (see Figure 4.6) are made of IPE300 sections that act compositely with the 150 mm thick concrete slab. The slab is poured on a 55 mm deep trapezoidal composite steel deck (Brollo EGB210 profile). The flutes of the deck are spaced at 150 and are oriented perpendicular to the direction of the moment frames. Shear studs arranged in pairs are used at every rib to ensure composite action with the beams. The shear connection degree between the steel profile and the concrete slab is full. For the prototype structure, the slab extends 500 mm beyond the exterior column lines in both directions.

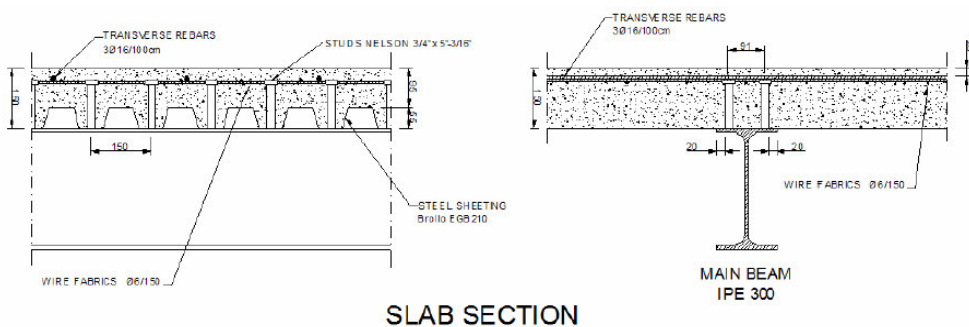


Figure 4.6. Details of the floor slab/beam assembly

The beam-to-column joint has been designed so as to provide adequate structural performances both under monotonic and cyclic loading. To this aim, a relatively

4. SEISMIC RESPONSE OF PARTIAL-STRENGTH COMPOSITE JOINTS

thin end-plate connection, illustrated in Figure 3, has been chosen, which guarantees predictable and efficient performance for seismic actions. The details of an exterior beam-to-column joint are illustrated in Figure 4.7. The connections are partially restrained, or semi-rigid, extended end plate connections. On the basis of constructional considerations and of the favourable seismic behaviour of the column web panel, the solution adopted relies on naked steel columns. In detail, the reinforced concrete encasement is interrupted in the connection, as shown in Figure 4.7. A pair of stiffening plates, set horizontally and welded to the column, guarantees full exploitation of the web panel's inelastic resources. Additional $\phi 12$ transverse and longitudinal reinforcing steel is placed in the floor slab at joint locations so that the slab participates to the transfer of bending moments between the columns and the beams.

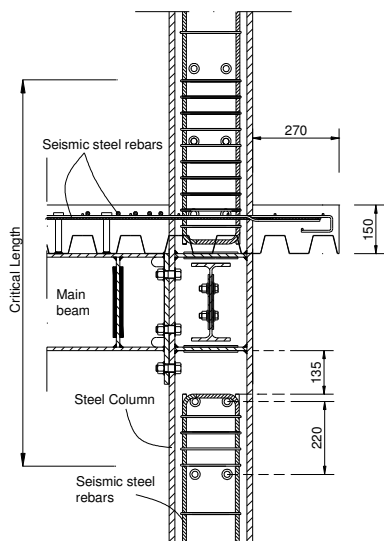


Figure 4.7. Details of the beam-column at the exterior joints

The transverse beams are IPE240 sections and simple shear connections are used at their ends. No shear studs are welded to the beams, so that their contribution to the lateral resistance in the direction of loading is negligible. The transverse lateral bracing is an X-bracing made with L50x100x8 angles, as shown in Figure 4.8.

The specifications for the structural materials are:

- Structural steel: Class S235 ($f_y = 235$ MPa, $f_u = 360$ MPa, $\epsilon_u = 28\%$)
- Concrete: Class C25/30 ($f'_c = 25$ MPa)
- Reinforcing Steel: Class B450-C ($f_y = 450$ MPa, $f_y/f_u < 1.35$, $\epsilon_u = 7.5\%$)

4. SEISMIC RESPONSE OF PARTIAL-STRENGTH COMPOSITE JOINTS

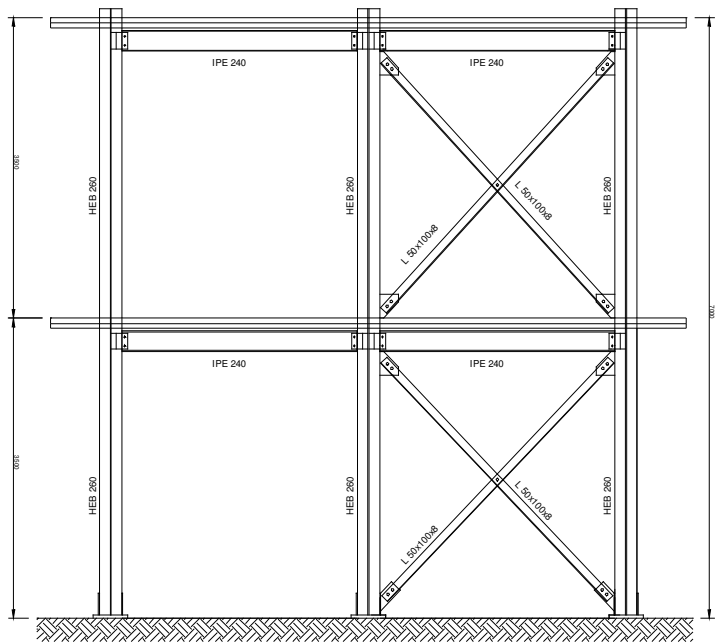


Figure 4.8. Elevation of the frames perpendicular to the direction of loading (Ispra test frame)

4.4 Seismic design of the prototype structure

The seismic design of the prototype structure, carried out by the research groups of the Universities of Pisa and Trento, has been executed by using the rules included in the following standards:

- prEN 1991-1-1:2001 “Actions on structures, Part 1-1: general actions, densities, self-weight, imposed loads for buildings” - Final Draft, July 2001;
- prEN 1992-1:2001 “Design of concrete. Part 1: general rules and rules for buildings” –Draft n° 2, January 2001;
- prEN 1993-1-1:2001 “Design of steel structures. Part 1.1: general rules” Draft n° 2, 2001;
- prEN 1994-1-1:2001 “Design of composite steel and concrete structures. Part 1-1: general rules and rules for buildings” – Draft n° 3, March 2001;
- prEN 1998-1:2002 “Design of structures for earthquake resistance. Part 1: general rules, seismic actions and rules for buildings” –Draft n° 5, January 2002.

4. SEISMIC RESPONSE OF PARTIAL-STRENGTH COMPOSITE JOINTS

University of Pisa acts as responsible of the design and execution of the 3D tests in the framework of the ECSC project 7210-PR-250 “*Applicability of composite structures to sway frames*”, coordinated by RWTH, Aachen, while University of Trento is the coordinator of a Ecoleader-Jrc project for access to the ELSA infrastructure entitled “*Cyclic and PsD testing of a 3D steel-concrete composite frame*”.

Only the main aspects that are relevant to the seismic resistance of the moment resisting frames in the direction of loading are summarised herein.

The uniformly distributed gravity dead load at both floors, w_D , was taken equal to 4.68 kPa, including the weight of the floor slab-steel deck assembly (3.18 kPa) and an additional dead load of 1.5 kPa (mechanical equipments, finishes, etc.). The weight of the beams and columns must be added to these values: IPE300 beams = 0.42 kN/m, IPE240 beams = 0.31 kN/m, HEB260 partially encased columns = 2.33 kN/m, and HEB280 partially encased columns = 2.67 kN/m. A uniformly distributed imposed live load, w_L , of 5.0 kPa was assumed at both levels.

The design seismic loads at each level, F_i , were determined by using the simplified modal response spectrum analysis method:

$$F_i = F_b \cdot \frac{z_i \cdot m_i}{\sum_i (z_i \cdot m_i)} \quad (4.1)$$

where F_b is the seismic base shear, and z_i and m_i are respectively the height from the base and the masses at each level. The seismic base shear is given by:

$$F_b = S_d(T_1) \cdot W \cdot \lambda \quad (4.2)$$

where $S_d(T_1)$ is the ordinate of the design spectrum at the fundamental period of vibration of the building for translational motion in the direction considered, T_1 , W is the total weight of the building, and λ is a corrective factor. The equations and the values of the soil parameter, S , and the reference periods T_B , T_C , and T_D that are required to construct Types 1 and 2 design spectra are given for different subsoil conditions. For this project, the following key parameters were adopted:

- Type 2 spectrum
- Peak ground acceleration, $a_g = 0.40$ g
- Subsoil Class A (Rock site, or alike, with $V_{s,30} > 800$ m/s)
- Behaviour factor, $q = 6.0$ (Concept a, Structural ductility Class S dissipative composite structure, with assumed multiplier $\alpha_u/\alpha_1 = 1.2$)

4. SEISMIC RESPONSE OF PARTIAL-STRENGTH COMPOSITE JOINTS

For these conditions, $S = 1.0$ and the reference periods T_B , T_C , and T_D are respectively equal to 0.05 s, 0.25 s, and 1.2 s. The period T_1 for the structure was calculated with the formula: $T_1 = 0.05 \cdot H^{0.75}$, with $H = 7.5$ m (total structure height), giving $T_1 = 0.22$ s. The value of S_d (0.22 s) = 0.167.

The seismic weight at each level includes the total gravity loads and the following fraction of the imposed live load: 48% at the first level ($\phi = 0.8$, $\psi_{2i} = 0.6$) and 60% at the second level ($\phi = 1.0$, $\psi_{2i} = 0.6$). The resulting total seismic weight, W , including the weight of the structural members is given in Table 4.1. In this calculation, the weight of a 3.5 m and a 1.75 m long column segments were applied respectively at the first and second levels. Assuming rigid diaphragm response, the seismic weight was divided equally between the 5 moment resisting frames, resulting in $W = 552$ kN/frame. The parameter λ in Eq. (4.2) is equal to 0.85 because $T_1 < 2 T_C$. Substituting these values, the base shear, F_b , is equal to 78.2 kN per frame. In Table 4.1, the base shear force was distributed at each level using Eq. (4.1) and assuming $m_i = W_i/g$.

Level	z (m)	w_d (kPa)	$\psi_e w_L$ (kPa)	TOTAL W (kN)	W / Frame (kN)	F / Frame (kN)
2	7.0	3.94	3.00	1398	280	52.6
1	3.5	3.94	2.40	1361	272	25.6
				2759	552	78.2

Table 4.1. Calculation of the seismic weights and seismic loads (torsion excluded)

The design was performed only for one of the interior moment resisting frames. Accidental torsion was included in the design and the most critical frames are those located at 3.0 m from the center of the structure. For these frames, an amplification factor, δ , equal to 1.15 (= 1.0 + 0.6 · 3.0/12.0) was used. Therefore, the final seismic loads were: 60.5 kN and 29.4 kN at levels 1 and 2 with a total base shear of 89.9 kN. In the design of the frames, these loads were combined with the total gravity dead load and 60% of the imposed live loads.

4. SEISMIC RESPONSE OF PARTIAL-STRENGTH COMPOSITE JOINTS

4.5 Seismic design of the composite joint

For moment resisting frame structures, the maximum structural ductility is attained through the formation of global mechanisms (Gioncu et al., 2002). To this end, it is necessary to foresee sufficient overstrength of the columns satisfying the relation:

$$\sum M_{Rc} \geq 1.3 \cdot \sum M_{Rb} \quad (4.3)$$

where

$\sum M_{Rc}$ is the sum of moments corresponding to the development of the design values of the resisting moments of the columns;

$\sum M_{Rb}$ is the sum of moments corresponding to the development of the design values of the resisting moments of the partial strength joints.

The ductile behaviour of the joints is guaranteed by defining an appropriate hierarchy of resistance for each component. In this respect, with reference to sagging moments, the end-plate and the column flange under bending as well as the column web panel in shear have to be considered ductile components; whereas the concrete slab under compression and the bolts under tension are assumed to be brittle.

With regard to hogging moments, the steel rebars under tension and, once again, the end-plate and the column flange under bending, as well as the column web panel under shear are considered ductile components; while the column web panel and the beam flanges under compression are assumed to be brittle. Brittle failure of the bolts in tension before yielding of the end plate and/or of the column flange can be easily averted by satisfying the following relation:

$$t \geq 0.36 \cdot d \cdot \sqrt{\frac{f_{ub}}{f_y}} \quad (4.4)$$

where t is the thickness of the end plate or of the column flange; d and f_{ub} are the nominal diameter and ultimate tensile stress of the bolts, respectively; and f_y the yielding stress of the base materials of the considered component (prEN 1993-1, 2000). For the remaining components, we applied the capacity design according to Table 4.2 and Table 4.3, respectively. It is also necessary to ensure that the joint possesses adequate resistance and rotational capacity.

4. SEISMIC RESPONSE OF PARTIAL-STRENGTH COMPOSITE JOINTS

Component	(1)	(2)	(3)
End plate and column flange in bending (1)	---	$F_{Rd.2} \geq 1.3F_{Rd.1}$	$F_{Rd.1} = F_{Rd.3}^{(+)}$
Concrete slab in compression (2)	$F_{Rd.2} \geq 1.3F_{Rd.1}$	---	$F_{Rd.2} \geq 1.3F_{Rd.3}$
Web panel in shear (3)	$F_{Rd.3}^{(+)} = F_{Rd.1}$	$F_{Rd.2} \geq 1.3F_{Rd.3}$	---

Table 4.2. Joint capacity design for sagging bending moment

Component	(1)	(2)	(3)
Reinforcing bars and I bolt-row in tension (1)	---	$F_{Rd.2} \geq 1.3F_{Rd.1}$	$F_{Rd.1} = F_{Rd.3}^{(+)}$
Beam flange in compression (2)	$F_{Rd.2} \geq 1.3F_{Rd.1}$	---	$F_{Rd.2} \geq 1.3F_{Rd.3}$
Web panel in shear (3)	$F_{Rd.3}^{(+)} = F_{Rd.1}$	$F_{Rd.2} \geq 1.3F_{Rd.3}$	---

Table 4.3. Joint capacity design for hogging bending moment

As far as resistance is concerned, particular attention must be paid for the definition and calculation of the strength of the concrete slab in compression (component 2 in the Table 2) and of the column web panel in shear (component 3)

4.5.1 Concrete slab resistance

Eurocode 8 Annex C (2002) contains some formulas that refer to the design of the slab and of its connection to the steel frame in moment resisting frames in which beams are composite T-beams comprising a steel section with a slab. The Annex has been developed and validated experimentally in the context of composite moment frames with rigid connections and plastic hinges forming in the beams; it is clearly stated that the expressions in the Annex have not been validated for cases with partial strength connections in which deformations are more localised in the joints. According to this Annex two conditions have to be fulfilled to ensure that a high ductility in bending is obtained:

- early buckling of the steel part shall be avoided;
- early crushing of the concrete of the slab shall be avoided.

The first condition imposes an upper limit on the cross-sectional area A_s of the longitudinal reinforcement in the effective width of the slab. The second condition imposes a lower limit on the cross-sectional area A_t of the transverse reinforcement in front of the column.

4. SEISMIC RESPONSE OF PARTIAL-STRENGTH COMPOSITE JOINTS

Under sagging bending moments, composite T sections can be ductile if the crushing of the concrete is avoided. The buckling failure of the steel walls normally does not control the ultimate limit state of composite beams under sagging bending moments, because of the connections between the upper flange and the concrete. To avoid concrete failure under sagging bending moment, the proportions of a composite steel-concrete section must be such that the steel on the bottom side yields before the concrete strain ϵ_c at the top of the section are too high; for reinforced concrete elements submitted to cycling loading, this is deemed to be satisfied when $\epsilon_c \leq 2 \cdot 10^{-3}$, when the strains ϵ_s in steel are high enough to obtain the required local ductility μ . Under earthquake loading at the connection of beam to column, a sagging bending moment on one side, and a hogging bending moment on the other side, are transmitted to the column. This implies one transfer of forces from the steel part of the composite section, which takes place through steel connecting elements and for which a design practice does exist, and another transfer of two forces F_{sc} and F_{st} from the slab. F_{sc} is the resulting compression force in the slab, on the sagging moment side, while F_{st} is the resulting tension force of the re-bars, on the hogging moment side (Plumier et al, 1998).

The transfer of the compression force F_{sc} from the slab to the column can be realised through two mechanisms, as illustrated in Figure 4.9.

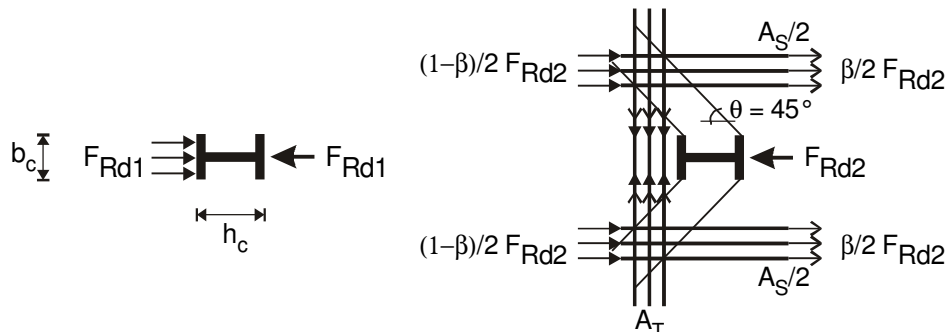


Figure 4.9. Two basic mechanisms of force transfer from the slab to the column

Mechanism 1 is the direct compression of concrete on the flange of the column. Mechanism 2 is a truss with two compressed struts and one steel tie in tension. This mechanism can be developed only when the column cross-section has some concave zones or special connecting devices on the sides. The design resistance of these two mechanisms can be estimated in a way similar to the one used in the design of reinforced concrete structure.

The design resistance F_{Rd1} of Mechanism 1 is simply:

4. SEISMIC RESPONSE OF PARTIAL-STRENGTH COMPOSITE JOINTS

$$F_{Rd1} = f_{cd} \cdot t_{slab} \cdot b_c \quad (4.5)$$

where f_{cd} is the strength of the concrete in compression, t_{slab} is the thickness of the concrete slab and b_c is the column width. F_{Rd1} is a rather concentrated force, which is spread through the width of the slab and induces a transverse tension force F_{t1} , which requires transverse anti bursting reinforcements. The spreading of this force approximately takes place on a distance equal to the half effective width b_{eff} of the slab and generates a transverse tension force F_{t1} , which can be computed explicitly if b_{eff} is defined. Under seismic action $l_0 = 0.7\ell$ is a reasonable estimate for the length l_0 of the beam between two points of moment reversal. Then according to Eurocode 4 we obtain:

$$b_{eff} = 2 \cdot b_e = 2 \cdot (0.7\ell) / 8 = 0.175\ell \quad (4.6)$$

The section of the steel needed for F_{t1} should be realized with several re-bars spread in a zone width equal to $0.6b_{eff}$, starting at a distance h_c of the column flange, as illustrated in Figure 4.10. Normally, the amount of the required re-bars is low and effectively already covered by the reinforcements needed for the gravity and live load resistance.

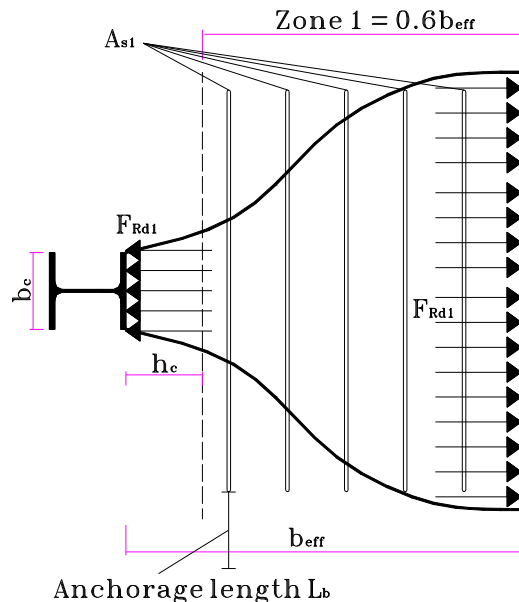


Figure 4.10. The spreading of F_{Rd1} and re-bars A_{s1} required by mechanism 1

4. SEISMIC RESPONSE OF PARTIAL-STRENGTH COMPOSITE JOINTS

For Mechanism 2, assuming an inclination $\theta = 45^\circ$ of the concrete struts, we have that the resistance of a compressed concrete strut, F_{ccs} is equal to:

$$F_{ccs} = \nu f_{cd} \cdot t_{slab} \cdot b_s \approx 0.6 \cdot f_{cd} \cdot t_{slab} \cdot \frac{h_c}{\sqrt{2}} \quad (4.7)$$

The resistance of the mechanism 2 results the sum of the component of two compressed struts in the direction of the force transferring in the column.

$$F_{Rd2} = 2 \cdot \frac{F_{ccs}}{\sqrt{2}} = 0.6 \cdot f_{cd} \cdot t_{slab} \cdot h_c \quad (4.8)$$

As Mechanism 2 is not intended to be the dissipative mechanism, an overstrength factor must be introduced; we must also take into account the fact that the concrete resistance νf_{cd} usually considered in Eurocode 2 for compressed struts is a safe side value. With an overstrength factor of 1.2 we obtain the formula contained in the current version of the Eurocode 8 (2002):

$$F_{Rd2} = 0.7 \cdot f_{cd} \cdot t_{slab} \cdot h_c \quad (4.9)$$

Because F_{t2} is equal for geometry to the resistance $F_{Rd2}/2$, the section A_{s2} of the steel re-bars into the main beam should comply with:

$$A_{s2} \geq \frac{F_{Rd2}}{2 \cdot f_{yd,T}} \quad (4.10)$$

These re-bars should be spread in a zone width equal to the dimension of the column flange as illustrated in Figure 4.11.

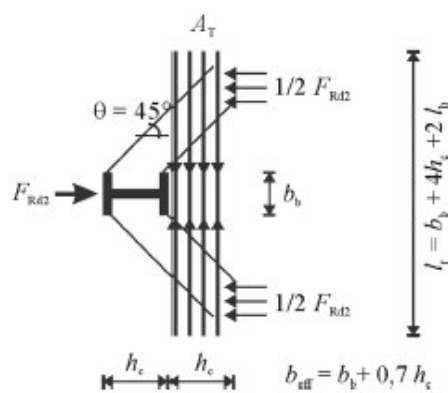


Figure 4.11. Re-bars A_{s2} required by mechanism 2

4. SEISMIC RESPONSE OF PARTIAL-STRENGTH COMPOSITE JOINTS

The transfer of the compression force from the slab, on the sagging moment side, can only take place through the two mechanisms described above. The highest resistance F_{Rd} offered at a beam-to-column connection can be estimated as the sum of F_{Rd1} and F_{Rd2} :

$$F_{Rd} = F_{Rd1} + F_{Rd2} = (b_c + 0.7 \cdot h_c) \cdot t_{slab} \cdot f_{cd} \quad (4.11)$$

Then, the effective width of concrete in the connection zone is, at the most:

$$b_{eff,conn} = b_c + 0.7 \cdot h_c \quad (4.12)$$

In general $b_{eff,conn} \ll b_{eff} = 0.175 \ell$ so that $b_{eff,conn} \approx 0.5 b_{eff}$. As the highest sagging bending moment in the beam under earthquake action is precisely developed in the connection zone, this result means that:

- the connection zone is the critical zone in which the highest strains are developed in both the concrete and the steel of the composite section;
- the plastic moment of the composite beam in that section should be computed considering an effective width $b_{eff,conn}$. As a consequence, the plastic neutral axis of the composite section is lower in the beam end section than in the mid-span section and it is practically impossible that the ratio between the steel and the concrete strains is such that ductility criteria for the composite section can be verified.

Considering the above evaluations, it can be concluded that it is impossible to develop a reliable composite plastic hinge at the end of the beams for sagging bending moments. Without other force transfer, the concrete in the beam-to-column connection zone will necessarily be crushed around the column after relatively low plastic rotations.

4.5.2 Column web panel shear resistance

The panel zone is the portion of the column contained within the beam–column joint. When a moment frame is subject to lateral loads, high shear forces develop within the panel zone. The resulting deformations of the panel zone can have an important effect on the response of the frame in both the elastic and inelastic ranges of frame behaviour (Tsai and Popov, 1988; Kim and Engelhardt, 1995). Numerous tests have been performed in the past three decades to investigate the load–deformation behaviour of the joint panel using connection subassemblies. Some significant observations from these tests are (Kim and Engelhardt, 2001):

4. SEISMIC RESPONSE OF PARTIAL-STRENGTH COMPOSITE JOINTS

- Joint panel zones often develop a maximum strength that is significantly greater than the strength at first yield. This additional strength has been attributed to strain hardening and to contributions of the column flanges in resisting panel zone shear forces. Large inelastic panel zone deformations are typically required in order to develop the maximum panel zone strength.
- Panel zone deformations can add significantly to the overall deformation of a moment resisting frame, for both elastic and inelastic ranges of behaviour.
- Panel zone stiffness and strength can be increased by the attachment of web doubler plates to the column within the joint region. The effectiveness of doubler plates is affected by the method used to connect them to the column.
- In the inelastic range, panel zones can exhibit very ductile behaviour, both for monotonic and cyclic loading. Experimentally observed hysteresis loops are typically very stable, even at large inelastic deformations.

Current US building code provisions (AISC, 1997; FEMA 350, 2000) permit the formation of plastic hinges in the panel zones of steel moment frames under earthquake loading. Thus, rather than forming plastic flexural hinges only in the beams or columns, a primary source of energy dissipation in a steel moment frame can be the formation of plastic shear hinges in the panel zones. Consequently, an accurate analytical model is needed to predict the response of the panel zone in order to predict accurately the response of a steel moment frame under earthquake loading,. The traditional center-to-center line representation of the frame must be modified to include panel zone deformation in frame analysis.

Several researchers, including Krawinkler et al. (1971) and Wang (1988) proposed relationships between panel zone shear force V and panel zone deformation γ for monotonic loading. These relationships have been used as the basis of mathematical models for non-linear rotational springs representing the panel zone. Krawinkler's $V-\gamma$ relations have been adopted in several building codes (ICBO, 1997; AISC, 1997) as a basis for computing the shear strength of panel zones. However, it was pointed out by Krawinkler that a new model might be needed for joints with thick column flanges since his $V-\gamma$ relations were derived from experimental and analytical results for panel zones with relatively thin column flanges. Wang also showed that Krawinkler's $V-\gamma$ relations may overestimate panel zone shear strength for panel zones with thick column flanges.

The mathematical model for strength and stiffness calculations is shown in Figure 4.12. It consists of an elastic-perfect plastic shear panel surrounded by rigid

4. SEISMIC RESPONSE OF PARTIAL-STRENGTH COMPOSITE JOINTS

boundaries with springs at the four corners. These springs simulate the resistance of the elements surrounding the panel zone, in particular the bending resistance of the column flanges.

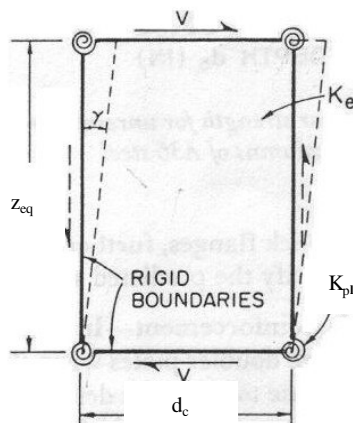


Figure 4.12. Mathematical model for the web panel in shear

If we use the mathematical model proposed by Krawinkler, it is possible to calculate the elastic stiffness of the web panel as follows:

$$K_{el} = G_{el} \cdot (H_c - t_{cf}) \cdot t_{cw} \quad (4.13)$$

where G_{el} is the elastic shear modulus; H_c is the column height; t_{cf} and t_{cw} are the thickness of the column flange and of the column web, respectively. This equation is valid until $\gamma < \gamma_y$: this value is achieved when the shear force at general yielding is equal to:

$$V_y = (H_c - t_{cf}) \cdot t_{cw} \cdot \frac{f_{y,cw}^*}{\sqrt{3}} \quad (4.14)$$

The $f_{y,cw}^*$ is the yield strength of the column web calculated adopting the Henky-Von Mises yield reduction criterion, when the column axial force is not negligible. The strength of the column web can be computed by means of the following relationship:

$$f_{y,cw}^* = f_{y,cw} \cdot \sqrt{1 - \left(\frac{\sigma_{sd,col}}{f_{y,cw}} \right)^2} \quad (4.15)$$

4. SEISMIC RESPONSE OF PARTIAL-STRENGTH COMPOSITE JOINTS

where $\sigma_{\text{Sd, col}}$ is the average normal stress in the panel zone. In the current Draft of Eurocode 3 (2001), the influence of the normal stress σ due the column axial force is approximately accounted for by means of a reduction coefficient equal to 0,9. In particular, the codified value of the reduction factor is on the safe side up to a column axial load equal to 45% of the column squash load.

After yielding, the rotational stiffness of the web panel zone can be attributed to the bending of the column flanges. It is computed as:

$$K_{pl,1} = \frac{24}{5} \frac{EI_{fc}}{t_{fc} Z_{eq}} \quad (4.16)$$

where I_{fc} is the inertia moment of the column flanges:

$$I_{fc} = \frac{b_c t_{fc}^3}{12} \quad (4.17)$$

We obtain:

$$k_{pl,1} = 1.04 \cdot G_{el} \cdot b_c \cdot \frac{t_{cf}^2}{Z_{eq}} \quad (4.18)$$

If it is assumed that the post-elastic stiffness of the joint $K_{pl,1}$ is valid for a range $\Delta\gamma = 3\gamma_y$, the strength $V_{pl,1}$ of the joints at an angle of distortion equal to $4\gamma_y$ is then given:

$$V_{pl,1} = k_{el} \cdot \gamma_y + k_{pl,1} \cdot 3\gamma_y \quad (4.19)$$

At an angle of distortion equal to $4\gamma_y$ it is possible to assume that strain hardening in the web panel in shear begins. The strain hardening branch stiffness $K_{pl,2}$ is suggested as follows:

$$k_{pl,2} = G_{sh} \cdot (h_c - t_{cf}) \cdot t_{cw} \quad (4.20)$$

where G_{sh} is the strain hardening shear modulus that can be assumed equal to $G_{sh} = 1/100 G_{el}$.

The column web panel must withstand the shear stresses acting when the global frame mechanism arises, that is, it must support that. In accordance with Eurocode

4. SEISMIC RESPONSE OF PARTIAL-STRENGTH COMPOSITE JOINTS

3 (2001), in frame web panels of beam-to-column connections the following assessment is permitted:

$$\frac{V_{wp,Ed}}{V_{wp,Rd}} \leq 1,0 \quad (4.21)$$

where

$V_{wp,Ed}$ is the design shear force in the web panel due to the action effects, taking into account the plastic resistance of the adjacent dissipative zones in beams or connections;

$V_{wp,Rd}$ is the shear resistance of the web panel according to J 3.5.1 of Annex C of the Eurocode 3. It is not required to take into account the effects of the stresses of axial force and bending moment on the plastic resistance in shear. The shear resistance of the columns, in dissipative zones, should be determined on the basis of the structural steel section alone, unless special details are provided to mobilize the shear resistance of the concrete encasement.

A possible system of internal actions that the panel zone of an interior beam-to-column connection may have to withstand is shown in Figure 4.13. Under this system of forces, shear deformation of the web panel zone occurs. A key simplification in this analysis is that the beam moments are replaced by an equivalent couple, with the forces acting at mid-depth of the beam flanges.

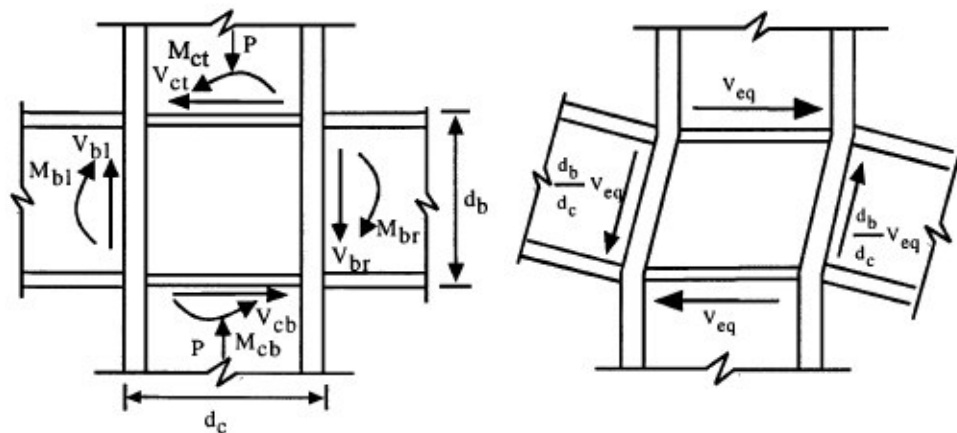


Figure 4.13. Internal actions of an interior beam-to-column joint

Under the assumption, the effective shear force in the web panel $V_{wp,Ed}$ of an interior column at the structure collapse in the seismic design situation can be calculated as follows:

4. SEISMIC RESPONSE OF PARTIAL-STRENGTH COMPOSITE JOINTS

$$V_{wp,Ed,eff} = \frac{M_{pl,Rd,conn}^- + M_{pl,Rd,conn}^+ - 2 \cdot M_{gravity}^-}{z_{eq}^-} - V_c \quad (4.22)$$

where:

$M_{pl,Rd,conn}^-$ is the ultimate strength of the connection for hogging bending moments;

$M_{pl,Rd,conn}^+$ is the ultimate strength of the connection for sagging bending moments;

$M_{gravity}^-$ is the bending moment, due to dead loads;

z_{eq}^- is the equivalent lever arm in the connection for hogging moment;

z_{eq}^+ is the equivalent lever arm in the connection for sagging moment;

V_c is the average shear force at collapse in the web panel equal to:

$$V_c = \frac{V_{column,up} + V_{column,botton}}{2} = \frac{M_{pl,Rd,conn}^- + M_{pl,Rd,conn}^+}{\left(H_c - \frac{z_{eq}^- + z_{eq}^+}{2} \right)} \quad (4.23)$$

where H_c is the height of the web panel.

In obtaining the shear forces in the column segments outside of the panel zone, it is often assumed that:

(a) the zero-moment points are located in the middle section of the columns;

(b) the equilibrium condition $\sum M_{pl,Rd,conn} = \sum M_{column}$ is satisfied.

4.5.3 Joint rotational capacity evaluation

With regard to rotational capacity, every joint must be able to develop the necessary plastic rotation upon formation of a global mechanism. Eurocode 8 (2002) prescribes that the rotational capacity θ_p of the plastic hinges, defined as $\theta_p = \delta / 0.5 L$, see Figure 4.14, should be greater than 35 mrad for structures of ductility class H, and 25 mrad for ductility class M structures, with behavioural coefficient $q > 2$. Such values must be obtained for cyclic loads with a reduction in strength and/or stiffness of less than or equal to 20%, and must be corroborated by experiments (prEN 1998-1, 2001).

The rotational capacity of the beam-to-column joint was computed using the component method (Eurocode 4, 2001), suitably modified in order to take into

4. SEISMIC RESPONSE OF PARTIAL-STRENGTH COMPOSITE JOINTS

account inelastic phenomena. The design is such that the joint behaviour is governed by ductile components: the end plate and column flange under bending; the column web panel under shear; and the concrete-slab rebars under tension. More specifically, in the case of hogging moment, the connection is governed by the rebars under tension. In this case, the bond between rebars and concrete limits the yielding between the cracks, so that the total elongation can be evaluated as the sum of the strains of the rebars near the cracks (ECCS-109, 1999). Therefore, the joint rotation results to be

$$\phi_U = \frac{\Delta_{U,S,Tot}}{D_S + D_R} \quad (4.24)$$

where $\Delta_{U,S,Tot}$ is the total elongation capacity of the rebars, D_S is the height of the steel profile and D_R the distance between the edge of the upper flange and the centroid of the steel reinforcements.

Conversely, in the case of sagging moment, the rotation of the joint is determined by the capacities of the column flange and of the end plate on an experimental basis (Bursi et al., 2002). As a result, the total rotation of the joint reads

$$\phi_U = \frac{\Delta_{U,S}}{D_S + D_C} \quad (4.25)$$

where $\Delta_{U,S}$ is the total displacement of the T-stubs, D_s the height of the steel profile and D_C the distance between the edge of the upper flange of the steel profile and the centroid of the concrete slab. The joint response is also governed by the deformational capacity of the web panel under shear forces. Thus, in applying the component method in order to account for such rotational capacity, we limited the maximum rotation to 30 mrad.

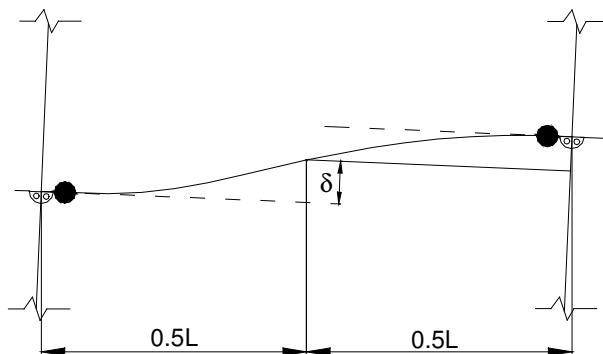


Figure 4.14. Deformed configuration of a sub-frame

4. SEISMIC RESPONSE OF PARTIAL-STRENGTH COMPOSITE JOINTS

4.6 Mechanical properties of materials

Production standards set strict lower limits for the yield stress, but they leave to the designer nearly complete freedom with regard to the upper limits. European standard ENV 206 (1990) on concrete production does not, for instance, require, on one hand, controls of the maximum resistance, just as in the case of EN 10025 (1993) for structural steels. Eurocode 8 (prEN 1998-1, 2002), on the other hand, recommends that the actual yield stress of steel be such as not to modify the localization of the plastic hinges considered during design. In the case of the beam-to-column joints under study, all the materials were checked preliminarily. The results, reported in Table 4.4, confirm the extremely wide scatter of the resistance values that can, in practice, be obtained.

	Design yield strength [N/mm ²]	Measured yield strength [N/mm ²]
BEAM FLANGE (IPE300 S235)	235	370
Beam web (IPE300 S235)	235	313
Column flange (HEB280/260 S235)	235	341
Column web (HEB280/260 S235)	235	300
End plate (S235)	235	383
Reinforcing bars (B450C)	450	537
Concrete (class 25/30)	25	35

Table 4.4. Design and actual yield strength

4.7 Seismic performance evaluation for the prototype structure

The principal objective of this project is the evaluation of the performance of the composite construction with semi-rigid partial-strength beam-to-column joints and partially encased columns in earthquake-prone regions. Performance is defined in terms of probabilistic performance objectives. A performance objective consists of

4. SEISMIC RESPONSE OF PARTIAL-STRENGTH COMPOSITE JOINTS

the specification of a performance level and an acceptable low probability that poorer performance could occur within a specific period of time. To evaluate a performance objective, selection of a performance level of interest is required. The performance levels can be, for example, the ultimate state limits or the service state limits. A desired probability that damage in a period of time will be worse than this performance level has to correspond for each selected level. Moreover an average estimate of the ground shaking intensity at the probability of exceedance identified in the performance objective definition has to be determined for each probabilistic performance objective.

The performance of a building during an earthquake depends on many factors including: the structure's configuration and proportions, its dynamic characteristics, the hysteretic behaviour of the elements and joints, the type of non-structural components employed, the quality of materials and workmanship, the adequacy of maintenance, the site conditions, and the intensity and dynamic characteristics of the earthquake ground motion experienced. Consequently, seismic performance prediction for buildings, either as part of a design or evaluation, should consider, either explicitly or implicitly, all of these factors.

Therefore, a reliability-based performance-oriented approach, adopted by the SAC project for design and evaluation, was taken in order to explicitly account for uncertainties and randomness in seismic demand and capacities in a consistent manner and to satisfy with defined reliability identifiable performance objectives corresponding to various occupancies, damage states and seismic hazards.

Consistently with the Eurocode 8 (2002) and on the basis of the FEMA 302 NEHRP Recommended Provisions for Seismic Regulation for New Buildings and Other Structures (BSSC, 1998a) and the FEMA 273 NEHRP Guidelines for Seismic Rehabilitation of Buildings (BSSC, 1997), two performance levels are considered. These are termed *Serviceability Limit State* (S.L.S.) and *Ultimate Limit State* (U.L.S.):

- The *Serviceability Limit State* (named *Immediate Occupancy* (IO) level in the FEMA Provisions) is defined as the post-earthquake damage state where only minor structural damage has occurred with no substantial reduction in building gravity or lateral resistance. Damage in this state could include some localized yielding and limited fracturing of connections. Damage is anticipated to be so slight that if it is not found during inspection there is no cause for concern. For pre-Northridge buildings, fewer than 15% of the connections on any floor may experience connection fractures without exceeding the IO level.
- The *Ultimate Limit State* (named *Collapse Prevention* (CP) level in the FEMA Provisions) is defined as the post-earthquake damage state, in

4. SEISMIC RESPONSE OF PARTIAL-STRENGTH COMPOSITE JOINTS

which the structure is on the verge of experiencing either local or total collapse. Significant damage to the building has occurred, including significant degradation in strength and stiffness of the lateral force resisting system, large permanent deformation of the structure and possibly some degradation of the gravity load carrying system. However, all significant components of the gravity load carrying system must continue to function.

The probability that a building may experience greater damage than foreseen depends on the vulnerability of the building and the seismic hazard to which it is exposed. Vulnerability is related to the capacity of the building, which may be a function of the global or interstory drift, plastic rotations or member forces. Ground accelerations associated with an earthquake cause building response resulting in global and interstorey drifts and member forces, all of which can be classified as demands. If both the demand produced by ground motion and the capacity of the structure to resist this demand could be predicted with certainty, the engineer could design a building and have 100% confidence that the building would achieve the desired performance objectives. Unfortunately, neither capacity nor demand can be precisely determined because of uncertainties and randomness inherent in our prediction of the ground motion, the structure's response to this motion and its capacity to resist damage, given these demands.

On the basis of the important advancements in performance evaluation, developed under the SAC project, a procedure for associating a level of confidence with the conclusion that the designed structure is capable of meeting the aforementioned performance levels (S.L.S. or S.L.U.) has been performed. The procedure includes the following steps:

- i. *Determining the structure performance objective to be evaluated.* This requires the selection of one or more performance levels, that is, either S.L.S. or U.L.S., and the appropriate hazard level, that is exceedance probability desired for this performance. The NEHRP guidelines (BSSC, 1998) recommend that design solutions provide a 90% level of confidence that the building satisfy desired performance from a global perspective and a 50% level of confidence that it satisfy the performance at a local level.
- ii. *Determining the ground motion characteristics for the chosen performance objective.* The ground motion intensity for each performance level should be chosen in order to have the same probability of exceedance as the hazard level of the design objective. It is assumed that a peak ground acceleration, p.g.a. equal to = 0.40 g should have the 90 % probability of not being exceeded in 50 years for the U.L.S. According to a Poisson model, this corresponds to a reference return period of 476.7 years; conversely a p.g.a. = 0.1 g should have the 90 % probability of not being exceeded in 10 years for

4. SEISMIC RESPONSE OF PARTIAL-STRENGTH COMPOSITE JOINTS

the S.L.S. According to a Poisson model, this corresponds to a reference return period of 95.4 years.

- iii. *Calculating the structural demand for the pre-selected earthquake intensity.* The demand parameters, such as the maximum interstory drift, are computed using standard methods of structural analysis (Non-linear Pushover analysis and Time-History analysis) taking into account possibly stiffness deterioration and strength degradation of members and connections of the structure (the effect of residual drift contributes about one-third to the loss in frame stability, and the remaining two-third drop is due to stiffness/strength degradation).
- iv. *Determination of global and local collapse capacity,* i.e. estimating the capacity of the structure and of its components (maximum rotation, interstorey, etc) for the defined limit states (damage and the collapse limit state).
Local Drift Capacity will be determined from cyclic tests of full-size connection specimens conducted by the Laboratory of the University of Pisa. The cyclic tests are used to determine load-deformation hysteresis behaviour of the system and the maximum drift for which gravity loads may still be carried by the girders. This gravity-induced drift limit is reached when a low-cycle fatigue crack develops in the end plate or the load-deformation behaviour of the moment connection has completely deteriorated. A standard test protocol, based on the ECCS Procedure (1986) was used for the tests. The moment vs. plastic rotation of a beam-column assembly representative of a single test is shown in Figure 4.15. The hysteretic behaviour is characterized by gradual strength degradation with increasing plastic rotation. For the specific connection tested, it appeared that the shear-carrying capacity was reached at a plastic rotation of about 0.06 radians. In order to use such data in the reliability framework it is necessary to have several such tests, from which we can obtain statistics on the likely distribution of important design parameters, such as plastic rotation at peak load and plastic rotation at loss of capacity. Statistics that must be obtained include the median value of the parameter and the standard deviation of the logarithm of the values obtained from the testing.
Global Drift Capacity of the prototype building will then be determined using the non-linear pushover analysis (NLP) or the incremental dynamic analysis (IDA) procedure that is based on the use of non-linear time-history analysis. It is important that the analytical model used for determining the global drift demand reproduces the major features of the measured response such as sudden loss of strength. This means that the measured hysteresis behaviour must be modeled reasonably well and the model must include all significant components of building stiffness, strength and damping.

4. SEISMIC RESPONSE OF PARTIAL-STRENGTH COMPOSITE JOINTS

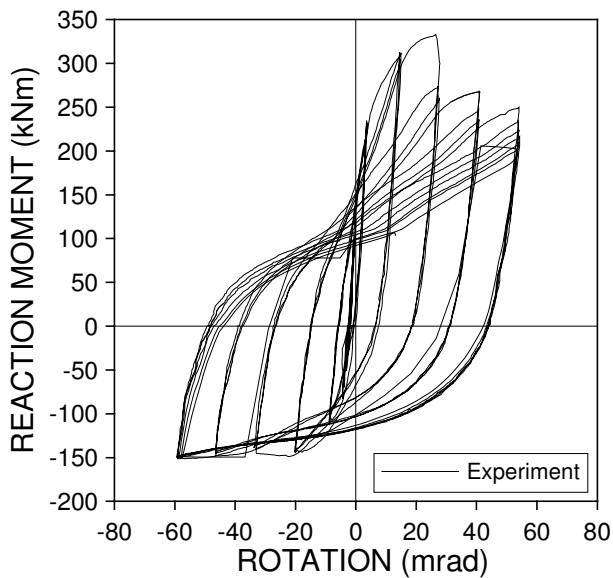


Figure 4.15. Measured moment vs. rotation behaviour of the connection

- v. *Determining the demand-to-capacity ratio.* Once calculated, the ratio between the demand obtained from aforementioned frame analyses and the obtained capacity allow to estimate the performance of the structure and of the components, i.e. the probability that the structure or a component will have less than a specified probability of exceedance of a desired performance level. The EC8 code requirements impose two primary controls on the structural design: minimum strength and minimum stiffness (as specified through the deflection limit). These two requirements are interrelated and competing. For instance, if the stiffness of a structure is increased so that it meets the drift requirements, then the period will shorten, which often results in a larger design base shear and a correspondingly larger drift. Moreover, the strength and stiffness of the building are coupled, and thus the minimum stiffness requirement adds considerably to the system overstrength. The structural overstrength results from a number of factors including internal force redistribution, code requirements for multiple loading combinations, code minimum requirements regarding proportioning and detailing, material strength higher than that specified in the design, strain hardening, deflection, constraints on system performance, member oversize and strain rate effect.

4. SEISMIC RESPONSE OF PARTIAL-STRENGTH COMPOSITE JOINTS

4.8 Cyclic tests of full-scale composite joint subassemblages

This Section presents results obtained from tests carried on three full-scale composite beam-to-column joint subassemblages, which were replicas of parts of the two-storey prototype structure. One monotonic test and one test in cyclic regime both on an interior (CJ-INT) and an exterior (CJ-EXT) joint were conducted. The steelwork connection consists of an extended end plate welded to the beam end and bolted to the column flange. As illustrated in Figure 4.16 and Figure 4.17, all the specimens had steel deck supported concrete slab acting compositely with the beam and partially encased steel-concrete composite columns. Moment–rotation curves obtained from the tests are compared with those predicted by an analytical model. Plastic analysis based on the theoretical developments of the previous sections is used to develop the analytical model for the prediction of moment capacity. A rotational spring model for the composite beam, as proposed in revised Annex J of EC4, combined with a translational spring model for the steel web panel, is used to assess the strength and the stiffness of the composite joints. The model tends to over-predict the behaviour of the joint. To better understand the transfer mechanism activated in the composite beam and in the web panel numerical finite element (FE) analyses were carried out by means of the ABAQUS code. The FE model was calibrated and the stress and strain state of the aforementioned connections was simulated in the monotonic displacement regime.

4.8.1 Test set-up and procedure

The basic set-up included a test frame and a loading system (Figure 4.18). The test frame was designed to be sufficiently stiff to minimize the lateral movement of the system. The lower hinges were fastened directly to the test floor. The horizontal displacement-controlled load was applied by a hydraulic jack at the upper end of the composite column. The jack was mounted on the pedestal and was connected to the column through a load cell. The height of the columns of the test specimens, measured from the point of load application to the center of the hinge, was 3500 mm, which was the storey height of the prototype structure. This selection was made by assuming that the points of contra-flexure occurred at the midheight of the adjacent stories.

In order to characterize the behaviour of the specimens under hysteretic loading a predefined representative displacement history was applied. The procedure follows the ECCS recommendation n° 45 (1986), as illustrated in Chapter 2. The instrumentation of the specimens was designed to determine the applied loads, to

4. SEISMIC RESPONSE OF PARTIAL-STRENGTH COMPOSITE JOINTS

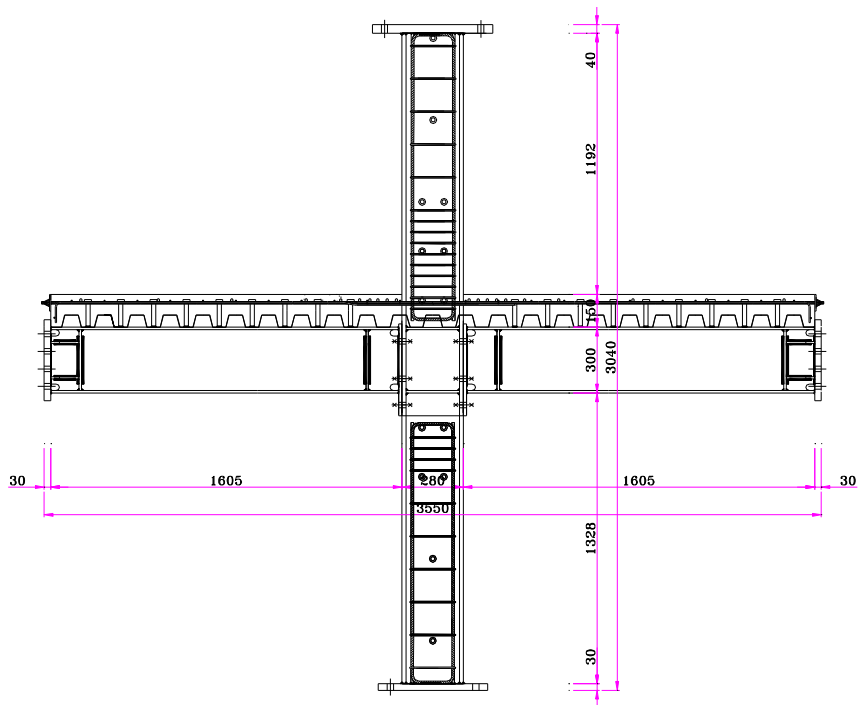


Figure 4.16. Dimensions and layout of the specimen CJ-INT

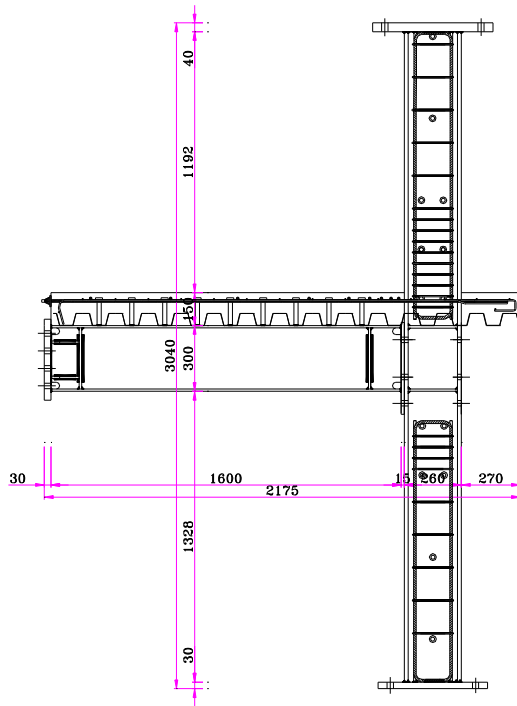


Figure 4.17. Dimensions and layout of the specimen CJ-EXT

4. SEISMIC RESPONSE OF PARTIAL-STRENGTH COMPOSITE JOINTS

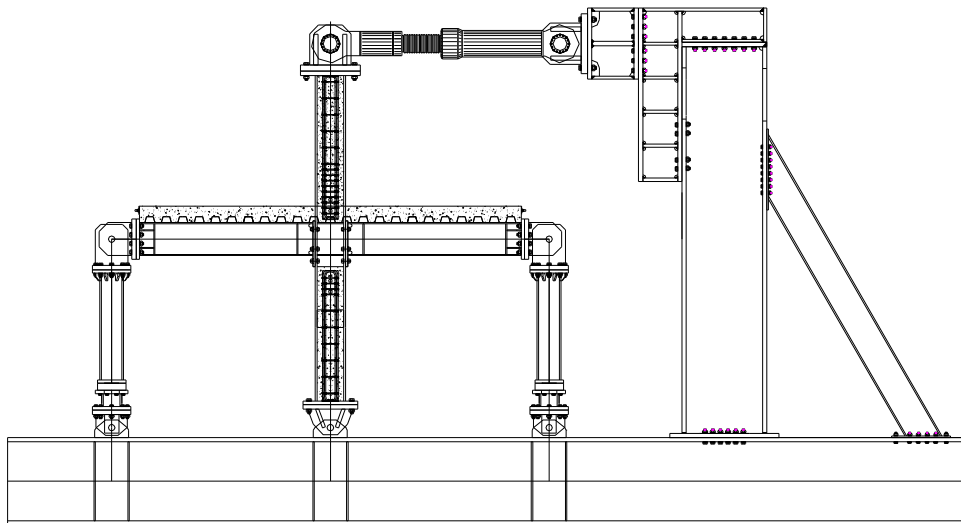


Figure 4.18. Test set-up for the interior joint CJ-INT

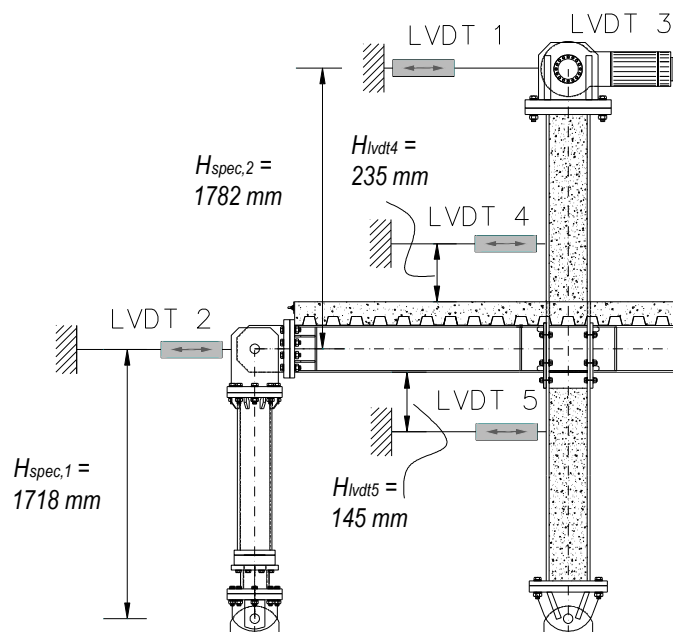


Figure 4.19. Global instrumentation for the specimen CJ-INT

check the reactions at the supports and to measure the deformation and internal stresses of the specimens. By means of LVDT transducers and inclinometers, positioned as illustrated in Figure 4.19, was possible to determine the global deformed configuration. Moreover, in the zone of the joint, LVDT transducers (see

4. SEISMIC RESPONSE OF PARTIAL-STRENGTH COMPOSITE JOINTS

Figure 4.20) and strain gauges were positioned in order to investigate the transfer mechanisms from the composite beam to the column; in detail the shear deformation of the web panel and the strain distribution in the concrete slab and in the reinforcing bars were well monitored.

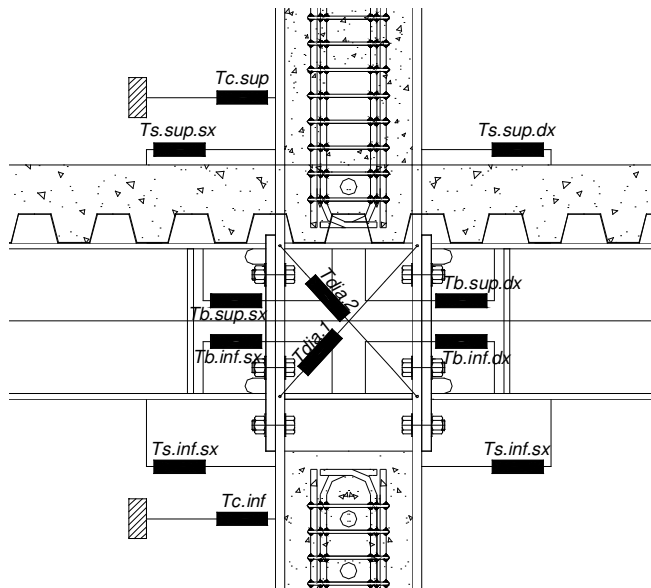


Figure 4.20. LVDT Transducer in the joint

4.8.2 Specimen behaviour and test results

The test results of the four specimens are shown as load-deformation relationships. The number of peaks indicates the cycle numbers. The hysteresis diagrams, characterizing the overall behaviour of the specimen and the behaviour of its components, are as follows:

- M- ϕ hysteresis diagram of the overall behaviour of the specimen;
- M- θ hysteresis diagram of composite beam connection rotation;
- V- γ hysteresis diagram of web panel zone distortion.

Interior Complete Joint CJ-INT

For this specimen both the monotonic and the cyclic test were performed. In the following Figure 4.21, Figure 4.22 and Figure 4.23 the moment vs. plastic rotation of a beam-column assembly, the moment vs. plastic rotation of the composite beam connection and the shear vs. plastic distortion of the column web panel are shown.

4. SEISMIC RESPONSE OF PARTIAL-STRENGTH COMPOSITE JOINTS

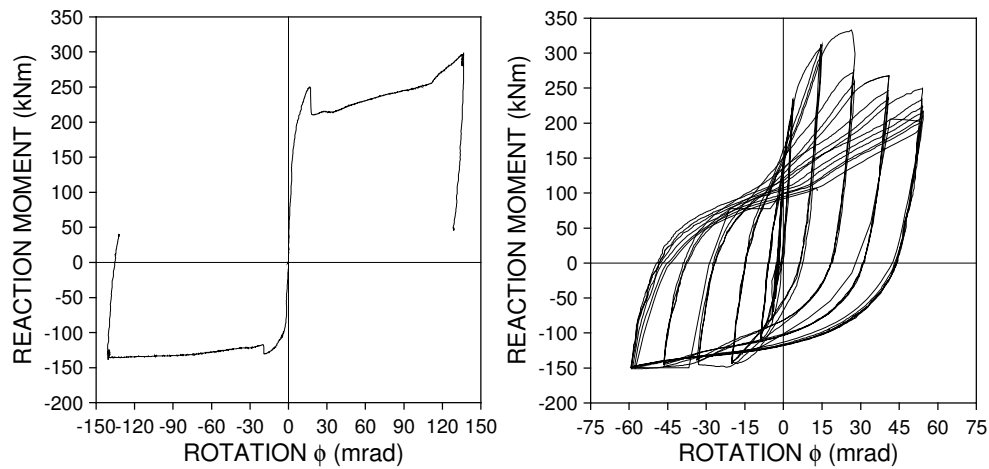


Figure 4.21. $M-\phi$ diagram of the overall behaviour of the CJ-INT specimen

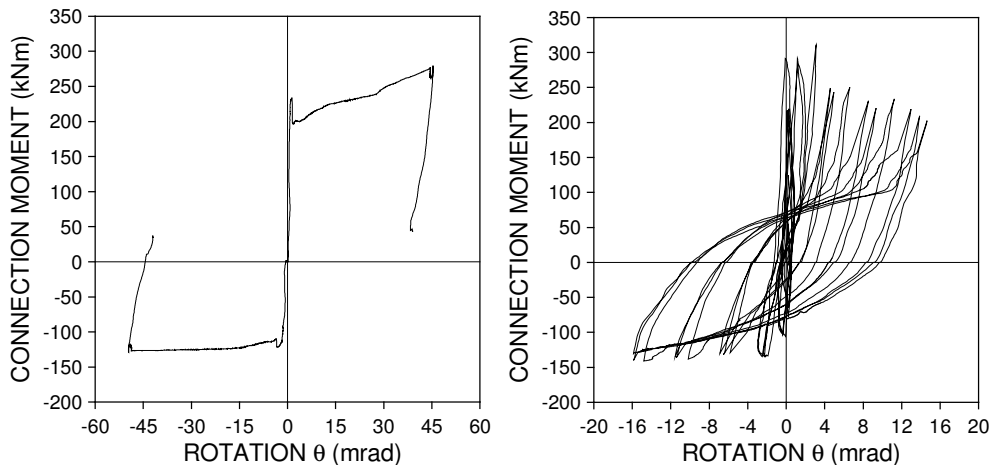


Figure 4.22. $M-\theta$ diagram of composite connection rotation of the CJ-INT specimen

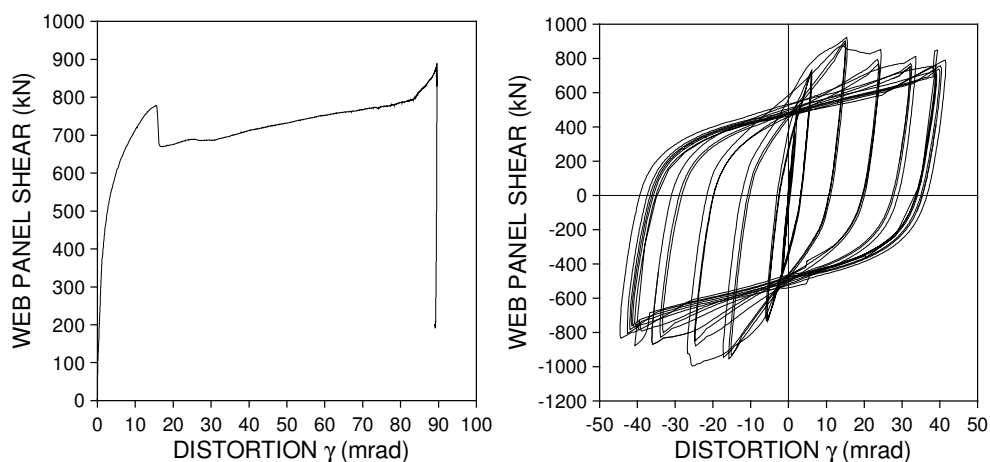


Figure 4.23. $V-\gamma$ diagram of web panel zone distortion of the CJ-INT specimen

4. SEISMIC RESPONSE OF PARTIAL-STRENGTH COMPOSITE JOINTS

The monotonic test shows clearly that, at an imposed global plastic rotation equal to 15 mrad (interstorey drift equal to 2%), a marked and sudden loss of moment resistance characterizes the positive branch of the joint behaviour. This is due to the fact that the concrete in the beam-to-column connection zone has been crushed around the column flange, as shown in Figure 4.24. From this point, the behaviour of the joint is similar to that of a composite joint with not-restrained slab (Lee and Lu, 1989; Ryan and Bitar, 2002). The loss of resistance is evident in the diagram of connection response too.



Figure 4.24. Crushed concrete in the beam-to-column connection zone around the column flange

From the re-assessment of data collection of the strain gauges in the slab and imposing the equilibrium condition between beam and column actions, it was possible to demonstrate that only the mechanism 1 was mobilized to react to the column action. In Figure 4.25 it is possible to underline the correspondence during the test between the maximum strength reached in the concrete slab (38 MPa) and the loss of resistance of the specimen. Due to this unexpected phenomenon the panel zone underwent very large shear distortions, but it did not show any sign of distress. The web panel rotation alone represents more than the 65% of the total joint rotation.

Under cyclic loading history, the specimen CJ-INT shows the same properties illustrated in monotonic regime. Moreover, the hysteretic behaviour is characterized by gradual strength degradation with increasing plastic rotation. However, the specimen exhibited considerable reserve of strength and one can observe that

4. SEISMIC RESPONSE OF PARTIAL-STRENGTH COMPOSITE JOINTS

total rotations of CJ-INT reach values greater than 50 mrad both under sagging and hogging bending moment, implying a suitable ductile behaviour for high ductile (class H) structures in seismic applications (Eurocode 8, 2002).

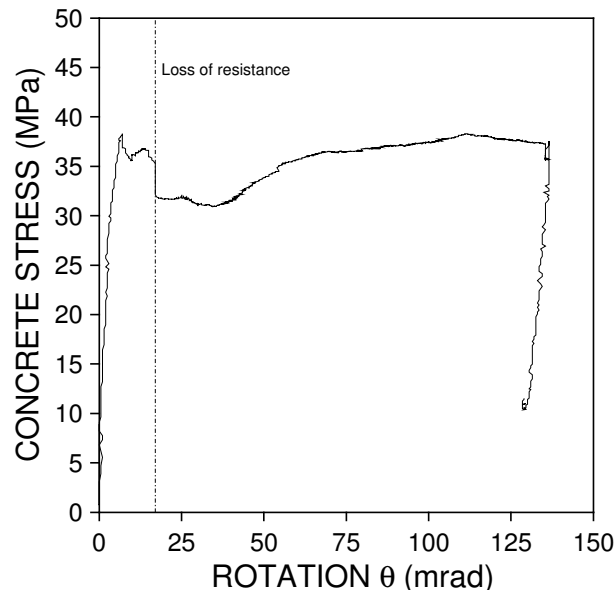


Figure 4.25. Concrete stress vs. global rotation in CJ-INT

Exterior Complete Joint CJ-EXT

Both the monotonic and the cyclic test were performed. In the monotonic test an imposed displacement load that would produce compression in the concrete slab was selected. The moment vs. plastic rotation of a beam-column assembly, the moment vs. plastic rotation of the composite beam connection, and the shear vs. plastic distortion of the column web panel are shown in the following Figures. The joint behaviour, and in particular the contribution of the concrete slab in compression, is very similar to that obtained for the interior joint CJ-INT. Also in this case, as shown in Figure 4.26, the crushing of the concrete in compression around the column flange brings about the loss of resistance in the global joint response. The same phenomenon is evident in the behaviour of the connection (see Figure 4.27) and in the response of the column web panel (see Figure 4.28), that distortion alone represents more than the 64% of the total joint rotation.

The behaviour of the exterior joint during the cyclic test resulted different from that of the interior joint. Under hogging bending moment, the exterior portion of the concrete slab in compression was able to absorb large plastic deformations with formation of evident cracks at an inclination of 45 degree, as shown in Figure 4.29.

4. SEISMIC RESPONSE OF PARTIAL-STRENGTH COMPOSITE JOINTS

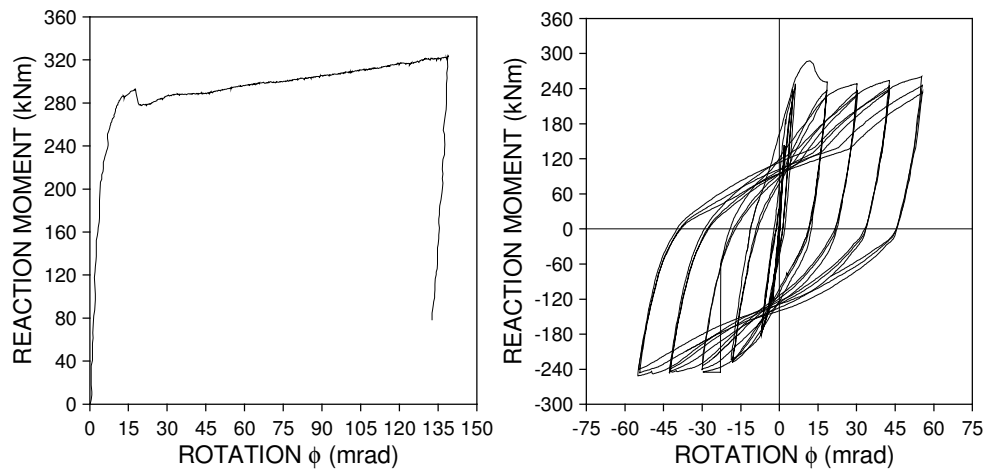


Figure 4.26. $M-\phi$ diagram of the overall behaviour of the CJ-EXT specimen

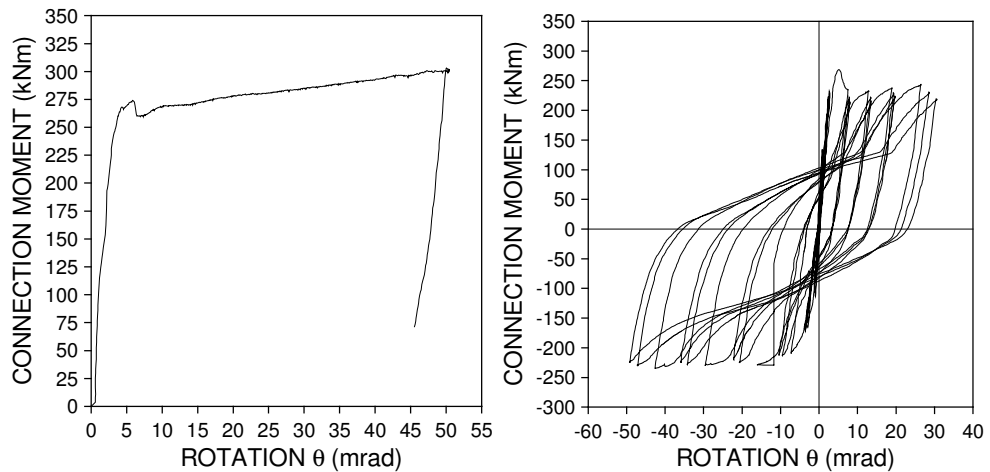


Figure 4.27. $M-\theta$ diagram of composite connection rotation of the CJ-EXT specimen

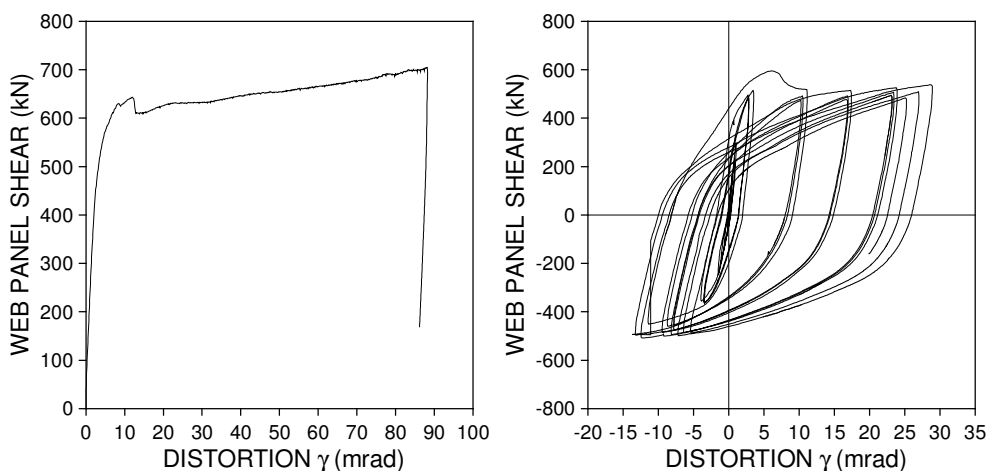


Figure 4.28. $V-\gamma$ diagram of web panel zone distortion of the CJ-INT specimen

4. SEISMIC RESPONSE OF PARTIAL-STRENGTH COMPOSITE JOINTS

In the transfer of the forces from the concrete slab to the column under hogging bending moment the longitudinal re-bars have played a relevant role. From the analysis of the strain gauges data it resulted that the reinforcing bars deform plastically.



Figure 4.29. Cracks at an inclination of 45° in the exterior portion of the concrete slab

Moreover, the good behaviour of the composite section under hogging bending moment is evident in the analysis of the response of the web panel too. In this case the distortion of the panel zone is only the 19% of the total joint rotation, and the transmitted shear force is smaller. This means that the connection worked well with maximum rotation of about 50 mrad greater than those observed in the column web panel.

4. SEISMIC RESPONSE OF PARTIAL-STRENGTH COMPOSITE JOINTS

4.8.3 Validation of the analytical model

The composite beam-to-column joint, named CJ type, is modelled using a rotational spring to simulate the connections and a rectangular articulated polygon, whose dimensions are represented in the Figure 4.30, with a non linear translational spring simulating the column web panel.

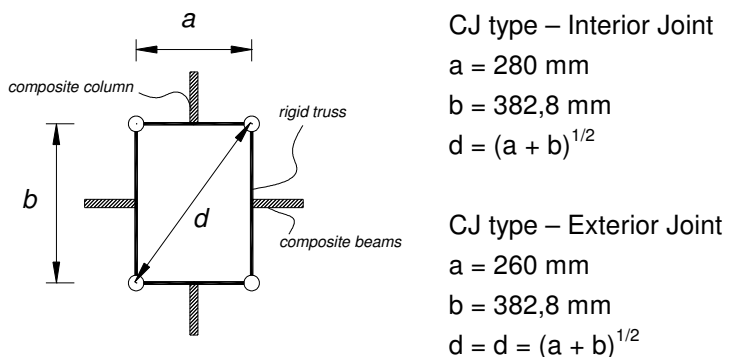


Figure 4.30. Dimensions of rectangular articulated polygon

The mechanical properties of the rotational spring are obtained using the *Component Method* according with ECCS - n°109 Procedure (1999); for the column panel in shear the Krawinkler's model has been used. To model the rotational spring of the connection in a way that closely reproduces the expected behaviour, each component is modelled separately, taking account of the interior moments and forces in the members acting at the periphery of the web panel. The modelling of the actual behaviour of the connection is different in the case of sagging or hogging bending moment. The basic components identified in this design are given in Table 4.5, for sagging and hogging bending moment respectively.

The design moment resistance $M_{j,Rd}$ of this rotational spring is determined for sagging bending moment from:

$$M_{j,Rd} = \sum_j F_{t,j,Rd} \cdot z_j \quad (4.26)$$

where:

- $F_{t,j,Rd}$ is the effective design tension resistance of the bolt-row j;
- z_j is the distance from the component j in tension to the center of the compression.

4. SEISMIC RESPONSE OF PARTIAL-STRENGTH COMPOSITE JOINTS

The center of the compression is assumed to be in line with the mid-thickness of the compression concrete slab (see Figure 4.31a).

MOMENT-ROTATION CHARACTERISTIC FOR SAGGING BENDING MOMENT	
<i>Components in compression</i>	Concrete Slab in compression
	Beam flange and web in compression
	Column web in compression
<i>Components in tension</i>	Column web in tension
	Beam web in tension
	Bolt in tension
<i>Components in bending</i>	Column flange in bending
	Interior end-plate in bending
	Exterior end-plate in bending
MOMENT-ROTATION CHARACTERISTIC FOR HOGGING BENDING MOMENT	
<i>Components in compression</i>	Beam flange and web in compression
	Column web in compression
<i>Components in tension</i>	Column web in tension
	Beam web in tension
	Bolt in tension
	Longitudinal slab re-bars in tension
<i>Components in bending</i>	Column flange in bending
	Interior end-plate in bending

Table 4.5. The basic components identified in this design for sagging and hogging bending moment

Moreover, the design moment resistance $M_{j,Rd}$ of this rotational spring is determined for hogging moment from:

$$M_{j,Rd} = \sum_j F_{t,j,Rd} \cdot z_i \quad (4.27)$$

4. SEISMIC RESPONSE OF PARTIAL-STRENGTH COMPOSITE JOINTS

where:

$F_{t,j,Rd}$ is the effective design tension resistance of the row of reinforcing bars or bolts;

z_j is the distance from the component j in tension to the center of the compression.

The centre of the compression is assumed to be in line with the mid-thickness of the compression flange of the connected beam (see Figure 4.31b).

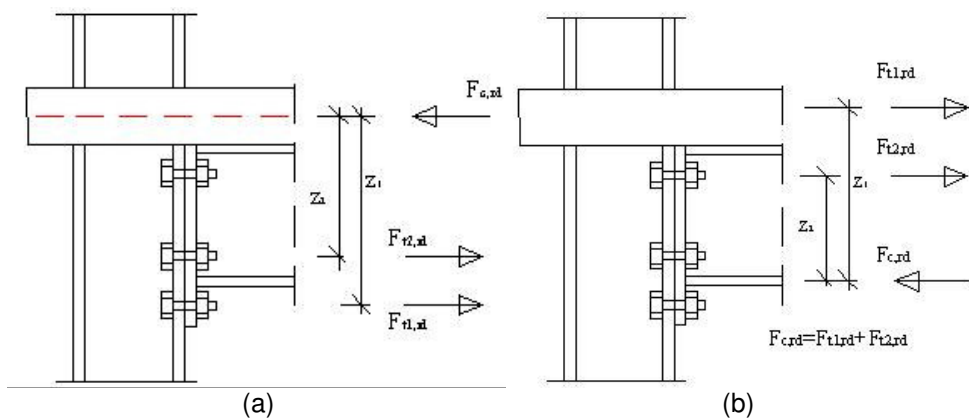


Figure 4.31. Moment resistance $M_{j,Rd}$ calculation for: a) Sagging bending moment; b) Hogging bending moment

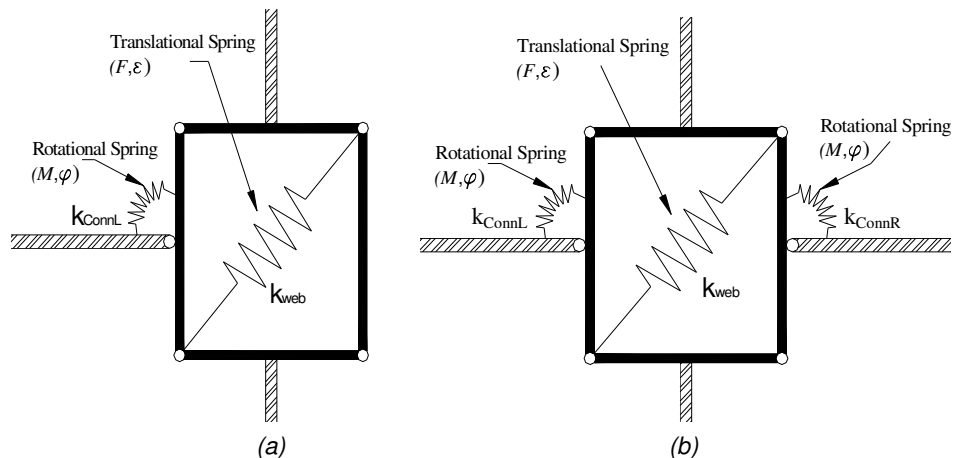


Figure 4.32. Joint configuration for: (a) Exterior joint with HEB 260 Column; (b) Interior joint with HEB 280 Column

The effective design tension resistance of a bolt-row is taken as the smallest values of the tension resistances of the basic components (bolts in tension, column web in tension, column web in bending, end-plate in bending, beam web in

4. SEISMIC RESPONSE OF PARTIAL-STRENGTH COMPOSITE JOINTS

tension). For the calculation of resistance, the actual values of the yield strength as well as the elasticity modulus of the material are used.

The rotational stiffness of the spring is determined from the flexibilities of its basic components, each represented by its stiffness coefficient k_j obtained in accordance with the Eurocode 3. Moreover, for ductile components an elastic-plastic stiffness coefficient is used; conversely, for the other components only an elastic stiffness coefficient is used. In Figure 4.32 the characteristics for the two single-sided and double-sided beam-to-column joint configurations respectively are shown. Moreover, the moment-rotation relationship for both the two joint configurations are shown in Figure 4.33: the calculated rotation capacity limits are in evidence in this figure. These vertical limits in the rotation of the complete joints are due to both the rotation capacity of the equivalent T-Stub that model the end-plate in bending (± 15 mrad), and the rotation capacity of the column web panel in shear (± 35 mrad), as illustrated in Section 3.5.3.

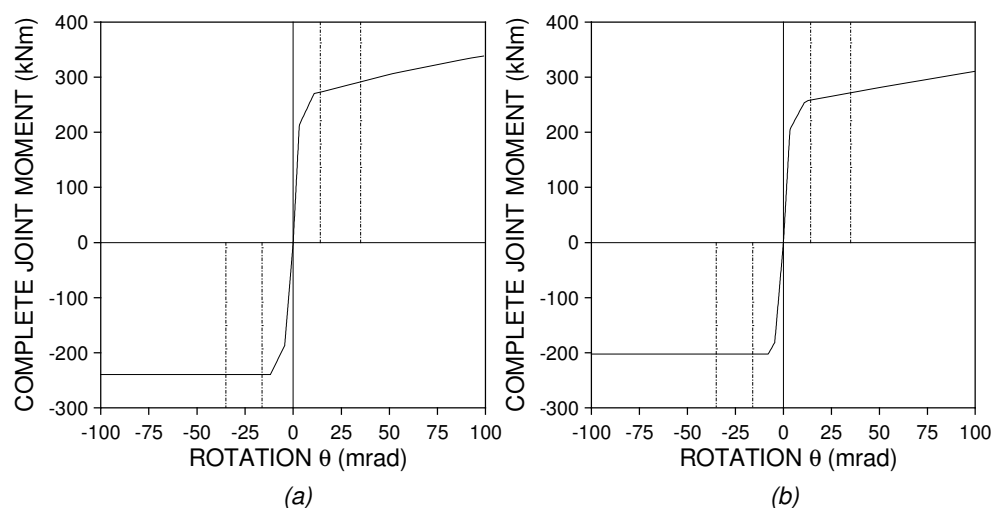


Figure 4.33. Moment-rotation relationship for the two joint configurations: (a) CJ-INT Joint; (b) CJ-EXT joint

The analytical models are then compared with the experimental results. The attention is hence focused on the use of these data for checking the general validity of the joint model by component with reference to the approximation of the monotonic and cyclic response.

With regard to the specimen CJ-INT the overall M-θ relationship is compared in Figure 4.34. Under sagging bending moment the analytical model tends to overestimate the experimental response and is not able to capture the loss of resistance due to the crushing of the concrete slab in compression around the column flange. Similar results are obtained under hogging bending moment, due to

4. SEISMIC RESPONSE OF PARTIAL-STRENGTH COMPOSITE JOINTS

the fact that, when the concrete slab is crushed, the joint loses its performance in term of resistance. A detailed comprehension can be obtained by analysing the response of the connection, under sagging and hogging bending moment.

In Figure 4.35 the experimental connection response of the CJ-INT specimen,

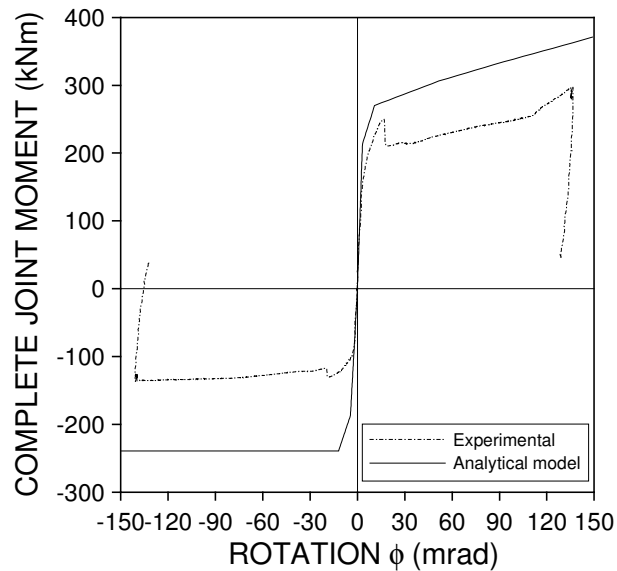


Figure 4.34. Comparison between experimental and numerical joint response of the CJ-INT specimen

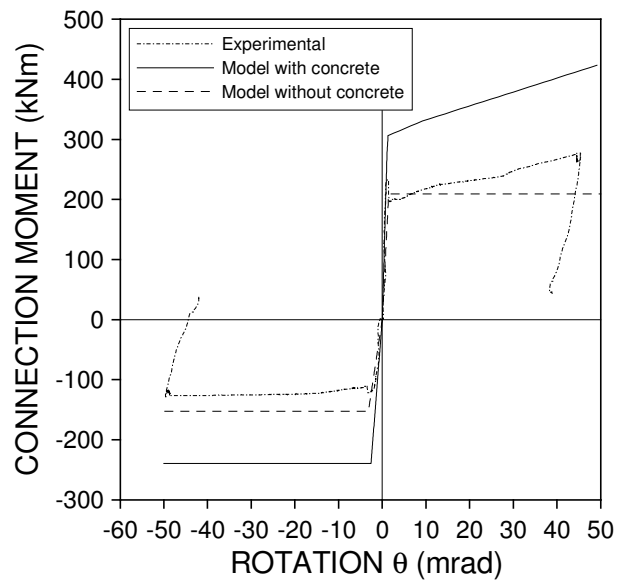


Figure 4.35. Comparison between experimental and numerical (with and without concrete contribution) connection response of the CJ-INT specimen

4. SEISMIC RESPONSE OF PARTIAL-STRENGTH COMPOSITE JOINTS

compared with the analytical prediction obtained from the model are shown. It is evident that the theoretical and the experimental results do not agree closely. It is interesting to underline that with a modified model in which the contribution of the composite section is not taken into account, the analytical prediction agrees quite well with the experimental results. This means that after the crushing of the concrete the benefit composite action of the beam is lost and the joint behaves simply as steel joint. Similar results are obtained for the exterior joint, as depicted in Figure 4.36; however, different considerations have to be made.

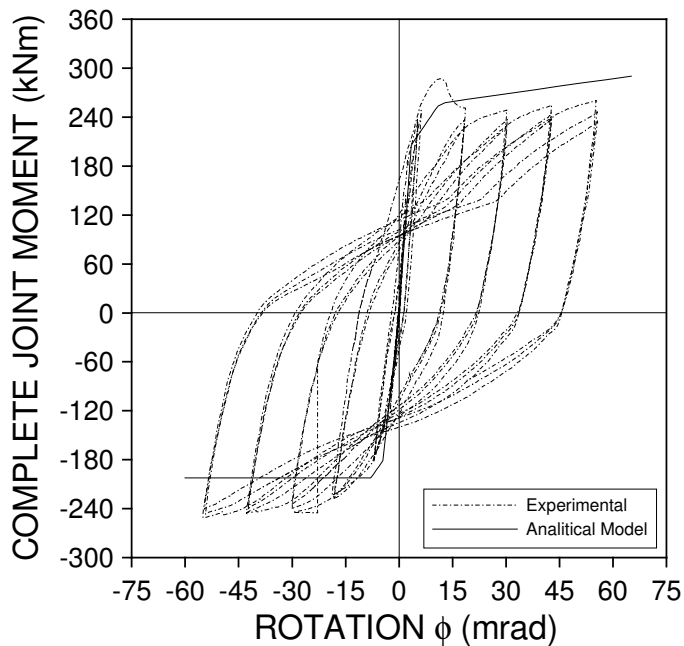


Figure 4.36. Comparison between experimental and numerical joint response of the CJ-EXT specimen

Under sagging bending moment, the analytical model is capable to predict correctly the maximum strength of the connections, as shown in Figure 4.37, but it is not able to predict the loss of strength due to the crushing of the concrete. Under hogging bending moment the analytical model captures very well the behaviour of the connection, in term both of stiffness and strength. The combination of the response under sagging and of the response under hogging bending moment of the specimen produces a different redistribution of force between connection and web panel in shear, which the model is not able to reproduce. This fact can explicate the differences in the global behaviour between experimental and analytical results.

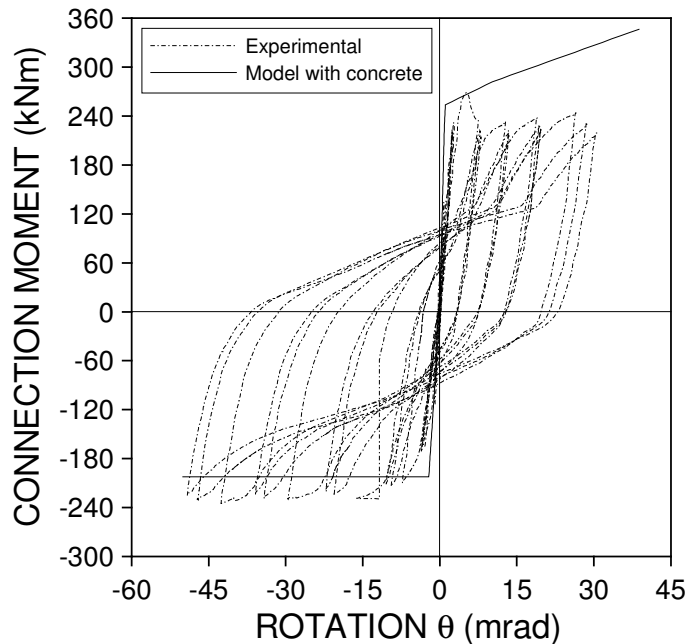


Figure 4.37. Comparison between experimental and numerical connection response of the CJ-EXT specimen

4.8.4 3D finite element (FE) model

To better understand the stress state in the web panel zone and in the concrete slab and therefore the activation of the transfer mechanisms idealized in Section 4.5.1, 3D finite element (FE) models of the composite joints have been developed, such as the one depicted in Figure 4.38. On the basis of the experimental results and the data collection, inelastic FE analyses carried out by means of the ABAQUS code (2001) on the exterior tested complete joints (CJ-EXT) have been calibrated and the stress and strain state of the aforementioned connection was simulated in the monotonic displacement regime.

The model includes details such as all re-bars in the concrete slab, boltholes and bolts; surface-to-surface contact elements are used to model the surface interaction. Moreover, constraint equations are introduced to make the bolt heads continuous with the end plate. Bolt pre-tensioning is applied by prescribed displacements at the end of the bolt shank. These displacements are held constant throughout the loading. The end of the beam and the bottom of the column in the model have roller and pin boundary conditions, respectively.

The material models exploited for 3D elements are those available in the ABAQUS code (2001). Elasto-plastic simulations of composite substructures are performed

4. SEISMIC RESPONSE OF PARTIAL-STRENGTH COMPOSITE JOINTS

by means of a macro-level approach for concrete fracture, in which plain concrete is assumed to be an equivalent isotropic continuum. The material model for concrete is developed within the framework of the theory of plasticity. Though it does not predict explicitly crack initiation and evolution, as the companion model based on the coaxial rotating crack formulation does, it is more doubtless robust from a computational standpoint. In particular, the pressure-dependent Drucker-Prager yield criterion formulated in stress space is adopted.

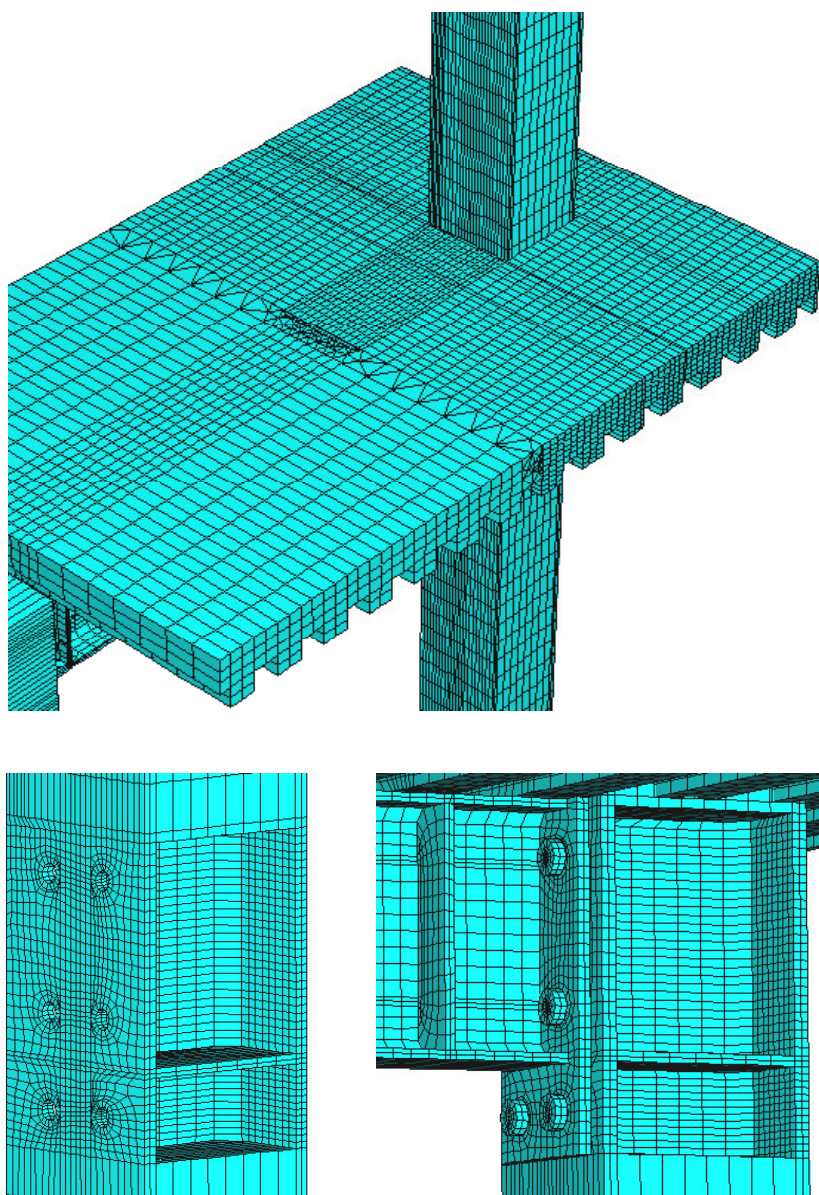


Figure 4.38. General view and details for the 3D Finite Element (FE) model of the CJ-EXT specimen

4. SEISMIC RESPONSE OF PARTIAL-STRENGTH COMPOSITE JOINTS

The two material constants are linked to the Mohr-Coulomb constants, viz. the cohesion and the angle of internal friction, by matching the fictitious tensile strength f_t and the biaxial compressive strength f'_{bc} of concrete according to transformation formulae in Chen (1982). Moreover, a non-associated flow rule is exploited. The strain-hardening behaviour of concrete is governed by means of the stress-strain law of concrete in uniaxial compression or uniaxial tension, complemented with appropriate post-peak softening rules. In detail, the tension-softening behaviour of concrete related to its progressive fracturing or tension-stiffening behaviour owing to the presence of reinforcements is reproduced with exponential decay curves (Stevens et al, 1991). Confining effects owing to transversal reinforcements and profiled-steel sheeting are considered in the compression regime by means of the model of Mander et al. (1988). The concrete model does not embody the specific fracture energy G_f , to overcome mesh-dependent results (Hilleborg et al, 1976). However, as the concrete slab is moderately reinforced both in the longitudinal and transversal direction, the mesh-dependency is small. Moreover, the FE analyses account for steel nonlinearities using the von Mises yield criterion. Isotropic hardening is assumed for the analyses. In the analysis the measured stress-strain properties of the materials obtained by tensile test were used. The elastic modulus and the Poisson's ratio were assumed as $E=210000$ and $\nu=0.3$, respectively. Longitudinal rebars in the slab are assumed to be made with a hardening elasto-plastic material and modelled using discrete two-noded beam elements for 3D models. The discrete representation of the reinforcements is adopted because the influence of bond-slip is of interest. Thereby, dimensionless bond-link elements are adopted to connect concrete and steel nodes. In detail, the bond stress-slip relation is modulated according to the law proposed in Stevens et al. (1991). Friction between the structural steel and the concrete slab is not modelled because it has little influence on the substructure responses. Elastic and inelastic convergence studies have been conducted to evaluate and arrive at the final mesh for the finite element models.

The reaction force vs. the controlled displacement is illustrated in Figure 4.39, where the numerical simulations are compared to the envelope curve of the cyclic experimental response. One may observe that experimental data and numerical prediction are in a good agreement. Under sagging bending moment the specimen yield strength is well captured as expected; moreover the numerical simulation captures very well the hardening branch of the experimental response, both in term of strength and stiffness; this indicates a satisfactory behaviour of the numerical model. The model clearly shows the evolution of the distribution of the principal stresses of compression in the slab for the specimen subjected both under sagging and hogging bending moment.

4. SEISMIC RESPONSE OF PARTIAL-STRENGTH COMPOSITE JOINTS

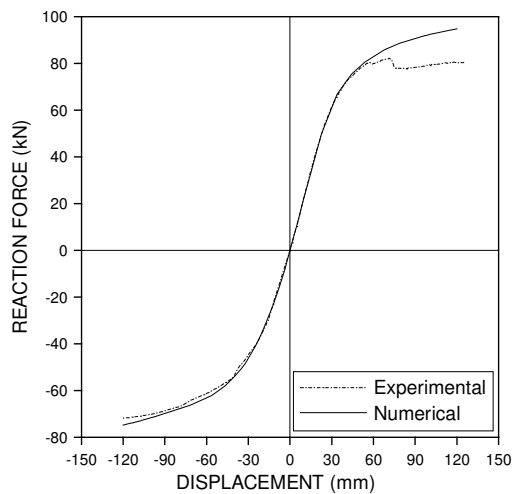


Figure 4.39. Experimental and predicted force vs. displacement of CJ-EXT specimen

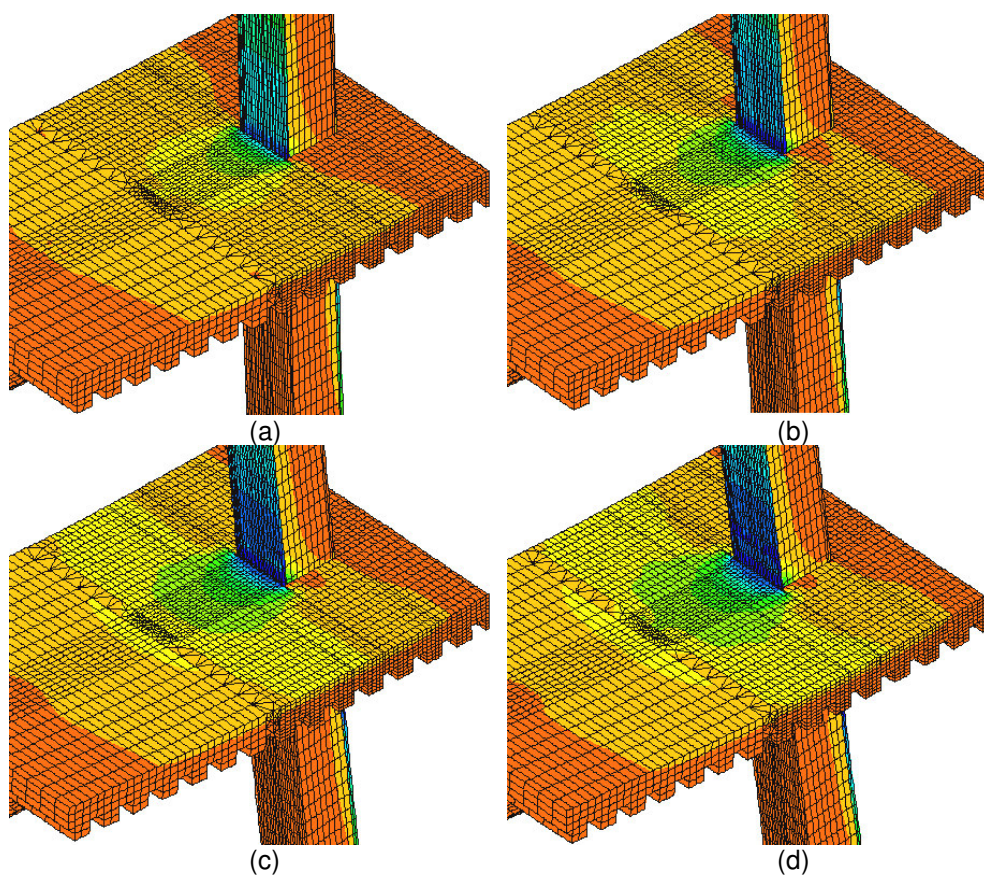


Figure 4.40. Evolution of the principal stresses of compression in the slab under sagging bending moment for a top displacement equal to: (a) 50 mm; (b) 75 mm; (c) 100 mm; (d) 125 mm

4. SEISMIC RESPONSE OF PARTIAL-STRENGTH COMPOSITE JOINTS

For sagging bending moment, as depicted in Figure 4.40, the localization of the stresses in the front of the column flange is evident. Moreover, under hogging bending moment, the model clearly shows the distribution of the stresses in the slab, due to the transfer of forces from the reinforcing bars in tension to the partially encased column. Such distribution explicates well the cracks in the concrete slab observed during the test, as depicted in Figure 4.41.

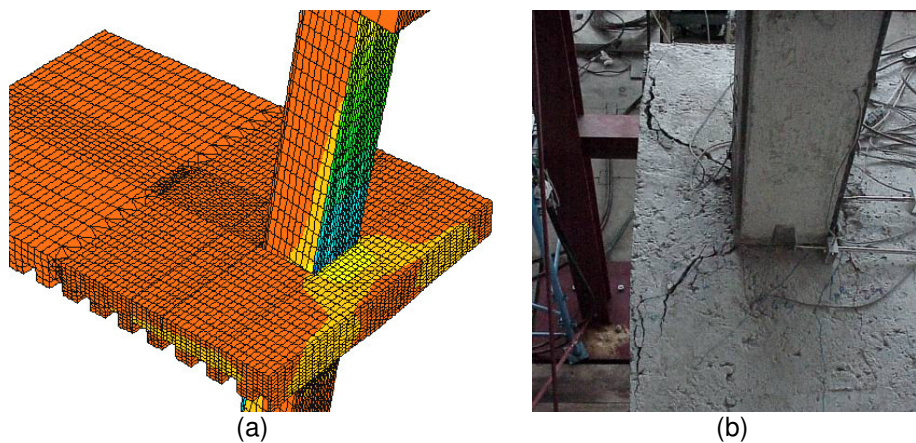


Figure 4.41. (a) Numerical distribution of the principal stresses of compression in the slab under hogging bending moment; (b) cracks in the concrete slab due to the transfer of force from the concrete slab to the column during the experimental test

Moreover, the model captures very well the deformed configuration of the joint, with localization of plastic hinges in the flanges of the steel column, in correspondence of the stiffeners and the yielding of the end plate in tension, as depicted in Figure 4.42. Moreover, the stress concentration due to the mobilization of the column web panel in shear is evident in the panel zone.

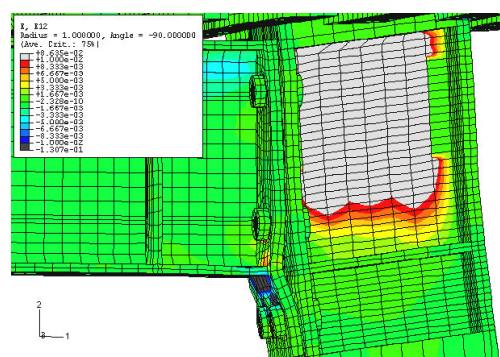


Figure 4.42. Plastic hinges in the flanges of the steel column and yielding of the end plate in tension

4. SEISMIC RESPONSE OF PARTIAL-STRENGTH COMPOSITE JOINTS

The strut and tie mechanisms to be activated in the slab depend on the joint flexibility. The numerical analyses carried out under sagging bending moment have evidenced the presence of high gradients of compression stresses in front of the column flanges. It is impossible to appreciate the formation of the idealized Mechanism 2, proposed in Section 4.5.1. In fact, in the portion of the concrete slab around the column, the numerical model evidences tensile stresses that do not permit the presence of an idealized concrete strut. This means that, under sagging bending moment, the resistance of the composite connection depends only on the resistance of the proposed Mechanism 1. The experimental loss of resistance of the joint is due to the high level of stresses that the concrete slab should transmit from the composite section of the beam to the column.

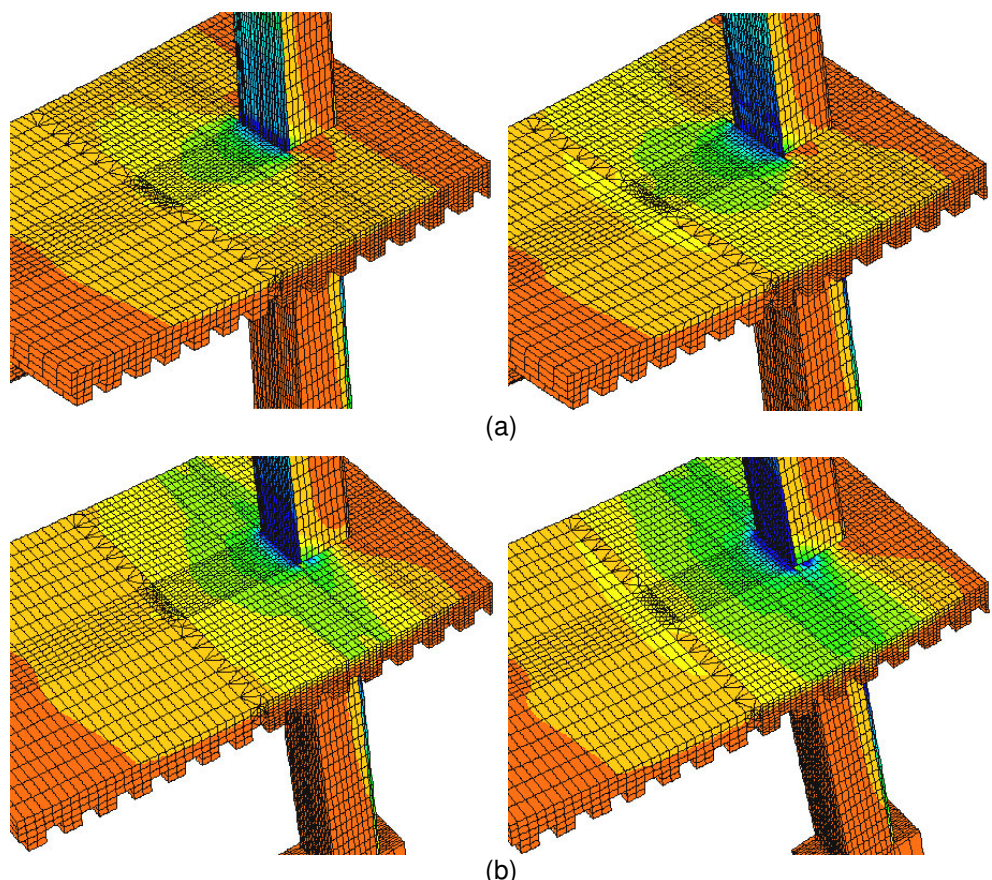


Figure 4.43. Evolution of the compression stress distribution in the concrete slab due to: (a) activation only of Mechanism 1; (b) Activation of Mechanisms 1 and 2

On the basis of the observations that have been brought to light, it is possible to design some constructional details that permit the formation of the Mechanism 2 in

4. SEISMIC RESPONSE OF PARTIAL-STRENGTH COMPOSITE JOINTS

the concrete slab, with an increase of the global joint resistance and ductility. The numerical model aims to calibrate the difference, in term of global response and local stress distribution, between the experimental specimen and the improved model. In fact, to better evidence the formation of Mechanism 2, the surfaces of the concrete slab and of the concrete portion of the column have been merged by means of constraint relation introduced in the numerical model. As depicted in Figure 4.43, the improved model clearly shows a uniform distribution of the compression stresses in the concrete slab with the increase of the imposed top displacement; in detail, it is possible to evidence that for an imposed displacement equal to 50 mm Mechanism 1 results completely activated in the frontal zone of the column flange. Successively, Mechanism 2, formed by the idealized concrete struts balanced by the transversal reinforcing bars, is put in action up to a top displacement equal to 120 mm, in which both the mechanisms develop the maximum permitted strength of the concrete. The reported results evidence that:

- Mechanism 1 doesn't activate at the same time of Mechanism 2. This means that Mechanism 1 results more rigid than Mechanism 2;
- only through constructional and designed details it is possible to activate Mechanism 2 in the transfer of forces from the concrete slab to the column;
- the compression struts in the concrete slab of Mechanism 2 don't have, as assumed, an inclination of 45 degrees;

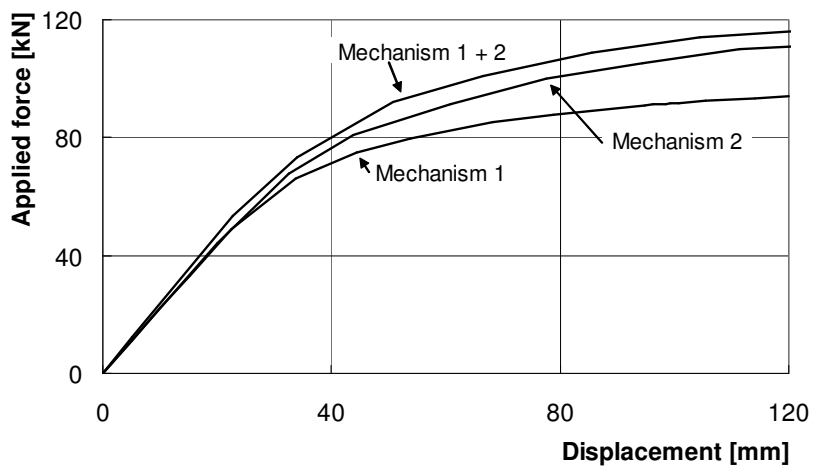


Figure 4.44. Monotonic applied force vs. top-displacement of an exterior joint under sagging bending: experimental response and numerical response for different activations of Mechanisms 1 and 2.

Both mechanisms cause a stiffening and strengthening of the exterior joint as illustrated in Figure 4.44. Finally, it is important to underline that the constraint

4. SEISMIC RESPONSE OF PARTIAL-STRENGTH COMPOSITE JOINTS

between concrete slab and column imposed in the model can be realized reality by means of some designed rebars or stirrups, which connect the two portions of concrete and permit the formation of the concrete struts due to presence of high resistance in shear, directly by friction, indirectly by shear yielding of the rebars or of the stirrups. The above-mentioned details are reported in Figure 4.45.

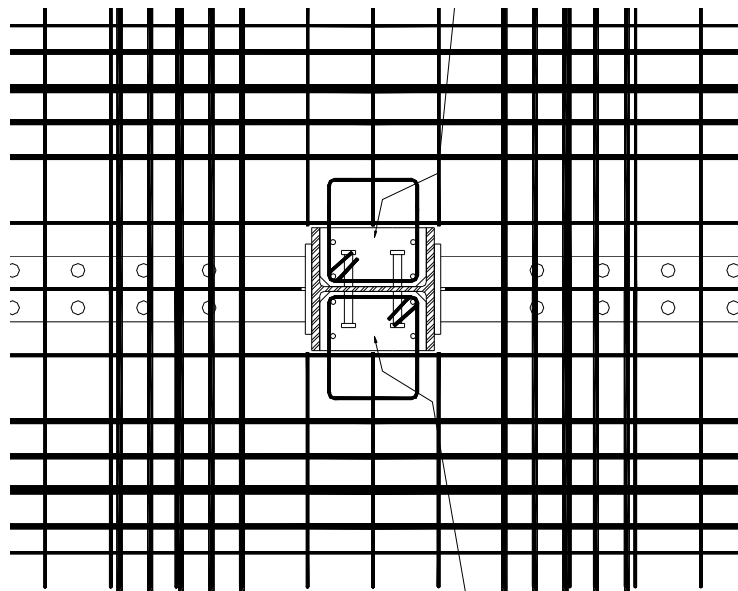


Figure 4.45. Detail in the concrete slab for activating Mechanism 2

4. SEISMIC RESPONSE OF PARTIAL-STRENGTH COMPOSITE JOINTS

4.9 Numerical analyses of the prototype structure

The behaviour of the prototype structure described above was simulated by means of a 2D numerical model of the main frame. All the constitutive elements, i.e. composite beams, composite partially encased columns, base joints, were modelled by using their actual geometrical and mechanical characteristics. Moreover, on the basis of the results obtained from the analyses of the tested specimens, it was possible to calibrate the analytical model of the semi-rigid partial strength joint, both for the exterior and for the interior configuration. As said before, the composite beam-to-column joint is modelled using a rotational spring to simulate the connections and a rectangular articulated polygon with a translational spring simulating the column web panel. Due to the inaccuracy of the analytical model obtained by applying the component method (Eurocode 3, 2001), the experimental response was reproduced by means of a hysteretic *Bouc-Wen* model with damage rules implemented in the program IDARC 2D (Valles et al, 1996): the smooth hysteretic model of Sivaselvan and Reinhorn (1999). In Figure 4.46 a scheme of the numerical model used for the simulations is represented.

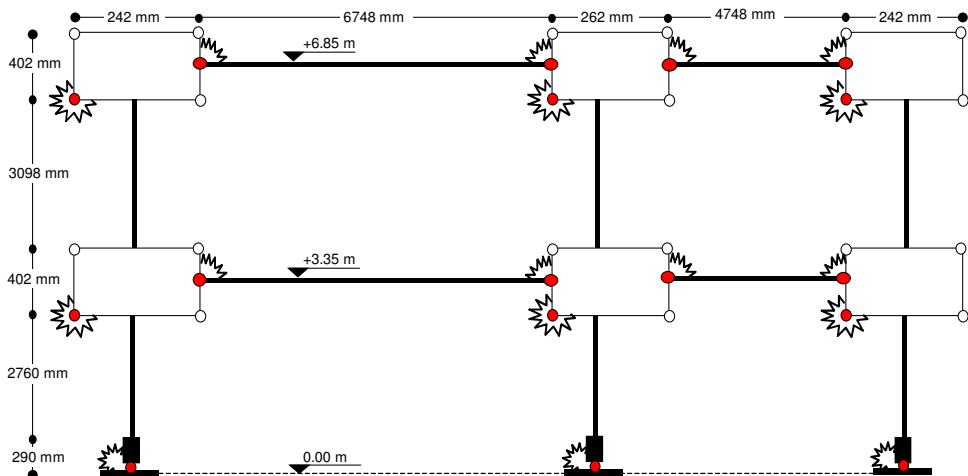


Figure 4.46. Scheme of the numerical model used for the simulations

By means of this numerical model both the non-linear static pushover (NSP) analysis and the incremental dynamic analysis (IDA) have been conducted. Hereinafter, the main results of these analyses will be discussed. The results of these analyses in term of maximum plastic rotation at the joint, total amount of dissipated energy and cumulated damage in the dissipative zones, have permitted to choose the correct accelerogram to impose on the prototype structure in the ELSA laboratory by means of the Pseudo-Dynamic (PsD) technique.

4. SEISMIC RESPONSE OF PARTIAL-STRENGTH COMPOSITE JOINTS

4.9.1 Pushover vs. incremental dynamic analysis results

Pushover analysis

As said in Chapter 2 Subsection 4, the purpose of the pushover analysis is to evaluate the expected performance of a structural system by estimating its strength and deformation demands in design earthquakes by means of a static inelastic analysis, and comparing these demands to available capacities at the performance levels of interest (Krawinkler and Seneviratna, 1998). By means of the numerical model above described, which implements the non-linear behaviour of the structural members of the prototype structure, the NSP analysis based on the Capacity Spectrum Method (CSM) and on the Performance Point Method proposed in the Eurocode 8 (2002) and FEMA-273 (1997) were performed. As explained in Chapter 2, the pushover analysis based on the CSM obtains the performance point in the ADRS space (standard pseudo-acceleration S_a vs. deformation spectrum S_d). Differently from this, the response curve based on the EC8 and FEMA assumptions is determined by nonlinear static analysis of the structure subjected to lateral forces with invariant distribution over the height but gradually increasing values until a target value of roof displacement is reached (*Target Displacement*). The floor displacements, storey drifts, joint rotations, plastic hinge rotations, etc., computed at the target displacement represent the earthquake induced demands on the structure. Three distributions of lateral forces are specified in FEMA-273 (1997):

- (a) uniform distribution: $s_j^* = m_j$ (where $j = 1, 2, \dots, N$ is the floor number);
- (b) equivalent lateral force (ELF) distribution: $s_j^* = m_j h_j^k$, where h_j is the height of the j -th floor above the base, and the exponent k varying linearly from the value 1 for fundamental period $T_1 < 0.5$ sec and the value 2 for $T_1 \geq 2.5$ sec;
- (c) SRSS distribution: s^* is defined by the lateral forces back-calculated from the storey shears determined by response spectrum analysis of the structure, assumed to be linearly elastic. This last distribution is not present in the Eurocode 8 (2002) recommendations.

The lateral force profiles in static pushover analyses influence the structural response. The first distribution represents the lateral forces that are proportional to the vertical distribution of the mass at various levels. The use of the uniform load shape may be justified in the light of a possible soft storey mechanism of irregular buildings. If this mechanism occurs, the response will be controlled by a large drift in the first storey. Therefore, this load distribution may give better predictions of the overall response. On the other hand, the code lateral load shape represents the forces obtained from the predominant mode of vibration. The inverted triangular (code) and the rectangular (uniform) load shapes also represent the extreme cases

4. SEISMIC RESPONSE OF PARTIAL-STRENGTH COMPOSITE JOINTS

from the linear distribution point of view. Moreover, the third shape, calculated as SRSS combinations of the load distributions is obtained from modal analyses of the buildings. The choice of this load shape is made to take into consideration the anticipated effect of higher modes of vibrations for moderate long period and irregular structures, as well as for buildings with hybrid lateral resistance systems. Another difference between the two approaches, i.e. the EC8 procedure and the FEMA-273 procedure, is the evaluation of the target displacement. Following the indication contained in the EC8 (2002), the capacity curve, which represents the relation between base shear force and control node displacement, is determined by pushover analysis for values of the control displacement ranging between zero and the value corresponding to 150% of the target displacement. The target displacement is defined as the seismic demand derived from the elastic response spectrum in terms of the displacement of an equivalent SDoF system. The procedure presented in the Annex B of the EC8 (2002) is articulated as follows.

- i. The MDof system is firstly converted into an SDoF system. The following relation between normalized lateral forces \bar{F}_i and normalized displacements Φ_i is assumed:

$$\bar{F}_i = m_i \Phi_i \quad (4.28)$$

where m_i is the mass in the i -th storey. Displacements are normalized in such a way that $\Phi_n=1$, where n is the control node (usually, n denotes the roof level), so that $\bar{F}_n = m_n$. The mass of an equivalent SDoF system m^* is determined as:

$$m^* = \sum m_i \Phi_i = \sum \bar{F}_i \quad (4.29)$$

and the transformation factor is given by:

$$\Gamma = \frac{m^*}{\sum m_i \Phi_i^2} = \frac{\sum \bar{F}_i}{\sum \left(\frac{\bar{F}_i^2}{m_i} \right)} \quad (4.30)$$

The force F^* and the displacement d^* of the equivalent SDoF system are then computed as:

$$F^* = \frac{F_b}{\Gamma}, \quad d^* = \frac{d_n}{\Gamma} \quad (4.31)$$

4. SEISMIC RESPONSE OF PARTIAL-STRENGTH COMPOSITE JOINTS

where F_b and d_n are, respectively, the base shear force and the control node displacement of the MDof system.

- ii. Definition of the yield force F_y^* , which also represents the ultimate strength of the idealized system; it is equal to the base shear force at the formation of the plastic mechanism. The initial stiffness of the idealized system is determined in such a way that the areas under the actual and the idealized force-deformation curves are equal (see Figure 4.47).

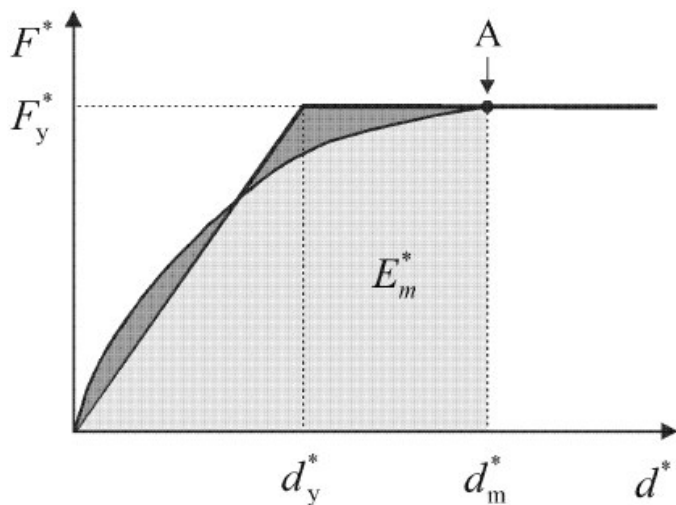


Figure 4.47. Determination of the idealized elasto-perfectly plastic force-displacement relationship (EC8, 2002)

Based on this assumption, the yield displacement of the idealized SDof system d_y^* is given by:

$$d_y^* = 2 \left(d_m^* - \frac{E_m^*}{F_y^*} \right) \quad (4.32)$$

where E_m^* is the actual deformation energy up to the formation of the plastic mechanism.

- iii. Determination of the period T^* of the idealized equivalent SDOF system, determined by:

$$T^* = 2\pi \sqrt{\frac{m^* d_y^*}{F_y^*}} \quad (4.33)$$

4. SEISMIC RESPONSE OF PARTIAL-STRENGTH COMPOSITE JOINTS

- iv. Determination of the target displacement for the equivalent SDOF system with period T^* and unlimited elastic behaviour, given by:

$$d_{et}^* = \left(\frac{T^*}{2\pi} \right)^2 S_e \quad (4.34)$$

where $S_e(T^*)$ is the elastic acceleration response spectrum at the period T^* . For the determination of the target displacement d^* for structures in the short-period range and for structures in the medium and long-period ranges different expressions should be used as indicated below. The corner period between the short- and medium period range is T_C .

If $T^* < T_C$:

$$d_t^* = \frac{d_{et}^*}{q_u} \left(1 + (q_u - 1) \frac{T_C}{T^*} \right) \geq d_{et}^* \quad (4.35)$$

where q_u is the ratio between the acceleration demands in the structure with unlimited elastic behaviour S_e and in the structure with limited strength.

$$q_u = \frac{S_e m^*}{F_y^*} \quad (4.36)$$

If $F_y^* / m^* \geq S_e$, the response is elastic and $d_t^* = d_{et}^*$.

- v. Determination of the target displacement for MDOF system, given by:

$$d_t = \Gamma d_t^* \quad (4.37)$$

The target displacement corresponds to the control node. Moreover, the relation between different quantities can be visualized in Figure 4.48 and in Figure 4.49). The figures are plotted in acceleration - displacement format. The period T^* is represented by the radial line from the origin of the coordinate system to the point at the elastic response spectrum defined by coordinates $d^* = (T^*/2\pi)^2 \cdot S_e$ and S_e .

4. SEISMIC RESPONSE OF PARTIAL-STRENGTH COMPOSITE JOINTS

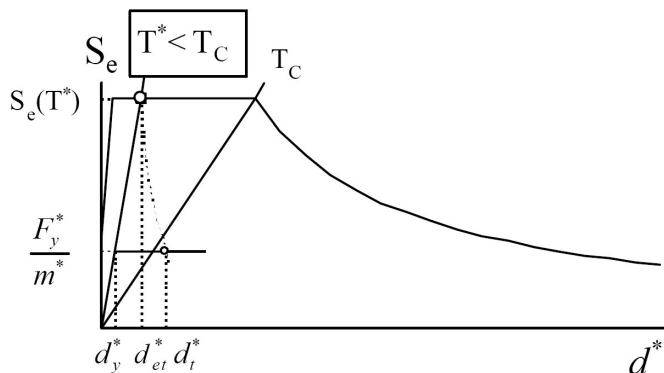


Figure 4.48. Relation between $S_e(T^*)$ and d^* for $T^* < T_c$

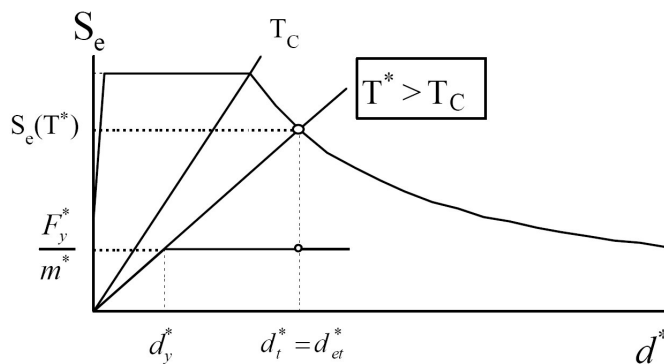


Figure 4.49. Relation between $S_e(T^*)$ and d^* for $T^* > T_c$

Incremental dynamic analysis

As said in Chapter 2, the Incremental Dynamic Analysis (IDA) technique consists of a series of non-linear analyses of the structure for a ground motion that is increased in amplitude, until instability of the structure is predicted. This analysis is repeated for multiple ground motions, so that statistics on the variation of demand and capacity with ground motion character can be attained. This procedure was followed in doing this analysis as follows:

- Choice of a suite of accelerograms representative of the site and hazard level.
- Performance of an elastic time history analysis of the building for one of the accelerograms. Plotting of the point on a graph whose vertical axis is the spectral ordinate for the accelerogram at the first period of the building and horizontal axis is the maximum calculated drift at any story. Drawing of a straight line from the origin of the axis to this point. The slope of this line is

4. SEISMIC RESPONSE OF PARTIAL-STRENGTH COMPOSITE JOINTS

referred to as the elastic slope for the accelerogram. Calculation of the slope for the rest of the accelerograms using the same procedure and calculation of the median slope. The slope of this median line is referred to as the elastic slope, S_e .

- c. Performance of a non-linear time history analysis of the structure subjected to one of the accelerograms. Plotting of this point, called Δ_1 , on the graph.
- d. Increase of the amplitude of the accelerogram and repeat step c. This may be done by multiplying the accelerogram by a constant, which increases the spectral ordinates of the accelerogram by 0.1g. Plotting of this point as Δ_2 . Repetition of step 4 until the structure will be a mechanism or the maximum rotation capacity of the components will be reached. When this condition is reached, Δ_i is the global drift capacity for this accelerogram.
- e. Choice of another accelerogram and repetition of steps c through d this for each accelerogram. The median capacity for global collapse is the median value of the calculated set of drift limits.

The factors that affect the curve of the Incremental Dynamic Analysis (IDA) are P- Δ effects, increment used for the analysis, ground motions used, strain hardening ratio, shifting of fundamental period due to non-linearity, higher mode effects, and shifting of maximum story drift location.

The accelerograms employed are characterized by strong motion duration of 10 sec with rise and decay periods of 2,5 and 5,0 secs respectively as shown Table 4.6. The generation of the spectrum compatible accelerograms was done according to the method provided by Clough and Penzien (1993). At the end of the generation process, in order to remove the drift in terms of displacement and velocity in all the accelerograms, the method of the linear baseline correction proposed by Meskouris (2000) was applied.

Δt_r [sec]	Δt_{sm} [sec]	Δt_d [sec]
2,5	10,0	5,0

Table 4.6. Rise, decay and strong motion durations employed for the generation of the accelerograms

The generated spectrum compatible accelerograms were three and they were referred to as A-03, A-12 and A-14. It is important to underline that the accelerogram employed for the pseudo-dynamic tests on the prototype structure was sorted out basing on the possible values and localization of the damage induced into the structure at the collapse limit state. The selection of the accelerogram was done considering the following parameters:

4. SEISMIC RESPONSE OF PARTIAL-STRENGTH COMPOSITE JOINTS

- the maximum rotation and local damage in the joints;
- the local damage in the columns;
- the value of the ratio between the input energy and the total hysteretic energy dissipated.

After the elaboration of the numerical analyses, the accelerogram A-14 was chosen because of the highest level of damage induced in the joints and the lower values of damage in the columns. This last parameter was taken into account in order to avoid dangerous global collapse due to the loss of stability at the base level. The main characteristics of the accelerogram A-14 are reported in Figure 4.50.

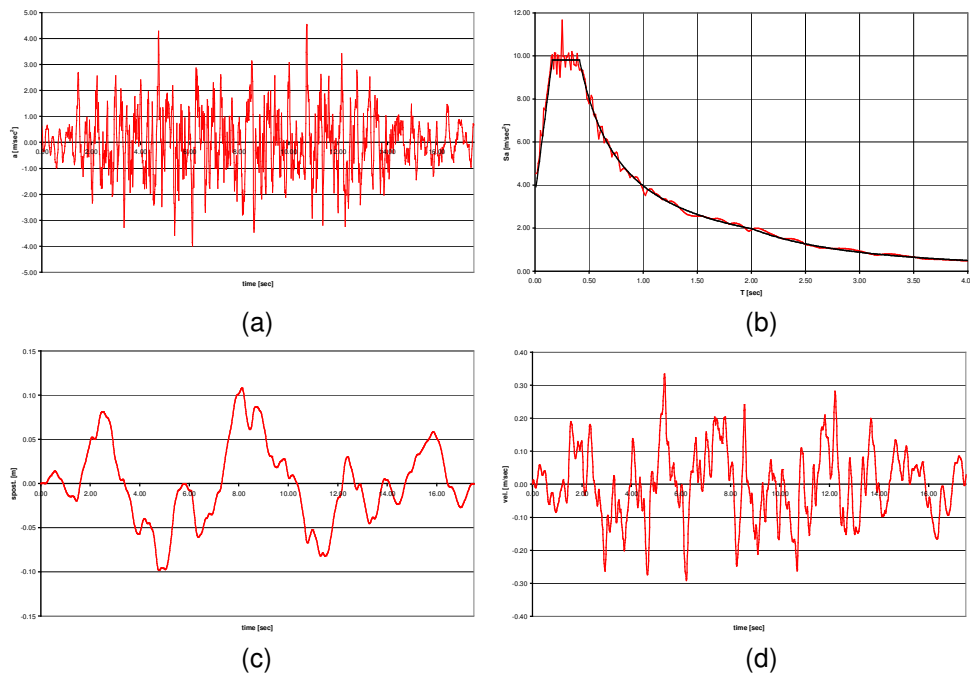


Figure 4.50. (a) Accelerogram A-14 employed for the analyses; (b) Elastic response spectrum of the accelerogram A-14 with ξ equal to 5%; (c) Integrated base displacements after the application of the baseline correction; (d) Integrated base velocity after the application of the baseline correction

Main results

The pushover and the incremental dynamic analysis was performed and then compared. Hereinafter the main results are reported in Table 4.7, whereas the obtained response curves are plotted in Figure 4.51. The uniform and triangular curves of the pushover analysis represent the upper and lower limit of the response curve obtained by the IDA (Antoniou et al, 2002). Moreover, in our case,

4. SEISMIC RESPONSE OF PARTIAL-STRENGTH COMPOSITE JOINTS

the curve that corresponds to lateral load proportional to the 1st modal shape underestimates the response curve of the IDA in the zone with large non-linear deformations; the curve obtained with a uniform load distribution overestimates the IDA curve in the first zone of the structural response up to a peak ground acceleration equal to 1.40g.

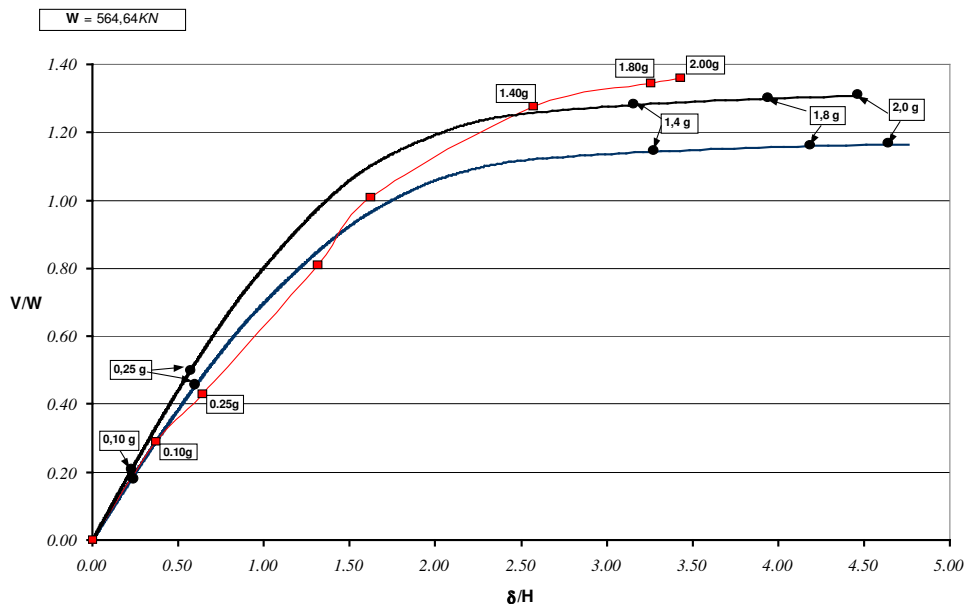


Figure 4.51. Pushover vs. IDA curve obtained by the numerical analyses

p.g.a.	EC8 pushover analysis				IDA	
	First Modal		Uniform			
	δ (mm)	Shear (kN)	δ (mm)	Shear (kN)	δ (mm)	Shear (kN)
0.10 g	16.2	109.0	15.7	115.85	23.4	164.2
0.25 g	40.6	265.4	39.2	283.5	43.7	253.1
1.40 g	227.2	638.1	219.8	717.1	179.8	720.2
1.80 g	292.1	649.3	282.6	734.1	227.8	759.6
2.00 g	324.6	655.0	313.9	739.7	240.0	768.2

Table 4.7. Pushover vs. IDA data obtained by the numerical analyses

On the basis of the numerical results it was possible to determine the behaviour factor of the designed structure. Two different method were used:

4. SEISMIC RESPONSE OF PARTIAL-STRENGTH COMPOSITE JOINTS

- The first one calculates the value of the behaviour factor as the ratio between the p.g.a. at the ultimate limit state, and the p.g.a. at the first yielding of the structure.

$$q_{dyna} = \frac{pg a_u}{pg a_y} \quad (4.38)$$

- The second one uses the results obtained from the non-linear static analysis (pushover curve) and determines the value of the behaviour factor by means the following formula:

$$q_{stat} = \mu_d \Omega \quad (4.39)$$

where μ_d represents the ductility factor, while Ω is the overstrength factor (Eurocode 8, 2002).

The two obtained values are reported in Table 4.8. One may observe that the results are in a good agreement with the design behaviour factor $q = 6$ proposed by the Eurocode 8 (2002). Nevertheless, in the same Table the calculated design overstrength factor Ω_d is reported. This parameter is obtained by using the formula

$$\Omega_d = \frac{pg a_y}{pg a_d} \text{ con } pg a_d = \frac{a_g}{q_d} = \frac{0,40}{6} \quad (4.40)$$

where $p.g.a_d$ is the design value of the base acceleration.

<i>Dynamic analysis</i>		<i>Pushover analysis</i>	
p.g.a. _y	0.25g	Overstrength factor Ω	
		α_1	0.459
		α_u	1.164
p.g.a. _u	1.54g	$\Omega = \alpha_1 / \alpha_u$	2.533
		Ductility factor μ_d	
		μ_d	3.11
q_{dyna}	6.16	q_{stat}	7.89
p.g.a. _d	0.07g		
p.g.a. _y	0.25g		
Ω_d	3.75		

Table 4.8. Values of the behaviour factor obtained from the analyses

4. SEISMIC RESPONSE OF PARTIAL-STRENGTH COMPOSITE JOINTS

The possible factors that have influenced the overestimation of the design overstrength factor should be:

- the partial safety factors used during the design of the structure;
- the design action amplification for accidental torsional effects;
- the interstorey drift limits that should be satisfied in the design;
- the difference between the design strength and the actual strength value of the materials;

4.10 Pseudo-Dynamic tests on the prototype structure

It is worthwhile to emphasize that quasi-static cyclic loading tests are no doubt the most effective tests to acquire data on the capacity of the structure, such as the maximum resistance and ductility. Nonetheless, to evaluate the performance of the structure in terms of complex hysteretic behaviour under earthquake-like loading pseudo-dynamic tests (PsD) are needed. Pre-test analyses of the specimen and post-test comparisons will be performed.

Basing on the Performance Based Seismic Engineering (PBSE) method, the values of the peak ground acceleration (PGA) employed for the pseudo-dynamic tests were chosen, as reported in Table 4.9.

PsD Tests	PGA [g]	OBJECTIVES
1	0,10	<i>Elastic Test</i>
2	0,25	<i>Serviceability Limit State: SLS</i>
3	1,40	<i>Ultimate Limit State: ULS (joints' maximum rotation equal to 35 mrad)</i>
4	1,80	<i>Collapse Limit State CLS</i>

Table 4.9. Values of the PGA's for the pseudo-dynamic tests

1. Snap back PsD test with a value of acceleration equal to 0.1g was performed to measure dynamic elastic properties of the frame, viz. eigenvalues, eigenvectors and equivalent viscous damping as well as to verify the precision of the PsD algorithm.
2. The objective of the second test was to lead the structure to the elastic limit, so as provided by the EC8 for the structural Serviceability Limit State. As a result, the basic vertical- and lateral force resisting system of the structure substantially retain original strength and stiffness. Only limited structural

4. SEISMIC RESPONSE OF PARTIAL-STRENGTH COMPOSITE JOINTS

damage has occurred. Basing on the numerical results taken out from IDA and from the Pushover analysis, the value of PGA employed for the 20% Earthquake was estimated at 0.25g.

3. The 100% earthquake PsD test was conducted by applying the input earthquake. So as provided by EC8, the minimum capacity in terms of plastic rotation of the beam-to-column joints is equal to 35 mrad. For the estimation of the PGA at the Ultimate Limit State, this last parameter was so considered. From IDA and Pushover analysis the value of acceleration equal to 1.4g was taken out. As a result, a significant amount of damage is inflicted to the structures. As a matter of fact, an artificial accelerogram will provide more large inelastic cycles for observation, but may damage the structure too much before the cyclic test.
4. For the *Near to Collapse* test, the values of PGA - equal to 1.8g - were calculated.
5. A final cyclic test is conducted according to the ECCS 45 (1986) procedure to study a severe amount of damage in the members and connections in a controlled and systematic way, which is not possible by means of earthquake PsD tests.

4.10.1 Testing apparatus and instrumentation

Four actuators are needed (two for each storey) together with the relevant exterior digital transducers (see Figure 4.52 and Figure 4.53). For the measurement of the rotation capacity of the joints and the deformation of the structural element (composite beam, partially encased column and connection) inclinometers, strain gages and LVDTs will be used.

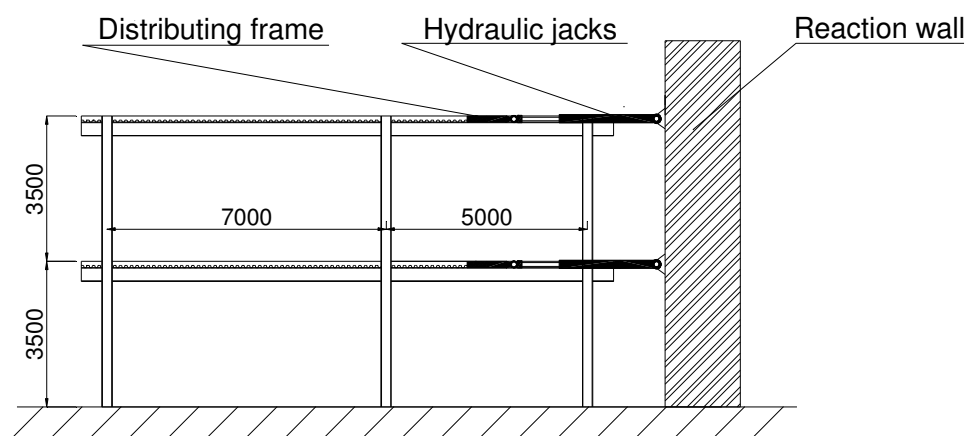


Figure 4.52. Lateral view of the 3D frame

4. SEISMIC RESPONSE OF PARTIAL-STRENGTH COMPOSITE JOINTS

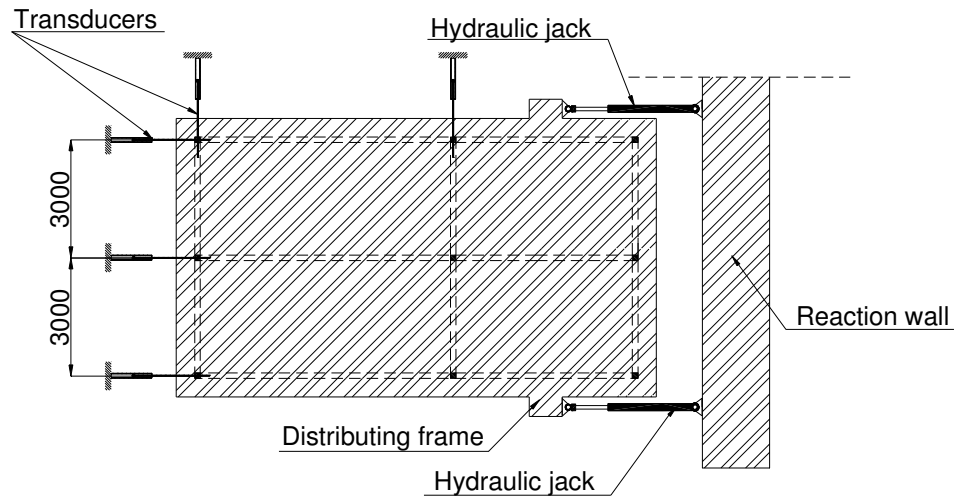


Figure 4.53. Plan view of the frame

Only two of the frames of the test structure, then referred to as exterior and interior ones, were instrumented. Moreover, the interior and the exterior frames were characterized by two different instruments arrangement. The locations of the aforementioned instruments in the exterior and interior frame are shown in Figure 4.54 and Figure 4.55.

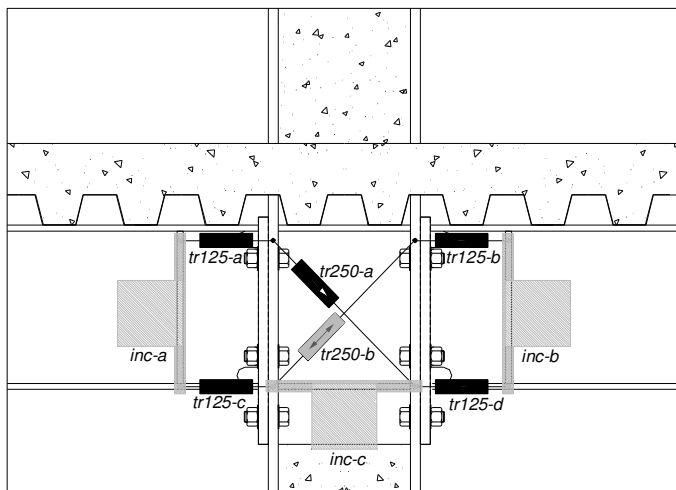


Figure 4.54. Exterior beam-to-column joint measurement equipment

4. SEISMIC RESPONSE OF PARTIAL-STRENGTH COMPOSITE JOINTS

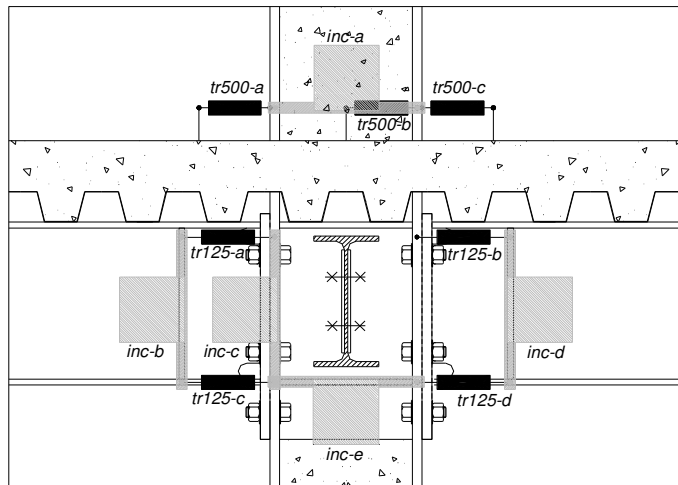


Figure 4.55. Interior beam-to-column joint measurement equipment

4.10.2 Results of the PsD test n°1

The behaviour of the structure was essentially elastic and no damage could be observed at the beam-to-column joints and at the base joints. Only at the bottom storey some little cracks were present on the slab in the joint areas, all parallel to the transverse beams and starting from the edges of the steel sections of the columns. Due to the presence of the concrete blocks at the second level, cracking developed in the transverse direction, mainly on the column line. At the first step of the *Spatial Model* procedure the frequencies of the first and second mode have values equal to 2.31 Hz and to 7.81 Hz, respectively. The mean value of the modal damping is very low, equal to 1.03% for the first mode and to 0.69% for the second one. The maximum interstorey drifts reached at the first and second level are -9.7 mm and -12.3 mm, respectively. These correspond to a value of about 0.35% of the interstorey height.

4.10.3 Results of the PsD test n°2

The objective of the second test was to induce into the structure a first yielding with no excessive damage. From a first visual inspection it could be observed that:

- no damage occurred at the column base, no crashing or spalling of the concrete and no local buckling in the steel flanges;

4. SEISMIC RESPONSE OF PARTIAL-STRENGTH COMPOSITE JOINTS

- thin cracks developed transversally in the mortar under the base plates and in the concrete blocks in line with the hooked rebars and the middle of the column section;
- there was no visible gap between the end plate and the column flange;
- new cracks developed in the concrete slab.

The cracks induced into the slab were found to be more evident at the bottom storey and in the exterior beam-to-column joints. Therefore, damage seemed to be more pronounced on the exterior frames than on the interior ones, probably due to a larger effective slab width of the first, combined with possible in-plane deformations of the floor diaphragm at level 1. In the beam-to-column joint areas, on the interior side of the columns, cracks developed mainly parallel to the transverse beams in line with or in front of the interior columns, while, on the exterior one, an inclined cracking pattern formed under hogging bending moment. No spalling of the compressed concrete could be observed. At the column base no damage developed, no cracking and no local instabilities could be observed. On the contrary in the grout at the base joints some thin vertical cracks appeared in the transverse direction, on the line of the hooked rebars.

From the experimental results it was possible to recognize, directly from the measurement equipment, how the joints worked in terms of rotation. In Figure 4.56 the maximum rotation reached by the beam-to-column joints (web panels, connections and global joints) are shown. The values of rotation of the web panels and the connections are evaluated at the instant of maximum rotation in the joint.

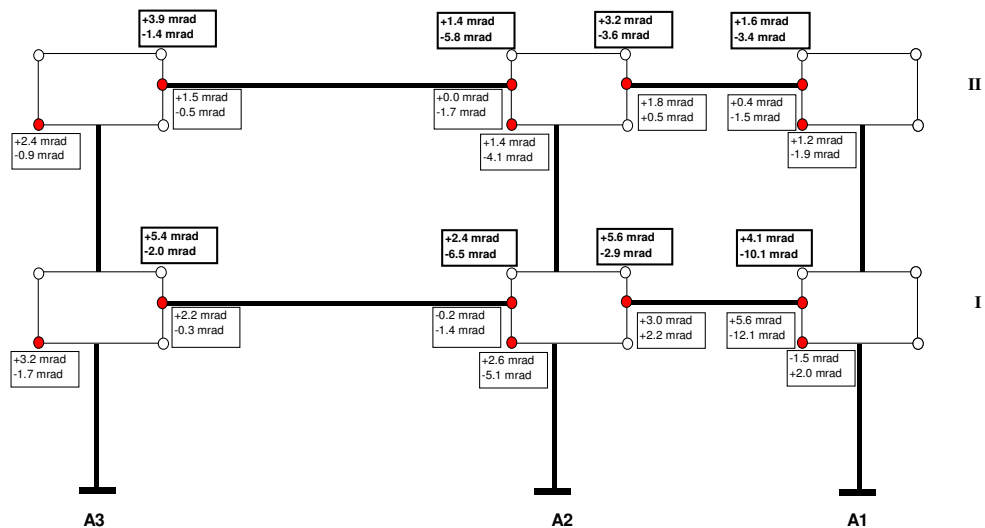


Figure 4.56. Maximum values of rotation reached by the beam-to-column joints of the interior frame during the PsD test n°2

4. SEISMIC RESPONSE OF PARTIAL-STRENGTH COMPOSITE JOINTS

Some remarks can now be made:

- the joints of the interior instrumented frame, where only the web panels reached the elastic limit while no connection yielded at this point, are lower than the exterior ones;
- the values of rotation are greater at the first level and on the column line 1.

The behaviour of the interior joints was quite elastic and no permanent rotation could be recognized. Conversely, in the exterior frame, all the joints reached the elastic limits. The main plastic mechanism started at about 12 sec, when probably the main inclined cracks on the exterior part of the slab developed. Nevertheless, the behaviour of the structure was essentially elastic and no damage could be observed.

4.10.4 Results of the PsD test n°3

The objective of the third test was to simulate the Ultimate Limit State, trying to make the joints rotate at least 35 mrad in the plastic range. From a first visual inspection of the beam-to-column joints, so as for the previous test, the damage was located more at the first level on the column line 1 and on the exterior frames. In the beam-to-column joints at Level 1, shear yielding of the web panel at the interior joints was observed, while at the exterior joints, under hogging bending moment, a flexural behaviour of the beam end plates was noticed. After the test, only little permanent deformations could be observed in the steel elements.



Figure 4.57. Rupture of the compressed concrete on the interior side of the C1-I joint

4. SEISMIC RESPONSE OF PARTIAL-STRENGTH COMPOSITE JOINTS

The shape of the cracks on the slab was quite the same as in test n° 2, even if their extension increased and spalling of the compressed concrete at level 1 was observed, as depicted in Figure 4.57. This last phenomenon was present only on the interior side of the joints. Gaps between the steel column flanges and the concrete slab were also observed at all joints, both the interior and the exterior ones.

So as for the previous test, at the column base no damage developed, no cracking and no local instabilities could be observed. Nevertheless, rotation at the base joints under the bending moment transferred by the columns was observed during the test. This was mainly due to the extension of the column anchor rods, and the failure of the grout in compression. Because of the gap between the upper side of the base plate and the nuts, it could be probably stated that yielding of the anchor rods had occurred. After the test, cracking were also noticed in the concrete blocks under the test structure.

While processing the experimental results, it was noticed that no beam-to-column joint reached 35 mrad of plastic rotation. In Figure 4.58 the maximum rotations of the joints are shown.

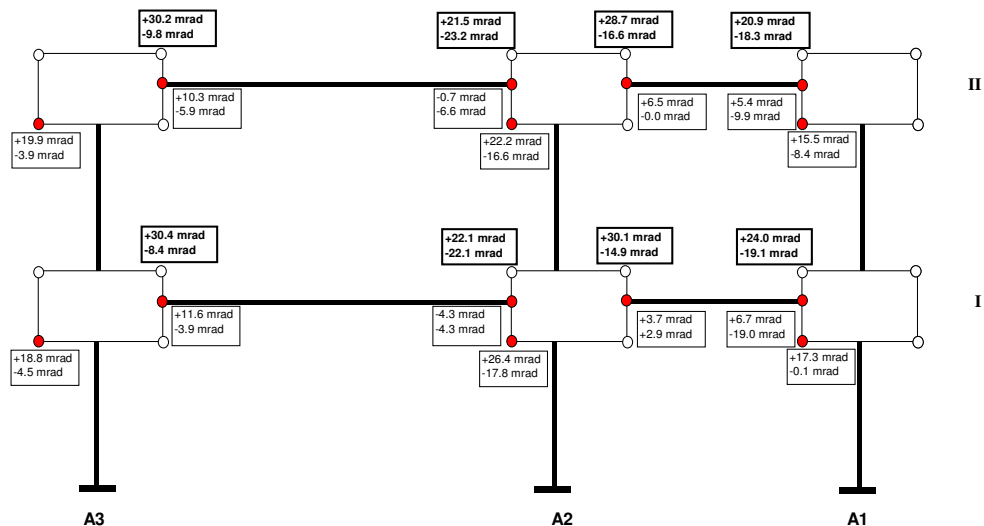


Figure 4.58. Maximum values of rotation reached by the beam-to-column joints of the exterior frame during the PsD test n°3

Other remarks can now be made:

- the maximum rotations of the joints at the first and second levels are quite the same;
- the joints on the span 1-2 of the interior frame rotated more than the exterior ones, thanks to a higher contribute of the web panels;

4. SEISMIC RESPONSE OF PARTIAL-STRENGTH COMPOSITE JOINTS

- on the exterior frame, the connection of the joint A1-I reached a value of rotation, under hogging bending moment, equal to 19 mrad. The main reason for this behaviour is the failure of the concrete on the exterior side, probably due to local tensile stresses grown in a reduced effective width. The same behaviour was observed in the tests conducted at the University of Pisa on the joint substructures;
- in all the other joints the web panel rotated more than the connections.

The displacements, the interstorey drifts, the restoring forces and the shear forces at the two levels are shown in Figure 4.59, while the results in terms of frequencies and modal damping are shown in the Figure 4.60. In this case the equivalent damping reached higher values, due to the hysteretic behaviour of the structure. The maximum value of the interstory drift is 110 mm while the maximum displacement at the second level is 198 mm.

4.10.5 Results of the PsD test n°4

The objective of the 4th test was to simulate the Collapse Limit State. From the visual inspection and the processing of the experimental results it could be observed that the behaviour of the beam-to-column and the base joints was comparable with that of the 3rd test. The only difference was the increase of the values of the maximum rotations. At the base columns no cracking of concrete or local buckling was seen. In this test the maximum value of the interstorey drift is 154 mm, which corresponds to a value of 4.43% of the height. The maximum displacement at the second level is 266 mm.

4.10.6 Results of the cyclic test

As described in the previous paragraph, the cyclic test was performed by imposing the displacements at the top storey and fixing the ratio between the reactions at the two levels R_1/R_2 . This factor was estimated by applying the spectral theory of the equivalent static analysis. From the results of the last PsD test it was possible to perform a calculation of the four elements of the stiffness matrix (as functions of time) and, by imposing the same interstorey drifts at the two levels, it could be observed how the ratio was equal to the one previously calculated. While on the A1-I joint the cracks on the slab were similar to those seen after the PsD tests, on the A3-I and C3-I joints the diagonal cracking at the exterior side started from the interior corner and the middle of the columns.

4. SEISMIC RESPONSE OF PARTIAL-STRENGTH COMPOSITE JOINTS

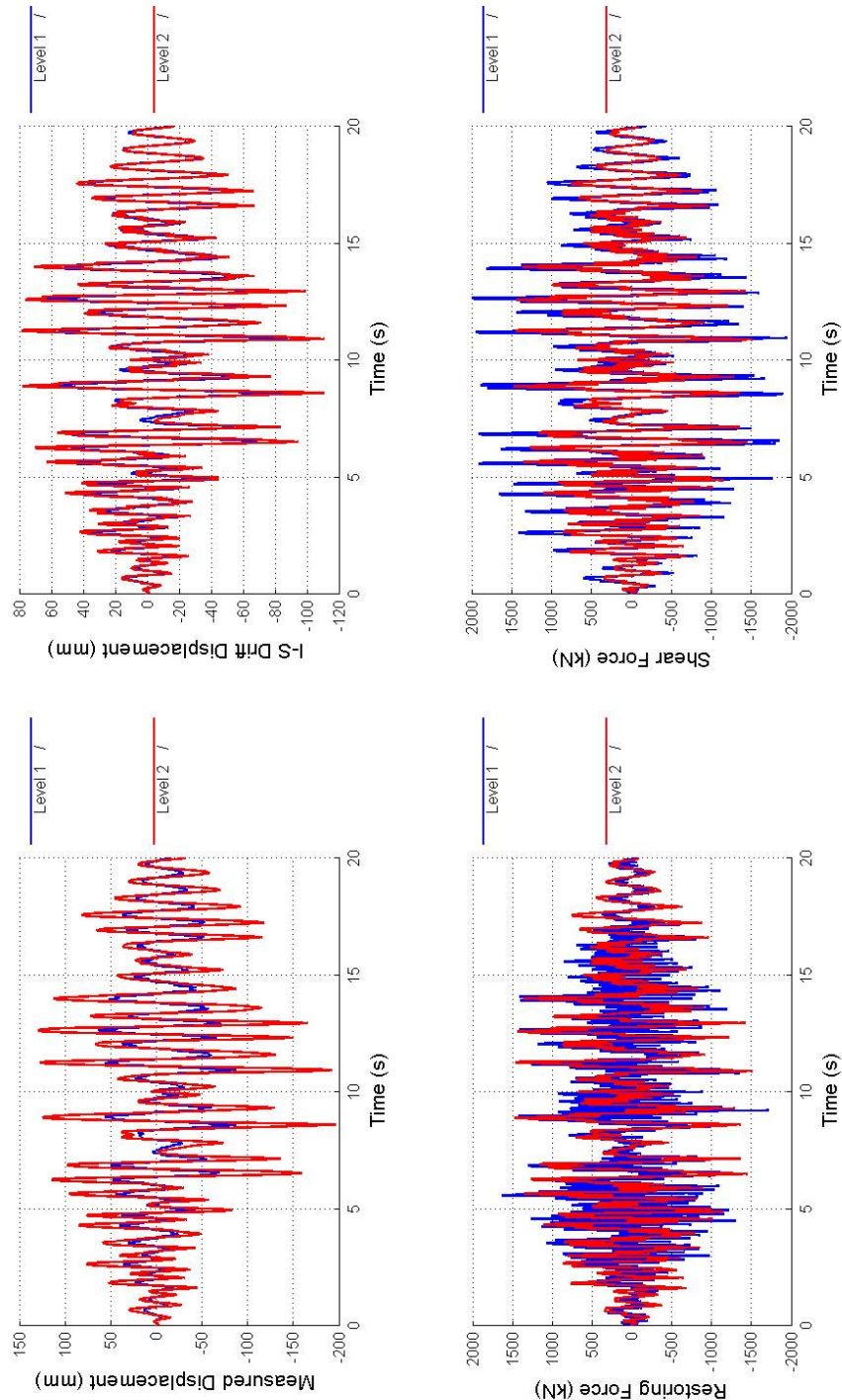


Figure 4.59. Results in terms of displacements, interstorey drifts (I-S Drift), restoring forces and shear forces at the two levels for the PsD test n°3

4. SEISMIC RESPONSE OF PARTIAL-STRENGTH COMPOSITE JOINTS

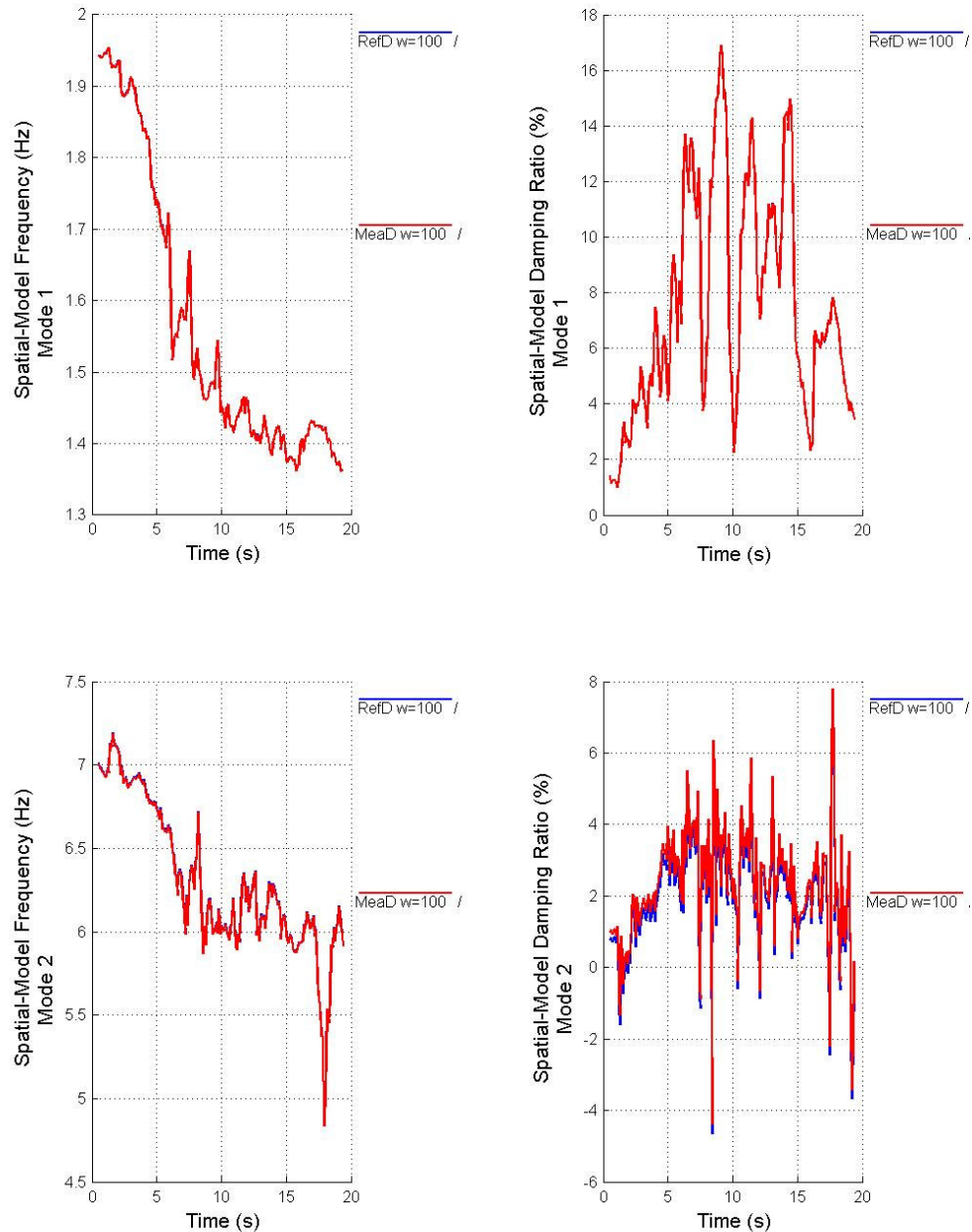


Figure 4.60. Results in terms of modal frequencies, modal damping for the PsD test n°3

4. SEISMIC RESPONSE OF PARTIAL-STRENGTH COMPOSITE JOINTS

From the processing of the experimental results it could be observed that the beam-to-column joints rotated more at the first level. Some remarks can be made:

- at the interior joints the web panels in shear contributed more than the connections while on the contrary at the exterior joints the connections rotated more;
- the joints A1 and A3 (the exterior joints on the exterior instrumented frame) worked quite in the same way as in the PsD tests.

Although we tested a composite structure the behaviour of all the joints was quite symmetric. This phenomenon was probably due to the damage induced during the PsD tests on the concrete slab.

4.11 Conclusions

The objective of this study has been the investigation of the seismic performance of a realistic size moment resisting frame structure of high ductility class according to Eurocode 8 (2002) under various levels of earthquake. Dissipative elements were conceived to be partial strength beam-to-column joints and column base joints at later stages. Some full-scale substructures, representing the interior and exterior joints, have been subjected to monotonic and cyclic tests at the Laboratory for Materials and Structures Testing of the University of Pisa in Italy.

Moreover, a new mechanical model of the partial strength beam-to-column joint has been described. The model, which still relies on experimental data, is capable of simulating the behaviour of the steel-concrete composite partial strength joints subjected to monotonic loading. In detail, the model is capable of defining yielding and failure evolution of different components. The component models of the slab have indicated clearly that the compressive strut strength of the composite slab bearing on the column flange depends on the shear stiffness of the column web panel. Moreover, the activation of diagonal compressive struts on column sides induced by transversal reinforcing bars is hindered by the direct bearing of the compressive strut. Some force-displacement relationships provided by the proposed mechanical model have been compared with analytical formulae and current European standards. The principles set forth have then been applied to the design of beam-to-column joints and columns of a full-scale frame structure that has been built and subjected to pseudo-dynamic tests at the ELSA Laboratory of the Joint Research Centre in Ispra. The construction of the full-scale structure proved that the construction of steel-concrete composite structures with partial strength beam-to-column joints and partially encased columns is highly efficient.

4. SEISMIC RESPONSE OF PARTIAL-STRENGTH COMPOSITE JOINTS

Pseudo-dynamic and cyclic test results confirmed that properly designed and constructed partial strength beam-to-column joints and partially encased columns without concrete in column web panels exhibit a favourable behaviour in terms of energy dissipation, limited strength degradation and ductility.

4.12 References

- AISC (1997), *Seismic provision for structural steel buildings*, Task Committee 113.
- Braconi A., Caramelli S., Cioni P., Salvatore W. (2003): *Earthquake-resistant composite steel-concrete frames: some constructional considerations*. Proceedings of the International Conference on Metal Structures, ICMS 2003. University of Miskolc, Hungary.
- Bursi O.S., Ferrario F., Fontanari V. (2992): *Non-linear Analysis of the Low-cycle Fracture Behaviour of Isolated Tee Stub Connections*. Computers and Structures, 80, 2333-2360.
- Bursi O.S., Lucchesi D, Salvatore W. (2003): *Beam-to-column connections for steel-concrete composite moment resisting frame designed for ductility class H*. To be presented in the Ninth International Conference on Civil and Structural Engineering Computing. Egmond aan Zee.
- Caramelli S., Salvatore W., Bursi O.S., Braconi A., Ferrario F. (2002): *ECSC Project 7210-PR-250 Ecoleader Project, Steel-concrete composite 3D Frame - Design according to Eurocodes*, University of Pisa and University of Trento.
- Chen, W. F. (1982): *Plasticity in reinforced concrete*. McGraw-Hill, New York, 270.
- Clogh R.W., Penzien J. (1993): *Dynamics of Structures*. Second Edition, McGraw-Hill ed.
- ECCS (1986): *Recommended Testing Procedure for Assessing the Behaviour of Structural Steel Elements under Cyclic Loads*. ECCS Publication n° 45.
- ECCS (1999): *Design of composite joints for buildings*. N° 109.
- FEMA 273 (1997): *HEHRR Guidelines for the seismic rehabilitation of buildings*. Federal Emergency Management Agency.
- FEMA 350 (2000): *Recommended seismic design criteria for new steel moment-frame buildings*. Federal Emergency Management Agency.
- Gioncu, V. and Mazzolani, F.M. (2002): *Ductility of seismic resistant steel Structures*. Spon Press, London, 1-40.

4. SEISMIC RESPONSE OF PARTIAL-STRENGTH COMPOSITE JOINTS

- Hibbit, Karlsson & Sorenson (2001): *ABAQUS user's manual – version 6.2.4.* Pawtucket. R.I.
- Hilleborg A., Modéer M. and Peterson, P.E. (1976): *Analysis of crack formation and crack growth in concrete by means of fracture mechanics and finite elements.* Cement and Concrete Research, 6, 773-782.
- International Conference of Building Officials (1997) *Uniform building code, ICBO*, Whittier, CA.
- Kim K., Engelhardt, M.D. (1995): *Development of analytical models for earthquake analysis of steel moment frames.* Report no. PMFSEL 95-2, Phil M. Ferguson Structural Engineering Laboratory, The University of Texas at Austin, Austin, TX; 1995.
- Kim K., Engelhardt, M.D. (2001): *Monotonic and cyclic loading models for panel zones in steel moment frames.* Journal of Constructional Steel research. Elsevier. Article in press.
- Krawinkler H. (1978): *Shear in Beam-Column Joints in Seismic Design of Steel Frames.* Engineering Journal AISC Vol. 3.
- Krawinkler H, Bertero V.V. and Popov E.P. (1971): *Inelastic behavior of steel beam-to-column subassemblages.* Report No. EERC 71/07, University of California, Berkeley, CA.
- Krawinkler, H. and Seneviratna, G.D.P.K. (1998): *Pros and cons of a pushover analysis of seismic performance evaluation.* Journal of Engineering Structures, Vol. 20, No. 4-6, 452-464.
- Lee S.J., Lu L.W. (1989): *Cyclic Tests of Full-Scale Composite Joint Subassemblage.* Journal of Structural Engineering, Vol. 115, n° 8.
- Mander, J. B., Priestley, M. J. N., Park, R. (1988): *Theoretical stress-strain model for confined concrete.* Journal of Structural Engineering, ASCE, 114, 8, 1804-1826.
- Meskouris K. (2000): *Structural Dynamics: models, methods, examples.* Berlin : Ernsted.
- prEN 1991-1-1:2001: *Actions on structures, Part 1-1: general actions, densities, self-weight, imposed loads for buildings - Final Draft.*
- prEN 1992-1:2001: *Design of concrete. Part 1: general rules and rules for buildings – Draft n° 2.*
- prEN 1993-1-1:2001: *Design of steel structures. Part 1.1: general rules - Draft n° 2.*
- prEN 1994-1-1:2001: *Design of composite steel and concrete structures. Part 1-1: general rules and rules for buildings – Draft n° 3.*
- prEN 1998-1:2002: *Design of structures for earthquake resistance. Part 1: general rules, seismic actions and rules for buildings - Draft n°5.*

4. SEISMIC RESPONSE OF PARTIAL-STRENGTH COMPOSITE JOINTS

- Ryan I., Bitar D. (2002): *Applicability of Composite Structures to Sway Frames*. ECSC Contract n° 7210-PR-250, CTICM.
- Sivaselvan M.V., Reinhorn A.M. (1999): *Hysteretic Model for Cyclic Behaviour of Deteriorating Inelastic Structures*. Technical Report MCEER-99-0018.
- Stevens N. J., Uzumeri S. M., Collins M. P., Will G. T. (1991): *Constitutive model for reinforced concrete finite element analysis*. ACI Structural Journal, 88, 1, 49-59.
- Tsai K.C., Popov E.P. (1988): *Steel beam-column joints in seismic moment resisting frames*. Report no. EERC 88/19, University of California, Berkeley, CA.
- University of Pisa et al. (2004): *Applicability of Composite Structure to Sway Frames*, ECSC Project n. 7210-PR-250, Eur Report, European Community.
- Valles R.E., Reinhorn A.M., Kunnath S.K., Madan A. (1996): *IDARC2D Version 4.0: A Program for the Inelastic Damage Analysis of Buildings*. Technical Report NCEER-96-0010.
- Wang S.J. (1988): *Seismic response of steel building frames with inelastic joint deformation*. PhD thesis, Department of Civil Engineering, Lehigh University, Bethlehem, PA.

5 SEISMIC BEHAVIOUR OF RC COLUMNS EMBEDDING STEEL PROFILES

5.1 Introduction

On August 17, 1999, a M_w 7.4 earthquake occurred on the 1500-km-long North Anatolian fault in north-western Turkey. The epicentre of the earthquake was near Izmit, 90 km east of Istanbul (Figure 5.1). After this seismic event, the Pacific Earthquake Engineering Research Center dispatched a "Reconnaissance Team" in the region of the epicentre to learn first hand about the performance of the civil infrastructure.

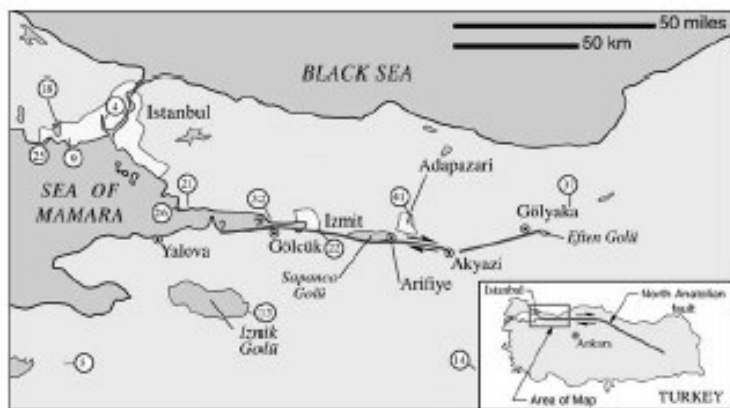


Figure 5.1. Map of affected region showing recorded peak ground accelerations in circles (as percentage of acceleration of gravity)

The geographic region impacted by the earthquake was somewhat narrow banded, centred on the fault and stretched from Istanbul in the west to Golyaka and Duzce in the east. Damage to concrete construction was severe and widespread (Sezen

5. SEISMIC BEHAVIOUR OF RC COLUMNS EMBEDDING STEEL PROFILES

et al., 1999; Aschheim, 2000; Scawthorn, 2000). Estimates for economic losses were around 20 billion US dollars. The official death toll was over 17,200, with some 44,000 people injured and thousands left homeless. Some 77,300 homes and businesses were destroyed, and 244,500 were damaged. The majority of deaths and injuries were in the cities of Kocaeli, Sakarya, and Yalova, as reinforced concrete moment-resisting frame buildings behaved poorly during the earthquake.

According to official estimates, more than 20,000 moment frame buildings collapsed, and many more suffered moderate to severe damage. Three- to seven-storey apartment buildings were hard hit, although many were constructed in the past 20 years. These buildings were probably designed and detailed to comply with the requirements of the building code (TS-500 code, 1975) and of the earthquake Turkish code (1975) for construction in a first-degree seismic zone. Nevertheless, the ductile reinforcement details described in the 1975 earthquake code were rarely observed in buildings inspected after the August 17th 1999 earthquake. Moreover, many of the failures and collapses of engineered construction observed by the reconnaissance team, and reported in Sezen et al. (1999), can be attributed to the formation of soft first storeys as a result of differences in frame systems and in-fill wall geometry especially between the first and upper stories; to the realisation of non-ductile details; and to the utilisation of material of too poor quality in some cases. It was clear that the Turkish earthquake code provisions were rarely enforced for the engineering of commercial and residential construction. On the basis of the aforementioned consideration, this last research activity, conducted in the third year of the Ph.D. course, is part of another European Project (INERD Project), promoted by the E.U. through the E.C.S.C. European Coal and Steel Community and R.F.C.S. Research Fund for Coal and Steel, that deals with the improvement of the resistance and ductility of reinforced concrete (RC) structures using the performance of structural steel profiles.

5.2 The INERD project

The European INERD (acronym of Innovations for Earthquakes Resistant Design) project consists in promoting one specific construction measure for lower storeys of RC structures, by which steel profiles would be encased in the RC columns in order to provide them with a basic reliable shear and compression resistance. The general objective is to establish an innovative concept through new standard

5. SEISMIC BEHAVIOUR OF RC COLUMNS EMBEDDING STEEL PROFILES

design rules able to improve the global safety of reinforced concrete structure, without great changes of the traditional constructional practice. The introduction of this new concept can obviate the most frequent failure mode of RC buildings, the so-called *soft storey* mechanism, which consists in a localisation of buildings seismic deformations and rupture in the one or two lower storeys. The cause of the manifestation of this mechanism is the surplus effort the columns at ground level have to stand, basically due to a big difference in stiffness between the first and the upper storeys. After some seismic events, experience on the spot provided evidence of a collapse behaviour not predicted at the design stage for many RC buildings. More precisely, some local brittle mechanisms occurred in the columns, generating the complete collapse of most buildings: 90% of failures in Kocaeli 1999 Turkey earthquake were of this nature, as illustrated in Figure 5.2.



Figure 5.2. Collapse of building in Kocaeli Turkey earthquake (1999) due to soft-storey mechanism

The “dirty job” is completed by the poor capacity of the reinforced concrete RC columns to develop adequate ductile resources as plastic elongation and by the difficulty in realising RC structures that behave in accordance with the *Strong column-Weak beam Principle*. The first aspect is well known by the in field engineers since the only ductile resource for concrete members, when subjected to tensile and compressive stresses due to cycling loading, arises from the plastic yielding of the steel re-bars; the concrete material alone showing typical brittle failure. The second aspect may be fulfilled following the prescriptions stated by the *Capacity Design Principle* built-in most Codes, which recommend the prevention of any kind of global collapse by concentrating the hinges development in some strategic points of the structure. In few words, the dissipating mechanisms are to form in the beams and not in the columns or joints, providing ductility for beams and a sort of over-strength for columns and joints. An explanation of this *Soft Storey Mechanism* was pursued and the answer obtained, taking into account the role played in practice by the in-fill walls combined with the usual weakening of the lower storeys due to the presence of wide openings as generally requested by

5. SEISMIC BEHAVIOUR OF RC COLUMNS EMBEDDING STEEL PROFILES

contractors. The in-fills force the RC structure above the first storey to act as a rigid body, thus the significant seismic forces and deformations shift in the columns of the lowest storey where the in-elastic buckling take place (see Figure 5.3). Considering also the low shear resistance belonging to RC members in general, it is immediate to understand why the first storey columns fail when subjected to cycling loading, generating the global structural collapse indeed.

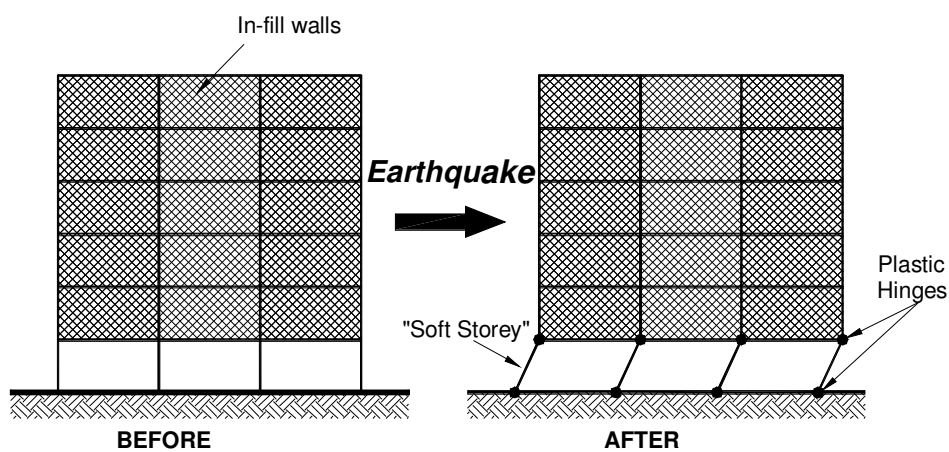


Figure 5.3. Sketch explaining the "Soft Storey Mechanism"

The proposed idea is to use encased steel section as ductile fuses able to dissipate cyclically the energy of the earthquake in the lower storeys of buildings which otherwise remain reinforced concrete buildings. The objective is to promote safety for the people without too much changing the constructional practice of RC structures. This way to set the problem is intended to be the most effective for an easy gain in the structural reliability in those areas where the civil engineering market mainly considers the use of cement, gravel and water

The research can be subdivided into a set of four operational tasks:

- Task 1: definition by calculations of H steel sections able to substitute reinforced concrete column of typical sizes, without working in a composite way with concrete;
- Task 2: definition, execution and analysis of tests aiming to set forward the composite shear resistance of encased steel sections in zone of columns submitted to cyclic plastic bending;
- Task 3: definition of a computation method of the shear resistance of composite columns submitted to cyclic bending;

5. SEISMIC BEHAVIOUR OF RC COLUMNS EMBEDDING STEEL PROFILES

- Task 4: definition of design rules and preparation of a design tool for practice: Tables of H steel sections able to substitute reinforced concrete column of typical sizes, considering a minimum composite activation.

The seismic design of the columns embedding steel profiles, successively verified on the basis of experimental tests, has been executed by using the rules included in the following standards:

- prEN 1991-1-1:2001 "Actions on structures, Part 1-1: general actions, densities, self-weight, imposed loads for buildings" - Final Draft, July 2001;
- prEN 1992-1:2001 "Design of concrete. Part 1: general rules and rules for buildings" –Draft n° 2, January 2001;
- prEN 1993-1-1:2000 "Design of steel structures. Part 1.1: general rules" Draft n° 2, August 2000;
- prEN 1994-1-1:2001 "Design of composite steel and concrete structures. Part 1-1: general rules and rules for buildings" – Draft n° 3, March 2001;
- prEN 1998-1:2001 "Design of structures for earthquake resistance. Part 1: general rules, seismic actions and rules for buildings" –Draft n°3, May 2001.

Moreover, the steel profiles for strong and weak axis bending have been chosen by matching simple design criteria developed at the University of Liege. They should aim to provide a simple constructional measure, which obviate the *soft storey* type failure of a building. This constructional measure should:

- provide ductility;
- provide a column which, at the ultimate stage where concrete would be locally crushed in plastic hinges, the steel section would provide enough axial strength and a plastic moment and a stiffness similar to those of the reinforced concrete column.

From the obtained knowledge on joint and member responses, a numerical FE model of the beam-to-column joint sub-assemblage has been developed to examine its seismic behaviour through non-linear analyses. This analytical work permitted to predict the performance of the joint and to propose appropriate analytical formulas for the estimation of the yield and ultimate strength both of the columns and of the beam-to-column joint subjected to very high seismic shear forces.

5. SEISMIC BEHAVIOUR OF RC COLUMNS EMBEDDING STEEL PROFILES

5.3 Description of the prototype structure

The prototype structure considered in this study is shown in Figure 5.4. It is a 5-storey, 30.0m long x 12.0m wide x 21.0m high structure, which includes six equal two-bay moment resisting frames with different bay length (5m and 7m), as illustrated in Figure 5.4a. In the direction perpendicular to the main moment resisting frames, simply supported secondary beams are foreseen at column lines to provide a better out of plane resistance. The structure was thought as a moment resisting (MR) type without core system, shear walls or other kinds of sub-structure able to transfer downwards the horizontal forces when subjected to the seismic load combinations and as having a core system resisting horizontal loads when subjected to the static load combinations.

From a finite element analysis and design of this prototype structure the overall geometrical and mechanical properties of the columns of the first floor will be determined.

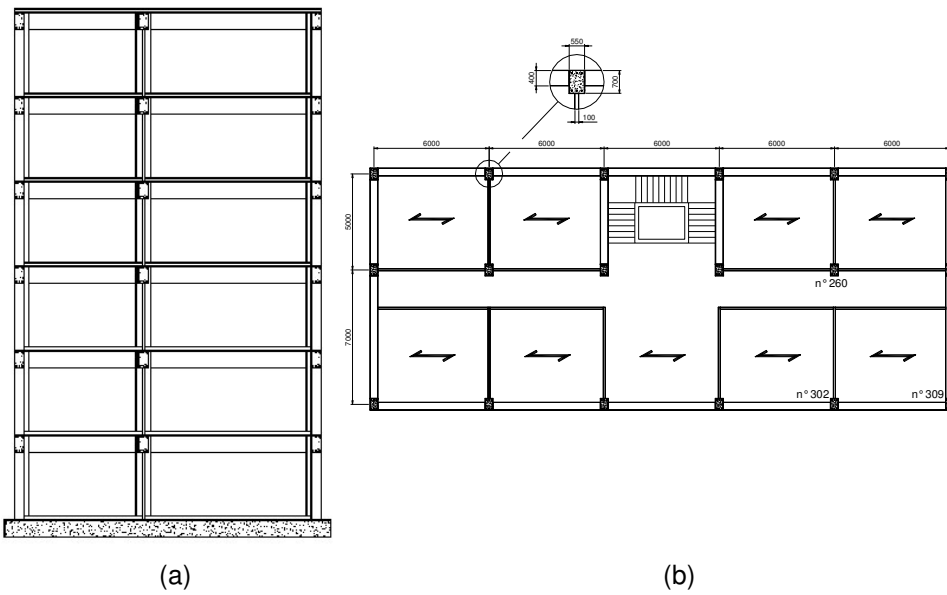


Figure 5.4. (a) Plan and (b) lateral view of the building

5.3.1 Materials and mechanical properties

The material classes adopted in the design are:

- Concrete: Class C 25/30

The mechanical properties of the concrete used in the design are the same as those reported in Table 3.1 of Eurocode 2. Wherever relevant, the beneficial

5. SEISMIC BEHAVIOUR OF RC COLUMNS EMBEDDING STEEL PROFILES

effects of the concrete confinement due to the presence of the stirrups are taken into account (Mander, 1988). The concrete confinement results in a modification of the effective stress-strain relationship: higher strength and higher critical strains are achieved (see Figure 5.5). The other basic material characteristics are considered as unaffected for the design.

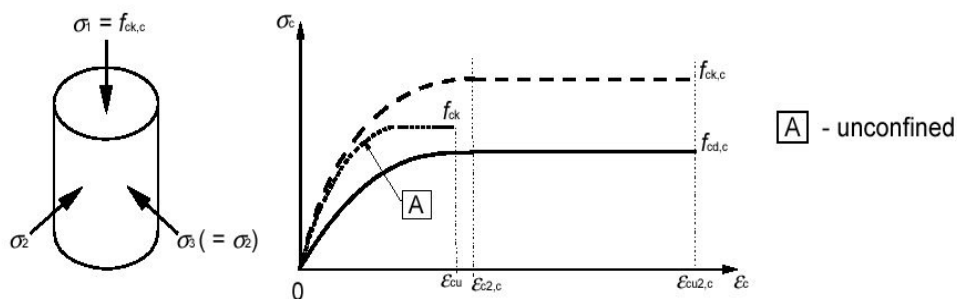


Figure 5.5. Stress-strain relationship for confined concrete

- Steel rebars: Class B 450 C

Following the prescription reported in Section 5.3.2.(1) and 5.4.1.1.(3) of the Eurocode 8 (2001), when considering critical parts of primary elements in seismic design, reinforcing steel bars of class B and C as indicated in Table 3.3 of Eurocode 2 shall be used. Consequently, the following properties are guaranteed:

Characteristic yield strength f_{yk} :	450 MPa
$k = (f_t / f_y)_k$:	$1,15 \leq k < 1,35$
Characteristic strain at maximum force $\epsilon_{uk} (\%)$:	$\geq 7,5\%$

- Structural Steel: Class S 235

When the design of steel structural members is required, the use of Structural Steel Class S 235 will be implied. Following the prescription of Eurocode 8 (2001), the possibility that the actual steel yield strength will be higher than the value of the nominal yield strength is taken into account by a material over strength factor γ_{ov} equal to 1.25. In structural members designed with the purpose of dissipating seismic energy, the value of the material yield strength utilised during the erection of the building must not exceed $f_{y\max} = 1.1 \cdot \gamma_{ov}$ times the yield strength defining the material steel grade: e.g., for S235 class not higher than ≈ 320 MPa. As an alternative way, it is allowed to determine the actual yield strength of the material utilised for the structure, taking it as the effective value in the design verifications. Having considered these prescriptions we are to use a steel grade S235 with a $f_y = 355$ MPa, value

5. SEISMIC BEHAVIOUR OF RC COLUMNS EMBEDDING STEEL PROFILES

guaranteed by tests carried out at the ProfilArbed laboratories. For an economical design of the steel members we considered this upper limit. The elastic modulus E is to be 210000 MPa.

5.3.2 Load combinations

In the present paragraph a base column of a five-storey building is designed for each of the three different load combinations listed below:

1. Gravity Load Combination, designing the columns only according to Eurocode 2.

$$q_1 = \Sigma_1(\gamma_G G_{K,i}) + \gamma_Q Q_{K,1} + \Sigma_2(\gamma_Q \psi_0 Q_{K,i}) \quad (5.1)$$

2. Seismic Load Combination A, assuming the structural elements in the Low Ductility Class designing the columns only according to Eurocode 2.

$$q_2 = \Sigma_1(G_{K,i}) + A_{E,d} + \Sigma_1(\psi_2 Q_{K,i}) \quad (5.2)$$

3. Seismic Load Combination B, assuming the structural elements in the Medium Ductility Class, and for that reason designing the columns according to Eurocode 2 and Eurocode 8.

$$q_3 = \Sigma_1(G_{K,i}) + A_{E,d} + \Sigma_1(\psi_2 Q_{K,i}) \quad (5.3)$$

where:

- $G_{K,i}$ is the dead load
 $Q_{K,1}$ is the imposed live load
 $Q_{K,2}$ is the wind load
 $A_{E,d}$ is the horizontal seismic action: $E_{Edx} + 0,3 E_{Edy}$.

γ_G Unfavourable	γ_Q Unfavourable	ψ_0	ψ_2	γ_G Favourable	γ_Q Favourable
1.35	1.5	0.7	0.3	1	0

Table 5.1. Values of the coefficients for the load combinations

The uniformly distributed loads to be vertically applied to the structural members have been calculated from the combinations above assuming typical values, found

5. SEISMIC BEHAVIOUR OF RC COLUMNS EMBEDDING STEEL PROFILES

in the design tables, for what concerns the material specific weights. A uniformly distributed live load of 3.0 kPa was assumed at each storey level (mechanical equipments, finishes, etc.). Different values of the dead and live loads were calculated for the roof; in this case the live load is equal to 2.0kPa.

Subsequently, the horizontal seismic forces acting at each storey height according to Eurocode 8 have been determined; being the structure regular both in plan and in height (prEN 1998-1, 2001), it is allowed to carry out a simplified planar static analysis, the so-called Lateral Force Method Analysis. The equivalent horizontal seismic forces, represented as nodal forces acting at each storey height, have been determined for the seismic study cases denominated above as A and B. For the two load combinations we assumed the same peak ground acceleration, i.e. 0.20g, which implies that the construction site belongs to a low seismicity area. Only the main aspects that are relevant to the seismic resistance of the moment resisting frames in the direction of loading are summarised herein.

The design seismic loads at each level, F_i , were determined using the simplified modal response spectrum analysis method:

$$F_i = F_b \cdot \frac{z_i \cdot m_i}{\sum_i (z_i \cdot m_i)} \quad (5.4)$$

where F_b is the seismic base shear, and z_i and m_i are respectively the height from the ground level and the masses at each storey of the building. The seismic base shear force is given by:

$$F_b = S_d(T_1) \cdot W \cdot \lambda \quad (5.5)$$

where $S_d(T_1)$ is the ordinate of the design spectrum at the fundamental period of vibration of the structure for translational motion in the direction considered, T_1 , W is the total weight of the building, and λ is a correction factor. The equations and the values of the soil parameter, S , and the reference periods T_B , T_C , and T_D that are required to construct Types 1 and 2 design spectra are given below. For this project, the following key parameters were adopted:

- Type 1 spectrum;
- Peak ground acceleration, $a_g = 0.20$ g;
- Subsoil Class A (Rock site, or alike, with $V_{s,30} > 800$ m/s);
- Behaviour factor, $q = 1.5$ for Ductility Class LOW and $q = 3.9$ for Ductility Class MEDIUM.

Therefore, $S = 1.0$ and the reference periods T_B , T_C , and T_D are respectively equal to 0.15 sec, 0.5 sec, and 2.0 sec. The fundamental period T_1 of the structure was

5. SEISMIC BEHAVIOUR OF RC COLUMNS EMBEDDING STEEL PROFILES

provided by linear analysis conducted in SAP2000 both for the x- and y-direction, giving $T_{1,x} = 0.302$ sec and $T_{1,y} = 0.267$ sec. The inertial effects of the seismic action are evaluated through the combination below:

$$W_k = \sum G_{kj} + \sum \psi_{Ei} \cdot Q_{kj} \quad (5.6)$$

Being:

$$\psi_{Ei} = \varphi \cdot \psi_{2i}$$

with

$$\varphi = \begin{cases} 1,0 & \text{for roof} \\ 0,8 & \text{for other storeys with correlated occupancies} \\ 0,3 & \text{for offices and residential buildings} \end{cases}$$

Thus:

$$\text{I-V Storey} \quad \psi_{E\ 1-5} = 0,24$$

$$\text{Roof} \quad \psi_{E\ Roof} = 0,3$$

$$\begin{array}{lll} G_{1-5} = 3561 \text{ KN} & G_{\text{roof}} = 2125 \text{ KN} \\ Q_{1-5} = 1011 \text{ KN} & Q_{\text{roof}} = 720 \text{ KN} \\ W_{1-5} = 3804 \text{ KN} & W_{\text{roof}} = 2341 \text{ KN} \end{array}$$

$$W_{\text{Tot}} = 5 \cdot W_{1-5} + W_{\text{roof}} = 21361 \text{ KN}$$

is the total weight of the building

$$M = 2177 \text{ tons}$$

is the total mass of the building

Hence, we can derive the total base shear force for each seismic design case and the horizontal seismic forces acting at the different storey heights. The main results of these calculations are reported in Table 5.2. Moreover, in order to cover uncertainties in the location of masses and in the spatial variation of the seismic motion, the calculated centre of mass at each floor i will be displaced from its nominal location by an accidental eccentricity in each direction:

$$e_{1i} = \pm 0,05 \cdot L_i \quad (5.7)$$

where e_{1i} is the accidental eccentricity of storey mass i from its nominal location, and L_i is the floor-dimension perpendicular to the direction of the seismic action. We obtain e_{1x} equal to 1500 mm and e_{1y} equal to 600 mm.

5. SEISMIC BEHAVIOUR OF RC COLUMNS EMBEDDING STEEL PROFILES

Design case: LOW DUCTILITY			Design case: MEDIUM DUCTILITY		
Total base shear force = 8716 kN			Total base shear force = 3353 kN		
Floor level	F_x (kN)	F_y (kN)	Floor level	F_x (kN)	F_y (kN)
1	477.0	477.0	1	180.0	180.0
2	933.0	933.0	2	359.0	359.0
3	1399.0	1399.0	3	539.0	539.0
4	1866.0	1866.0	4	718.0	718.0
5	2332.0	2332.0	5	897.0	897.0
Roof	1722.0	1722.0	Roof	633.0	633.0

Table 5.2. Lateral seismic forces obtained for the two ductility design cases

5.3.3 3D frame modelling

After a rough estimation of the geometry of all the structural elements by simplified drafts and schematic diagrams, a simulation of the building behaviour was implemented applying both vertical and horizontal forces to a 3D model drawn by the finite element program SAP2000 (see Figure 5.6).

The contribution of a single masonry in-fill was taken into account by an equivalent compression diagonal model endowed the following stiffness:

$$K_w = 0.6 \frac{E_w \cdot w \cdot t \cdot \cos^2 \theta}{d} \quad (5.8)$$

in which the value 0.6 accounts for the presence of openings, doors, etc. Two different models have been considered:

- the first one (see Figure 5.6a) in which the structure was modelled with the masonry in-fill present on each floor of the building (Structure I);
- the second one (see Figure 5.6b) in which the structure was modelled without the masonry infill on the first floor. This case, named *Pilotis Case* (Structure II), was considered with the purpose of maximizing the design action on the base columns and of incrementing the second order effects (inter-storey drift sensitivity). In fact, this model implements the aforementioned *Soft Storey* situation.

From these analyses it was found that the most adverse conditions applied to three representative base columns of the building labelled as n° 260, n° 302 and n° 309 (as indicated in Figure 5.4); we also paid particular attention to how the masonry

5. SEISMIC BEHAVIOUR OF RC COLUMNS EMBEDDING STEEL PROFILES

wall stiffness modifies the re-distribution of the internal member actions going from the top storey to the ground level.

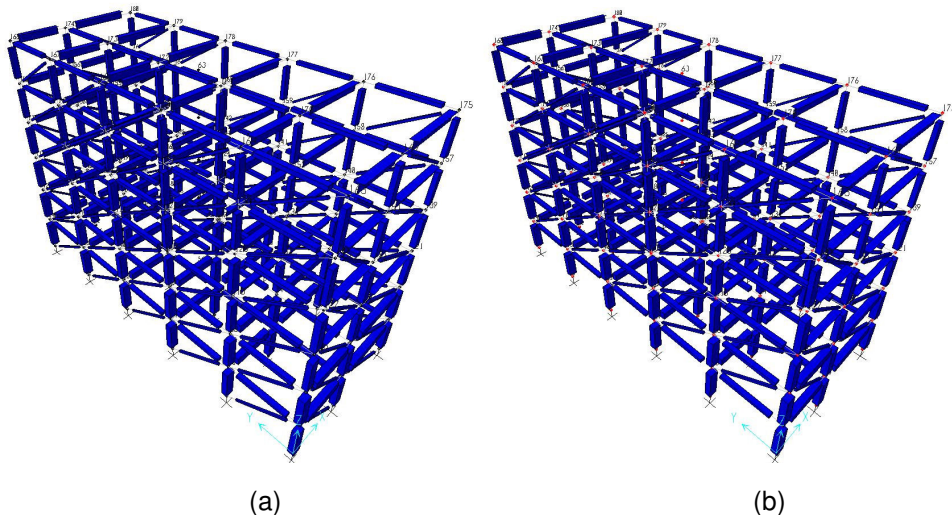


Figure 5.6. Building structures modelled by the SAP2000 program: a) structure with the masonry infill present in each floor; b) Pilotis Case - structure without the masonry infill at the first floor

For the assumed load combination, *Static*, *Seismic A* and *Seismic B*, all comes down to the design of one column (taken with rectangular geometry) which complies with the worst case of forces among those acting on the considered elements (n° 260, n° 302 and n° 309) for the load combination under exam. Nonetheless, as the heaviest forces to be withdrawn arise from the *seismic combination A* (*Low ductility* and behaviour factor $q = 1,5$), the column width and depth were fixed in this case varying only the number and distribution of the reinforcing bars in the others.

In order to have an approximate idea of the re-distribution of internal forces on the structural members once loaded, some diagrams obtained from SAP2000 and representing respectively the deformed shape, axial force and bending moment are shown below.

Moreover, on the basis of the results obtained by applying the forces defined according to the load combinations A and B to the structure and considering the seismic wave load acting alternatively in the two directions of the 3D frame, it was possible to verify the values of the inter-storey drift coefficients. The value of the inter-storey drift is $d_r = q \cdot d_e$ where d_e is the displacement of the considered point in the structural system as determined by a linear analysis based on the design response spectrum. The value of the inter-storey drift sensitivity coefficient is equal to:

5. SEISMIC BEHAVIOUR OF RC COLUMNS EMBEDDING STEEL PROFILES

$$\theta = \frac{P_{\text{tot}} \cdot d_r}{V_{\text{tot}} \cdot h} \quad (5.9)$$

where P_{tot} is the total weight above and at the considered floor system, according to the equivalent seismic effect hypotheses; V_{tot} is the total shear force for the considered floor system due to the seismic equivalent action; and h is the distance between two adjacent floor systems. On the basis of the numerical simulations, the frame results not sway for the Seismic combinations; therefore second-order effects need not to be taken into account.

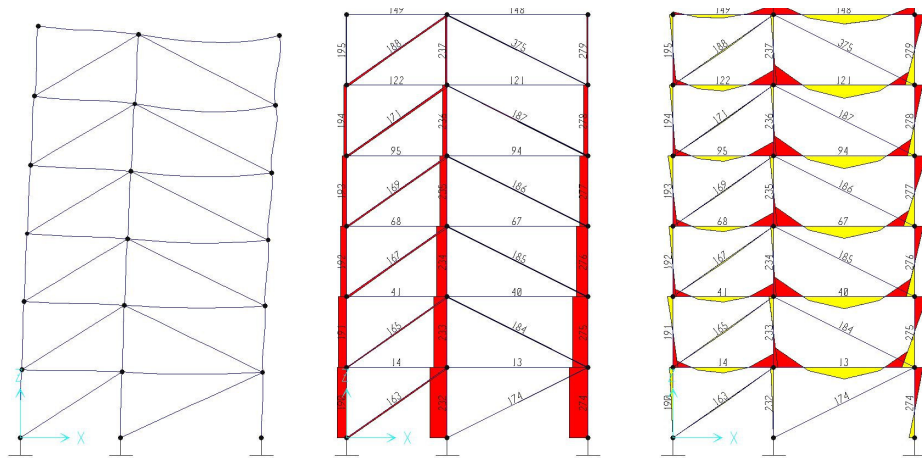


Figure 5.7. Output results from the SAP 2000 for the Static load combination

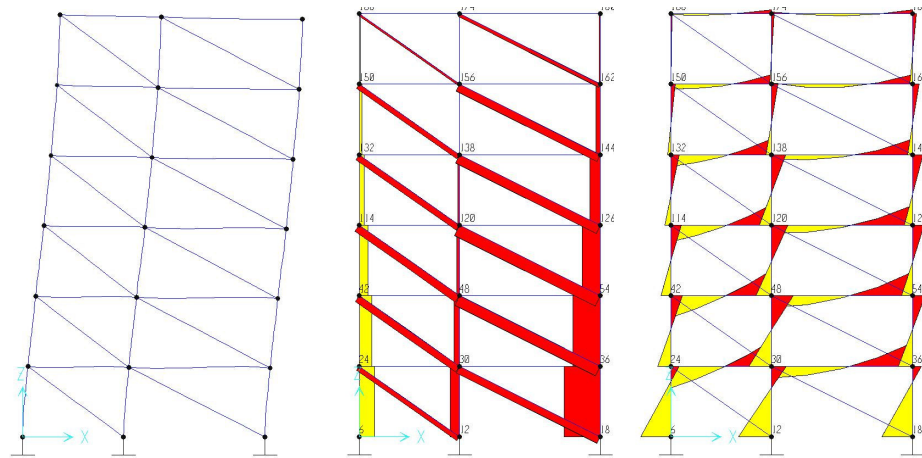


Figure 5.8. Output results from the SAP 2000 both for A and for B Seismic load combinations

5. SEISMIC BEHAVIOUR OF RC COLUMNS EMBEDDING STEEL PROFILES

5.3.4 Design of the reinforced concrete columns

On the basis of the numerical simulation, the column section has been verified for axial bending, compression and shear in both directions. The 2nd order effects need not to be considered, being the columns not slender in plan ($\lambda < \lambda_{CR} = 25$). As example, the M-N diagrams for designing the three rectangular columns corresponding to the Static combination, the Seismic combination A and the Seismic combination B are illustrated below (Figure 5.9, Figure 5.10 and Figure 5.11), respectively.

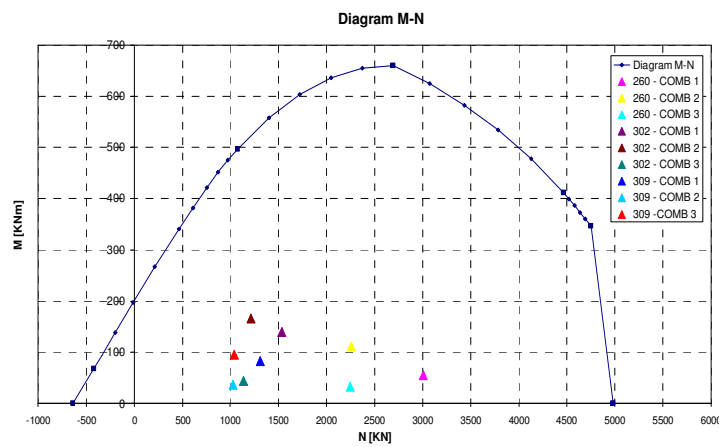


Figure 5.9. M-N diagram illustrating the column resistance for the Static load combination.

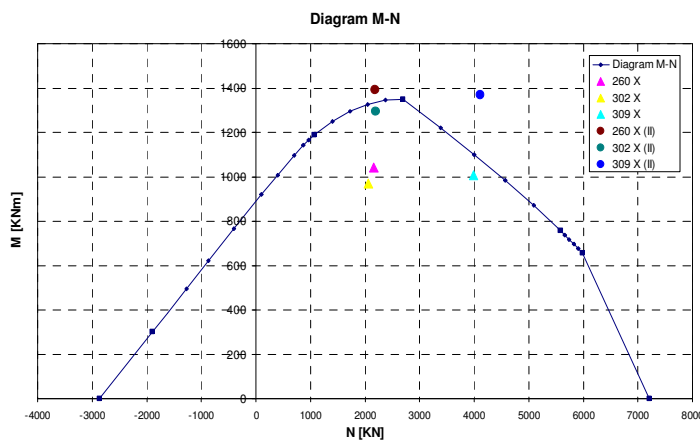


Figure 5.10. M-N diagram illustrating the column resistance for the Seismic load combination A (Low)

5. SEISMIC BEHAVIOUR OF RC COLUMNS EMBEDDING STEEL PROFILES

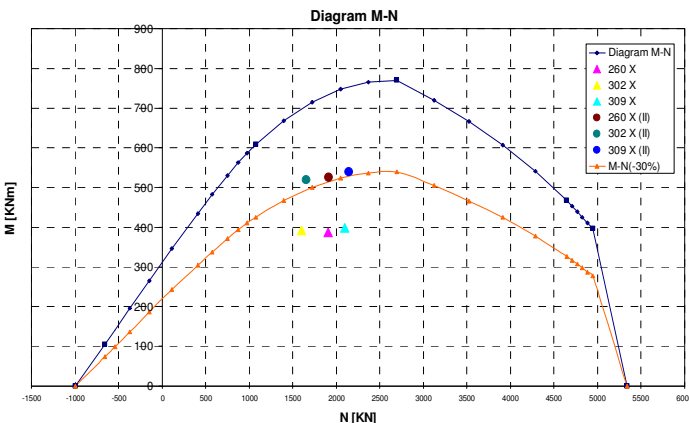


Figure 5.11. M-N diagram illustrating the column resistance for the Seismic load combination B (Medium)

For the design of MEDIUM ductility members prescriptions from Eurocode 8 (2001) have also been taken into account. This means a reduction of 30% in the resisting moment M_{Rd} and an N_{Sd} axial force to be not greater than $0,65N_{Rd}$. Besides, all necessary prescriptions for both end sections of the primary columns to be considered as critical regions have been matched (Eurocode 8, 2001).

Moreover, in accordance with the design rules of Eurocode 2 (2001) and Eurocode 8 (2001) the following details for the columns are chosen. Note that for the design of MEDIUM ductility members also prescriptions of Eurocode 8 (2001) clause have been taken into account.

- Details of the concrete section designed for the Gravity load combination

Maximum longitudinal hoops spacing	300 mm
Maximum transversal hoops spacing	510 mm
Minimum shear reinforcement ratio ρ_w	0,0011

Concrete column depth	700 mm
Concrete column width	550 mm
Number of longitudinal rebars along major axis	4
Number of longitudinal rebars along minor axis	4
Longitudinal rebars diameter	16 mm
Longitudinal hoops spacing	300 mm
Hoops diameter	10 mm
Hoops arm number	4

Table 5.3. Geometrical properties of the cross section

5. SEISMIC BEHAVIOUR OF RC COLUMNS EMBEDDING STEEL PROFILES

In the critical region (in accordance with Eurocode 2):

L_{CR} (critical regions length): 720 mm

Maximum hoops spacing in the critical regions: 180 mm

- Details of the section designed for the Seismic load combination A

Maximum longitudinal hoops spacing 300 mm

Maximum transversal hoops spacing 300 mm

Minimum shear reinforcement ratio ρ_w 0,0011

Concrete column depth	700 mm
Concrete column width	550 mm
Number of longitudinal rebars along major axis	8
Number of longitudinal rebars along minor axis	6
Longitudinal rebars diameter	25 mm
Longitudinal hoops spacing	300 mm
Hoops diameter	10 mm
Hoops arm number	4

Table 5.4. Geometrical properties of the cross section

In the critical region (in according with Eurocode 2):

L_{CR} (critical regions length): 720 mm

Adopted hoops spacing in the critical regions: 180 mm

- Details of the section designed for the Seismic load combination B

Maximum longitudinal hoops spacing 300 mm

Maximum transversal hoops spacing 300 mm

Minimum shear reinforcement ratio ρ_w 0,0011

Concrete column depth	700 mm
Concrete column width	550 mm
Number of longitudinal rebars along major axis	4
Number of longitudinal rebars along minor axis	4
Longitudinal rebars diameter	20 mm
Longitudinal hoops spacing	300 mm
Hoops diameter	10 mm
Hoops arm number	4

Table 5.5. Geometrical properties of the cross section

5. SEISMIC BEHAVIOUR OF RC COLUMNS EMBEDDING STEEL PROFILES

By considering the prescription both of Eurocode 2 and Eurocode 8, within the critical region the most restrictive of the following conditions should be satisfied.

Eurocode 2

L_{CR} (critical regions length):	720 mm
Hoops spacing in the critical regions:	180 mm

Eurocode 8: to satisfy plastic rotation demands and to compensate for loss of resistance due to spalling of concrete cover

L_{CR} (critical regions length):	700 mm
Hoops spacing in the critical regions:	150 mm

5.3.5 *Design of the fully encased composite columns*

To ease and promote the utilisation of composite columns in seismic geographical areas in order to obviate the Soft Storey type of building failure, the steel profiles for strong and weak axis bending have been chosen by matching simple design criteria developed at the University of Liege. This constructional measure should:

- provide ductility;
- maintain axial strength, (plastic) shear and moment resistance, and stiffness similar to those of the RC column at the ultimate stage when concrete is locally crushed.

The following design criteria have been defined, in order to allow the achievement of the mentioned target.

1. The steel section should at least be able to take alone the design axial force of the seismic loading case:

$$N_{Rd} \geq N_{Sd} (\gamma_g G + \gamma_q Q) \quad (5.10)$$

with:

$$\gamma_g = 1$$

$$\gamma_q = 0.3$$

2. The steel section alone (not acting composedly) should be able to substitute the deficient concrete section:

$$M_{Rd,steel} \geq M_{Rd,concrete} \quad (5.11)$$

$$V_{Rd,steel} \geq V_{Rd,concrete} \quad (5.12)$$

5. SEISMIC BEHAVIOUR OF RC COLUMNS EMBEDDING STEEL PROFILES

Eq. (5.10) should entail the erection of composite columns, which resist more than the dead load of the structure under severe seismic conditions providing enough residual stiffness to minimise the risk of collapse. Moreover, criteria defined in 1 and 2 should provide a beneficial residual strength after the concrete crushing that should lead to improved ductility.

3. The section profiles should not much modify the local stiffness EI of the single RC columns (maximum modification level in the order of 10%) in order not to change the distribution in stiffness of the entire concrete structure. In fact, a change in the stiffness distribution may also signify a variation of the building periods of vibration closely tied with the inertial forces, e.g. seismic forces.
4. The following ratio

$$r_{\text{major}} / r_{\text{minor}} = [M_{Rd,\text{comp}} / M_{Rd,\text{concrete}}]_{\text{major}} / [M_{Rd,\text{comp}} / M_{Rd,\text{concrete}}]_{\text{minor}} \quad (5.13)$$

should be close to 1 in order to achieve a suitable performance of the steel section both along major axis bending and minor axis bending.

The steel section design is performed using the structural steel class S235 with a value of $f_y = 355$ MPa guaranteed by ProfilArbed. The steel profile sections that ensure the above mentioned design criteria were chosen considering this limit for the structural steel yield strength.

For each load combination, Static, Seismic A and Seismic B, two steel cross sections were chosen, being a HEM and a HEB type cross section. The choice fell upon these two sections mainly for a matter of constructability of the specimens to be tested. It is not to forget that the steel profiles are inserted in some critical and tied up regions, e.g. the joint regions, with a quite high quantity of horizontal, vertical and transversal reinforcing bars. Other types of cross section (IPE or UB sections) did not give enough guarantees regarding the feasibility of the composite joints. The resulting sections are reported hereinafter for the three design cases.

5. SEISMIC BEHAVIOUR OF RC COLUMNS EMBEDDING STEEL PROFILES

- Details of the steel profile for the Gravity load combination (Design Case 1)

HEM 160					
<i>Major Axis</i>			<i>Minor Axis</i>		
N_{Sd}	3008,4	kN	N_{Sd}	3008,4	kN
$M_{Rd,conc}$	201,2	kNm	$M_{Rd,conc}$	154,8	kNm
$V_{Rd,conc}$	554,3	kN	$V_{Rd,conc}$	508,7	kN
$N_{Rd,steel}$	3132,07	kN	$N_{Rd,steel}$	3132,07	kN
$M_{Rd,steel}$	217,71	kNm	$M_{Rd,steel}$	105,05	kNm
$V_{Rd,steel}$	574,07	kN	$V_{Rd,steel}$	1422,79	kN
A_{steel}	9705	mm ²	A_{steel}	9705	mm ²
A_{steel}/A_{conc}	2,52%		A_{steel}/A_{conc}	2,52%	
$N_{Pl,Rd,comp}$	10113,52	kN	$N_{Pl,Rd,comp}$	10113,52	kN
$M_{Rd,comp}$	778,89	kNm	$M_{Rd,comp}$	608,54	kNm
$M_{Rd,comp}/M_{Rd,conc}$	3,87		$M_{Rd,comp}/M_{Rd,conc}$	3,93	

Table 5.6. Details of the HEM 160 steel profile

HEB 220					
<i>Major Axis</i>			<i>Minor Axis</i>		
N_{Sd}	3008,4	kN	N_{Sd}	3008,4	kN
$M_{Rd,conc}$	201,2	kNm	$M_{Rd,conc}$	154,8	kNm
$V_{Rd,conc}$	554,3	kN	$V_{Rd,conc}$	508,7	kN
$N_{Rd,steel}$	2938,11	kN	$N_{Rd,steel}$	2938,11	kN
$M_{Rd,steel}$	266,90	kNm	$M_{Rd,steel}$	127,12	kNm
$V_{Rd,steel}$	520,22	kN	$V_{Rd,steel}$	1311,74	kN
A_{steel}	9104	mm ²	A_{steel}	9104	mm ²
A_{steel}/A_{conc}	2,36%		A_{steel}/A_{conc}	2,36%	
$N_{Pl,Rd,comp}$	9929,78	kN	$N_{Pl,Rd,comp}$	9929,78	kN
$M_{Rd,comp}$	778,19	kNm	$M_{Rd,comp}$	612,58	kNm
$M_{Rd,comp}/M_{Rd,conc}$	3,87		$M_{Rd,comp}/M_{Rd,conc}$	3,96	

Table 5.7. Details of the HEB 220 steel profile

5. SEISMIC BEHAVIOUR OF RC COLUMNS EMBEDDING STEEL PROFILES

- Details of the steel profile for the Seismic load combination A (Design Case 2)

HEM 280					
Major Axis			Minor Axis		
N _{Sd}	3992,9	kN	N _{Sd}	3152,3	kN
M _{Rd,conc}	963,07	kNm	M _{Rd,conc}	552,39	kNm
V _{Rd,conc}	711,8	kN	V _{Rd,conc}	534,4	kN
N _{Rd,steel}	7751,91	kN	N _{Rd,steel}	7751,91	kN
M _{Rd,steel}	957,21	kNm	M _{Rd,steel}	450,85	kNm
V _{Rd,steel}	1342,11	kN	V _{Rd,steel}	3541,70	kN
A _{steel}	24020	mm ²	A _{steel}	24020	mm ²
A _{steel} /A _{conc}	6,24%		A _{steel} /A _{conc}	6,24%	
N _{Pl,Rd,comp}	16825,28	kN	N _{Pl,Rd,comp}	16091,10	kN
M _{Rd,comp}	2151,84	kNm	M _{Rd,comp}	1342,58	kNm
M _{Rd,comp} /M _{Rd,conc}	2,16		M _{Rd,comp} /M _{Rd,conc}	2,36	

Table 5.8. Details of the HEM 280 steel profile

HEB 360					
Major Axis			Minor Axis		
N _{Sd}	3992,9	kN	N _{Sd}	3152,3	kN
M _{Rd,conc}	963,07	kNm	M _{Rd,conc}	552,39	kNm
V _{Rd,conc}	711,8	kN	V _{Rd,conc}	534,4	kN
N _{Rd,steel}	5828,45	kN	N _{Rd,steel}	5828,45	kN
M _{Rd,steel}	865,88	kNm	M _{Rd,steel}	333,05	kNm
V _{Rd,steel}	1129,14	kN	V _{Rd,steel}	2515,41	kN
A _{steel}	18060	mm ²	A _{steel}	18060	mm ²
A _{steel} /A _{conc}	4,69%		A _{steel} /A _{conc}	4,69%	
N _{Pl,Rd,comp}	10033,85	kN	N _{Pl,Rd,comp}	9299,67	kN
M _{Rd,comp}	2042,2	kNm	M _{Rd,comp}	1256,90	kNm
M _{Rd,comp} /M _{Rd,conc}	2,30		M _{Rd,comp} /M _{Rd,conc}	2,28	

Table 5.9. Details of the HEB 360 steel profile

5. SEISMIC BEHAVIOUR OF RC COLUMNS EMBEDDING STEEL PROFILES

- Details of the steel profile for the Seismic load combination B (Design Case 3)

HEM 200					
<i>Major Axis</i>			<i>Minor Axis</i>		
N_{Sd}	2098,1	kN	N_{Sd}	1782,8	kN
$M_{Rd,conc}$	311,8	kNm	$M_{Rd,conc}$	239,1	kNm
$V_{Rd,conc}$	604,5	kN	$V_{Rd,conc}$	570,5	kN
$N_{Rd,steel}$	4237,41	kN	$N_{Rd,steel}$	4237,41	kN
$M_{Rd,steel}$	366,30	kNm	$M_{Rd,steel}$	174,31	kNm
$V_{Rd,steel}$	764,50	kN	$V_{Rd,steel}$	1919,16	kN
A_{steel}	13130	mm ²	A_{steel}	13130	mm ²
A_{steel}/A_{conc}	3,41%		A_{steel}/A_{conc}	3,41%	
$N_{Pl,Rd,comp}$	7886,17	kN	$N_{Pl,Rd,comp}$	7887,17	kN
$M_{Rd,comp}$	925,12	kNm	$M_{Rd,comp}$	798,28	kNm
$M_{Rd,comp}/M_{Rd,conc}$	2,97		$M_{Rd,comp}/M_{Rd,conc}$	3,34	

Table 5.10. Details of the HEM 200 steel profile

HEB 240					
<i>Major Axis</i>			<i>Minor Axis</i>		
N_{Sd}	2098,1	kN	N_{Sd}	1782,8	kN
$M_{Rd,conc}$	311,8	kNm	$M_{Rd,conc}$	239,1	kNm
$V_{Rd,conc}$	604,5	kN	$V_{Rd,conc}$	570,5	kN
$N_{Rd,steel}$	3420,91	kN	$N_{Rd,steel}$	3420,91	kN
$M_{Rd,steel}$	339,83	kNm	$M_{Rd,steel}$	160,85	kNm
$V_{Rd,steel}$	619,16	kN	$V_{Rd,steel}$	1520,43	kN
A_{steel}	10600	mm ²	A_{steel}	10600	mm ²
A_{steel}/A_{conc}	2,75%		A_{steel}/A_{conc}	2,75%	
$N_{Pl,Rd,comp}$	10725,46	kN	$N_{Pl,Rd,comp}$	10725,46	kN
$M_{Rd,comp}$	944,57	kNm	$M_{Rd,comp}$	737,42	kNm
$M_{Rd,comp}/M_{Rd,conc}$	3,03%		$M_{Rd,comp}/M_{Rd,conc}$	3,08%	

Table 5.11. Details of the HEB 240 steel profile

5. SEISMIC BEHAVIOUR OF RC COLUMNS EMBEDDING STEEL PROFILES

The ratio r_{major} / r_{minor} , that could estimate the performance of the different designed rectangular sections along the major and the minor bending axis, are reported in the following Table:

Load Combination	Profile	r_{major} / r_{minor}
Gravity load Combination (Case 1)	HEM 160	0,98
	HEB 220	0,98
Seismic load Combination A (Case 2)	HEM 280	0,92
	HEB 360	0,90
Seismic load Combination B (Case 3)	HEM 200	0,89
	HEB 240	0,98

Table 5.12. Value of the ratio r_{major} / r_{minor} for the used steel profiles

The cross sections designed following the simplified and aforementioned criteria, are illustrated in the following Figure 5.12. The sections appear to be composite concrete-steel sections despite not having been “ordinarily” designed like that. These sections are representative of the column specimens to be tested soon after.

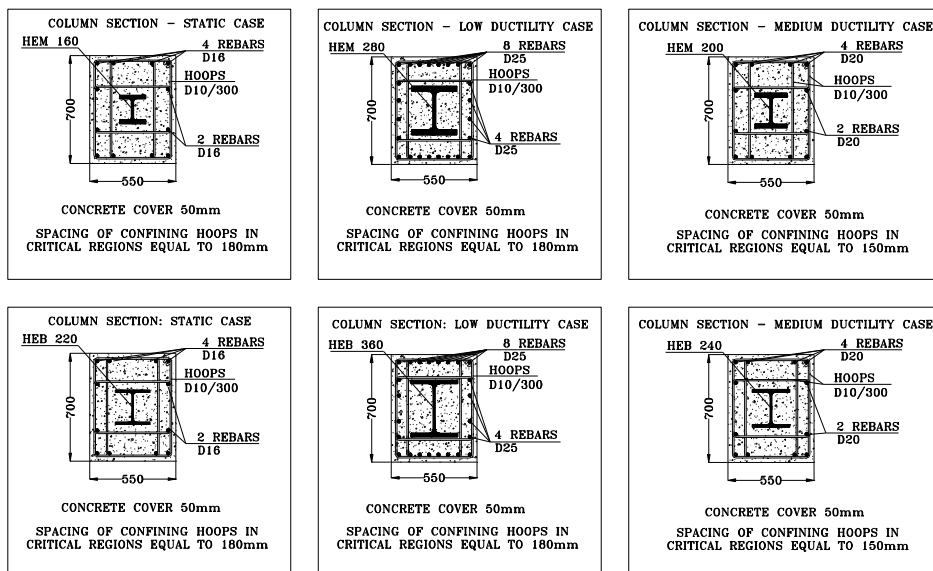


Figure 5.12. Composite section for the designed rectangular columns

The steel contribution ratio satisfies the condition given in Eurocode 4:

$$0,2 \leq \delta \leq 0,9 \text{ with } \delta = \frac{A_s f_yd}{N_{pl,Rd}} \quad (5.14)$$

5. SEISMIC BEHAVIOUR OF RC COLUMNS EMBEDDING STEEL PROFILES

For rectangular concrete sections with the HEM and HEB profiles return the following:

HEM 160	$\delta = 0,328$	HEB 220	$\delta = 0,296$
HEM 220	$\delta = 0,461$	HEB 360	$\delta = 0,581$
HEM 200	$\delta = 0,537$	HEB 240	$\delta = 0,319$

5.4 Design of beam-to-column joints

In the classic deflected shape of a structural frame subjected to lateral loading, where the load distribution is characterized by inflection points near the midpoint of the beams and columns, the maximum moments occurs at the joint. Such actions are shown acting on an interior joint in Figure 5.13. Satisfactory response for the frame requires the joint to transfer the large unbalanced beam and column moments with reasonable deformations at both service and ultimate conditions.

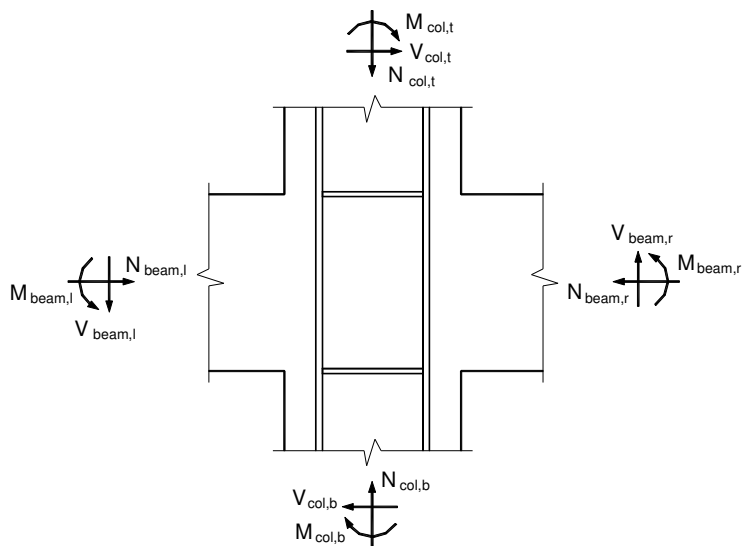


Figure 5.13. Actions on an interior composite joint

By means of the adjustment of an analytical model proposed by Kanno and Deierlein (2000) and Chou and Uang (2002) it is possible to quantify the shear resistance of the joint, consisting in the sum of different mechanisms activated in the connection. Furthermore, it is true that, up to now, the European Codes don't entirely cover the behaviour of the composite beam to column connections. In fact,

5. SEISMIC BEHAVIOUR OF RC COLUMNS EMBEDDING STEEL PROFILES

one of the goals of the InERD Project is to validate experimentally the joint mechanisms providing the shear resistance. Hence, once the presumed *Joint Formulation* had been derived, we were able to validate it thanks to the experimental data obtained from the tests.

The inner joint region behaviour is associated with two modes of failure, i.e. Shear and Bearing Failure and with the two correspondent resisting strengths in shear, $V_{joint,sp}$ and $V_{joint,hb}$, where $V_{joint,sp}$ is given by the sum of $V_{joint,wsp}$ and $V_{joint,ccs}$. The outer part of the joint deals with Shear and Bond Failure and with the associated shear strengths $V_{joint,cct}$ and $V_{joint,bf}$. As a result, the joint inner and outer resistances are evaluated as follows

$$V_{joint,inner} = \min \{V_{joint,ps}, V_{joint,hb}\} \quad (5.15)$$

and

$$V_{joint,outer} = \min \{V_{joint,cct}, V_{joint,bf}\} \quad (5.16)$$

where

$$V_{joint,ps} = V_{joint,wps} + V_{joint,ccs} \quad (5.17)$$

5.4.1 Strength of the Inner Elements

Inner joint behaviour is characterized by two primary modes of failure. Panel shear failure, see Figure 5.14a, is similar to the collapse typically associated with structural steel or reinforced concrete joints; but in composite joints both structural steel and reinforced concrete elements participate. The bearing failure, shown in Figure 5.14b, occurs at a location of high compressive stresses and permits rigid body rotation of the steel column within the concrete beam.

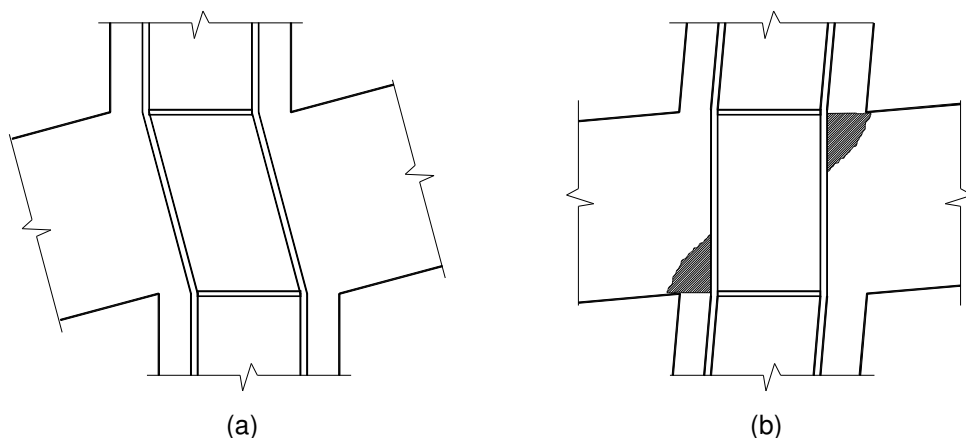


Figure 5.14. a) Panel shear failure; b) Bearing failure

5. SEISMIC BEHAVIOUR OF RC COLUMNS EMBEDDING STEEL PROFILES

Steel web panel, as shown in Figure 5.15a, acts similarly in composite and structural steel connections. The web is considered to carry pure shear stress over an effective panel length d_s , which is dependent on the location of the stiffeners in the column or on the distribution of horizontal bearing stresses.

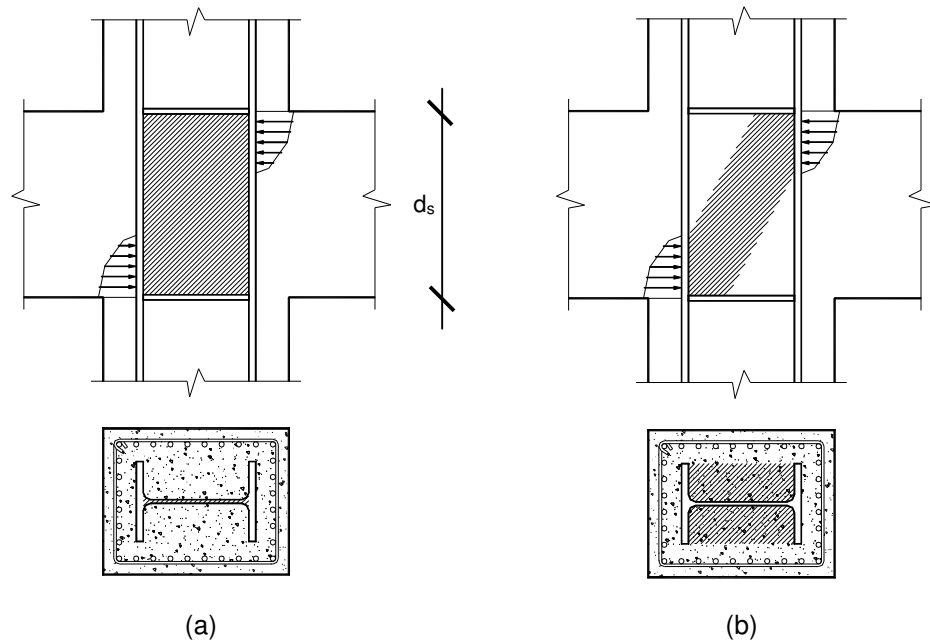


Figure 5.15. a) Steel web panel mechanism; b) Concrete compression strut mechanism

The shear resistance and the moment resistance for the steel web panel are calculated as follows:

$$V_{j,wps} = 0,7 \cdot \left(\frac{f_{ym,d,cw}}{\sqrt{3}} \cdot \min(A_v; t_{cw} \cdot 0,8d_s) + \Delta V_{j,wps} \right) \quad (5.18)$$

$$M_{Rd,j,wps} = V_{j,wps} \cdot (0,8 \cdot d_s) \quad \text{if } A_v < t_{cw} \cdot 0,8 \cdot d_s \quad (5.19)$$

$$M_{Rd,j,wps} = V_{j,wps} \cdot (h_c - t_{cf}) \quad \text{if } A_v > t_{cw} \cdot 0,8 \cdot d_s \quad (5.20)$$

Generally, lateral loads induced by seismic force govern composite connection design. Under seismic loading, the structure dissipates energy through several cyclic inelastic response. In steel structures, inelastic response can occur through plastic hinges, which, preferably, is limited to beam elements. For seismic design,

5. SEISMIC BEHAVIOUR OF RC COLUMNS EMBEDDING STEEL PROFILES

therefore, the composite connection and concrete column design strength should not be less than forces developed by plastic hinging of the steel beam adjacent to the connection.

Connection design strength is obtained reducing the nominal strength by a resistance factor ϕ . Since a large data base does not exists for statistical analysis of joint strength, the resistance factor is determined by calibration with relative factor of safety in the allowable stress specification for steel structures (AISC Specification, 1997). It practically corresponds to the inverse of the partial safety factor γ_{M0} used in European practice (where $\phi=0.9$ e $\gamma_{M0}=1.1$).

In the presented formula the resistance factor ϕ proposed by the AISC Specification (1997) is not directly take into account. The value of 0.7, that multiplies the formula, is based on the following assumption:

- The connections should have a greater reliability index (or factor of safety) than structural members. Allowable stress values reflect a factor of safety for connection that is 1.3 times greater than that for structural members;
- When the column axial force is not negligible, the shear resistance of the column web should be computed, by adopting the Hencky-Von Mises yield criterion, by means of the following relationship:

$$\sqrt{1 - \left(\frac{\sigma_{Sd,col}}{f_{yd,wc}} \right)^2} \cdot f_{yd,cw} \quad (5.21)$$

where $\sigma_{Sd,col}$ is the average normal stress in the panel zone. In the current Draft of EC3 (2000), the influence of the normal stress $\sigma_{Sd,col}$ due the column axial force, is approximately accounted for by means of a reduction coefficient equal to 0.9. In particular, the codified value of the reduction factor is on the safe side up to a column axial load equal to 45% of the column squash load. The use of the above equations, i.e. the use of a first yield criterion for evaluating the panel zone shear resistance, should be preferred when the effect of the panel zone deformation on frame stability is not considered in the structural analysis (Liew and Chen, 1994) or when is desired to limit the panel zone behaviour to the elastic range (Mazzolani and Piluso, 1996).

Thus, it is simple to obtain that $0.7 = 0.9 / 1.3$.

For the calculation of the shear area in the web panel zone the minimum value of two different contributions is take into account. Shear area A_v proposed by EC3 that may be taken as:

$$A_v = A_{s,tot} - 2 \cdot b_{cf} \cdot t_{cf} + (t_{cw} + 2 \cdot r) \cdot t_{cf} \quad (5.22)$$

5. SEISMIC BEHAVIOUR OF RC COLUMNS EMBEDDING STEEL PROFILES

Shear area calculated on the basis of the length j_h , used to regulate the effective length of the web panel and the distance between vertical resultant forces coupled in the compression strut. It is proposed to use a fixed value of $j_h = 0.8d_s$ based on comparison with test data.

Moreover, experimental tests have demonstrated that the panel zone is able to provide a significant post-yield resistance (Krawinkler, 1978). When the panel zone has uniformly reached yielding, an additional increase in shear strength $\Delta V_{j,wps}$ can be attributed to the resistance in flexion of the elements surrounding the panel. This resistance can be approximated by springs at the four corners whose stiffness is that corresponding to rotations of the column flanges concentrated at each corner. When the boundaries of the panel zone are assumed to be rigid, the post-elastic stiffness of the joint, attributable to the four springs, is computed as:

$$\Delta V_{j,wps} = \min \left\{ \frac{\frac{4 \cdot M_{Pl,cf,Rd}}{d_s} = \frac{4 \cdot \sqrt{4} b_{cf} t_{cf}^2 f_{ym,d,cf}}{d_s} = \frac{b_{cf} t_{cf}^2 f_{ym,d,cf}}{d_s}}{\frac{2 \cdot M_{Pl,cf,Rd} + 2 \cdot M_{Pl,st,Rd}}{d_s} = \frac{b_{cf} t_{cf}^2 f_{ym,d,cf} + b_p t_{sp}^2 f_{ym,d,s}}{2 \cdot d_s}} \right\} \quad (5.23)$$

Where the steel column web is encased in concrete the design shear resistance of the panel may be increased with the contribution of the inner concrete strut V_{ccs} , that is the design shear resistance of the concrete encasement to the web panel. The concrete compression strut, shown in Figure 5.15b, is similar to the mechanism used to model shear in a reinforced concrete connection. In composite connections, the concrete compression strut could be mobilized in resisting the connection shear either due to the presence of the horizontal stiffener plates welded to the column or due to the friction and the flexural forces acting in the steel column flange. In case of presence of the stiffener plates, the location and width of these determine how effectively the concrete strut is mobilized. The shear resistance and the moment resistance for the concrete compression strut are calculated as follows:

$$V_{j,ccs} = \frac{1}{1.3} \cdot V \cdot f'_{cd} \cdot A_c \cdot \sin\theta = \frac{1}{1.3} \cdot V \cdot \frac{0.85 \cdot f_{ck}}{\gamma_c} \cdot A_c \cdot \sin\theta \quad (5.24)$$

$$M_{Rd,j,ccs} = V_{j,ccs} \cdot (0.8 \cdot d_s) \quad (5.25)$$

5. SEISMIC BEHAVIOUR OF RC COLUMNS EMBEDDING STEEL PROFILES

For a single-sided joint, or a double-sided joint in which the beam depths are similar, the design shear resistance of concrete encasement into the column web panel depends by the following geometrical and mechanical parameters:

$$A_c = [0.8 \cdot (h_c - 2 \cdot t_{cf}) \cdot \cos \theta] \cdot (b_{cf} - t_{cw}) \quad (5.26)$$

$$\nu = 0.55 \cdot \left(1 + 2 \cdot \frac{N_{sd}}{N_{pl,Rd}} \right) \leq 1.1 \quad (5.27)$$

$$\theta = \tan^{-1} \left(\frac{h_c - 2 \cdot t_{cf}}{z} \right) \quad (5.28)$$

For connections with contact plates, the center of compression should be assumed to be in line with the mid-thickness of the compression flange. For connections with contact plates and only one row of reinforcement active in tension, the lever arm z should be taken as the distance from the center of compression to the row of reinforcement in tension. For connections with contact plates and two rows of reinforcements active in tension the lever arm z should be taken as the distance from the center of compression to a midway point between these two rows, provided that the two rows have the same cross-sectional area. In the formulation above, ν is a multiplier factor which accounts for the column axial load effects on the joint shear resistance, following the prescriptions of Eurocode 2.

Bearing Failure

The horizontal bearing strength $V_{joint,hb}$ is determined through a standard Stress Block model similar to that used for flexural strength calculation in reinforced concrete members. The shear resistance and the moment resistance for the concrete compression strut are calculated as follows:

$$V_{j,hb} = \frac{1}{1.3} \cdot \left(0.85 \cdot \frac{f_{ck,c}}{\gamma_c} \right) \cdot a_c \cdot b_{cf} \quad (5.29)$$

$$M_{Rd,j,hb} = V_{j,hb} \cdot (h_b - a_c) \quad (5.30)$$

To evaluate this resistance it is of primary importance to be able to guarantee an adequate concrete confinement inserting a proper ties quantitative which enhances the concrete performance. Confinement of concrete results in a modification of the effective stress-strain relationship: higher strength and higher critical strains are

5. SEISMIC BEHAVIOUR OF RC COLUMNS EMBEDDING STEEL PROFILES

achieved (Mander, 1988). The other basic material characteristics may be considered as unaffected for design. In the absence of more precise data, the stress-strain relation with increased characteristic strength and strains may be used, according to:

$$f_{ck,c} = f_{ck} \cdot \left(1 + 5 \cdot \frac{\sigma_2}{f_{ck}} \right) \quad \text{if } \sigma_2 \leq 0.05 \cdot f_{ck} \quad (5.31)$$

$$f_{ck,c} = f_{ck} \cdot \left(1.125 + 2.5 \cdot \frac{\sigma_2}{f_{ck}} \right) \quad \text{if } \sigma_2 > 0.05 \cdot f_{ck} \quad (5.32)$$

where σ_2 ($= \sigma_3$) is the effective lateral compressive stress at the ULS due to confinement. The value a_c is the stress block depth equal to $0.58 h_b/2$.

5.4.2 Strength of the Outer Elements

Shear Failure

The concrete compression field mechanism, shown in Figure 5.16, consists of several compression struts that act with horizontal reinforcement to form a truss mechanism (often used for modelling shear in reinforced concrete beams). Shear is transferred horizontally from the beam into the compression field through bearing against the embedded steel column.

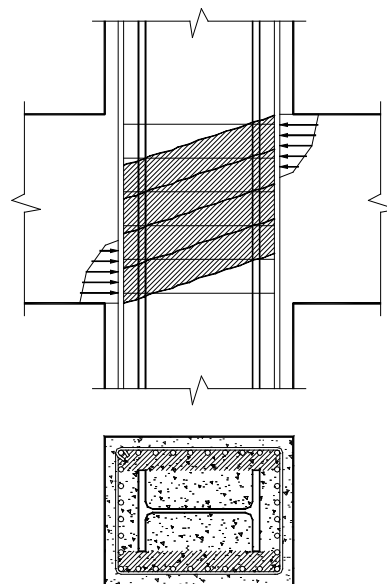


Figure 5.16. Concrete compression field mechanism

5. SEISMIC BEHAVIOUR OF RC COLUMNS EMBEDDING STEEL PROFILES

The shear resistance of this mechanism was evaluated following the prescriptions of prEN 1992-1, Final draft. In the latest version of Eurocode 2, for members not subjected to axial forces and with transverse reinforcement, $V_{\text{joint,ccf}}$, is evaluated as the smaller quantity between the concrete compressive strength V_c and the tensile strength of the transverse reinforcement V_s , where:

$$V_c = V_{Rd,\max} = \nu \cdot \frac{f_{ck}}{\gamma_c} \cdot b_{cs} \cdot 0.9 \cdot d \cdot \frac{1}{(\cot \theta + \tan \theta)} \quad (5.33)$$

and

$$V_s = V_{Rd,sy} = \frac{A_{sw}}{s} \cdot \frac{f_{yk,w}}{\gamma_s} \cdot 0.9 \cdot d \cdot \cot \theta \quad (5.34)$$

where $\nu = 0.6 (1 - f_{ck} / 250)$; θ is the angle between the concrete struts and the column longitudinal axis and it should be chosen such that the condition $1 \leq \cot \theta \leq 2.5$ is satisfied; b_{cs} is the effective width of the outer concrete strut equal to $b_{cs} = b_c - b_{cf} - 2c_c$.

In the case of members subjected to axial compressive forces, the maximum concrete shear resistance increases of the quantity α_c , defined as follows:

$$\begin{aligned} \alpha_c &= (1 + \sigma_{cp}/f_{cd}) && \text{for } 0 < \sigma_{cp} \leq 0.25 f_{cd} \\ \alpha_c &= 1.25 && \text{for } 0.25 f_{cd} < \sigma_{cp} \leq 0.5 f_{cd} \\ \alpha_c &= 2.5 (1 - \sigma_{cp}/f_{cd}) && \text{for } 0.5 f_{cd} < \sigma_{cp} < 1.0 f_{cd} \end{aligned}$$

σ_{cp} is the average concrete compressive stress (taken as positive) of the composite column due to the design axial load obtained also considering the longitudinal rebars.

The transverse reinforcement in the connection region plays a primary role both for the concrete confinement and to ensure the joint resistance. Precise guidelines are contained in the Eurocodes. First of all, the ties diameter must be equal to or greater than 6mm and not smaller than $1/4$ of the maximum re-bar diameter. The maximum amount of transverse reinforcement $A_{sw,max}$ must reflect the conditions:

$$\frac{A_{sw,max} \cdot f_{yd,w}}{b_w \cdot s_{tie}} \leq \frac{1}{2} \nu \cdot f_{cd} \quad (5.35)$$

Moreover, to allow the required plastic rotation, we need to verify for the confining reinforcement in joints of primary seismic beams with columns (in joints of primary importance for resisting the seismic actions), that:

5. SEISMIC BEHAVIOUR OF RC COLUMNS EMBEDDING STEEL PROFILES

$$\alpha \omega_{wd} \geq 30 \mu_\phi v_d \epsilon_{sy,d} \frac{b_c}{b_0} - 0,035 \quad (5.36)$$

with:

α global confinement effectiveness factor, equal to $\alpha = \alpha_n \times \alpha_s$ with, for rectangular cross sections:

$$\alpha_n = 1 - \sum \frac{b_i^2}{6b_0 h_0} \quad (5.37)$$

$$\alpha_s = \frac{1 - \frac{s}{2b_0}}{1 - \frac{s}{2h_0}} \quad (5.38)$$

ω_{wd} mechanical volumetric ratio of confining hoops within the critical regions equal to:

$$\frac{\text{Volume of the confining hoops}}{\text{Volume of concrete core}} \cdot \frac{f_{yd,w}}{f_{cd}} \quad (5.39)$$

μ_ϕ required value of the curvature ductility factor equal to:

$$\begin{cases} 2q-1 & \text{if } T_1 \geq T_c \\ 1+2(q-1) \frac{T_c}{T_1} & \text{if } T_1 < T \end{cases} \quad (5.40)$$

v_d normalized design axial force, equal to $\frac{N_{Ed}}{A_c f_{cd}}$

$\epsilon_{sy,d}$ design value of tension steel strain at yield

b_c gross cross-sectional width

b_0 width of confined core (to the centerline of the hoops)

h_0 depth of confined core (to the centerline of the hoops)

for the critical regions of columns l_{cr} , except as specified follows:

1. If beams frame into all four sides of the joint and their width is at least three-quarter of the parallel cross-sectional dimension of the column, the spacing of the horizontal confinement reinforcement in the joint may be increased to twice that required, but not to exceed 150 mm.

5. SEISMIC BEHAVIOUR OF RC COLUMNS EMBEDDING STEEL PROFILES

2. At least one intermediate (between column corner bars) vertical bar shall be provided at each side of a joint of primary seismic beams and columns.

In the absence of more precise information, the length of the critical region l_{cr} may be computed as follows:

$$l_{cr} = \max (h_c ; l_{cl} / 6 ; 450 \text{ mm}) \quad (5.41)$$

Bond Failure

An idealization of the bond failure $V_{joint,bf}$ provided by the longitudinal reinforcing bars acting in friction with concrete and embedded in the outer joint region is shown in Figure 5.17. The bond failure occurs in the outer elements if the compression and tension forces (due to moment equilibrium), along with the forces mobilised in the concrete compression field, are greater than the strength of the bond mechanism of a set of main longitudinal re-bars.

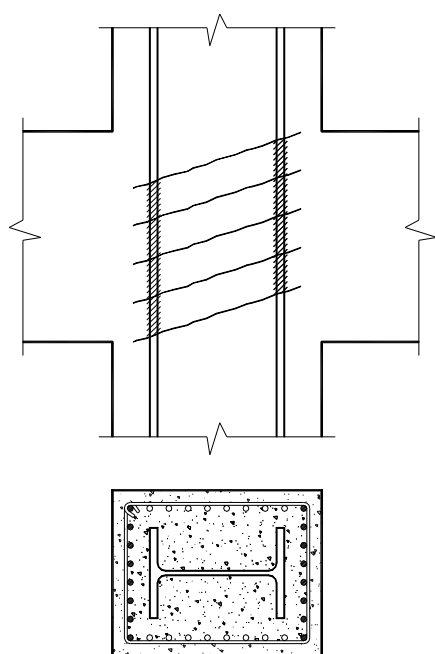


Figure 5.17. Bond failure mechanism

The shear resistance and the moment resistance for bond mechanism is calculated as follows:

$$V_{j,b} = \frac{1}{1.3} \cdot f_{bd} \cdot \phi_b \cdot x_{rb,c} \quad (5.42)$$

5. SEISMIC BEHAVIOUR OF RC COLUMNS EMBEDDING STEEL PROFILES

$$M_{Rd,j,b} = V_{j,b} \cdot d_s \quad (5.43)$$

It is assumed that bond failure occurs in the outer elements when the sum of the forces is equal to the bond strength of a set of main reinforcing bars.

$$T_{cb} + T_{ib} = T_{bf} \quad (5.44)$$

The bond failure strength should be calculated as follows:

$$T_{bf} = f_{bd} \cdot \phi_b \cdot d_s \quad (5.45)$$

The design value of the ultimate bond stress f_{bd} for ribbed bars may be taken as:

$$f_{bd} = 2.25 \cdot \eta_1 \cdot \eta_2 \cdot f_{ctd} = 2.25 \cdot \eta_1 \cdot \eta_2 \cdot \frac{0.7 \cdot 0.3 \cdot f_{ck}^{2/3}}{\gamma_c} \quad (5.46)$$

where:

- η_1 is a coefficient related to the quality of the bond condition and the position of the bar during concreting:
1,0 when *good* conditions are obtained;
0,7 for all other cases and for bars in structural elements built with slip-forms, unless it can be shown that *good* bond conditions exist;
- η_2 is a coefficient related to the bar diameter ϕ equal to:
1.0 for $\phi \leq 32$ mm
 $(132 - \phi)/100$ for $\phi > 32$ mm

Where not otherwise indicated in Eurocode 8, for frame systems the beam-to-column joints are required to have an increased moment resistance $M_{joint,Rd}$ in order to enhance the ductile capacity of the columns avoiding, in this way, the local formation of plastic hinges. Provided that, at the design stage, the plastic hinge formation in the beams is envisaged, it is necessary in any case to take into account the increase in the beam moment values in order to derive the design joint forces. Focusing the attention on the behaviour of an internal beam-to-column joint belonging to a frame free to deform in plane and subjected both to gravitational

5. SEISMIC BEHAVIOUR OF RC COLUMNS EMBEDDING STEEL PROFILES

and seismic loads, as depicted in Figure 5.18, it is possible to define the following relations for the bending moments acting at the left and at the right of the joint.

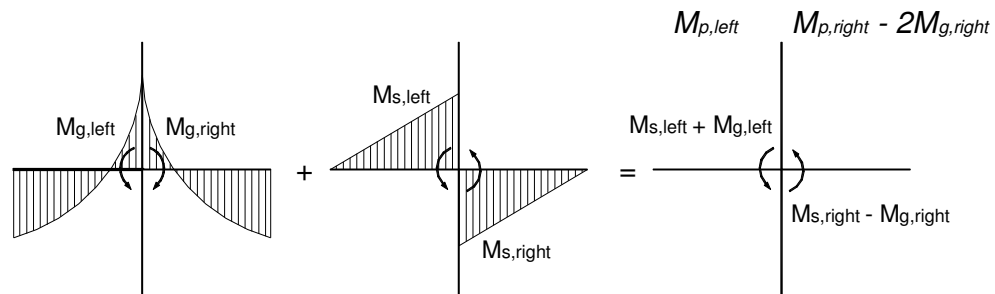


Figure 5.18. Gravitational and seismic action in an interior joint

$$M_{left} = M_{s, left} + M_{g, left} \quad (5.47)$$

$$M_{right} = M_{s, right} - M_{g, right} \quad (5.48)$$

If it is assumed that during a seismic event the left bending moment of the beam reaches the value of the bending plastic moment, as a consequence:

$$M_{p, left} = M_{s, left} + M_{g, left} \quad (5.49)$$

Moreover, if the same allowances for the beam bending moment acting on the right side are made, we obtain:

$$M_{p, right} = M_{s, right} + M_{g, right} \quad (5.50)$$

Hence, combining Eqs (5.48) and (5.50), it is easy to obtain that the bending moment acting on the right of the joint is equal to:

$$M_{right} = M_{s, right} - M_{g, right} = M_{p, right} - 2M_{g, right} \quad (5.51)$$

This equation underlines that the gravitational loads reduce the effects of the seismic action in terms of bending moment acting at the joint. This beneficial effect of the gravitational loads is not included in the Eurocode prescriptions. Nevertheless, the AISC provisions (1997) approximately account for it by means of a reduction coefficient equal to 0,8. Besides, it has to be noted that the column shear reduces the total joint shear action at the beam-to-column joint position and

5. SEISMIC BEHAVIOUR OF RC COLUMNS EMBEDDING STEEL PROFILES

thus increases the shear joint strength. In accordance with these assumptions, for the two seismic load combination (design case 2 and design case 3), we must check that:

$$1. \quad V_{j,Rd} \geq V_{j,Sd} = 0,8 [(M_{beam,Rd,right} + M_{beam,Rd,left}) / d_s - V_c] \quad (5.52)$$

where V_c is the average shear force at collapse in the web panel equal to:

$$(V_{column,top} + V_{column,bottom}) / 2 = (M_{column,Rd,top} + M_{column,Rd,bottom}) / (H_c - d_s) \quad (5.53)$$

assuming that the zero-moment points are located in the middle section of the columns the equilibrium condition $\sum M_{beam} = \sum M_{column}$ is satisfied.

$$2. \quad M_{j,Rd} \geq 1,3 (M_{beam,Rd,right} + M_{beam,Rd,left}) \quad (5.54)$$

In view of the resistance evaluation, the following equations obtained from equilibrium of forces in the joint panel zone are used:

$$M_{j,Rd} = V_{joint,inner} \cdot d_{inner} + V_{joint,outer} \cdot d_{outer} \quad (5.55)$$

$$V_{j,Rd} = M_{j,Rd} / d_s \quad (5.56)$$

5.5 The experimental test programme

5.5.1 Design of the reduced section of the specimen to be tested

For what concerns the laboratory experimentation feasibility, it was suggested to test the specimens in $1/2$ scale. Hence, some geometrical and mechanical reducing factors had to be applied to the section properties which include:

- exterior geometrical dimensions of the concrete column (b and h);
- amount of longitudinal reinforcing bars in the column ($A_{s,long}$);
- amount of transverse reinforcing bars in the column ($A_{s,stirrup}$);
- dimension of the steel profile.

Concerning the reduction of the steel profile two different possibilities were taken into account. The steel profile may be reduced either in term of the cross area $A_{s,steel}$ or in term of plastic modulus $W_{pl,steel}$. The first solution ensures that the axial

5. SEISMIC BEHAVIOUR OF RC COLUMNS EMBEDDING STEEL PROFILES

and shear resistance of the steel sections reduces of a half factor, while the second one guarantees the resistance in bending to be half of that belonging to the original section. Nevertheless, by diminishing the geometrical properties of the concrete sections we obtained a reduction of the bending resistance equal to one fourth of the original section. Hence, the assumptions made for the reduction of the steel profile properties were not adoptable. Indeed, it was necessary to calculate the reduced steel sections following the design criteria already presented in a previous paragraph for the full-scale steel-concrete composite columns, and briefly summarised below:

- the steel section should at least be able to take alone the design axial force of the seismic loading case;
- the steel section alone (not acting composedly) should be able to substitute the deficient concrete section;
- the sections have been chosen in order to not modify the local stiffness EI of the columns and the total stiffness of the original concrete structure (maximum level of modification of the order of 10%);
- the sections have been chosen in order to achieve a favourable performance both along their major axis bending and along their minor axis bending.

In the following Figure 5.19 the reduced composite column cross sections adopted in the experiments at the University of Trento are shown.

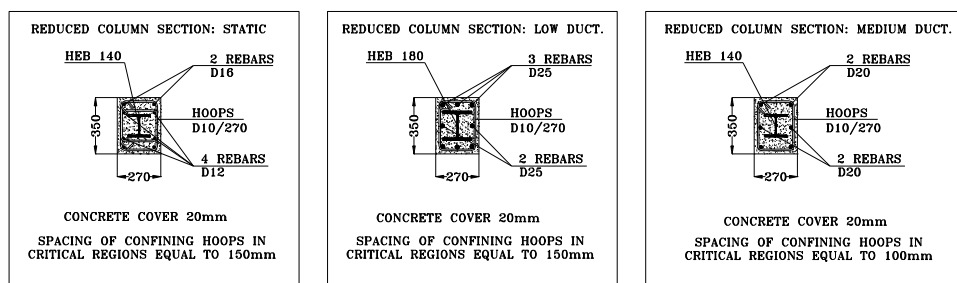


Figure 5.19. Reduced sections for the composite columns to be tested

From these sections, corresponding to the respective load cases under study, we extrapolated the scaled 3D composite columns to be analysed. Each cross composite section generated four scaled samples, two with long steel profile (with or without steel plates in the joint), and two with short steel profile in the critical length (with or without horizontal steel plates) as illustrated in Figure 5.20. Therefore, to each design category (static and seismic) belong four composite samples plus another scaled sample without the encased steel profile. The latter operating as a comparison trial for the others. Also four tests along minor axis were

5. SEISMIC BEHAVIOUR OF RC COLUMNS EMBEDDING STEEL PROFILES

planned. One reinforced concrete (RC) column and one composite (CO) column both for the Static case and for the Seismic A case had to be analysed.

The stiffeners were considered with the aim of better understanding the behaviour of the joint panel, i.e. the continuity horizontal plates were welded to the steel profile at the height of the critical joint region to state whether their presence may modify or not the load transfer between concrete and steel.

In order to ensure that the load transfer between concrete and steel are efficiently mobilized in critical region of the composite column, an end plate welded at the end of the steel profile was designed. The alternative and possible use of shear connectors welded on the steel flanges in the critical zone was rejected, both to allow for a simplified technical solution and to minimise the fabrication costs of the samples under evaluation. The geometrical specifications for the design of the end plate are highlighted in Figure 5.20.

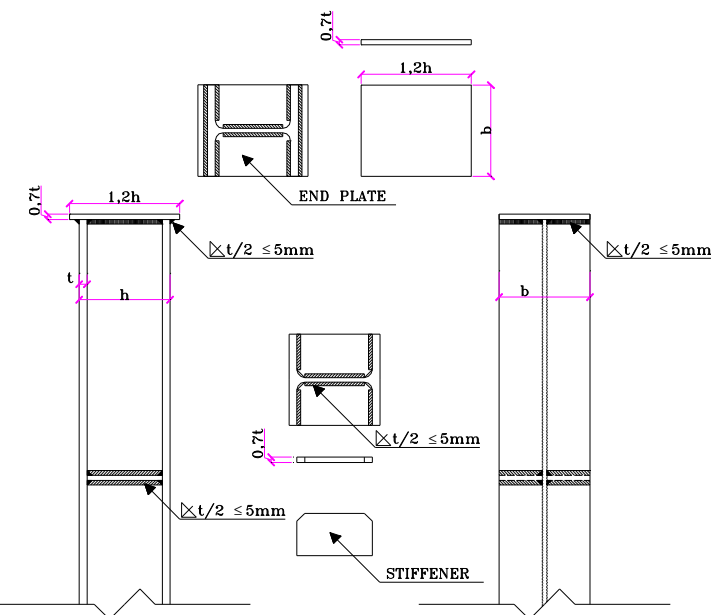


Figure 5.20. Geometrical characteristic of the end plate and stiffeners

It is to mention that the side beams were over-designed in respect of the column (not responding to the *Capacity Design* principle) specifically to allow the study of the joint and column behaviour. On the contrary, another research carried out at the University of Liège, in the presence of a frame, which did not permit the full frame deformation (due to the presence of a bracing system simulating the masonry in-fills), saw the plastic deformation occurring in the column without the

5. SEISMIC BEHAVIOUR OF RC COLUMNS EMBEDDING STEEL PROFILES

chance of studying the mechanisms mobilised in the joint. Actually, this last-mentioned frame had the purpose of better reproducing the boundary condition of a Soft Storey for a base column. Nevertheless, some other recent researches in this field have demonstrated that the masonry in-fills play a role, contributing to the overall structural stiffness, only in the very first phase of a seismic event.

5.5.2 Test set-up and test programme

The test configuration adopted at the University of Trento Laboratories is represented in Figure 5.21. It is to be noted that the frame does not exactly represent the Soft Storey configuration being free from the secondary forces transmitted in a presence of masonry in-fills. Besides, the beams were over-designed with respect to the columns not matching the Capacity Design philosophy of Eurocode 8 (2001). In the previous chapters we already discussed the choices made in relation to these issue. Nevertheless, this test configuration has the advantage that the determination of the internal actions in the members is easier. As a result, it is possible to catch the forces acting inside the joint in order to compare the results and to work out the relevant parameters indispensable for an excellent connection design under seismic loading.

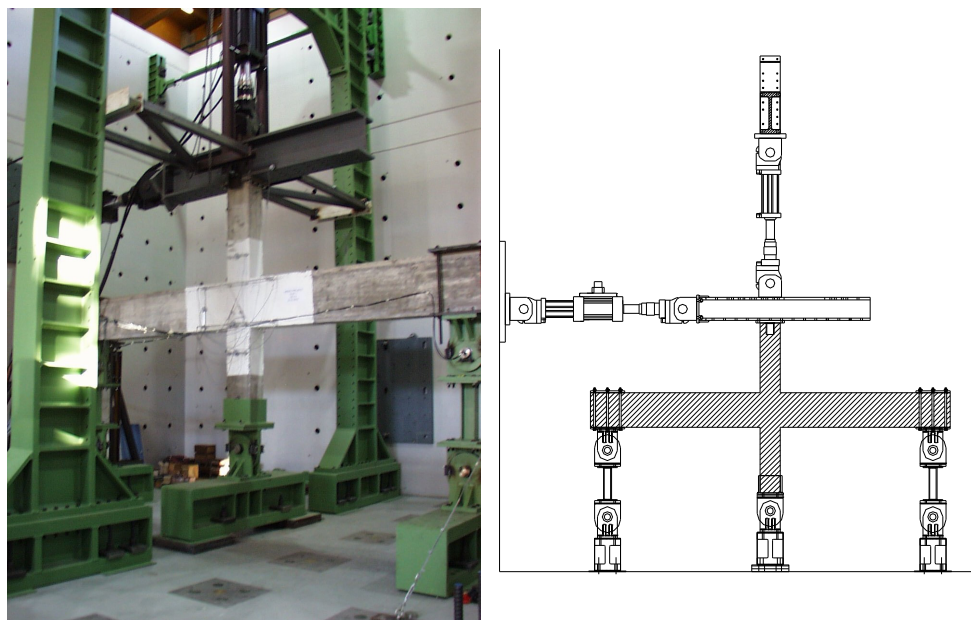


Figure 5.21. Test configuration adopted in Trento

The final test programme is reported in the following Table 5.13, in which it is possible to find all the characteristics of the specimens to be tested at the

5. SEISMIC BEHAVIOUR OF RC COLUMNS EMBEDDING STEEL PROFILES

University of Trento. It is important to highlight that the terms C1, C2 and C3 are essentially three different configurations of the steel profile, that will be used during the test; in detail, C1 is the configuration of the specimen with the steel profile extended beyond the depth of the beam; C2 is the configuration of the specimen with the steel profile at the level of the depth of the beam (not used in Trento); and C3 is the configuration of the specimen with a short steel profile in the critical length of the column.

		R.C.	COMPOSITE				
PHASE 1	Low ductility strong axis	RCT3	COT5	COT6	COT7	COT8	
			with stiffeners	without stiffeners	with stiffeners	without stiffeners	
			long (C1)	long (C1)	short (C3)	short (C3)	
PHASE 2	Medium ductility strong axis	RCT5	COT9	COT10	COT11	COT12	
			with stiffeners	without stiffeners	with stiffeners	without stiffeners	
			long (C1)	long (C1)	short (C3)	short (C3)	
PHASE 3	Static strong axis	RCT1	COT1	COT2	COT3	COT4	
			with stiffeners	without stiffeners	with stiffeners	without stiffeners	
			long (C1)	long (C1)	short (C3)	short (C3)	
PHASE 4	Weak axis	Static	RCT2	COT13			
				with stiffeners			
				long (C1)			
	Low ductility	RCT4	COT14				
				with stiffeners			
				long (C1)			

Table 5.13. Test programme

For each specimen 2 cubes and 1 cylinder are necessary:

2 cubes for compressive strength the day of the test

1 cylinder for tensile strength and modulus of elasticity the day of the test

Moreover additional cubes and cylinders are made to obtain:

1 cubes for compressive strength at 1 day

1 cubes for compressive strength at 3 days

1 cubes for compressive strength at 7 days

1 cubes for compressive strength at 14 days

1 cubes for compressive strength at 28 days

1 cylinder for tensile strength and modulus of elasticity at 14 days

5. SEISMIC BEHAVIOUR OF RC COLUMNS EMBEDDING STEEL PROFILES

5.5.3 Global test instrumentation

Different types of instruments were used to determine the behaviour of the specimens during the test, among them strain gauges, load cells, displacement transducers, inclinometers, etc. Preliminary analyses of the specimen and loading apparatus, by means of FE method, were conducted to estimate the displacement/strain/force ranges to be used in selecting and calibrating instruments. Hereafter the instrumentation that has been used in monitoring the specimens is presented, according to the test set-up illustrated in Figure 5.21.

Load cells

- Interior load cell located in the vertical actuator (Maximum capacity: 1000 kN in compression, 650 kN in tension);
- Interior load cell located in the horizontal actuator (Maximum capacity: 1000 kN in compression, 1000 kN in tension);
- LC-1: exterior load cell located as hinge (Maximum capacity: 1000 kN);
- LC-2: exterior load cell located as hinge (Maximum capacity: 1000 kN).

Displacement transducers

- Interior LVDT located in the vertical actuator (Maximum capacity: 500 mm);
- Interior LVDT located in the horizontal actuator (Maximum capacity: 500 mm);
- DT500-Column: exterior digital transducer Heidenhein-USL500 (Maximum capacity: 500 mm), located at the top of the column;
- DT500-Beam: exterior digital transducer Heidenhein-USL500 (Maximum capacity: 500 mm), located at the mid-height of the beam.

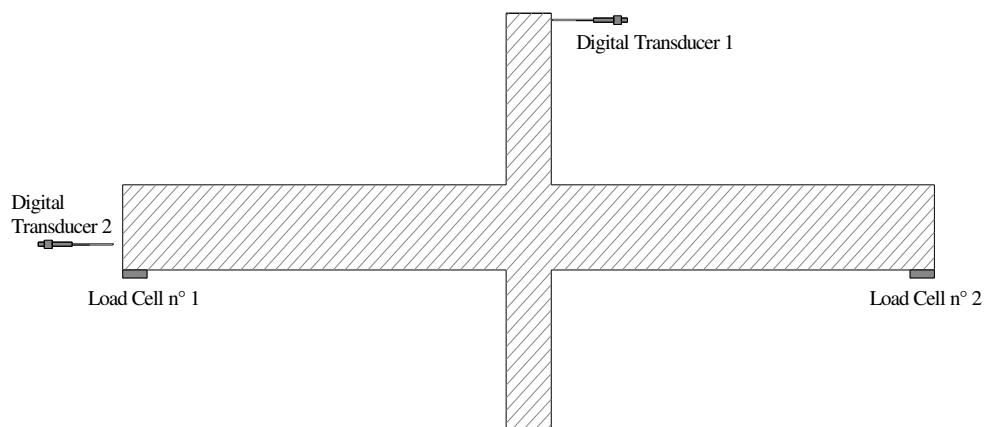


Figure 5.22. Exterior digital transducer and exterior load cells in the specimen

5. SEISMIC BEHAVIOUR OF RC COLUMNS EMBEDDING STEEL PROFILES

Additional instrumentation

Moreover, exterior instrumentation was used to obtain adequate information on the rotation of the column web panel and on the beam portion in the closeness of the joint. In details the instruments are listed below (see Figure 5.23):

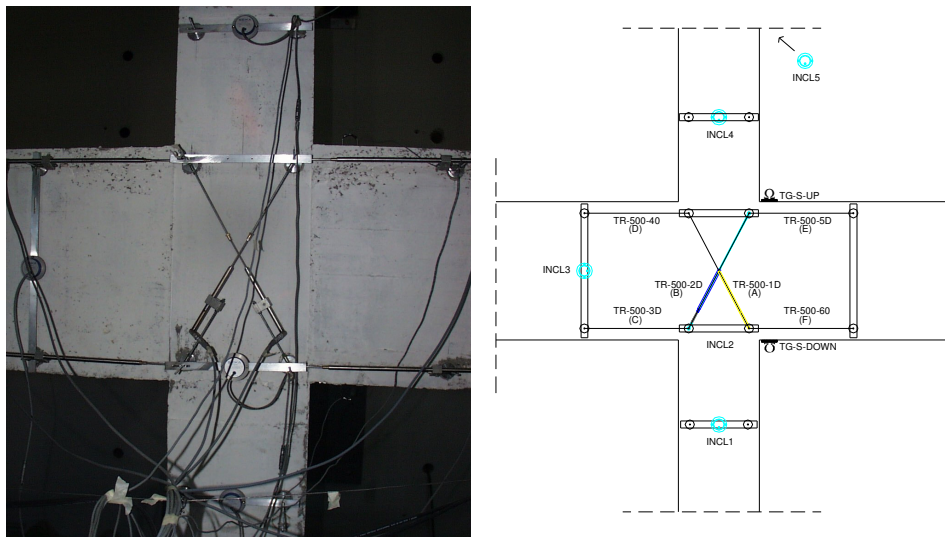


Figure 5.23. Exterior instrumentation in the joint

- Exterior LVDTs (Maximum capacity: 100 mm) located in the portion of the joint as seen in the pictures;
- Exterior inclinometers (INCL1-2-3-4 with maximum capacity of ± 14 degrees) located in the portion of the joint. One more inclinometer (INCL5) located on the force distributing steel beam at the top of the specimen to record the slope variation during the test; by means of this measurement it is possible to obtain the axial and shear load components (which vary during the test) originated by the actuators and acting on the specimen;
- Exterior omega (Ω) displacement transducer (TG-S-UP and TG-S-DOWN) located on the top-bottom face of the concrete beam in proximity to the connections; by means of this measurement it is possible to obtain information about the deformation of the beam section during the test, and then, to reproduce the bending moment acting at the joint.

5.5.4 Local test instrumentation

The local instrumentation (see the next Figure 5.24-Figure 5.26) was only applied to the specimens COT6-7 of the Phase 1 and COT9-10 of the Phase 2. It consisted of:

5. SEISMIC BEHAVIOUR OF RC COLUMNS EMBEDDING STEEL PROFILES

- Linear strain gauges SG-1 to 10 stuck on the steel profiles as shown in Figure 5.24. By means of this measurement it is possible to understand when the joint force transfer mechanism is activated in the portion of the steel profile. This mechanism represents the shear force carried by the steel column web behaving in an elastic-plastic regime.

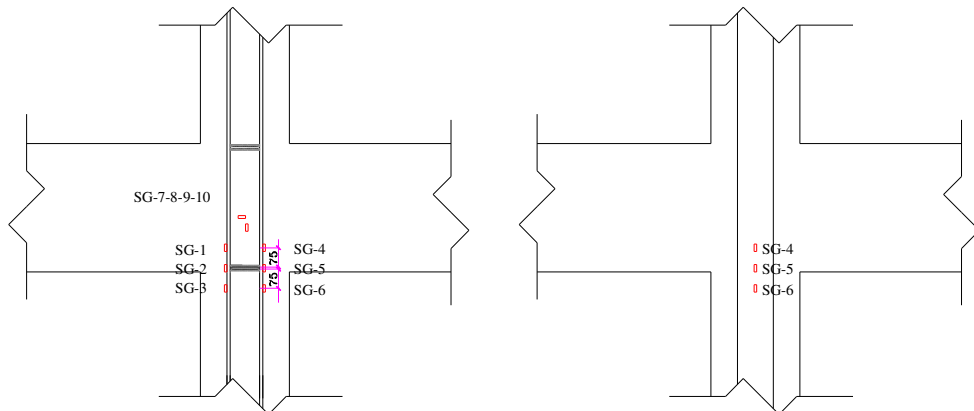


Figure 5.24. Interior strain gauges located in the steel profile

- Linear strain gauges SG-11 to 22 on the reinforcing bars and on the stirrups of the column as shown in Figure 5.25. By means of these measurements it is possible to understand when the force transfer mechanism is activated in the concrete portion of the joint.

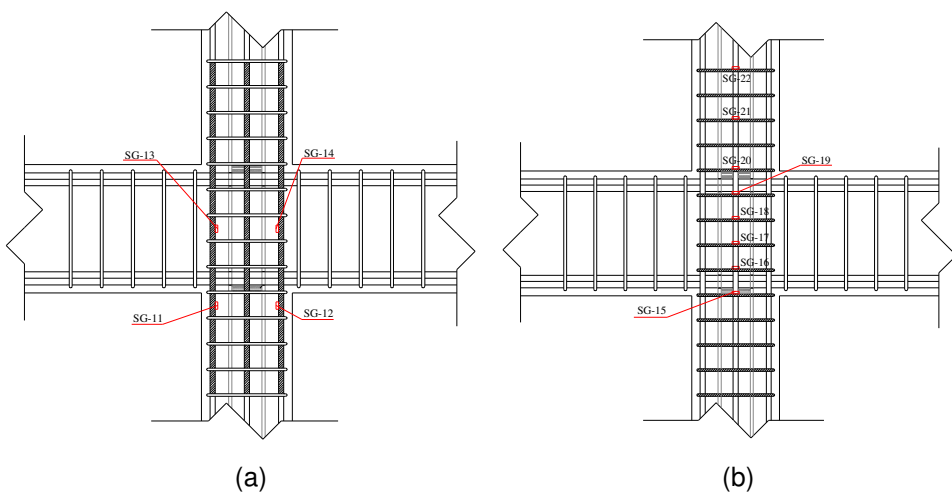


Figure 5.25. Interior strain gauges located (a) in the rebars and (b) in the stirrups of the concrete column

5. SEISMIC BEHAVIOUR OF RC COLUMNS EMBEDDING STEEL PROFILES

- Strain gauges SG-23 to 26 on the reinforcing bars of the beam as shown at Figure 5.26. All strain gauges are linear strain gauges. By means of these measurements, coupled with those recorded by the Ω -transducer, it is possible to obtain information about the deformation of the beam section in the closeness of the joint during the test; and then, to reproduce the bending moment acting in the joint.

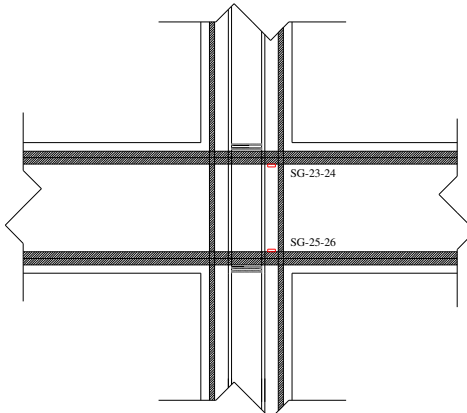


Figure 5.26. Interior strain gauges located in the rebars of the concrete beam

5.5.5 Test procedure and loading history

The choice of a testing program and associated loading history depends on the purpose of the experiment, type of test specimen, and type of expected failure mode. The following testing procedures are intended as a reference, to produce an adequate and, as much as possible, a unified way to carry out tests in order to characterize the structural behaviour of structural component substructures.

The ECCS Procedure (1986) should help to verify the common design relationship between a pseudo-static horizontal force and a specified ductility or displacement given by Codes and Recommendations, such as, for instance the ECCS Recommendations for Steel Structures in Seismic Zones. This procedure has been chosen to set forward the characteristics of the element in that peculiar context. The complete definition of the test also requires data on the combination of seismic and non-seismic loads. The testing procedure may include preliminary classical monotonic displacement increase tests or obviate them. In the first case, it is called *complete testing procedure*; in the opposite case, it is called *short testing procedure*. From the F-e curve recorded during the monotonic test, the conventional limit of elastic range F_y and the corresponding displacement e_y^+ may be deduced. In the present study case, F_y and e_y are not known at the beginning of

5. SEISMIC BEHAVIOUR OF RC COLUMNS EMBEDDING STEEL PROFILES

the test because only a cyclic test is executed, that is a test with increase of displacement. The principle is that a reference *yield displacement* e_y value in the form of an absolute value should be defined preliminarily and kept for all specimens, in order to make possible a direct comparison. For composite columns, the estimated interstorey drift angle θ_y at yielding is $0,5\% = 5$ mrad. The drift angle in the test is the displacement of the actuator divided by the height or length of the part of the specimen, which may deform during the test. The height of column which is free to deform is 3500 mm (storey height), i.e. from the actuator axis to the hinge axis, then, $e_y = \theta_y \times 3500 = 17,50$ mm is the yield displacement (+ and -) at the actuator (+ and -). The loading history is defined by the following sequences, reported hereafter in Figure 5.27:

- one cycle in the intervals:
 $e_y^+/4, e_y^-/4; 2e_y^+/4, e_y^-/4; 3e_y^+/4, 3e_y^-/4; e_y^+, e_y^-;$
- three cycles in the intervals:
 $2e_y^+, 2e_y^-; 4e_y^+, 4e_y^-; \dots; (2+2n)e_y^+, (2+2n)e_y^-$ with $n = 1, 2, 3, \dots$
- more cycles or more intervals may be used if necessary.

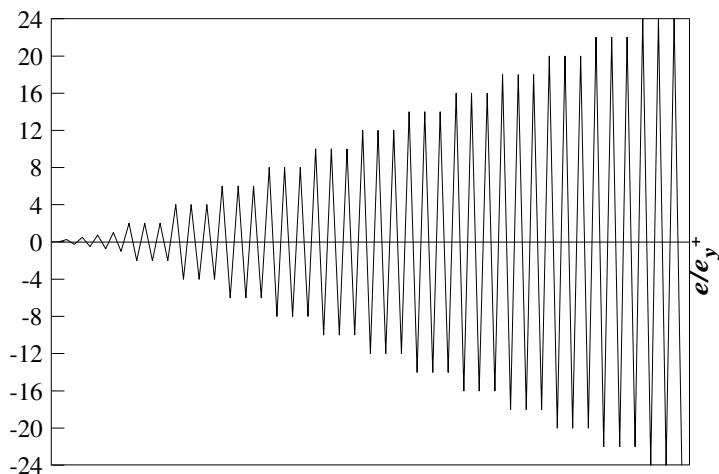


Figure 5.27. Multiple-Step Test: adopted ECCS loading history

Due to the set-up configuration used by the laboratory of the University of Trento, some calculations have been conducted in order to obtain the correct displacement and force loading history to be applied to the horizontal and the vertical actuators, respectively. During the test, because of the deformed configuration of the specimen, the steel distributing frame modifies the inclination with respect to the horizontal line in the un-deformed configuration. This means that, both the horizontal and the vertical actuators modify their original inclination, producing a

5. SEISMIC BEHAVIOUR OF RC COLUMNS EMBEDDING STEEL PROFILES

modification in the actual applied horizontal displacement and vertical axial force. Considering the geometry of the specimen and of the test set-up we obtain that:

- the imposed displacement of the horizontal actuator is greater than the horizontal displacement at the top face of the specimen, due to the angle formed by the top steel distributing beam in the deformed shape of the specimen. Obviously, this inclination depends on the specimen flexibility that varies during the test due to damage in some portions of the specimen. *A priori*, it is impossible to know correctly this aspect, even if we reconstructed the displacement loading history by means of an elastic numerical model. We have obtained that the ratio between the top displacement of the column and the displacement of the horizontal actuator is given by a factor equal to 1.214;
- moreover, the axial load imposed by the vertical actuator (assumed equal to 900 KN) must be maintained constant during the test. The top displacement of the column δ_x , imposed by the horizontal actuator, modifies the alignment between the specimen and the vertical actuator (see the deformed configuration in Figure 5.28). For this reason, only a component of the imposed axial load is applied to the column.

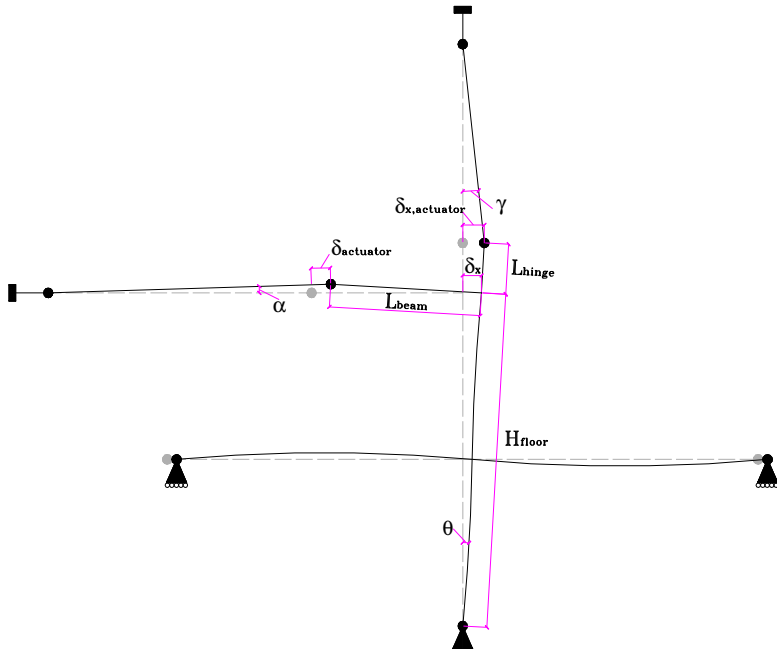


Figure 5.28. Deformed configuration of the specimen and of the test set-up during the test

Thus, a geometrical relation to maintain constant the axial load, as a function of the top displacement of the column, was deduced

5. SEISMIC BEHAVIOUR OF RC COLUMNS EMBEDDING STEEL PROFILES

$$\delta_{x,actuator} = \delta_x + L_{hinge} \cdot \tan \vartheta \cong \delta_x + L_{hinge} \cdot \vartheta \quad (5.57)$$

$$\delta_x = H_{floor} \cdot \tan \vartheta \cong H_{floor} \cdot \vartheta \quad (5.58)$$

Hence, combining the Eq. (5.57) with the Eq. (5.58) we obtain:

$$\delta_{x,actuator} = (H_{floor} + L_{hinge}) \cdot \vartheta \quad (5.59)$$

$$\gamma = \frac{\delta_{x,actuator}}{L_{actuator}} \quad (5.60)$$

$$N_{column} = N_{actuator} \cdot \cos(\vartheta + \gamma) \quad \text{with} \quad \vartheta = \frac{\delta_x}{H_{floor}} \quad (5.61)$$

Combining the Eq. (5.60) with the Eq. (5.61) and expressing $N_{actuator}$ in term of N_{column} we still get:

$$N_{actuator} = \frac{N_{column}}{\cos(\vartheta + \gamma)} = \frac{N_{column}}{\cos\left[\vartheta + \frac{H_{floor} + L_{hinge}}{L_{actuator}} \cdot \vartheta\right]} = \frac{N_{column}}{\cos\left[\left(1 + \frac{H_{floor} + L_{hinge}}{L_{actuator}}\right) \cdot \frac{\delta_x}{H_{floor}}\right]}$$

This relation produces a variation of the applied axial load that depends on the amplitude of the column top displacement. Only at large displacements the value of the imposed axial load varies significantly.

In order to investigate the forces acting on the frame system, an elaboration of the main parameters is due. As main parameters are intended the bending moment M , shear V , reaction forces and the values defining the deformed shape as rotations ϕ and displacements s . Taking the origins of an hypothetical coordinate system xy at both ends of the lateral beams, with the x -coordinate s_1 and s_2 , as indicated in Figure 5.29, we have the main parameters defined by:

$$M_c^-(s_2) = V_c^- s_2 \quad (5.62)$$

$$V_c^-(s_2) = R_{LC,dx} \cos(\varphi_{DEV}) \quad (5.63)$$

$$M_c^+(s_1) = V_c^+ s_1 \quad (5.64)$$

5. SEISMIC BEHAVIOUR OF RC COLUMNS EMBEDDING STEEL PROFILES

$$V_c^+ (s_1) = R_{LC,sx} \cos(\varphi_{DEV}) \quad (5.65)$$

$$R_V = F_{VJ} + R_{LC,dx} \cos(\varphi_{DEV}) - R_{LC,sx} \cos(\varphi_{DEV}) \quad (5.66)$$

$$R_H = F_{HJ} + R_{LC,dx} \sin(\varphi_{DEV}) - R_{LC,sx} \sin(\varphi_{DEV}) \quad (5.67)$$

Where M_c^+ , V_c^+ , M_c^- , V_c are the bending moments and shear forces acting in the beams at the two sides of the frame system. R_V and R_H are the vertical and horizontal reaction forces at the column base.

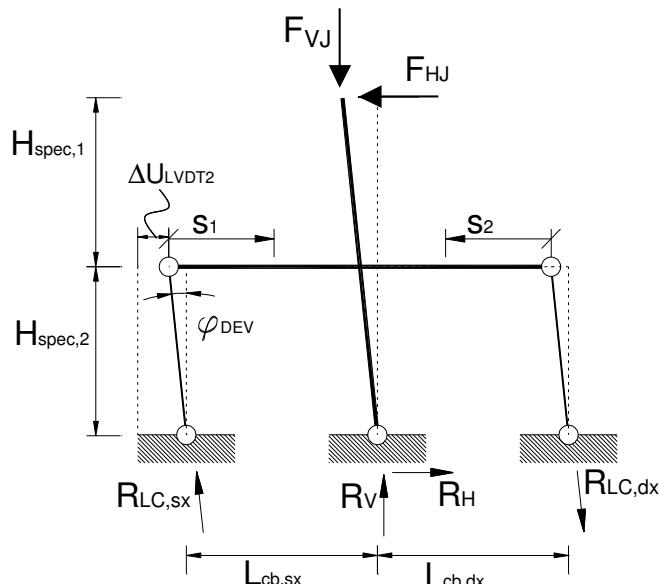


Figure 5.29. First order deformed shape to evaluate the forces acting on the frame system

The angle φ_{DEV} represents the slope of the vertical pendulum during the test, increasing with the horizontal displacement. Assuming the hypothesis of small angles we can state that:

$$\varphi_{DEF} = \frac{\Delta U_{DT,beam}}{H_{spec,2}} \quad (5.68)$$

where $\Delta U_{DT,beam}$ is the specimen displacement given by the digital transducer applied at the lateral concrete beam face.

5. SEISMIC BEHAVIOUR OF RC COLUMNS EMBEDDING STEEL PROFILES

The force reactions are measured by two load cells located under the extreme faces of the concrete beams, whereas the specimen displacements, slopes, and deformations are derived from the inclinometers (giving as measure absolute angles in respect to the vertical axis) and from the digital displacement transducers described above.

In order to understand the behaviour of the joint under cyclic loading, it is important to underline the rotation capability of the panel zone. For this reason, the angular distortion was monitored during the test through the measures of diagonal transducers TR500-2D, TR500-1D fitting their values in the Krawinkler (1978) equation:

$$\gamma_{conn} = \operatorname{tg}^{-1} \left[\sqrt{(h_j)^2 + (b_j)^2} \frac{(\Delta U_{TR500-2D} - \Delta U_{TR500-1D})}{2(h_j * b_j)} \right] \quad (5.69)$$

Where h_j and b_j are the net height and breadth of the panel zone subjected to shear given by $h_b - 2c_c$ and $b_c - 2c_c$. ΔU_{TR500} represent the diagonal LVDT joint measures. In this manner it is possible to underline the panel energy absorption and its performance in terms of ductility due to the plastic deformation.

The rotation of the beam in respect to the connection, φ_{conn} , gives the relative angle between the deformed joint panel and the concrete beam in the deformed shape. The following equations, based on the measure of the horizontal displacement transducers TR500 3O, 4O, 5O, 6O, can be utilised:

$$\varphi_{CONN.SX} = \frac{\Delta U_{TR500-40} - \Delta U_{TR500-30}}{h_j} \quad (5.70)$$

$$\varphi_{CONN.DX} = \frac{\Delta U_{TR500-50} - \Delta U_{TR500-60}}{h_j} \quad (5.71)$$

Another way to derive this quantities is to purify the measures from the "vertical" inclinometers attached to the two sides of the concrete beam by the reading of the "horizontal" inclinometer at the joint and adding the panel zone distortion, Equation [6.17], where $\square_{panel} = \square_{connection}$:

$$\varphi_{CONN.DX} = Incl_3 - Incl_2 + \gamma_{panel} \quad (5.72)$$

5. SEISMIC BEHAVIOUR OF RC COLUMNS EMBEDDING STEEL PROFILES

5.6 Results of the tests

As said before, the specimens belonging to the Static category have been designed only with regard to the gravity loads, whereas the specimens belonging to the Low Ductility and Medium Ductility categories have been designed both considering the gravity loads and the equivalent horizontal seismic loads. The Low Ductility and the Medium Ductility categories differ one from the other mainly for the magnitude of the seismic forces applied to the original RC structure, depending on the grade of ductility the designers are to attribute to it at the design stage. Consequently, the specimens differ on the amount of longitudinal reinforcement, on the spacing of stirrups placed in the critical zones of the main elements and on the dimensions of the embedded steel profiles. For this reason, only an abridgement of the results obtained from testing is hereafter illustrated along with some commentaries. The comments can be extended to the other study cases.

The $F-\Delta$ curves of five specimens belonging to the same study case are represented. In detail, the specimens RCT5, COT9-COT10, and COT11-COT12 for the medium ductility design case, according to the test programme illustrated in Subsection 5.5.2, have been presented. The test conducted on the specimen RC-T (sample without steel profile) is used as test control and reference for the other tests of the same category. In fact, the behaviour of this specimen relies only on the resistance and ductility of a reinforced concrete section. The previsions obtained in the design of the specimens have been confirmed, as the tests have shown that the specimen collapse has been caused by failure in the joint. The global behaviour for each test will be shown below with some pictures that illustrate clearly the problems occurred in the joints during the tests.

5.6.1 RCT5 Specimen

The test conducted on specimen RCT5 is used as test control and reference for the other tests of the same category. As illustrated in Figure 5.30, the behaviour of this specimen relies only on the resistance and ductility of a reinforced concrete section. Once again, the curves above show the classical aspects of a RC column: regular stiffness and resistance up to a $100 \div 110\text{mm} = 6e_y$ displacement from which the column loses very fast its mechanical properties (from the higher value of $\approx 110\text{kN}$ to the lower of $\approx 70\text{kN}$) anticipating the final failure at the beginning of the first $8e_y$ cycle. The column collapsed in a brittle way in the closeness of the connection with some cracks and spalling of the concrete at the joint panel. The joint region was rather deteriorated, as showed in the following Figure 5.31.

5. SEISMIC BEHAVIOUR OF RC COLUMNS EMBEDDING STEEL PROFILES

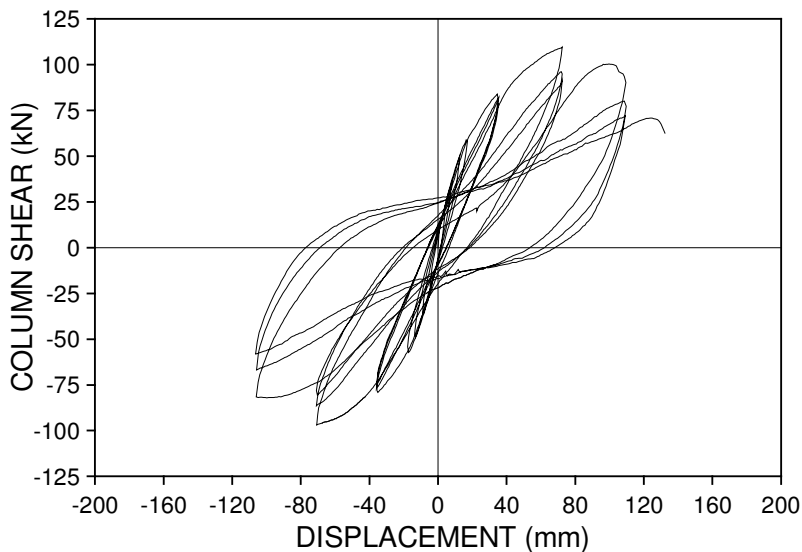


Figure 5.30. Column shear force vs. top displacement relationship for RCT5 specimen

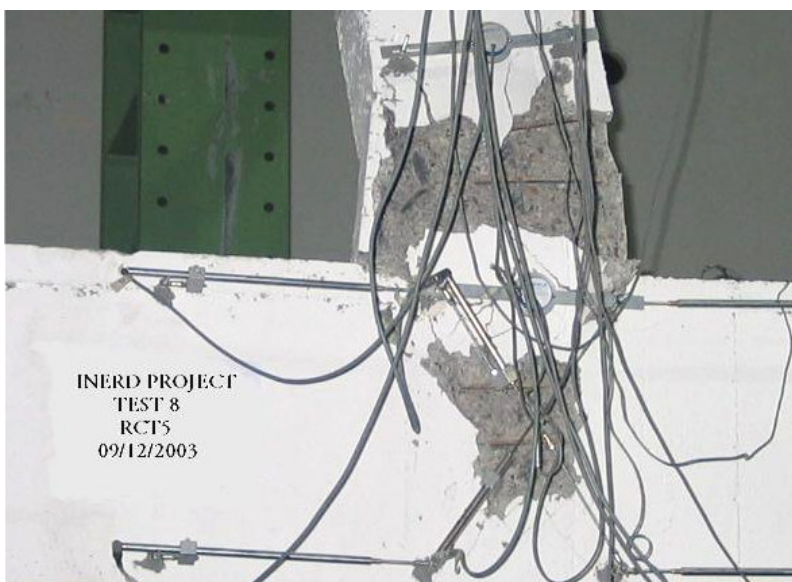


Figure 5.31. RC T5 collapse above the joint region

5.6.2 COT9-COT10 Specimens

The tests conducted on specimens COT9 and COT10 were utilised to compare the behaviour of the RC column with that of the strengthened samples through the steel column in the C1 configuration (long steel profile). As illustrated in Figure 5.32, after a first portion of the test ($60\text{--}80 \text{ mm} = 4e_y$), in which the stiffness and

5. SEISMIC BEHAVIOUR OF RC COLUMNS EMBEDDING STEEL PROFILES

resistance of the concrete section prevails, the specimen COT9 shows the typical behaviour for steel section: large hysteresis cycles with constant level of stiffness and modest loss of resistance. At the subsequent cycles ($6e_y$, $8e_y$ and $10e_y$), the specimen reacts to the imposed top displacement with a force equal to 85%, 70% and 35% of the maximum reached level (110 KN), respectively. One important aspect is that COT9 showed wide hysteresis cycles with the resisted shear force.

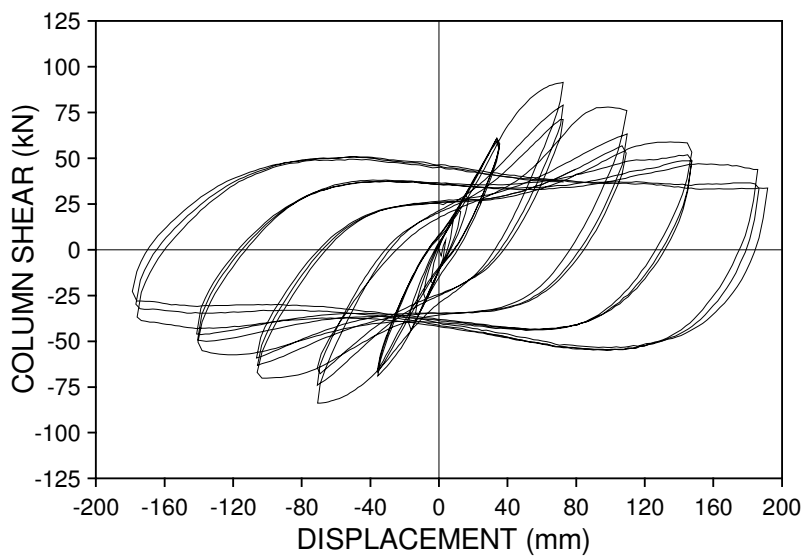


Figure 5.32. Column shear force vs. top displacement relationship for COT9 specimen

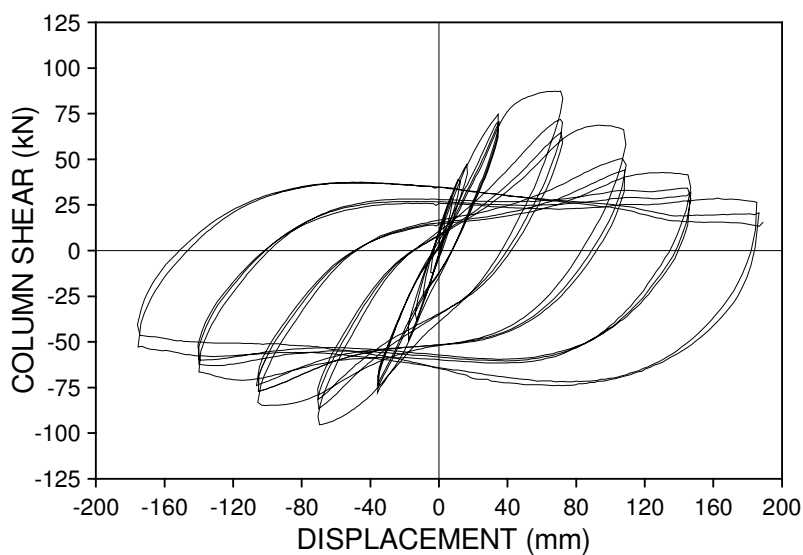


Figure 5.33. Column shear force vs. top displacement relationship for COT10 specimen

5. SEISMIC BEHAVIOUR OF RC COLUMNS EMBEDDING STEEL PROFILES

The previsions were respected. We can state that the sample failed due to the degraded joint mechanical properties and the test was stopped at the end of the $10e_y$ cycles. Also the COT10 specimen (see Figure 5.33) was able to reach the second $10e_y$ cycle with a residual strength of $\approx 20\text{kN}$ and a good resource in ductility thanks to the resistance and stiffness added by the steel profile. The collapse interested the entire column length. It was caused by a longitudinal crack that started from the joint region interesting the concrete cover thickness up to the column top (concrete cover separation), as showed in the Figure 5.34.

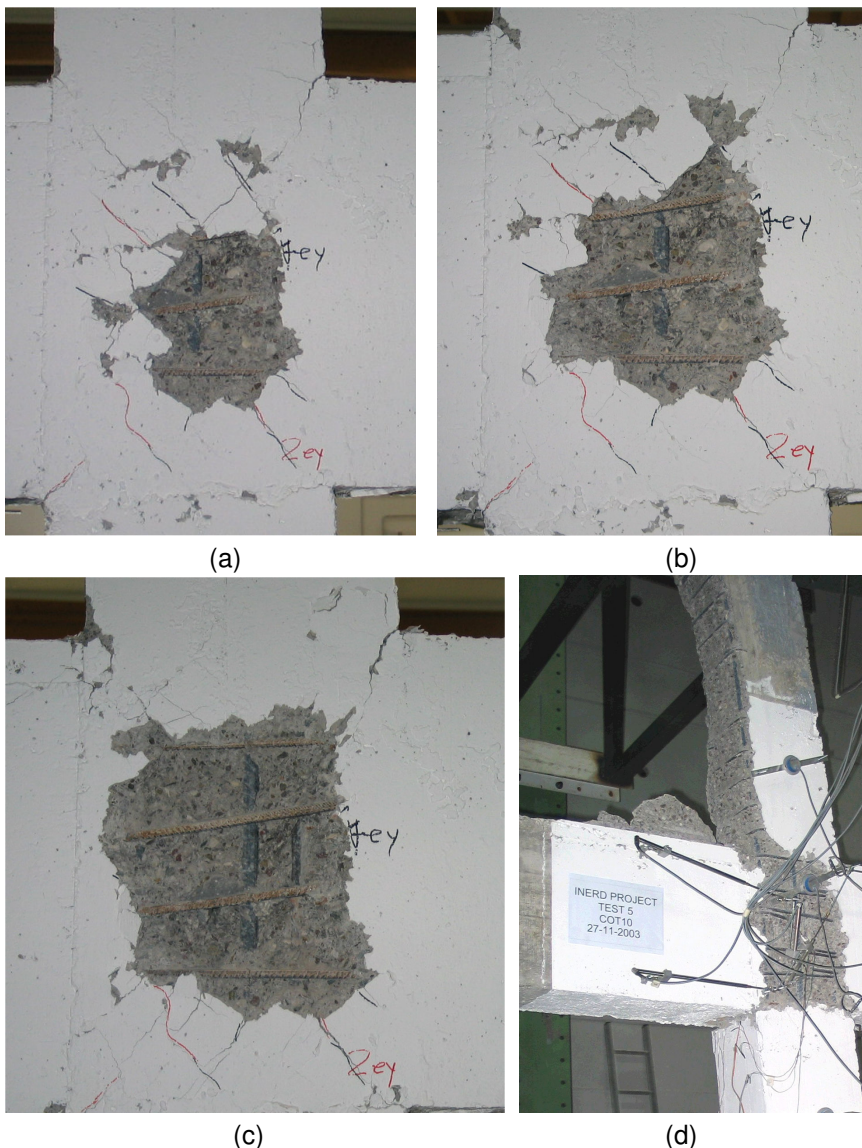


Figure 5.34. Evolution of cracks and spalling of the concrete in the joint for a top displacement varying equal to: (a) $4e_y$, (b) $6e_y$, (c) $8e_y$, (d) at collapse

5. SEISMIC BEHAVIOUR OF RC COLUMNS EMBEDDING STEEL PROFILES

In order to understand the behaviour of the joint under cyclic loading, it is important to evidence the rotation capacity that the panel zone can carry out. As explained before, the distortion of the panel zone was monitored during the test by means of the LVDT TR500-2D e TR500-1D. The transducer measurements are combined by the following formula (Krawinkler, 1978) to obtain the total distortion.

$$\gamma_{conn} = \operatorname{tg}^{-1} \left[\sqrt{(h_{sp})^2 + (b_{sp})^2} \frac{(\Delta U_{TR500-2D} - \Delta U_{TR500-1D})}{2(h_{sp} + b_{sp})} \right] \quad (5.73)$$

where h_{sp} e b_{sp} are the design height and depth of the web panel in shear; ΔU_{TR500} are the difference between the two measurement of the diagonal LVDT transducer. As depicted in Figure 5.35, it is possible to underline that the behaviour of the panel zone is characterized by large energy absorption and displacement ductility, due to the extensive plastic deformation occurring. One can observe that total distortions of the joint reach values greater than 35 mrad, implying a suitable ductile behaviour for high ductile structures in seismic applications. Progressive strength and stiffness deterioration is then occurring associated to the increase of plastic deformations of the steel profile and damage in the concrete.

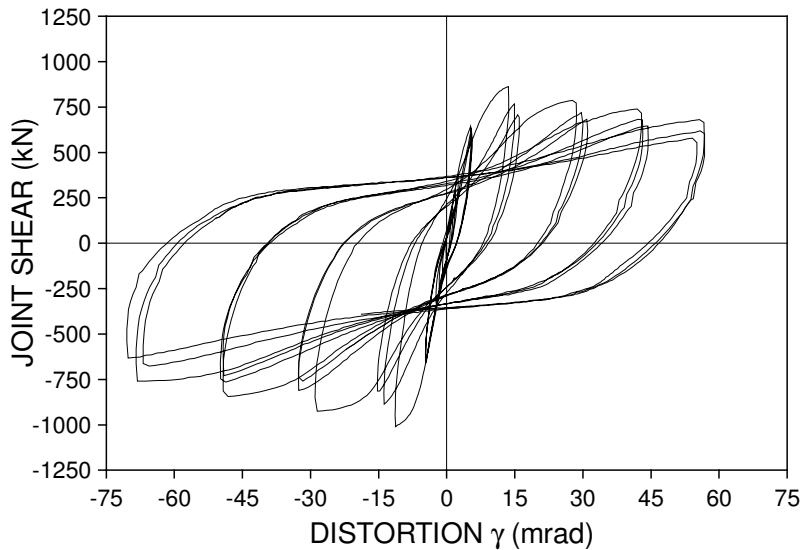


Figure 5.35. Joint shear force vs. distortion relationship for COT10 specimen

5. SEISMIC BEHAVIOUR OF RC COLUMNS EMBEDDING STEEL PROFILES

5.6.3 COT11-COT12 Specimens

The test conducted on specimen COT11, is the only one with available data representing the C3 configuration for the Medium Ductility Case. The test finished at the real begin of the $10e_y$ cycle with a residual resistance of $\approx 40\text{kN}$, after having reached the maximum value of $\approx 95\text{kN}$ at $4e_y$. The failure occurred up to the middle column height, again far from the joint, which appeared rather deteriorated. Also the COT12 rupture confirmed this tendency of the other specimens belonging to the configuration C3, i.e. to show a collapse far from the joint region before the conventional end of test fixed at $10e_y$.

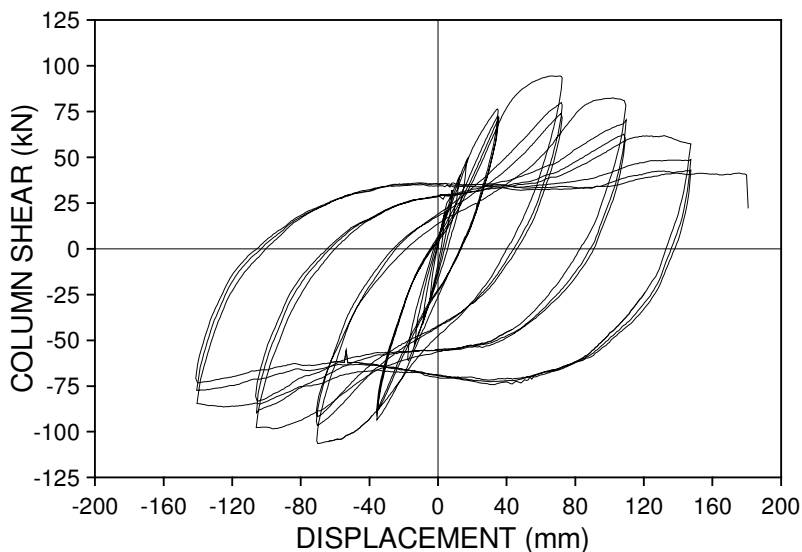


Figure 5.36. Column shear force vs. top displacement relationship for COT11 specimen

5.6.4 Comparison of the experimental results and comments

In order to better understand the improvement in the behaviour of the specimens in term of strength and ductility due to the use of the inserted steel profile is important to compare the obtained results. A directed comparison is done in Figure 5.37, in which the envelopes of the behaviour of the specimens in term of shear force–top displacement are reported. The reader can see clearly that the presence of the steel profile increases the level of ductility for each level of the reached force. In others words, the specimens COT9, COT10 and COT11 show a reserve of strength for each imposed displacement greater than the reaction force exhibited from the specimen RCT5. This difference has been summarized in Table 5.14.

5. SEISMIC BEHAVIOUR OF RC COLUMNS EMBEDDING STEEL PROFILES

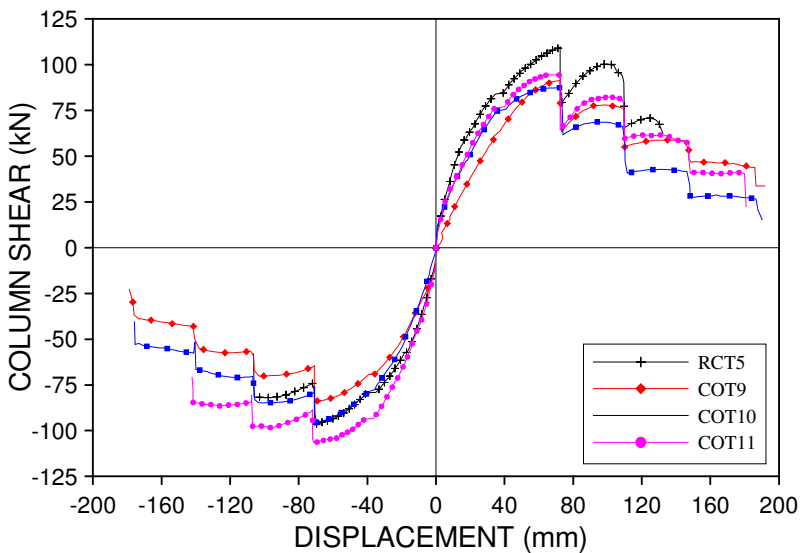


Figure 5.37. Envelope of the specimen responses in term of shear force-top displacement

IMPOSED DISPLACEMENT	MAXIMUM REACTION FORCE (kN)			DIFFERENCE IN PERCENTAGE (%) OF THE REACTION FORCE	
	RCT5	COT10	COT11	$\frac{COT10 - RCT5}{RCT5}$	$\frac{COT11 - RCT5}{RCT5}$
e_y	57,37	48,68	61,12	-15,2	8,15
$2e_y$	79,16	77,77	93,35	-1,76	20,56
$4e_y$	96,91	95,44	106,44	-1,52	11,39
$6e_y$	81,61	84,75	97,72	3,85	22,97
$8e_y$	68,95	66,46	84,54	-3,62	26,73
$10e_y$	/	52,84	40,43	/	/

Table 5.14. Comparison in term of reaction force for the tested specimens

Another important index for the comparison of the behaviour of the specimens is the accumulated energy, dissipated during the test. This index provides information about the ductility of the specimen, as the comparison is made in terms of absorbed energy for each level of imposed displacement; one may observe from Figure 5.38, that the specimens with the inserted steel profile dissipate an amount of energy that is double with respect to the dissipated energy of the reinforced concrete specimen. Moreover, the two configurations C1 and C3 are not so

5. SEISMIC BEHAVIOUR OF RC COLUMNS EMBEDDING STEEL PROFILES

different in term of dissipated energy; this means that only the portion of the steel profile in the web panel zone behaves in an inelastic range, whereas the other portion of the column behaves elastically, with a little contribution to the absorbed energy. This difference has been summarized in the following Table 5.15.

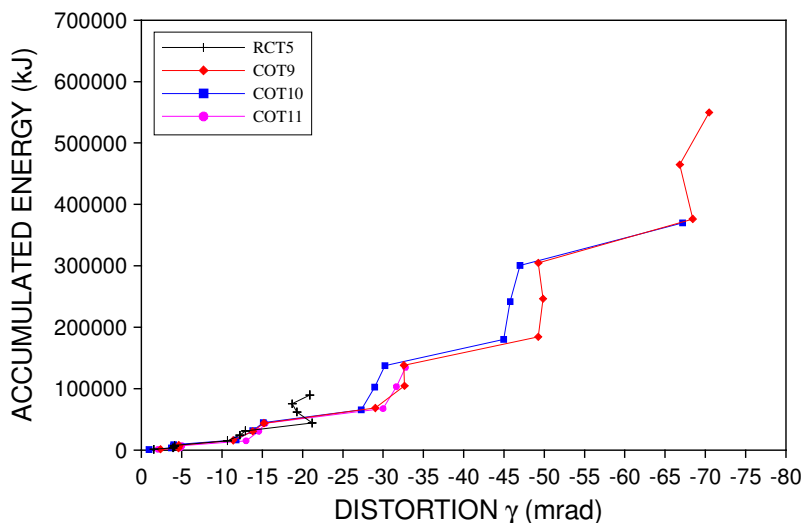


Figure 5.38. Comparison in term of accumulated energy for the tested specimens

		ACCUMULATED ENERGY (KJ)			DIFFERENCE OF THE ACCUMULATED ENERGY (%)	
IMPOSED DISPLACEMENT		RCT5	COT10	COT11	$\frac{COT10 - RCT5}{RCT5}$	$\frac{COT11 - RCT5}{RCT5}$
e_y^+		1244	1075	1135	-13,6	-8,8
$2e_y^+$	1° cycle	3089	2592	2882	-16,1	-6,7
	2° cycle	4705	3891	4908	-17,3	4,3
	3° cycle	5910	4815	6564	-18,5	11,1
$4e_y^+$	1° cycle	10612	8795	11355	-17,1	7,0
	2° cycle	15312	14477	19173	-5,5	25,2
	3° cycle	19008	19282	26032	1,4	37,0
$6e_y^+$	1° cycle	24873	26432	34778	6,3	39,8
	2° cycle	34685	38249	49915	10,3	43,9
	3° cycle	43604	49249	64246	12,9	47,3
$8e_y^+$	1° cycle		61747	80811	/	/
	2° cycle	/	82533	105833	/	/
	3° cycle		102310	129912		

Table 5.15. Comparison in term of cumulated energy for the tested specimens

5. SEISMIC BEHAVIOUR OF RC COLUMNS EMBEDDING STEEL PROFILES

Summarizing, we can say that the tests conducted on specimens COT9 and COT10 confirm to have a very similar behaviour regardless of the presence of the continuity plates. Both samples reached or nearly reached the conventional end of test. The important piece of information for COT11 and COT12 mostly concerns the type of failures occurred to these specimens. Hence, we have to judge whether the displacement level reached for the specimens belonging to the C3 configuration (normally $8e_y$) establish a sufficient amount of ductility or it simply shift the problem from the joint to another cross column section (the weakest one). In fact, the connection panel with short profile encased, showed a good resistance. Nonetheless, it may cause the brittle failure of the column before the requested time, necessary to resist a seismic event.

5.7 Numerical analyses and validation of the mechanisms

In this section, the inelastic finite element (FE) analyses carried out by means of the ABAQUS code (2003) are discussed. Thereby, the FE models were calibrated and the stress and strain state of the aforementioned joints was simulated in the monotonic displacement regime. Finally, by means of the analysis results a validation of the proposed analytical formulas have been determined. The modification in the dimension of some geometrical and mechanical parameters, obtained through the elaboration of the numerical evidences, has permitted to match better the experimental resistance of the joint subjected to shear loads.

5.7.1 *FE Model of the specimens*

Non-linear FE analyses of the tested specimens were carried out in a monotonic loading regime. The analyses have been developed with 3D FE models. The used model is reported in Figure 5.39 and represents the specimen COT9, endowed with an HEB 140 steel profile. It is characterized by reduced integration eight-node solid elements (C3D8R in the ABAQUS library). The FE analyses account for material non-linearities through classical plasticity based on the Von Mises yield criterion. Isotropic hardening is assumed for the analyses. The new model Concrete in ABAQUS code has been used. This model permits to define the correct strain-stress curve of the concrete both in tension and in the compression. Moreover, for cyclic loading history, it is possible to define a degradation law for the stiffness characteristics. The measured stress-strain properties of the different materials (column flange, column web, stiffeners, rebars in the beam and in the

5. SEISMIC BEHAVIOUR OF RC COLUMNS EMBEDDING STEEL PROFILES

column, concrete) obtained by test were used. Moreover, the confinement of the concrete due to the presence of the stirrups in the region of the joint is implicitly taken into account. As said in Subsection 5.3.1, the confinement results in a modification of the effective stress-strain relationship: higher strength and higher critical strains are achieved.

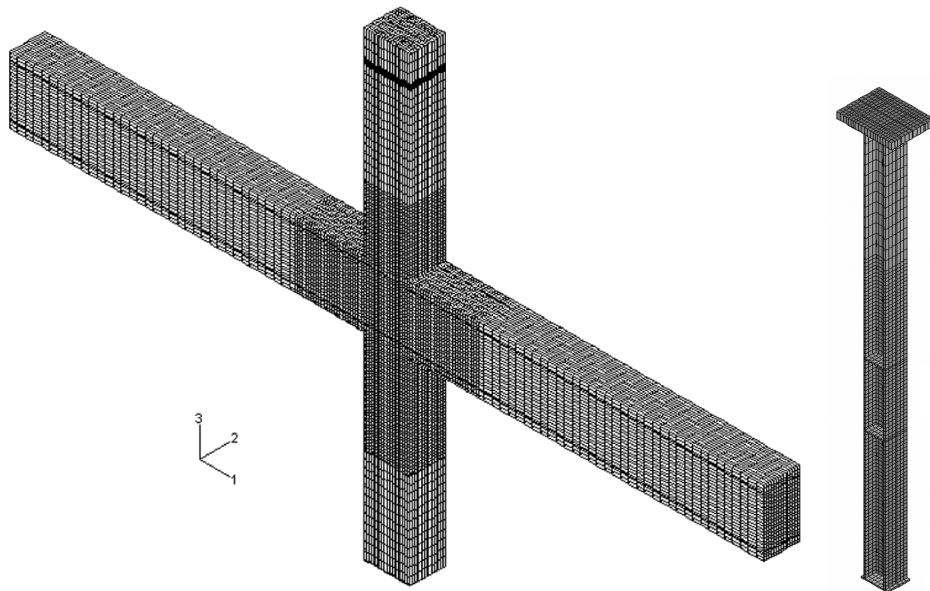


Figure 5.39. 3D numerical model of the COT9 specimen

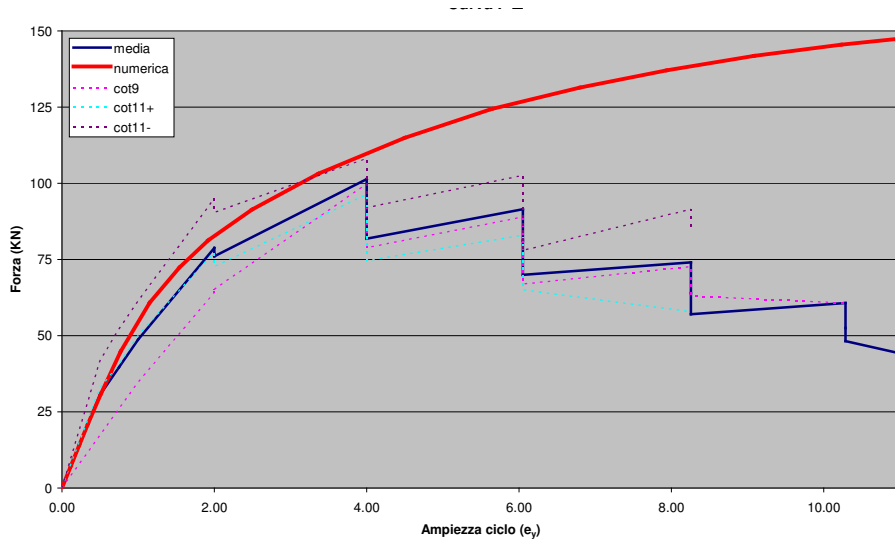


Figure 5.40. Predicted vs. numerical response of the specimen COT9

5. SEISMIC BEHAVIOUR OF RC COLUMNS EMBEDDING STEEL PROFILES

Elastic and inelastic convergence studies have been conducted to evaluate and arrive at the final mesh for the finite element models. The finite element model was verified by comparing the measured cyclic response of specimen with the predicted monotonic (see Figure 5.40). As far as concerns the cyclic test, the envelope curve of the experimental tests was found and compared to the curve found using the finite element model. Even if the model is not able to capture the loss of resistance and stiffness due to the crushing of the concrete after a certain level of the imposed displacement, the experimental data are in good agreement with the numerical simulation. The elaboration of the numerical evidences has led to the modification of some geometrical and mechanical parameters related to the formulae and it has permitted to better figure out the experimental response of the joint subjected to shear loading. Also the measurements obtained from the local instrumentation by means of strain gauges helped in the understanding of the activation and evolution of the resistance mechanisms, proposed in Section 5.4, while testing.

5.7.2 Steel web panel shear mechanism verification

By means of a set of elements extracted in the web panel zone of the steel profile, it was possible to monitor the evolution of the shear stress σ_{13} at the increasing of the imposed top displacement. As depicted in the following Table 5.16, and as expected, the stress state of web panel increases during the test until it yields uniformly for a top displacement equal to $6e_y$. From this point the concentration of the stresses moves in the four corners of the steel web panel, where the stiffeners are welded. In this moment the resistance of the panel zone in the steel profile is given to the contribution of four plastic hinges that have been formed.

This hypothesis results confirmed analysing the experimental results obtained from the strain gauges positioned in the web and in the flange of the steel profile in correspondence of the stiffeners. The graphs below, deduced from the experimental data (strain gauges), give explanation of the shear mechanisms activated in the steel web, steel flanges and stiffeners. To obtain the shear strain by the measurement the hypothesis that the principal stress σ_1 and σ_3 are aligned with the axes of the steel column is made. As depicted in Figure 5.41, the measured web strain increases uniformly up to a displacement equal to $4e_y \div 6e_y$ when it exceeds the steel yield strain. It is the central zone of the panel that deforms most. It can be imagined the web stresses increasing during the test until the panel zone yields uniformly for a top displacement equal to $6e_y$. From this point on, concentration of stresses shifts to the four corners of the steel web panel in correspondence of the stiffeners, and the resistance of the panel zone is given by the contribution of these four local plastic hinges.

5. SEISMIC BEHAVIOUR OF RC COLUMNS EMBEDDING STEEL PROFILES

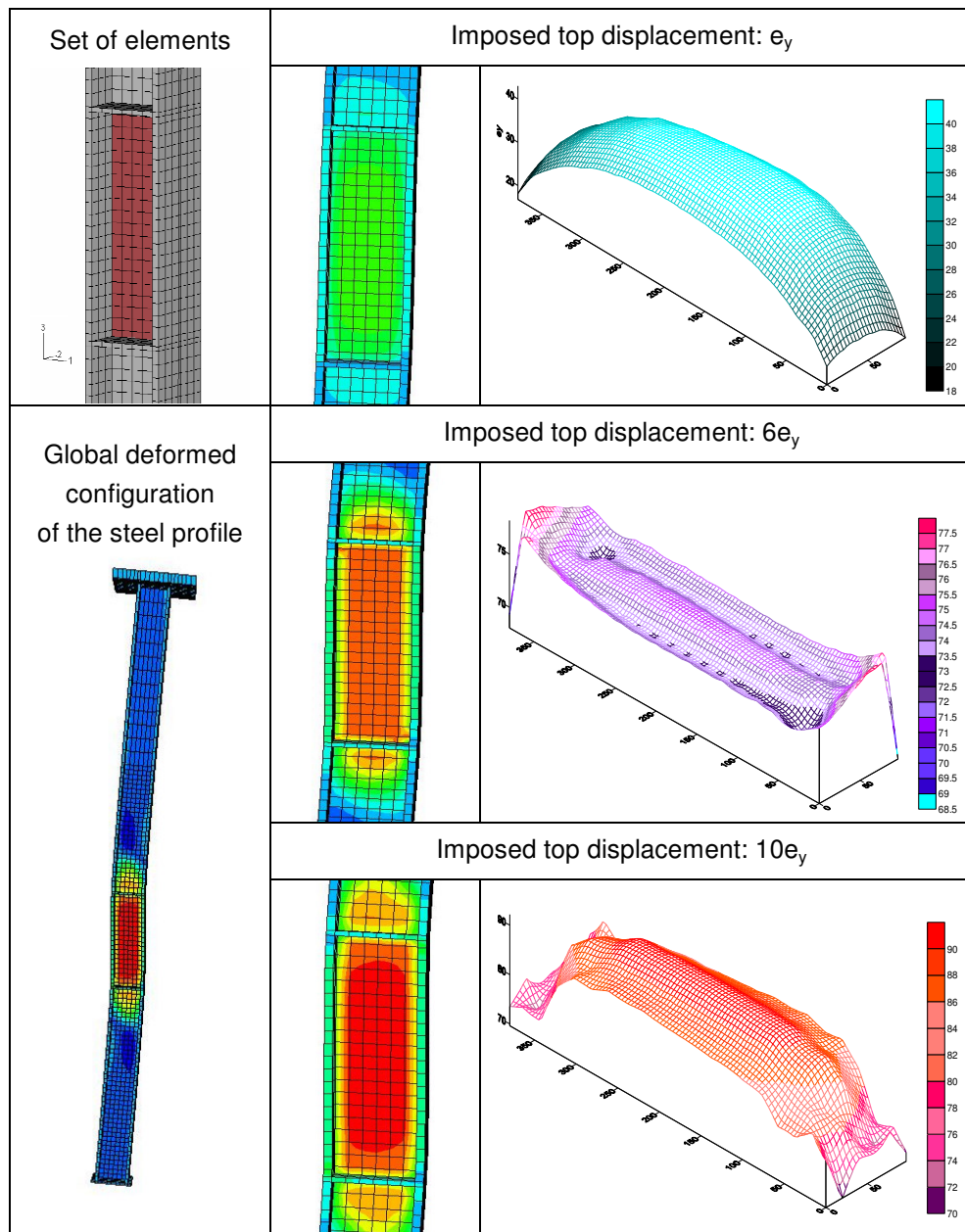


Table 5.16. Steel web panel mechanism $-\sigma_{13}$ stresses

In fact, as depicted in Figure 5.42, by means of the elaboration of the values of the strain gauges positioned in the flange of the steel profile it is possible to evidence that the deformation in the zone of the stiffeners is greater than that along the flange. High plastic deformations, intended as local plastic hinges, are well localised in these points where part of the shear forces are transmitted.

5. SEISMIC BEHAVIOUR OF RC COLUMNS EMBEDDING STEEL PROFILES

Nevertheless, it is of primary importance to point out that this behaviour was encountered also in the specimens without the horizontal steel plates. Therefore, the plastic hinges form at the four joint corners where the shear forces have to be transferred, regardless of the presence of the stiffeners.

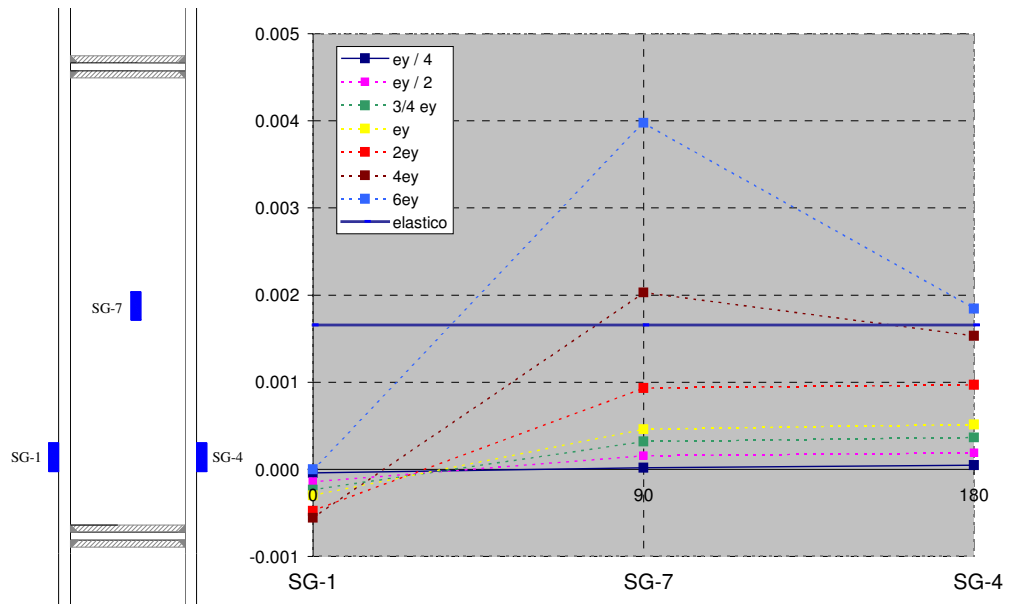


Figure 5.41. Evolution of the measured strain in the web panel of the steel profile

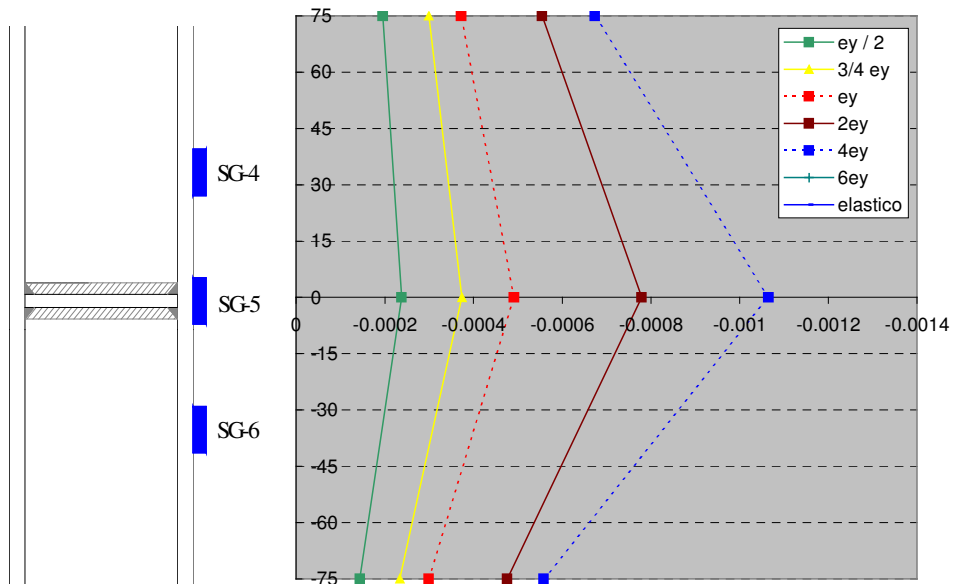


Figure 5.42. Evolution of the measured strain in the flange of the steel profile

5. SEISMIC BEHAVIOUR OF RC COLUMNS EMBEDDING STEEL PROFILES

5.7.3 Concrete compression strut mechanism verification

Where the steel column web is encased in the concrete, the design shear resistance of the panel may be increased with the contribution of the inner concrete strut V_{ccs} that is the design shear resistance of the concrete encasement of the web panel.

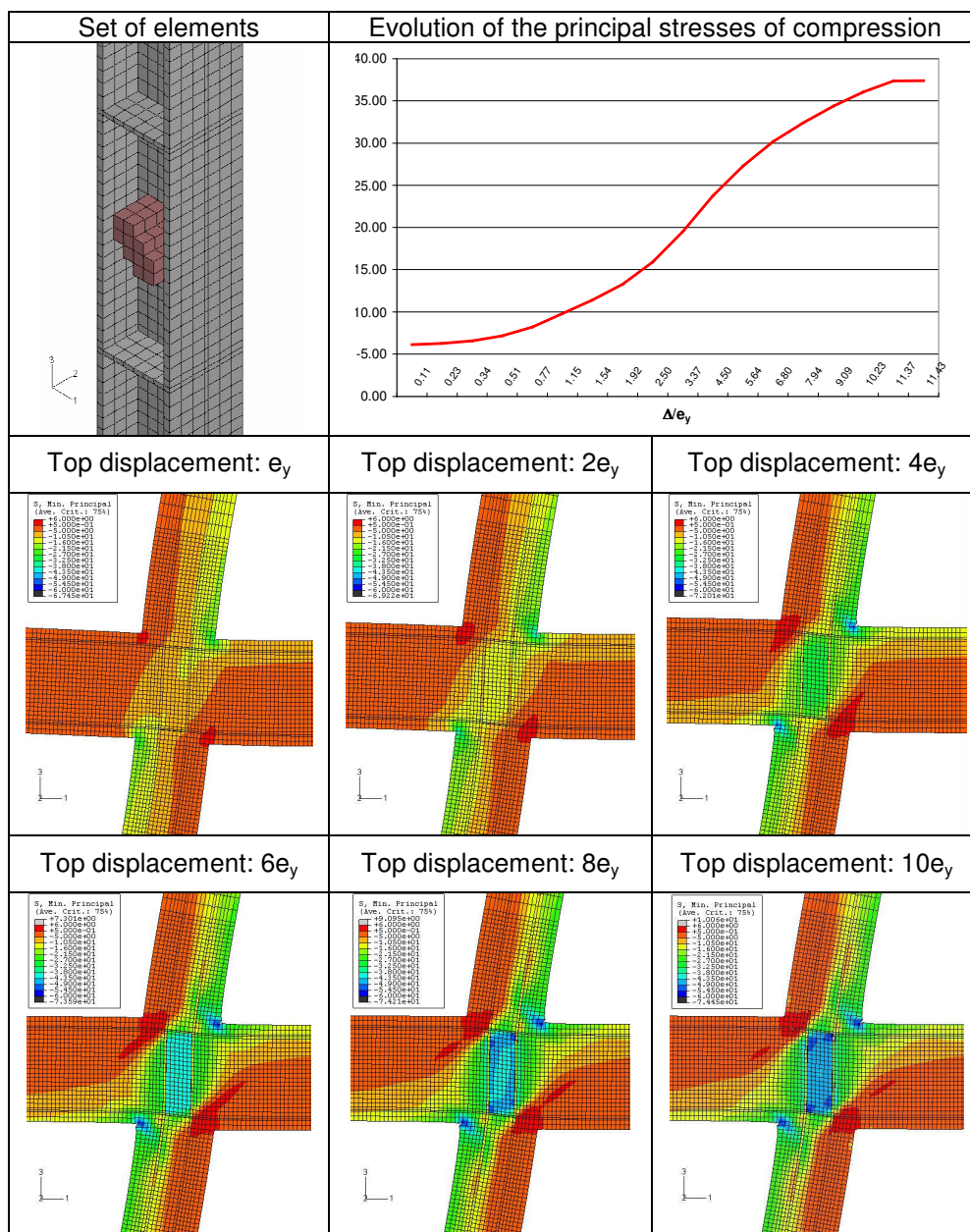


Table 5.17. Concrete compression strut mechanism – $\sigma_{min,prin}$ stresses

5. SEISMIC BEHAVIOUR OF RC COLUMNS EMBEDDING STEEL PROFILES

In composite connections, the concrete compression strut may be mobilised in resisting the shear either due to the presence of the horizontal plates welded to the column or simply due to friction and flexural forces acting in the steel column flanges. By means of a set of elements extracted in the concrete between the stiffeners and the web panel of the steel profile, it was possible to monitor the evolution of the principal stresses of compression for different imposed top displacement.

As evidenced in Table 5.17, with the increasing of the displacement imposed at the top of the column, high stresses of compression are mobilized in the concrete strut. For a displacement equal to $6e_y$, all the concrete in the zone reached the value of 40 MPa that represent the maximum allowed compression strength. Nevertheless, the effect of the confinement due to the presence of the steel profile and the stiffeners permits to reach greater value for an amplification of the top displacement. Finally, at an imposed displacement equal to $10e_y$ the concrete in the interior zone and around the joint is crushed. The numerical results are in a good agreement with the experimental test, as evidenced in Figure 5.43.



Figure 5.43. Failure of the joint during the experimental tests

The shear resistance given by the concrete horizontally compressed by the elements inside the column $V_{j,hbf}$, is determined through a standard Stress Block Model. For a good development of the Horizontal Bearing Mechanism it is important to provide a sufficient concrete confinement. The provided amount of stirrups in the tested specimens seems to be adequate to this aim.

5. SEISMIC BEHAVIOUR OF RC COLUMNS EMBEDDING STEEL PROFILES

5.7.4 Concrete compression field mechanism verification

In the numerical model the stirrups in the column are not directly modelled; the confinement effect is taken into account by a modification of the effective concrete stress-strain relationship. Nevertheless, the activation of the concrete compression field is verified by means of the strain gauges positioned in the stirrups. As evidenced in Figure 5.44, with the increase of the imposed top displacement the stirrups were mobilised to transfer the shear forces into the joint. At elevated displacements 8ey-10ey, the transversal re-bars are subjected to high tensile stresses that should equilibrate the compression struts in the outer concrete part of the joint. The equilibrium of forces results satisfied by the tension and compression stresses in the longitudinal re-bars, which transfer the relative component of the compression strut into the column. The evolution of the tensile and compressive stress in the column is reported in Figure 5.45, and was obtained through the elaboration of the numerical results. It is also possible to underline that, at elevated imposed top displacements, the deformations of the longitudinal re-bars in the panel zone increase due to the tensile and to the compressive forces transmitted by the concrete.

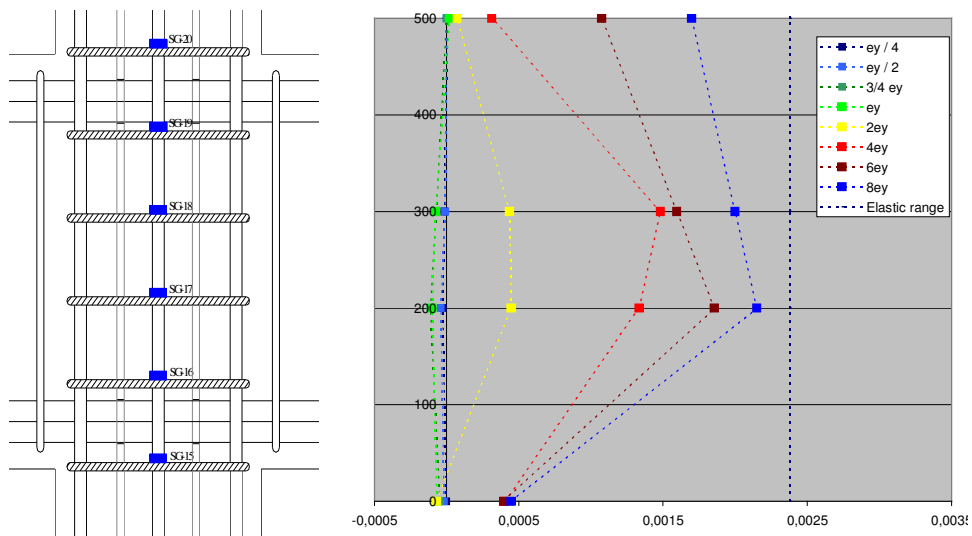


Figure 5.44. Evolution of the measured strain in the stirrups of the column

The Bond Resistance $V_{\text{joint,bf}}$ is provided by the longitudinal reinforcing bars acting in friction with concrete and embedded in the outer joint region. The bond failure occurs in the outer elements if the compression and tension forces (due to moment equilibrium), along with the forces mobilised in the concrete compression field, are greater than the strength of the bond mechanism of a set of main longitudinal re-

5. SEISMIC BEHAVIOUR OF RC COLUMNS EMBEDDING STEEL PROFILES

bars. In Figure 5.45, the strain values measured by means of the strain gauges stuck on the longitudinal re-bars of the column are reported. The augmentation of the strains tied to the increase of the top displacement can be noted.

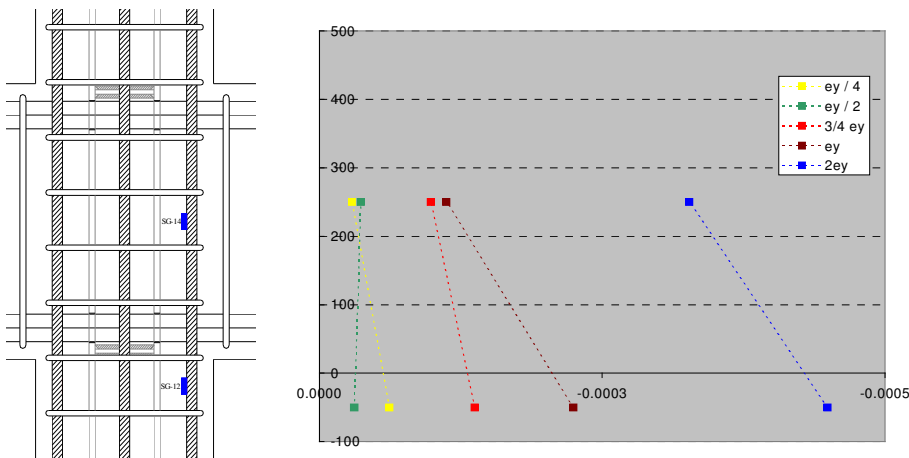


Figure 5.45. Strains of the longitudinal re-bars of the column

5.7.5 Calibration of the mechanisms

By means of the analysed numerical results it was possible to verify the activation of the proposed shear transfer mechanism in the joint. Moreover, by means of a detailed analysis of the stress and strain evolution obtained from the numerical model it was possible modify in the proposed analytical formulas the values of some geometrical and mechanical parameters.

In detail, the most important geometrical parameter that influences the shear resistance of the joint is the depth of the joint itself, j_h that is utilized both in the interior mechanisms and in the exterior mechanisms evaluation.

By the analysis of the numerical results (see Figure 5.46) it was possible to determine that:

- for the steel web panel mechanism, the joint depth j_h can be taken equal to the distance d_s of the stiffeners welded to the column;
- for the concrete compression strut, the joint depth j_h can be taken equal to $0.9d_s$ the distance of the stiffeners welded to the column, due to the fact that the center line of the compression results interior to the stiffeners;
- for the concrete compression filed mechanism, the joint depth j_h can be taken equal to $1.1d_s$ the distance of the stiffeners welded to the column, due to the fact that the center line of the shear force results localized at the level of the reinforcing bars in the beam.

5. SEISMIC BEHAVIOUR OF RC COLUMNS EMBEDDING STEEL PROFILES

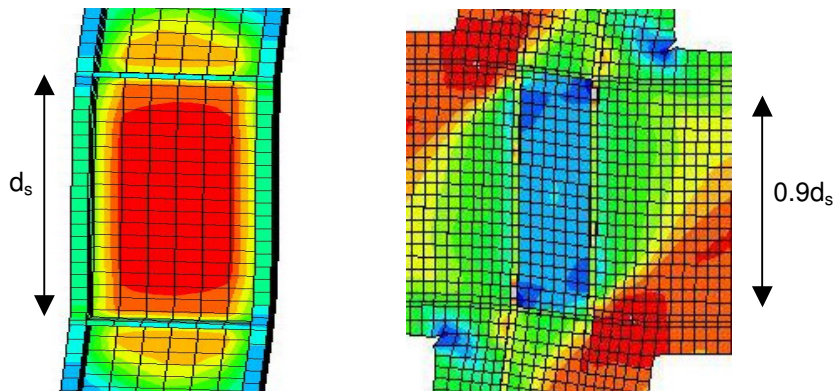


Figure 5.46. Modified joint depth after the numerical analyses

The differences between the analytical model, i.e. the equations previously illustrated necessary to determine the single joint mechanism resistance, and the experimental values obtained from the tests in terms of maximum average shear force resisted at the joint region are introduced in the following Table 5.18.

ANALYTICAL PROCEDURE					
Inner Resistance			Outer Resistance		
Mechanism	$V_{j,rd}$ [kN]	$M_{j,Rd}$ [kNm]	$M_{j,Rd}$ [kNm]	$V_{j,rd}$ [kN]	Mechanism
PANEL ZONE	583	230			
CONCRETE COMPRESSION STRUT	134	47	66	152	CONCRETE COMPRESSION FIELD
HORIZONTAL BEARING	1231	437	77	194	BOND
	$M_{j,Rd,MINIMUM}$	$M_{j,Rd,MINIMUM}$			
	277	66			
	$\Sigma M_{j,Rd,MINIMUM}$ [kNm]				
	344				
	$V_{j,rd}$ [kN]				
Analytical Value	871				
Experimental Value	915				
Difference	-4,8%				

Table 5.18. Comparison between numerical and experimental results after the numerical analyses

5. SEISMIC BEHAVIOUR OF RC COLUMNS EMBEDDING STEEL PROFILES

The analytical values obtained from the previous equations well agree with the true joint shear resistances obtained from the experimental tests in the case that, an increase in the shear resistance of the steel web panel (when subjected to high cyclic strains) is allowed. Hence, in equation 5.18, the factor $1/\sqrt{3}$ is substituted by a value equal to unity:

$$V_{j,wps} = 0,7 \cdot \left(\frac{f_{ym,d,cw}}{1} \cdot \min(A_v; t_{cw} \cdot d_s) + \Delta V_{j,swp} \right) \quad (5.74)$$

Note that, in this phase, the single mechanism resistance evaluated by means of the analytical model, does not take into account the partial safety factor value equal to 1,3 as prescribed by the Capacity Design Principle. Furthermore, the resistance values are determined considering the real material strengths obtained from specific tests conducted on concrete and steel samples. In fact, it is intended to make a direct comparison to establish the precision of the proposed analytical equations. Of course, at the design stage, it is necessary to account for all the relevant safety factors as already foreseen in the equations previously presented. By means of these modifications it was possible to calibrate the proposed analytical formulas: a substantial increase in the accuracy of the predicted joint shear resistance compared with that obtained from the experimental results. The difference between the analytical and experimental results has been modified from a 20% to a 5% of error, as reported in the Table.

5.8 Conclusions

This part of the Ph.D. thesis has been written with the intent of underlining the importance of the studies conducted on Innovative Beam-to-Column Composite Joints in order to provide the reinforced concrete structures of the necessary amount of ductility in those critical zones usually strongly affected by the occurrence of seismic events. The general recommendation is to reinforce some strategic points of the building, as the joints of the 1st storey, allowing in this manner to save the structure from a global collapse due to localised brittle type of failures. Both the solutions studied, with long and short steel profile encased in the concrete column, as expected, revealed to be effective in order to greatly improve the performance of the concrete members in terms of strength and ductility at large deformations. In fact, it can be stated that also the short steel profile stump is able to guarantee an adequate amount of resistance and ductility at the joint critical

5. SEISMIC BEHAVIOUR OF RC COLUMNS EMBEDDING STEEL PROFILES

region, even if some inconveniences occurred in the column length between the joint and the inflection point. It means that, a not accurate constructive process or the presence of not envisaged extra forces in the column may lead to an anticipated rupture in the absence of a full-length steel profile.

Having had the chance to go further into detail, also looking at the inside behaviour of the beam-to-column joints, the mechanisms activated in the shear load transfer were determined. The evidence is that the investigated solution with the continuity plates (stiffeners) welded to the steel column at the joint region seems not to give a substantial contribution in helping the load transfer at the beam-to-column joint. Thus, as not influencing significantly the global response of the joint under study, their usage in practice could be neglected also because of their remarkable effect on the overall cost of the assemblage.

Wishing to point out a commentary about the weak axis bending behaviour of the concrete frame structure, we underline the risk the building might run if the seismic wave comes along the minor axis bending and the columns were not specifically designed to withstand cyclic loads regardless the presence of the steel profile encased in the column.

Finally, we can say that, at the moment, the new applications are concentrated on the improvement of the analytical models to evaluate the shear resistance at the connection by means of further numerical simulations by means of a FE program. It may be also interesting to produce a procedure in order to evaluate the behaviour of the one-sided type of joints starting from the conclusions drawn for the two-sided type of joints considered in this research thesis.

5. SEISMIC BEHAVIOUR OF RC COLUMNS EMBEDDING STEEL PROFILES

5.9 References

- ACI American Concrete Institute (1995): *Building code requirements for structural concrete (ACI 318-95)*. Farmington Hills, MI.
- AISC (1997), Seismic provision for structural steel buildings, Task Committee 113.
- Aschheim M, Gulkan P., Sezen H. (2000): *Chapter 11: Performance of Buildings, in Kocaeli, Turkey earthquake of August 17, 1999 Reconnaissance Report*. Earthquake Spectra. Supplement A to Volume 16, 237–279.
- Chou C.C., Uang C.M. (2002): *Cyclic Performance Of A Type Of Steel Beam To Steel-Encased Reinforced Concrete Column Moment Connection*. Journal of Constructional Steel Research 58, 637-663.
- ECCS (1986): *Recommended Testing Procedure for Assessing the Behaviour of Structural Steel Elements under Cyclic Loads*. ECCS Publication n° 45.
- ECSC Project 7210-PR-316 (2001): *Earthquake Resistant Design: the INERD Project*.
- Hibbitt, Karlsson & Sorensen Inc (2003): *ABAQUS - User's Manual, Version 6.3*. Vol.1-3, 2003.
- Kanno R., Deierlein G.G. (2000): *Design Model Of Joints For Rcs Frames*. Composite Construction in Steel and Concrete IV – Proc. of Engrg. Found. Conference, Banff, May 28 – June 2, Banff, Alberta, 947-958.
- Krawinkler H. (1978): *Shear in Beam-Column Joints in Seismic Design of Steel Frames*. Engineering Journal AISC Vol. 3.
- Mander J.B., Priestley M.J. N., Park R. (1988): *Theoretical Stress-Strain Model For Confined Concrete*. Journal of Struct. Engrg., ASCE, vol. 114, No 8, 1804-1826.
- Ministry of Public Works and Settlement (1975): *Specification for structures to be built in disaster areas*. Government of Republic of Turkey.
- Penelis G.G., Kappos A.J. (1997): *Earthquake-Resistant Concrete Structures*. E & FN Spon, London.
- prEN 1991-1-1:2001: *Actions on structures, Part 1-1: general actions, densities, self-weight, imposed loads for buildings*. Final Draft, July 2001.
- prEN 1992-1:2001: *Design of concrete. Part 1: general rules and rules for buildings*. Draft n° 2, January 2001.
- prEN 1993-1-1:2000: *Design of steel structures. Part 1.1: general rules*. Draft n° 2, August 2000.
- prEN 1994-1-1:2001: *Design of composite steel and concrete structures. Part 1-1: general rules and rules for buildings*. Draft n° 3, March 2001.

5. SEISMIC BEHAVIOUR OF RC COLUMNS EMBEDDING STEEL PROFILES

- prEN 1998-1:2001: *Design of structures for earthquake resistance. Part 1: general rules, seismic actions and rules for buildings.* Draft n°3, May 2001.
- Scawthorn C.R. (2000): *Turkey earthquake of August 17, 1999: Reconnaissance Report.* Technical Report MCEER-00-0001. Buffalo, N.Y.: Multidisciplinary Center for Earthquake Engineering Research, State University of New York, NY. Editor. the Marmara.
- Sezen H., Elwood K.J., Whittaker A.S., Mosalam K.M., Wallace J.W., Stanton J.F. (2000): *Structural Engineering Reconnaissance of the August 17, 1999 Kocaeli (Izmit), Turkey Earthquake.* PEER 2000/09. Technical Report. Berkeley, CA.: Pacific Earthquake Engineering Research Center, University of California, CA. <http://nisee.berkeley.edu/turkey>.
- Turkish Standards Institute (1985). *TS-500 Building Code Requirements for Reinforced Concrete.* Ankara, Turkey.

6 SUMMARY, CONCLUSIONS AND FUTURE PERSPECTIVES

6.1 Summary

Mainly focusing the attention in new solutions assuring the necessary ductility, that can be obtained not only through careful study of building morphology, structural schemes and construction details, but also through a rational use of materials, this work constitutes an endeavour toward detailed analyses, design and tests of beam-to-column joints. The analysis started from the theoretical investigation of the so-called *Performance-Based Seismic Engineering approach*, that is defined as "identification of seismic hazards, selection of the performance levels and performance design objectives, determination of site suitability, conceptual design, numerical preliminary design, final design, acceptability checks during design, design review, specification of quality assurance during the construction and of monitoring of the maintenance and occupancy (function) during the life of the building." (Bertero and Bertero, 2002). Therefore, a comprehensive performance based design involves several steps:

- selection of the performance objectives;
- definition of multi-level design criteria;
- specification of ground motion levels, corresponding to the different design criteria;
- consideration of a conceptual overall seismic design;
- options for a suitable structural analysis method;
- carrying out comprehensive numerical checking.

On this basis an extensive study has been carried out on three main topics that are briefly summarized hereafter.

1. *Seismic behaviour of bolted end plate beam-to-column steel joints*: this research programme had a two-fold purpose: (i) to analyse the seismic

6. SUMMARY, CONCLUSIONS AND FUTURE PERSPECTIVES

- performance of partial strength bolted extended end plate joints with fillet welds, which represent an alternative to fully welded connections for use in seismic force resisting moment frames; (ii) to verify in a low-cycle fatigue regime, the feasibility of the mechanical approach adopted for joints undergoing monotonic loading, whereby the properties of a complete joint are understood and obtained by assembling the properties of its component parts.
2. *Seismic response of partial-strength composite joints:* in order to evaluate the feasibility and effectiveness of the composite constructions with partial-strength beam-to-column joints and partially encased columns in earthquake-prone regions, the study aimed at calibrating design rules affecting the aforementioned components and the participation of the concrete slab in the relevant transfer mechanisms. The results of this project led to improved design procedures for composite constructions (Section 7, Part 1 of EC8, 2002).
 3. *Seismic behaviour of RC columns embedding steel profiles:* this last research activity was part of another European Project titled Two Innovations For Earthquake Resistant Design - INERD Project, that deals with the improvement of the resistance and ductility of reinforced concrete (RC) structures using the performance of structural steel profiles. The general objective was to establish a new standard constructional rule able to improve the seismic safety of reinforced concrete structure, without great changes of traditional constructional practice. This rule consists in promoting one specific construction measure for lower storeys of reinforced concrete structures, by which steel profiles would be encased in RC columns in order to provide them with a basic reliable shear and compression resistance.

6.2 Conclusions and future perspectives

6.2.1 Seismic behaviour of bolted end plate beam-to-column steel joints

A general test programme was presented, comprising partial strength bolted extended end plate joints with fillet welds and component parts, which represent an alternative to fully welded connections for use in seismic force resisting moment frames. The main results indicate that partial strength bolted extended end plate connections are suitable for use in seismic moment resisting frames. They represent an alternative to fully welded connections, as together with the column

6. SUMMARY, CONCLUSIONS AND FUTURE PERSPECTIVES

web panel yielding, they can exhibit favourable ductility and energy dissipation properties.

As far as the understanding of the low-cycle fracture behaviour of ITS, CTS, and CJ connections is concerned, experiments and numerical analyses under monotonic and cyclic loading have provided insights in order to develop rules able to reduce fracture in the aforementioned connection components. The main conclusions of this study follow.

- vi. When proper consideration is given to material selection and detailing, extended end plates show a cyclic performance adequate for seismic design. The considered joints exhibit a plastic rotation greater than 35 mrad; therefore, they can be classified as *ductile* in accordance to Eurocode 8 (2002). In detail, test results on isolated bolted Tee stubs as well complete extended end plate bolted joints have shown that the overall behaviour of the specimens under investigation is governed by the material endowed with the lowest strength, viz. the base metal, in which yielding occurs, effectively. In fact, the weld metal persists in the elastic regime while the contiguous zones are weakened owing to the sharp thermal treatments and to structural as well as shape discontinuities.
- vii. Component cyclic tests enable identification of the failure mode. Moreover, they allow the Code requirements on the rotational capacity of the joint to be checked. Moreover, the mechanical models provided by the Eurocodes to determine the stiffness and strength characteristics of the individual components showed little agreement with the experimental data.
- viii. A *component model*, which approximates the cyclic response of the joints on the basis of the responses of the elemental components, does not seem to possess sufficient accuracy. Conversely, the use of *macro-components*, incorporating some of the interaction effects among elemental components, appears to be more adequate.
- ix. The simulations relevant to isolated Tee stub and Complete Joint connections indicate that the numerical model with isotropic hardening rule is able to capture both the monotonic and the cyclic responses but is not able to reproduce properly stiffness and strength degradation.
- x. A number of parametric analyses have been performed by considering fractures initiating from weld-root defects by means of the onset cracking method. Conclusions drawn from the models indicate that:
 - a. fracture driving force demands are reduced by using fillet welds matching the end plate material;
 - b. welding-induced residual stresses increase the fracture demand;

6. SUMMARY, CONCLUSIONS AND FUTURE PERSPECTIVES

- c. connections with $\sigma_y/\sigma_u = 0.9$ exhibit reduced fracture driving force demands but also limited plastic regions. The yield-to-ultimate strength reduction must comply with the requirements of plastic analysis.

Besides, the study is currently concentrating on the damage evolution aspect both for the components and the joint. The availability of adequate damage assessment methods is a pre-requisite to the development of reliable hysteretic models for research as well for design purposes. The confirmation of the above-mentioned conclusions to the complete joints tested deserves further studies.

6.2.2 Seismic response of partial-strength composite joints

The objective of this study was the investigation of the seismic performance of a realistic size moment resisting frame structure of high ductility class according to Eurocode 8 (2002) under various levels of earthquake. Dissipative elements were conceived to be partial strength beam-to-column joints and column base joints at later stages. Some full-scale substructures, representing the interior and exterior joints, have been subjected to monotonic and cyclic tests at the Laboratory for Materials and Structures Testing of the University of Pisa in Italy. Experimental results and three-dimensional finite element analysis of composite substructures has allowed the composite joints to be calibrated; and some inelastic phenomena characterizing their behaviour, such as the distribution of longitudinal stresses in the composite slab around the composite columns and the distribution of stresses in the column web panel and flanges to be understood. Moreover, analyses have demonstrated the adequacy of three-dimensional finite element models based on the smeared crack approach. The parametric analyses conducted both on exterior and interior joints have revealed that the full activation of Mechanisms 1 and 2 in the concrete slab causes a stiffening and strengthening of joints. This represents the most favourable design situation also due to a substantial increase of the effective breadth. Nonetheless, the aforementioned mechanisms have not the same stiffness, exhibiting Mechanism 1 a greater stiffness than Mechanism 2. Therefore, it is not easy to benefit from the strength of both mechanisms. For the exterior joint the full activation of Mechanism 2 is the most favourable design situation, while for the interior joint Mechanism 1 seems to be more effective, owing to the interaction phenomena between the two parts of the composite slab. The quantification of the stiffness corresponding to the activation of Mechanism 1 and of Mechanism 2 analysed in the parametric study performed in this work clearly imposes further study. Simulation and implementation in FE codes of the deteriorating behaviour of dissipative components of the joints, by means of robust hysteretic models, deserves further studies.

6. SUMMARY, CONCLUSIONS AND FUTURE PERSPECTIVES

Subsequently, a new mechanical model of the partial strength beam-to-column joint has been described. The model, which still relies on experimental data, is capable of simulating the behaviour of the steel-concrete composite partial strength joints subjected to monotonic loading. In detail, the model is capable of defining yielding and failure evolution of different components. The component models of the slab have indicated clearly that the compressive strut strength of the composite slab bearing on the column flange depends on the shear stiffness of the column web panel. Moreover, the activation of diagonal compressive struts on column sides induced by transversal reinforcing bars is hindered by the direct bearing of the compressive strut. Some force-displacement relationships provided by the proposed mechanical model have been compared with analytical formulae and current European standards.

The principles set forth have then been applied to the design of beam-to-column joints and columns of a full-scale frame structure that was built and subjected to pseudo-dynamic tests at the ELSA Laboratory of the Joint Research Centre in Ispra. The construction of the full-scale structure proved that the construction of steel-concrete composite structures with partial strength beam-to-column joints and partially encased columns is highly efficient.

Pseudo-dynamic and cyclic test results confirmed that properly designed and constructed partial strength beam-to-column joints and partially encased columns without concrete in column web panels exhibit a favourable behaviour in terms of energy dissipation, limited strength degradation and ductility.

6.2.3 Seismic behaviour of RC columns embedding steel profiles

This part of the Ph.D. thesis has been written with the intent of underlining the importance of the studies conducted on Innovative Beam-to-Column Composite Joints in order to provide the reinforced concrete structures of the necessary amount of ductility in those critical zones usually strongly affected by the occurrence of seismic events. The general recommendation is to reinforce some strategic points of the building, as the joints of the 1st storey, allowing in this manner to save the structure from a global collapse due to localised brittle type of failures. Both the solutions studied, with long and short steel profile encased in the concrete column, as expected, revealed to be effective in order to greatly improve the performance of the concrete members in terms of strength and ductility at large deformations. In fact, it can be stated that also the short steel profile stump is able to guarantee an adequate amount in terms of resistance and ductility at the joint critical region, even if some inconveniences occurred in the column length between the joint and the inflection point. It means that, a not accurate constructive process

6. SUMMARY, CONCLUSIONS AND FUTURE PERSPECTIVES

or the presence of not envisaged extra forces in the column may lead to an anticipated rupture in the absence of a full-length steel profile.

Having had the chance to go further into detail, also looking at the inside behaviour of the beam-to-column joints, the mechanisms activated in the shear load transfer were determined. The evidence is that the investigated solution with the continuity plates (stiffeners) welded to the steel column at the joint region seems not to give a substantial contribution in helping the load transfer at the beam-to-column joint. Thus, as not influencing significantly the global response of the joint under study, their usage in practice could be neglected also because of their remarkable effect on the overall cost of the assemblage.

Wishing to point out a commentary about the weak axis bending behaviour of the concrete frame structure, we underline the risk the building might run if the seismic wave comes along the minor axis bending and the columns were not specifically designed to withstand cyclic loads regardless the presence of the steel profile encased in the column.

Finally, we can say that, at the moment, the new applications are concentrated on the improvement of the analytical models to evaluate the shear resistance at the connection by means of further numerical simulations by means of a FE program. It may be also interesting to produce a procedure in order to evaluate the behaviour of the one-sided type of joints starting from the conclusions drawn out for the two-sided type of joints considered in this research thesis.

@Seismicisolation